

January 2016

MANUFACTURE OF INDIVIDUALIZED
DOSING: DEVELOPMENT AND CONTROL
OF A DROPWISE ADDITIVE
MANUFACTURING PROCESS FOR MELT
BASED PHARMACEUTICAL PRODUCTS

Elcin Icten
Purdue University

Follow this and additional works at: https://docs.lib.purdue.edu/open_access_dissertations

Recommended Citation

Icten, Elcin, "MANUFACTURE OF INDIVIDUALIZED DOSING: DEVELOPMENT AND CONTROL OF A DROPWISE ADDITIVE MANUFACTURING PROCESS FOR MELT BASED PHARMACEUTICAL PRODUCTS" (2016). *Open Access Dissertations*. 1289.

https://docs.lib.purdue.edu/open_access_dissertations/1289

This document has been made available through Purdue e-Pubs, a service of the Purdue University Libraries. Please contact epubs@purdue.edu for additional information.

**PURDUE UNIVERSITY
GRADUATE SCHOOL
Thesis/Dissertation Acceptance**

This is to certify that the thesis/dissertation prepared

By Elcin Icten

Entitled

MANUFACTURE OF INDIVIDUALIZED DOSING: DEVELOPMENT AND CONTROL OF A DROPWISE ADDITIVE
MANUFACTURING PROCESS FOR MELT BASED PHARMACEUTICAL PRODUCTS

For the degree of Doctor of Philosophy

Is approved by the final examining committee:

Gintaras V. Reklaitis

Chair

Zoltan K. Nagy

Co-chair

Lynne Taylor

Michael Harris

To the best of my knowledge and as understood by the student in the Thesis/Dissertation Agreement, Publication Delay, and Certification Disclaimer (Graduate School Form 32), this thesis/dissertation adheres to the provisions of Purdue University's "Policy of Integrity in Research" and the use of copyright material.

Approved by Major Professor(s): Gintaras V. Reklaitis, Zoltan K. Nagy

Approved by: John Morgan

Head of the Departmental Graduate Program

2/23/2016

Date

MANUFACTURE OF INDIVIDUALIZED DOSING: DEVELOPMENT AND
CONTROL OF A DROPWISE ADDITIVE MANUFACTURING PROCESS FOR
MELT BASED PHARMACEUTICAL PRODUCTS

A Dissertation

Submitted to the Faculty

of

Purdue University

by

Elçin İçten

In Partial Fulfillment of the
Requirements for the Degree

of

Doctor of Philosophy

May 2016

Purdue University

West Lafayette, Indiana

Beni her zaman destekleyen
anneciğim Aliye İçten ve babacığım Cengiz İçten'e

ACKNOWLEDGEMENTS

I would like to express my genuine gratitude to Prof. Gintaras V. Reklaitis and to Prof. Zoltan K. Nagy for their guidance, support and encouragement throughout my graduate career. I am truly honored and extremely lucky to have them as my graduate advisors, who I feel comfortable turning to both for research advice and for out of research discussions. I appreciate their constant support and guidance while evaluating my career choices. I would also like to thank Prof. Lynne Taylor and Prof. Michael Harris for serving on my committee and their contributions to my research. I would like to thank Dr. Seza Orçun for introducing me to research and encouraging me to attend graduate school.

Special thanks to staff member in the department who made my life easier. I would like to thank Teresa Cadwallader for going above and beyond the call of duty to help me and for being so kind. I would also like to thank Dr. Gabriela Nagy for her kindness and encouragement on Women in Chemical Engineering seminar. I would like to thank Deb Bowman, Bev Johnson and Corwin Green for their support as graduate administrators. I would like to thank business administrators for their help, especially Courtney Eddy, Amy Hayden and JoAnna Hadley. I appreciate the rest of the staff for all their help and friendly smiles, including Mike Harrington and Jeff Valley.

I would like to thank Dr. Arun Giridhar for his essential help in my research. It would not have been possible for me to reach this stage without his support in TB3. I would like to thank Dr. Laura Hirshfield for helping me get started with my research and for being a supportive friend. I would also like to thank Dr. Girish Joglekar for his contributions to my research. I would like to acknowledge my peers at the ERC-SOPS who I worked with closely, especially Dr. Niraj Trasi, Hitesh Purohit, Golshid Keyvan, Vicky Hsu, Christopher Anthony, Nur Atiqah Abd Rahman, Sierra Davis, Chelsey Wallace, Kristen Loehr and Jen Sacksteder.

I am very fortunate to be a part of an amazing research group. I would like to thank my office mates for enriching my Purdue life and providing entertainment in office life: Dr. Anshu Gupta, Dr. Jingjie Xiao, Dr. Ye Chen, Matt Louvier, Xiaohui Liu, Anuradha Bath, Omar Guerra, Mariana Moreno, Francesco Rossi, Daniel Casas, Ana Rosso, Sudarshan Ganesh, Andrew Radcliffe. I would also like to thank my group mates who I didn't get to share an office with, but enhanced my Purdue experience: Dr. Jose Miguel Lainez, Dr. Kris Villez, David Acevedo, Yang Yang, Ramon Pena, Jennifer Lu, Andy Koswara, Elena Simone, Akos Borsos and Boti Szilagyi.

I would like to thank my wonderful friends and family for being there for me during graduate school. I appreciate the support and encouragement of all my dear friends in all geographical locations, some of who could not physically be with me but always would care about me. I would like to thank my mother Aliye and my father Cengiz İçten for always supporting me and believing in me. I am blessed with the best parents I could

have ever asked for. I would also like to thank my sister Burçin İçten for entertaining me and being there for me. Lastly, I would like to thank Emre Gençer for his love and support. Making through graduate school would be impossible without his encouragements and cheering up. I feel lucky to share the good and bad times of our graduate lives together.

TABLE OF CONTENTS

	Page
LIST OF TABLES	xii
LIST OF FIGURES	xiv
ABSTRACT	xxii
CHAPTER 1. INTRODUCTION	1
1.1 Introduction	1
1.2 Project Motivation.....	3
1.3 Research Objectives	4
1.4 Thesis Overview.....	5
CHAPTER 2. DROPWISE ADDITIVE MANUFACTURING PROCESS FOR MELT BASED PHARMACEUTICAL PRODUCTS.....	8
2.1 Introduction	8
2.2 Dropwise Additive Manufacturing Process Description.....	12
2.2.1 Formulation Selection.....	17
2.2.2 Control of Operating Temperature	19
2.2.3 Drop Formation	20
2.2.4 Drop Monitoring and Deposition.....	25
2.2.5 Substrate Selection.....	27
2.2.6 Control of Substrate Conditions	28

	Page
2.2.7 Confirmation of Solid-State Form	28
2.2.8 Postprocessing	29
2.3 Materials and Methods for the Analysis of Melt Based Drug Products.....	29
2.3.1 Materials and Formulation Preparation	29
2.3.1.1 Film Preparation	30
2.3.2 Methodology.....	30
2.3.2.1 Hot Stage Microscopy Experiments	31
2.3.2.2 High Performance Liquid Chromatography Experiments.....	31
2.3.2.3 Reproducibility of Dosage Amounts	32
2.3.2.4 Dissolution Testing.....	32
2.3.2.5 X-ray Diffraction	33
2.4 Analysis of Melt-Based Dosage Forms.....	33
2.4.1 Reproducibility of Dosage Forms.....	35
2.4.2 Dissolution Testing.....	36
2.4.3 Effect of Formulation on Dissolution	38
2.5 Conclusions	42
CHAPTER 3. REAL TIME PROCESS MANAGEMENT STRATEGY FOR DROPSWISE ADDITIVE MANUFACTURING OF PHARMACEUTICALS.....	44
3.1 Introduction	44
3.2 Development of a Real Time Process Management Strategy	46
3.3 Automation.....	48
3.3.1 Program Inputs.....	50

	Page
3.3.2 Program Outputs	54
3.3.3 System Performance	56
3.4 Feedback Control	57
3.4.1 Process Temperature Control	59
3.4.1.1 Reservoir Temperature Control:	60
3.4.1.2 Pump Temperature Control:	61
3.4.1.3 Tubing and Nozzle Temperature Control:	61
3.4.2 Product Temperature Control	61
3.5 Online Monitoring Strategy	65
3.5.1 Image Acquisition.....	66
3.5.2 Volume Calculation.....	67
3.6 Conclusions	68
CHAPTER 4. A KNOWLEDGE PROVENANCE MANAGEMENT SYSTEM FOR DAMPP	70
4.1 Introduction	70
4.2 DAMPP Test Bed Operation.....	71
4.3 KProMS System.....	73
4.3.1 Using KProMS.....	73
4.3.2 Management of the DAMPP Test Bed	76
4.4 Data Extraction and Analysis	77
4.4.1 Operating Regime Determination.....	82
4.4.1.1 Operating Regime Based on Dimensionless Numbers.....	82

	Page
4.4.1.2 Operating Regime Based on Printing Parameters	85
4.5 Conclusions	89
CHAPTER 5. SUPERVISORY CONTROL OF DAMPP: EFFECT OF CRITICAL PROCESS PARAMETERS ON PRODUCT QUALITY OF MELT-BASED SOLID ORAL DOSAGES	91
5.1 Introduction	91
5.2 Supervisory Control Framework	92
5.3 Production of Dosage Forms with Different Critical Process Parameters	93
5.4 Analysis of Melt Based Solid Oral Dosages	95
5.4.1 Raman Microscopy: Crystallinity Study	95
5.4.2 Raman Mapping: Distribution of API throughout the Drop	97
5.5 Effect of Crystallization Temperature Control on Product Solid State	97
5.6 Effect of Critical Process Parameters on the Dissolution of Dosage Forms	102
5.7 Conclusions	108
CHAPTER 6. PROCESS CONTROL OF THE DROPWISE ADDITIVE MANUFACTURING SYSTEM USING POLYNOMIAL CHAOS EXPANSION BASED SURROGATE MODEL	110
6.1 Introduction	110
6.2 Process Control Strategy	111
6.2.1 Surrogate Model-based Hierarchical Control System	112
6.3 Polynomial Chaos Expansion Based Surrogate Model Development	113
6.4 Surrogate Model Based Optimization of Temperature Profiles	124

	Page
6.5 Conclusions	129
CHAPTER 7. MODELLING OF CRYSTALLIZATION OF MELT-BASED SOLID ORAL DRUG FORMS	130
7.1 Introduction	130
7.2 Crystallization Model Development	131
7.3 Determination of Kinetic Parameters	134
7.3.1 Induction Time.....	134
7.3.2 Nucleation Rate	135
7.3.3 Growth Rate.....	136
7.4 Crystallization Modelling Results and Discussion.....	138
7.5 Conclusions	141
CHAPTER 8. AMORPHOUS AND SELF-EMULSIFYING MELT-BASED SOLID ORAL DOSAGE FORMS.....	142
8.1 Introduction	142
8.1.1 Amorphous Drug Formulations.....	143
8.1.2 Self-Emulsifying Drug Delivery Systems	143
8.2 Investigation of Amorphous and Self-Emulsifying Drug Delivery Systems for DAMPP.....	144
8.3 Materials and Methods	148
8.3.1 Materials and Formulation.....	148
8.3.1.1 Film Preparation	149
8.3.2 Methodology.....	149

	Page
8.3.2.1 Reproducibility of Dosage Amounts	149
8.3.2.2 Raman Microscopy.....	150
8.3.2.3 X-ray Diffraction	150
8.3.2.4 Nanoparticle Tracking Analysis	151
8.3.2.5 Dissolution Testing and High Performance Liquid Chromatography Analysis	151
8.4 Results and Discussion.....	152
8.4.1 Reproducibility of Dosage Forms.....	152
8.4.2 Solid-State Analysis.....	153
8.4.3 Analysis of the Self-Emulsifying Drug Delivery System.....	156
8.4.4 Dissolution Testing.....	157
8.5 Conclusions	159
CHAPTER 9. FUTURE DIRECTIONS	161
9.1 Process.....	161
9.2 Process Monitoring and Control	163
9.3 Products	165
REFERENCES	167
APPENDICES	
Appendix A LabVIEW Flowsheets	177
Appendix B MATLAB Codes	204
VITA	209
PUBLICATIONS.....	211

LIST OF TABLES

Table	Page
Table 2.1 Nozzle sizes	25
Table 2.2 Reproducibility analysis of dosage forms.....	36
Table 3.1 Critical quality attributes and critical process parameters	46
Table 3.2 Process performance for different formulations	57
Table 4.1 Fluid properties for solvent-based formulations.....	82
Table 4.2 Dimensionless number calculations for solvent-based formulation Naproxen-PVPK90 (30:70).....	84
Table 4.3 Operating regime data for PEG:NAP (85:15) with nozzle N19 and workflow ID: 382.....	87
Table 5.1 Reproducibility analysis of dosage forms.....	95
Table 5.2 Induction points when different temperature profiles are applied	100
Table 6.1 Single input, multiple input, single output parameters for PCE based model development.....	122
Table 6.2 Mean square error of estimation (MSEE) and prediction (MSEP) values for single input (1-1) and multiple input (5-1) PCE based models	122
Table 7.1 Calculated and experimental solidification times under different cooling rates	139

Table	Page
Table 8.1 Lipid-based excipients used in DAMPP system and their properties.....	145
Table 8.2 Reproducibility of SEDDS	152

LIST OF FIGURES

Figure	Page
Figure 2.1 Dropwise additive manufacturing process for pharmaceuticals (DAMPP)	13
Figure 2.2 Dropwise additive manufacturing system (1: material reservoir, 2: precision P/D pump, 3: nozzle, 4: camera, 5: substrate, 6: xy-stage and the dotted box: online imaging system)	14
Figure 2.3 Process schematic of DAMPP	16
Figure 2.4 Critical cooling rates to avoid crystallization [31]	18
Figure 2.5 Piezoelectric DoD drop formation, modified from [39].....	22
Figure 2.6 Printable fluid properties for Newtonian fluids [24]	24
Figure 2.7 Images of PEG 3350 drops printed with DAMPP	26
Figure 2.8 Melt-based formulations during deposition on a. polymeric films b. placebo tablets	27
Figure 2.9 Dosage forms containing Naproxen/PEG 3350 formulation deposited on a. inert tablets b. HPMC film.....	34
Figure 2.10 Phase Diagram of Naproxen / Pluronic F38.....	35
Figure 2.11 Dissolution profiles of dosage forms created with different number of drops of the formulation containing PEG 3350.....	37

Figure	Page
Figure 2.12 Dissolution profiles of dosage forms created with different number of drops of the formulation containing Pluronic F38.....	38
Figure 2.13 Effect of formulation (PEG 3350 vs Pluronic F38) on the dissolution of dosage forms consisting of large drops.....	39
Figure 2.14 Effect of formulation (PEG 3350 vs Pluronic F38) on the dissolution of dosage forms consisting of small drops.....	40
Figure 2.15 XRD spectra of crystalline naproxen, PEG 3350, Pluronic F38, and physical mixtures of both formulations and resulting dosage forms.	41
Figure 3.1 RTPM strategy for DAMPP	47
Figure 3.2 The user interface of the LabVIEW- based automation program	49
Figure 3.3 Input file in CSV format.....	53
Figure 3.4 Automation process of DAMPP	54
Figure 3.5 Output file in CSV format.....	56
Figure 3.6 Boustrophedon movement path.....	57
Figure 3.7 Points of temperature control in DAMPP process	59
Figure 3.8 Labview program for product temperature control	64
Figure 3.9 Design program for product temperature setpoint profile.....	65
Figure 3.10 Images of non-uniform drops	67
Figure 4.1.a DAMPP system workflow, b. Data entry form for TB3Basic workflow, c. Data entry form for Material Source R1, d. Data entry form for IVEK pump setup task	75
Figure 4.2 Integration of KProMS and the DAMPP test bed	77
Figure 4.3 Scientific workflow for drawing plots.....	78

Figure	Page
Figure 4.4 Data selection through SelectData node.....	79
Figure 4.5 a. Drop number vs drop volume for instances 255-260, Basic statistics results for instances b. 255-257 and c. 258-260.....	81
Figure 4.6 Operating regime graph for solvent formulation Naproxen-PVPK90 (30:70)	85
Figure 4.7 Drop specification criteria.....	86
Figure 4.8 Workflow for determining the operating regime.....	86
Figure 4.9 Operating region plot.....	89
Figure 5.1 Supervisory control framework for DAMPP. TC: temperature controller, TT: temperature transmitter.	93
Figure 5.2 Raman spectra of a. pure NAP, b. pure PEG 3350, c. co-melt of NAP-PEG 3350 (15:85). Characteristic peaks at 760 and 1280 cm ⁻¹ are shown with red and blue arrows, respectively.	96
Figure 5.3 Raman map of melt-based deposits of NAP-PEG 3350 (15:85). Map Area 600 μm x 1000 μm.....	98
Figure 5.4 Temperature profiles applied on the substrate.....	99
Figure 5.5 Optical microscopy images of melt-based deposits (Naproxen-PEG 3350) after a. fast cooling, b. slow cooling, c. cycling.....	101
Figure 5.6 Effect of different cooling profiles on the dissolution of the dosage forms created with small drops.	103
Figure 5.7 Effect of different cooling profiles on the dissolution of the dosage forms created with small drops.	104

Figure	Page
Figure 5.8 Dissolution profiles of the dosage forms created with two different drop sizes and solidified at different temperature profiles: a. constant temperature, b. fast cooling, c. slow cooling, d. cycling.	105
Figure 5.9 Infrared camera image of melt-based deposits solidifying at room temperature	106
Figure 6.1 Process control strategy for DAMPP	112
Figure 6.2 PCE based surrogate model development	117
Figure 6.3 Input-output pairs for (1-1) and (5-1) PCE-based surrogate models.....	118
Figure 6.4 Crystallization temperature profiles used in the PCE model development...	121
Figure 6.5 Performance of 1 st order PCE model with validation and prediction for a. single input single output (1-1), b. multiple input single output (5-1) cases. Exp data: experimental data points used in PCE development, PCE: model validation points, Actual: the experimental time constant, which is predicted using the PCE model, Simulated: the model prediction	123
Figure 6.6 Optimized temperature profiles using (1-1) and (5-1) PCE models vs. the actual temperature profiles.....	126
Figure 6.7 Hierarchical temperature control strategy	128
Figure 7.1 Nucleation kinetics for different cooling rates	135
Figure 7.2 Optical microscopy images used for growth rate estimation with cooling rate 1°C/min	136
Figure 7.3 Optical microscopy images used for growth rate estimation with cooling rate 10°C/min	137

Figure	Page
Figure 7.4 Growth kinetics for different cooling rates	138
Figure 7.5 Solid percentages of the dosage forms using the developed crystallization model.....	139
Figure 7.6 Crystallization model results for mean crystal radius vs cooling rate.....	140
Figure 8.1 Hydrophilic – Lipophilic Balance (HLB) scale [89].....	146
Figure 8.2 Online drop images.....	153
Figure 8.3 Raman spectras of SEDDS formulation, pure gelucire 44/14 and pure crystalline celecoxib.....	154
Figure 8.4 Raman spectras of amorphous and crystalline celecoxib. Modified from Andrews, et al. (2010) [91].....	155
Figure 8.5 XRD spectra of crystalline celecoxib, pure gelucire 44/14 and SEDDS Formulation with 10% celecoxib and 90% gelucire 44/14.....	156
Figure 8.6 Size distribution profiles and particle images for SEDDSs.....	157
Figure 8.7 Dissolution of celecoxib found in SEEDS formulation and crystalline celecoxib	159
Appendix Figure	
Figure A.1 Reading the input information from the Intermediate file generated by KProMS	178
Figure A.2 Connecting to temperature controller visa ports.....	179
Figure A.3 Setting the substrate temperature controller to heating mode	180
Figure A.4 Turning the substrate temperature controller on.....	180

Appendix Figure	Page
Figure A.5 Setting the substrate temperature controller high operating temperature to 60 °C	180
Figure A.6 Setting the substrate temperature controller low operating temperature to 0 °C	181
Figure A.7 Turning the substrate temperature controller alarm on	181
Figure A.8 Setting the setpoint temperature for substrate temperature controller.....	181
Figure A.9 Setting the substrate temperature controller high alarm 20 °C above the setpoint temperature.....	182
Figure A.10 Setting the substrate temperature controller low alarm at 0 °C.....	182
Figure A.11 Turning the reservoir temperature controller on.....	183
Figure A.12 Setting the reservoir temperature controller setpoint temperature	183
Figure A.13 Setting the reservoir temperature controller alarm low to 10°C lower than setpoint.....	184
Figure A.14 Setting the reservoir temperature controller alarm high to 10°C higher than setpoint.....	184
Figure A.15 Turning the tubing temperature controller on.....	185
Figure A.16 Setting the tubing temperature controller setpoint temperature	185
Figure A.17 Setting the tubing temperature controller alarm low to 10°C lower than setpoint.....	186
Figure A.18 Setting the tubing temperature controller alarm high to 10°C higher than setpoint.....	186

Appendix Figure	Page
Figure A.19 Checking temperature range for reservoir and tubing controllers.....	187
Figure A.20 Checking temperature range for substrate temperature controllers.....	188
Figure A.21 Generating the output file, pulling up printing settings and connecting to pump and staging controllers	190
Figure A.22 Turn staging motor for x-direction on	191
Figure A.23 Turn staging motor for y-direction on	191
Figure A.24 Setting pump to move in forward direction.....	192
Figure A.25 Moving staging to home position in x-direction	192
Figure A.26 Moving staging to home position in y-direction	193
Figure A.27 Logic loops for boustrophedon stage movement.....	193
Figure A.28 Depositing drop	194
Figure A.29 Saving x-position on stage.....	194
Figure A.30 Saving y-position on stage.....	195
Figure A.31 True: Continue printing in the same row	195
Figure A.32 False: Move to next row y	196
Figure A.33 Read and record temperatures of tubing, reservoir and substrate and substrate power output	196
Figure A.34 Record output values for no temperature control	197
Figure A.35 Saving positions and temperatures to file.....	197
Figure A.36 Connect to camera	198
Figure A.37 Image processing code.....	199
Figure A.38 Merge drop deposition and camera files to the output file.....	200

Appendix Figure	Page
Figure A.39 Stop program after drop cycle is finished.....	200
Figure A.40 Connecting to the substrate temperature controller and generating output file	202
Figure A.41 Executing designed temperature profiles via substrate temperature control program and saving the time series data	203

ABSTRACT

İçten, Elçin. Ph.D., Purdue University, May 2016. Manufacture of Individualized Dosing: Development and Control of a Dropwise Additive Manufacturing Process for Melt Based Pharmaceutical Products. Major Professors: Zoltan K. Nagy and Gintaras V. Reklaitis.

The improvements in healthcare systems and the advent of precision medicine initiative have created the need to develop more innovative manufacturing methods for the delivery of individualized dosing and personalized treatments. In recent years, the US Food and Drug Administration (FDA) introduced the Quality by Design (QbD) and Process Analytical Technology (PAT) guidelines to encourage innovation and efficiency in pharmaceutical development, manufacturing and quality assurance. As a result of emerging technologies and encouragement from the regulatory authorities, the pharmaceutical industry has begun to develop more efficient production systems with more intensive use of on-line measurement and sensing, real time quality control and process control tools, which offer the potential for reduced variability, increased flexibility and efficiency, and improved product quality.

In accordance with the changes observed in health care systems towards more innovative personalized therapies, this dissertation presents a novel technology for small scale, distributed manufacturing of individualized dosing. A dropwise additive manufacturing process for melt-based solid oral drug production is developed, which utilizes the drop-

on-demand (DoD) printing technology for predictable and highly controllable deposition of active pharmaceutical ingredients (API) onto an edible substrate, such as a polymeric film or placebo tablet. This manufacturing method has tremendous potential in individualized dosing because through a combination of drop size and number of drops, the dosage can be precisely and reliably controlled to match the prescribed amount for a patient.

The real-time process management (RTPM) strategy is developed for the dropwise additive manufacturing of pharmaceutical products (DAMPP). The automation program assures synchronous operation of process units, while monitoring process parameters and maintaining process control. The automation program is integrated with the Knowledge Provenance Management System (KProMS) to record and make accessible the data provenance of each and every dosage produced via DAMPP.

For the dropwise additive manufacturing system, the critical process parameters (CPP) are controlled to achieve the desired critical quality attributes (CQA) of the dosage forms. The effect of the CPPs on the final drug property is investigated and it is shown that implementation of a supervisory control system on the process is essential for producing individual dosage forms with the desired CQAs. A polynomial chaos expansion based surrogate model is developed to predict the dissolution profile of the solidified drug deposition given the temperature profile applied on the substrate. Using this model, a hierarchical control system is implemented by monitoring the drop size on-line and predicting a temperature profile to achieve the desired dissolution profile for the dosage

forms created. The process control strategy effectively mitigates variations in the dissolution profiles due to variable dosage amounts, hence enabling the application of the DoD system for the production of individualized dosage regimens.

A crystallization model based on non-isothermal Avrami kinetic equation is developed for the cooling temperature dependent solid-state transformation of the melt-based solid oral dosages produced using the dropwise additive manufacturing process. This model increases the understanding of solidification and crystallization processes from undercooled melts. Using the proposed model, the effect of temperature profiles leading to differences in solid-state parameters such as the mean size can be investigated.

The DAMPP process is a viable method for on-demand production of various formulations. Melt-based dosage forms containing crystalline API and self-emulsifying drug delivery systems with amorphous API forms are produced and analyzed to demonstrate reproducibility of dosages and their dissolution behaviors.

The prototype system offers great promise as a tool for advancing personalized medicine by allowing the precise production of convenient solid oral dosages tailored to the patient on site at hospitals, clinics and even pharmacies. Future directions are suggested to further advance dropwise additive manufacturing of pharmaceutical products and lead to commercialization of this technology.

CHAPTER 1. INTRODUCTION

1.1 Introduction

The average life expectancy has increased dramatically during the 20th century. The ceaseless improvement in human health care systems consisting of the development of new treatments and the increasing accessibility to medicine has a significant effect on this achievement. Nevertheless, medicine still targets therapy to the broadest patient population that might possibly benefit from it, and it relies on statistical analysis of this population's response for predicting therapeutic outcome in individual patients [1]. Therapists make decisions both about the choice of drug and appropriate dosage based on information derived from population averages. Worldwide use of these drugs has revealed substantial interindividual differences in therapeutic response [1]. With the recent developments in pharmacology and genomics, this "one drug fits all" approach is evolving into a personalized approach to therapy [1]–[3]. It is paving the way towards future health care systems, which was also recently announced in the precision medicine initiative [4]. Personalized therapy is defined as therapy with the right drug at the right dose for the right patient, which implies the delivery of personalized medicine and individualized dosing [1]–[3], [5].

As health care systems keep improving not only discovery of new drugs and therapies but also development of innovative drug delivery and production methods become crucial. The current level of innovation in dosage form design and drug product manufacturing cannot meet the needs of personalized therapies [6]. While innovation is the key to success within the pharmaceutical industry, it has been largely sought through new drug discovery and development, while the development of new manufacturing methods has received inadequate attention. Traditionally the pharmaceutical industry has manufactured its products in large scale batch processes with nonexistent or limited on-line process monitoring and control. In recent years, the US Food and Drug Administration (FDA) introduced the Quality by Design (QbD) approach and Process Analytical Technology (PAT) guidance to encourage innovation and efficiency in pharmaceutical development, manufacturing and quality assurance [7]. As a result of encouragement from the regulatory authorities, the advent of globalization and the increasing awareness of environmental impact, the pharmaceutical industry has been reconsidering the way drug products are developed and manufactured [8], [9].

Thus, in accordance with the changes observed in health care systems towards more innovative personalized therapies, this dissertation focuses on the manufacture of individualized dosing by developing a dropwise additive manufacturing process for melt-based solid oral drug production. A novel manufacturing technology based on drop-on-demand printing is presented for small scale, distributed manufacturing of drug dosage, which enables cost-effective production of individualized dosing. This manufacturing method has tremendous potential in individualized dosing because through a combination

of drop size and number of drops, the dosage can be precisely and reliably controlled to match the prescribed amount for a patient. In addition, the ‘batch size’ can be as small as the number of tablets or drops required for one patient and the transitions from one dose to another made with minimal or no waste in very short time. The dropwise additive manufacturing system offers great promise as a tool for advancing personalized therapies by allowing the precise production of convenient solid oral dosages tailored to the patient on site at hospitals, clinics and even pharmacies.

1.2 Project Motivation

Accessibility to medicine designed for exclusive therapeutic needs of individual patients will be a tremendous achievement for the healthcare system. The research project aims to solve the challenge of manufacture of individualized dosing by the development and control of a dropwise additive manufacturing process for pharmaceutical products (DAMPP). As a part of the National Science Foundation supported Engineering Research Center for Structured Organic Particulate System (C-SOPS), a prototype system for DAMPP is developed, which uses the drop on demand (DoD) technology. The main advantages of using DoD technology for drug printing are the ability to produce small droplets of controlled sizes and to produce these drops with high placement accuracy onto selected substrates [10]. By changing the drop size and the composition of the formulation, the dosage amount can be tailored according to the patient’s needs.

C-SOPS focuses on advancing the scientific foundation and developing methodologies for the active control and manufacturing of pharmaceutical products and brings together a

multi-disciplinary team of engineers, scientists and industry leaders to improve pharmaceutical production processes [11]. C-SOPS supports the development of three test beds, which are TB1: Continuous Manufacturing of Tablets, TB2: Strip Films for Controlled Substance Delivery and TB3: Mini-Manufacturing using Drop-on-Demand Technology. The DAMPP process corresponds to TB3.

1.3 Research Objectives

The major focus of the research work is the development of the dropwise additive manufacturing process for pharmaceutical products. The advancement of the system to process melt-based dosage forms requires an assembly of various scientific and engineering principles including drop dynamics, heat transfer, automation, process control, data management, process analytics and pharmaceutical sciences. Here, a real time process management strategy is crucial to enable the application of this system for the production of dosage forms with the desired quality attributes matching individualized dosage regimens. Establishing automation and process control of the system, monitoring important process parameters online and managing process data are essential elements of a meticulous real time process management strategy. While developing a process to manufacture pharmaceutical dosage forms, the process parameters should be precisely controlled to reach the final product quality attributes. Therefore important quality attributes need to be identified and their relationship to quality attributes need to be modelled. Another objective is to demonstrate that the process can utilize various pharmaceutical formulations and to characterize the resulting dosage forms with various methods.

1.4 Thesis Overview

Chapter 2 presents dropwise additive manufacturing of pharmaceutical products for melt-based dosage forms. This chapter discusses the rationale for developing the drop-on-demand process for pharmaceutical applications and implementation of the DoD system for different pharmaceutical formulations with an emphasis on melt-based drug systems.

Chapter 3 describes the real time process management (RTPM) strategy developed for dropwise additive manufacturing of pharmaceutical products. The RTPM strategy consists of automation, online monitoring and process control. It is successful in controlling deposition of either solvent-based or melt-based dosage forms and ensures that every dosage unit meets quality specifications. It controls process and product temperature and monitors each drop visually. It records data pertinent to each deposited drop, determines the drop volume and thus API amount deposited, and conducts analyses that can detect process faults.

Chapter 4 presents a workflow based knowledge provenance management system, KProMS, developed for DAMPP. DAMPP requires and generates a range of data types, including camera and IR images, spectra and numerical parameter values, both of real time and off-line nature. KProMS is integrated with the automation program and captures relationships between the processing steps and material and information flows, and data input and output generated by DAMPP. Thus a complete data provenance is recorded for each dose produced.

In Chapter 5, a supervisory control system is presented, that is designed to ensure reproducible production of high quality of melt-based solid oral dosages. This control system enables the production of individual dosage forms with the desired critical quality attributes by monitoring and controlling critical process parameters. The effects of these process parameters on the final product quality are investigated and the properties of the produced dosage forms are characterized using various techniques.

Chapter 6 describes a process control framework for DAMPP to produce individual dosage forms with the desired critical quality attributes, including formulation composition, drop size, deposit morphology and dissolution performance. In order to achieve desired product morphology, a surrogate model based on polynomial chaos expansion is developed to relate the critical process parameters to deposit morphology using dissolution data of the active pharmaceutical ingredient. The proposed process control strategy can effectively mitigate variations in the dissolution profiles due to variable dosage amounts and enable the application of the DoD system for the production of individualized dosage regimens.

In Chapter 7, a model based on non-isothermal Avrami kinetic equation is developed to model the solidification and crystallization processes of the drug deposits under different cooling profiles using temperature dependent crystallization kinetics. Using the proposed model, the temperature profiles leading to the desired solid-state parameters such as the minimum mean size are determined.

In Chapter 8, dropwise additive manufacturing of amorphous and self-emulsifying melt-based solid oral dosage forms is demonstrated for improved oral delivery of lipophilic drugs. Different lipid carriers are investigated to increase the bioavailability of poorly water soluble drugs. The produced dosage forms are analyzed with various techniques.

Chapter 9 talks about future directions and suggested studies to further advance the drop on demand manufacturing system.

CHAPTER 2. DROPWISE ADDITIVE MANUFACTURING PROCESS FOR MELT BASED PHARMACEUTICAL PRODUCTS*

2.1 Introduction

The large-scale batch processing mode which the pharmaceutical industry has traditionally used to manufacture pharmaceutical products provides significant challenges, including high production costs, long manufacturing times, scale-up difficulties and recurring quality issues [12]. The increasing competition and payer pressures are driving the pharmaceutical industry to deliver drug products in shorter time and lower cost [13]. The US Food and Drug Administration (FDA) has promoted the Quality by Design (QbD) approach to increase process understanding and improve quality and efficiency while minimizing risk [14]. The Process Analytical Technology (PAT) guidance introduced by the FDA encouraged the monitoring of critical quality and performance attributes during processing with the goal of ensuring final product quality [7], [15].

As part of this renewed emphasis on improvement of manufacturing, the pharmaceutical industry has begun to shift towards continuous processing and to develop more efficient production systems with more intensive use of on-line measurement and sensing, real

* This chapter is based on: E. İçten, A. Giridhar, L. S. Taylor, Z. K. Nagy, and G. V. Reklaitis, "Dropwise Additive Manufacturing of Pharmaceutical Products for Melt-Based Dosage Forms.," *Journal of Pharmaceutical Sciences*, vol. 104, no. 5, pp. 1641–1649, 2015[19].

time quality control and process control tools, which offer the potential for reduced production costs, faster product release, reduced variability, increased flexibility and efficiency, and improved product quality [13], [16], [17].

This chapter presents a dropwise additive manufacturing process for pharmaceutical products (DAMPP) as an alternative to conventional methods. The process utilizes the drop-on-demand (DoD) printing technology for predictable and highly controllable deposition of active pharmaceutical ingredients (API) onto an edible substrate, such as a polymeric film or placebo tablet [18], [19]. This process uses fluid operations suitable for low volume production of personalized dosage forms.

The main advantages of using DoD technology for drug printing are the ability to produce small droplets of controlled sizes and to produce these drops with high placement accuracy onto selected substrates [10]. The advantages of liquid processing and reproducible production of small droplets create the special opportunity for the production of high potency, low dose drugs, which are difficult to produce with consistent quality via conventional powder processing methods. By changing the drop size and the composition of the formulation, the dosage amount can be adjusted according to the patient's needs. The ability to adjust the dosage amount according to patient's needs and layering of multiple drugs enable the process to produce individualized dosage products. For most drugs, a "one dose fits all" or standardized dosage regimen is recommended for patients regardless of their age, sex, or other physiologic factors [20]. Standardized dosing is preferred because it simplifies the

production/packaging processes, the associated product supply chain and the prescription of the drug by physicians [21].

However, given that interpatient variability in pharmacologic response can be large due to pharmacokinetic (PK) and pharmacodynamics (PD) differences, a “one dose fits all” approach may result in ineffective or excessive dosing [21]. Any given drug can be therapeutic in some individuals but ineffective in others, and some individuals experience adverse drug effects whereas others are unaffected [1]. It has been reported that optimization-based methods, which use PK-PD models with parameter distributions determined from population clinical data together with a limited number of plasma samples from a specific patient, can effectively predict a regimen that has the highest probability of meeting the therapeutic needs of that patient [22]. Thus the dosage regimen can be individualized to the patient and the DAMPP process can be employed to produce that predicted dose in a clinic or a pharmacy. This would change the supply chain structure of the industry from mass production of multiple dosages for each drug to bulk production of the formulation for that drug with the actual dosage produced on demand at distributed sites. Of course, the DoD technology can also be employed for commercial scale production of drug products, as is the case with GlaxoSmithKline’s Liquid Dispensing Technology© since DoD can produce multiple drops per second and can be scaled up further by using multiple nozzles [23].

The high placement accuracy of DoD also enables the production of multi-layered dosage forms which is a promising application since increasing number of treatment regimens

involve a cocktail of different drugs (e.g., HIV-AIDS, a number of cardiovascular conditions and most cancer treatments). The manufacturing of multiple drugs of the cocktail into a single tablet or capsule is an accepted strategy for mitigating one of the key related problems in medical practice: assurance of patient compliance.

Although different material systems with a wide range of properties can be deposited using DoD technology [24], until recently a limited range of materials have been used in the pharmaceutical drug printing applications, namely, solvent or nano-suspension based formulations [25], [26]. Using the developed dropwise additive manufacturing process for pharmaceuticals (DAMPP), different drug formulations including solvent based systems, i.e. solvent-polymer-API solutions, as well as melt based systems, i.e. polymer-API melts, can be printed. Recently, Hirshfield et al. (2014) and Icten et al. (2015), reported proof of concept of dropwise additive manufacturing process for solvent-based applications and for melt-based applications, respectively. Melt-based printing applications eliminate the solvent evaporation step after drop deposition and thus allow on demand production of individual dosage forms with good control of drug solid state and morphology.

In this chapter, the DAMPP process for melt-based dosage forms is discussed. First a detailed process description is presented, which is followed by the scientific and engineering principles of the manufacturing steps including formulation selection, control of operating temperature, drop formation, drop monitoring and deposition, substrate selection and control of substrate conditions. Then the application of DAMPP for melt-

based pharmaceutical dosage forms is demonstrated with flexible use of different formulations, good reproducibility and dissolution profiles.

2.2 Dropwise Additive Manufacturing Process Description

The proto-type DAMPP process for solid oral drug products is shown in Figure 2.1. The process utilizes the DoD printing technology for predictable and highly controllable deposition of API onto an edible substrate, such as a polymeric film or placebo tablet, using a semi-continuous operation suitable for low volume production of personalized dosage forms.

The DAMPP system consists of a material reservoir, precision positive displacement pump, xy-staging, a hot air based heating system, online imaging and sensing, and temperature, pump and stage controllers. The material reservoir, pump, nozzle, camera, substrate and staging are labelled in Figure 2.2 with numbers 1 through 6, respectively. The first step of the process is formulation preparation where the API is dissolved in a solvent- or melt-based formulation. For the melt-based formulation, a low melting point polymer (or alternatively a lipid or surfactant) such as polyethylene glycol, in which the drug dissolves once the polymer becomes molten, is used. The prepared formulation is placed in the reservoir, and heated until the polymer melts and the drug dissolves in the molten polymer. Next, the fluid formulation is pumped through an IVEK Digispense 10 single-channel positive displacement pump with a custom controller (IVEK Corporation, North Springfield, Vermont), which allows for the adjustment of the drop size by changing the pump parameters.

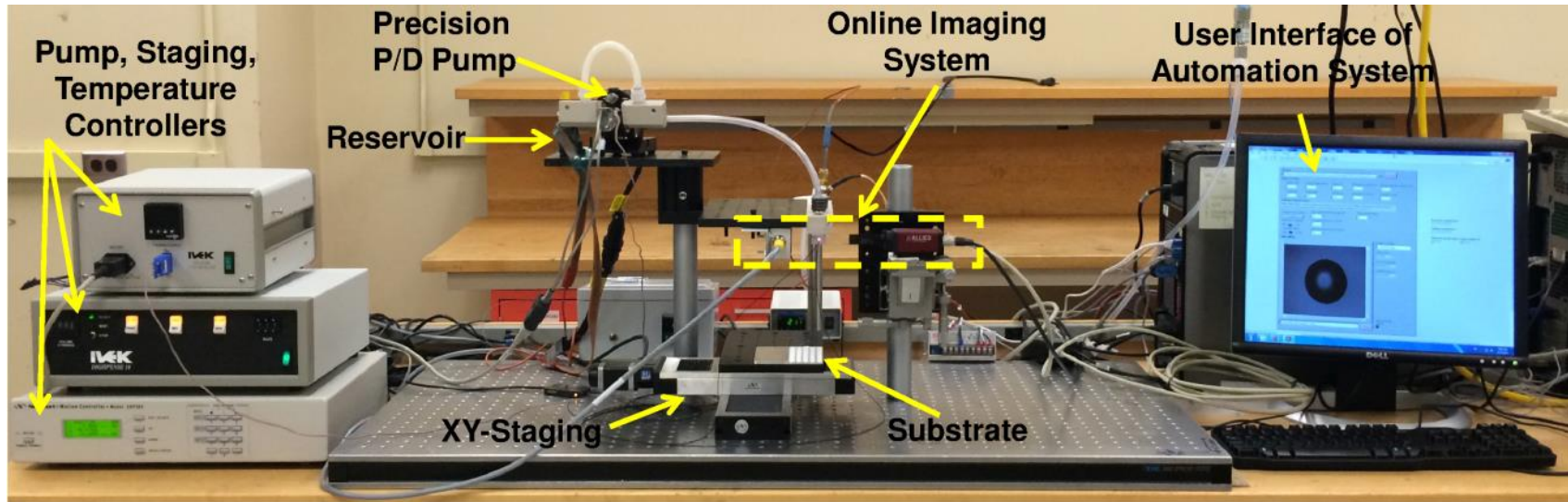


Figure 2.1 Dropwise additive manufacturing process for pharmaceuticals (DAMPP)

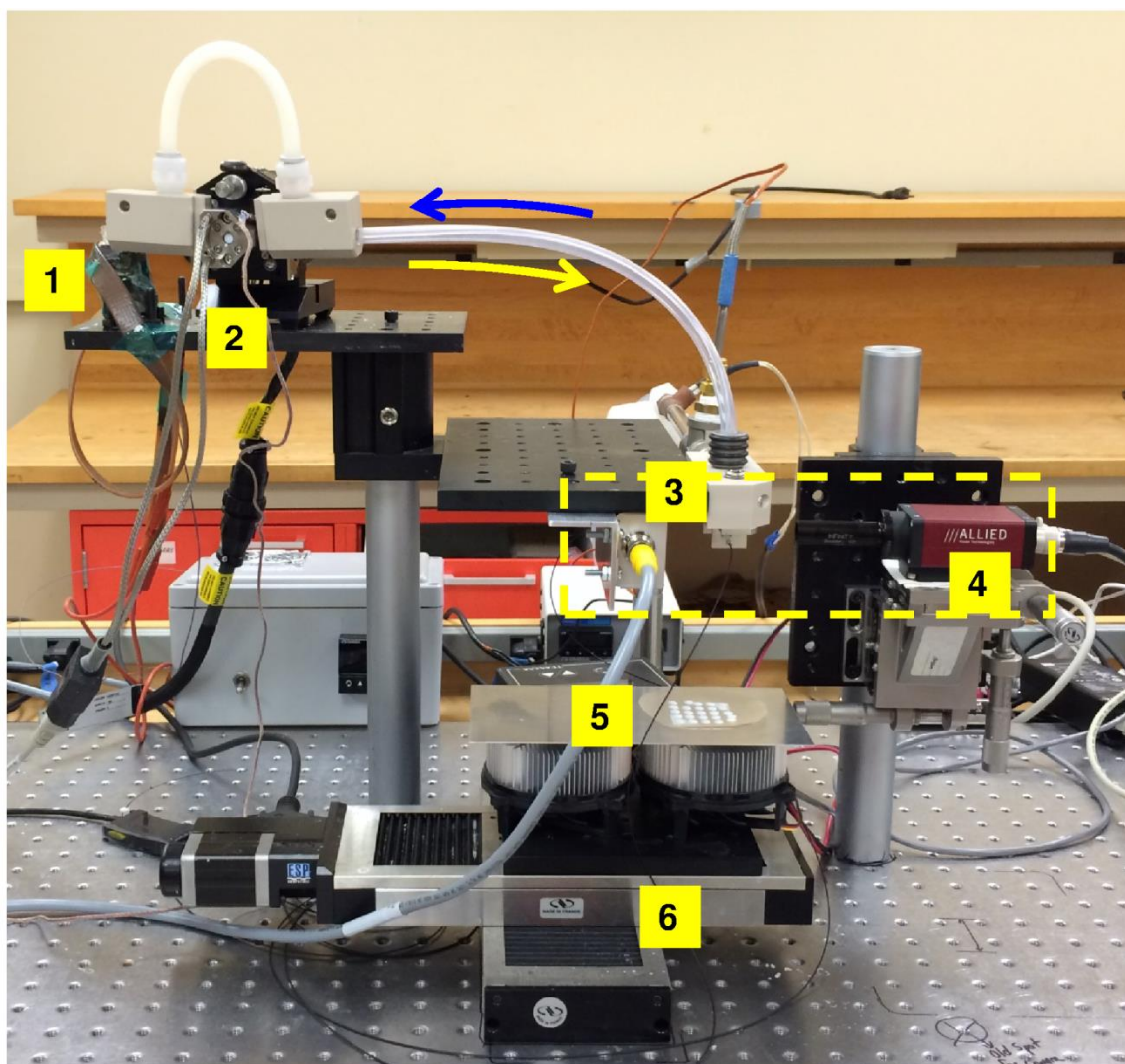


Figure 2.2 Dropwise additive manufacturing system (1: material reservoir, 2: precision P/D pump, 3: nozzle, 4: camera, 5: substrate, 6: xy-stage and the dotted box: online imaging system)

In order to maintain constant rheological properties of the printed formulation, temperature control is established on the whole process using hot air based heating system, a custom heater controller (IVEK Corporation, North Springfield, Vermont), and heating elements with PID controller units (Omega Engineering Inc., Stamford, Connecticut). After passing through the pump, the drops are ejected through a nozzle,

which can be of various internal diameter sizes as required by the specific formulation. An image of each drop is taken after it is ejected from the nozzle, while still on air, using a Manta camera with Banner motion sensors (Allied Vision Technologies, Exton, Pennsylvania). The size of each drop is monitored using real-time image analysis.

The drops deposit onto the substrate placed on the Newport ESP301 series xy staging controlled by the corresponding controller/driver unit (Newport Corporation, Irvin, California). The xy-staging and synchronization logic allows precise drop positioning on the substrate while printing. The temperature of the deposited drops is controlled indirectly by controlling the temperature of the substrate using a Peltier device with TC-48-20 PID controller (TE Technology, Traverse City, Michigan), which is placed on the xy-stage. This allows control of the rate of solidification of melts and thus control of nucleation and crystallization phenomena. Since the crystallization temperature profile has a strong effect on product solid state characteristics, influencing the dissolution properties and hence the bioavailability of the drug, precise control of the drop solidification process occurring on the substrate can be very important [27], [28]. The effect of controlled process parameters on the solid state and dissolution profiles of the dosage forms is further discussed in Chapter 5 [29].

The automation system of the process is developed using National Instruments' LabVIEW 2012. The synchronization logic allows execution of the pump, staging and temperature controllers and imaging system simultaneously. With this system, process data including the volume of each drop, the location on the substrate and temperature

values at various process units are recorded in a data management application, which serves as documentation for each dosage that is produced using the DAMPP [30]. The resulting validated documentation is an essential record of drug product quality. The details of the automation and data management systems for DAMPP are presented in Chapters 3 and 4.

Next, the details of the manufacturing steps for melt-based dosage forms are presented along with the scientific and engineering principles that are relevant to DAMPP. A detailed process schematic of DAMPP is shown in Figure 2.3.

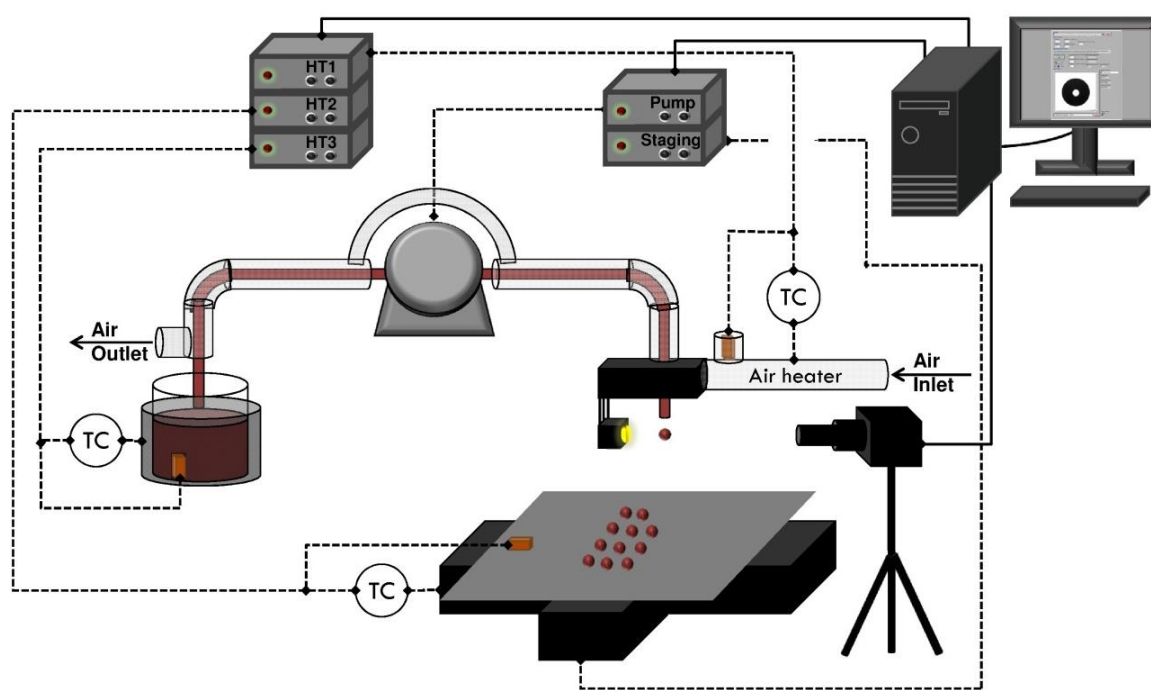


Figure 2.3 Process schematic of DAMPP

2.2.1 Formulation Selection

Using this process, different drug formulations including solvent-polymer-API systems and low melting point carrier-API systems, i.e. melts, can be used. The solvent-based formulation consists of an organic solvent, API and a polymer. The details for solvent-based formulations were studied by Hirshfield et al. (2014) [18]. The melt formulations consist of a low melting point carrier and an API, which are mixed and heated above the melting temperature of the mixture in order to produce hot-melts. Different carrier systems including low molecular weight polymers: PEG and Pluronic, surfactants: Gelucire and lipids: Compritol are studied. Depending on the desired final solid state form of the API, different carriers can be used in the formulation of solid dispersions. The key characteristics affecting the solid state form are the nucleation and crystallization growth rates of the API during melt cooling. Following Baird et al.[31], 2010, the crystallization tendency of organic molecules from undercooled melts can be grouped into three main classes, which are depicted in Figure 2.4. Class I molecules crystallize rapidly since they have fast nucleation and growth rates; class II molecules can either be crystalline or amorphous depending on the kinetics of the process relative to crystallization and nucleation kinetics; class III molecules stay amorphous when a nuclei free glass is prepared during cooling of the melts [31]. In addition to the crystallization cooling rates, selection of the polymer is an important factor in drug morphology, since the polymer may inhibit or promote crystallization of the drug [32], [33].

Polymers are added to the printing material not only to help control drug solid state properties, but also to establish formulation composition and material rheological

properties. Depending on the ratio of drug and polymer present in the formulation, the dosage amount can be adjusted. The material rheological properties of the formulation depend on the surface tension and viscosity values of different polymers used. Polymers or other carriers also have an effect on the bioavailability of the drug by enhancing the dissolution or by sustaining the release of the drug [34]–[36].

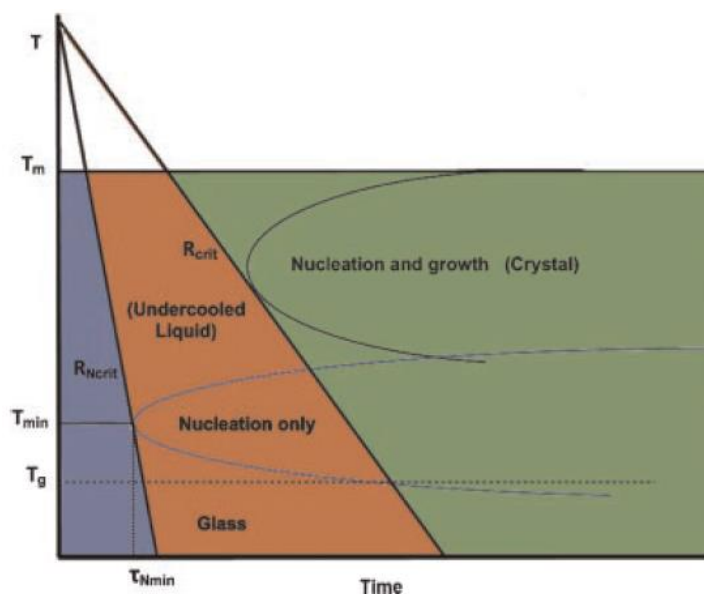


Figure 2.4 Critical cooling rates to avoid crystallization [31]

For the DAMPP process, polymers/carriers with low melting temperature (≤ 100 °C) and with low melt viscosity are preferred. The former is bounded by the operating temperature of the DAMPP system and the latter is a requirement for the printability of the melts. For instance, for hot melt extrusion, polyethylene glycol (PEG) with molecular weights of 1500-20000 are commonly used whereas for DAMPP process, PEGs at the

lower end of this bound are favorable since viscosity increases with an increase in the molecular weight [34].

Another limitation on the operating temperature is the stability of the drug used in the formulation. Although the API is not melted during DAMPP operation, the formulations are produced by dissolving the API in the molten carrier at relatively high temperatures (≤ 100 °C). Therefore stability of the drug products produced via DAMPP should be established and shelf life determined. Shelf-life is determined by testing samples for product attributes susceptible to change during storage and shipping, and likely to influence quality, safety and efficacy of the drug [37]. These include chemical attributes, e.g., pH, degradation; physical attributes, e.g., appearance, particle size; in vitro drug release, e.g., dissolution; and biological attributes, e.g., potency. Conventional drug products are tested for long term or accelerated storage conditions. Using the DAMPP system at distributed sites is envisioned to shorten the shelf-life of drug products. However a protocol for establishing stability of the drug products should be developed. Currently, for the dosage forms produced via DAMPP, the chemical stability of the API is verified using HPLC experiments and in vitro drug release is analyzed through dissolution testing.

2.2.2 Control of Operating Temperature

In order to produce melt-based dosage forms reproducibly, the complete system must be, maintained at suitable temperature, which is above the melting temperature of the formulation, below the potential degradation temperature of the drug substance and

within the desired operating limits of the equipment itself (≤ 100 °C). The printability and reproducibility of melt-based formulations depend on material properties of the fluid processed, especially viscosity and surface tension, which are generally highly dependent on temperature. Therefore temperature control on each process component, including reservoir, pump, tubing and nozzle, is implemented, as shown in Figure 2.3. The temperature of the fluid maintained in the reservoir and passing through the pump are controlled via the heating tape and the custom heater controller built in the pump, respectively. A concentric tube heat exchanger is designed to control the temperature of the tubing and the nozzle, where air is used as a heating medium. Air is heated by the custom air heater, which is connected to a proportional-integral-derivative (PID) temperature controller. The formulation material flows on the tube side, that is, inside the inner tube in the direction shown with the yellow arrow in Figure 2.2. The hot air flows on the shell side, that is, around the tubing and the nozzle in the countercurrent direction shown with the blue arrow in Figure 2.2. This structure prevents the melts from solidification inside the tubing and on the nozzle, and maintains the temperature at the desired set point.

2.2.3 Drop Formation

In the DAMPP system, the melt-based formulation contained in the reservoir is pumped through a DoD positive displacement pump. Drop on demand technology allows generation of individual drops by means of a pressure pulse upstream of the printing nozzle [24], [38]. Until the pressure pulse reaches a threshold value, the liquid will be held in place by the surface tension at the nozzle. Once the threshold value is exceeded a

drop is ejected [24]. By adjusting the pressure pulse used to form the drops, the drop size can be controlled within a defined range [24]. Different DoD printing methods, including thermal, piezoelectric or positive displacement pump can be used to generate the pressure pulse required for drop formation. In the DAMPP, the precision pump is connected to a custom controller that allows for variations in printing parameters such as the RPM, i.e. the speed of the piston rotation within the cylinder, and volume strokes, i.e. how many times the piston rotates within the cylinder in the pump per trigger. Besides the RPM and volume stroke, the displacement on the pump can also be used to adjust the size of drops generated.

Drop formation using DOD technology has the characteristic stages as seen in Figure 2.5. The first four images of Figure 2.5 exhibit ejection and stretching of the fluid. Once the fluid in the nozzle is pushed out of the nozzle, the meniscus extends outward and a liquid column is formed. After this step, the flow rate of the fluid decreases. Necking and pinch-off steps of the fluid are shown in images 5 to 9. The fluid at the nozzle exit necks and the radius of liquid thread continues to get thinner. Due to the high pressure in the tail, the surface contracts in order to decrease the surface energy, and the tail of the drop starts to recoil towards the head of the drop. The recoil step is displayed in images 10 to 12. The fluid thread continues to shrink and a second neck forms, through images 13 to 16. It breaks up into a primary and a satellite drop. In different conditions, the satellite drop can break up into more than one drop. In images 17 to 20, the satellite and primary drops merge to form a larger drop. Then the excessive surface energy is transformed into oscillatory kinetic energy and an equilibrium stage is reached [39].

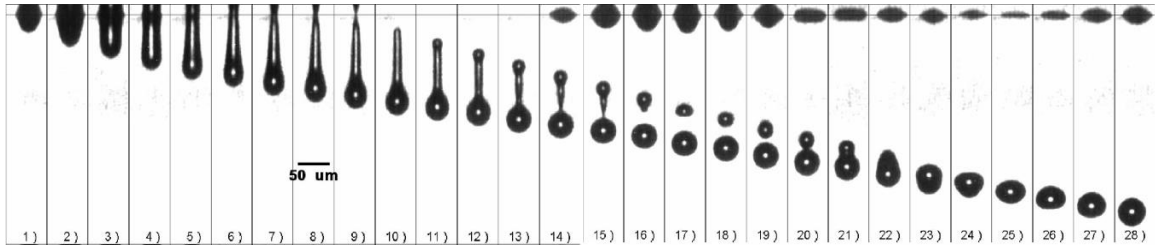


Figure 2.5 Piezoelectric DoD drop formation, modified from [39].

Drop dynamics is also known to be strongly influenced by surface tension and viscosity and can be characterized by dimensionless quantities, such as the Reynolds (Re), Weber (We), Ohnesorge (Oh) numbers, which are shown in Equations 2.1 to 2.3 [24], [38].

$$\text{Re} = \frac{v\rho d}{\mu} \quad \text{Eq. 2.1}$$

$$\text{We} = \frac{v^2\rho d}{\sigma} \quad \text{Eq. 2.2}$$

$$\text{Oh} = \frac{\mu}{\sqrt{\rho d \sigma}} = \frac{\sqrt{\text{We}}}{\text{Re}} \quad \text{Eq. 2.3}$$

where ρ = density [kg/m^3]

σ = surface tension [N/m]

v = velocity [m/s]

μ = dynamic viscosity [$\text{kg}/\text{s}\cdot\text{m}$]

d = characteristic length (nozzle diameter) [m]

The Ohnesorge number relates the viscous force relative to the surface tension force. Fromm has introduced a parameter to represent printability, which is the reciprocal of the Oh number as shown in Equation 2.4 [40]. He suggests that $Z > 2$ for stable drop formation. Another proposed range for stable drop formation is $10 > Z > 1$. At low values of Z , viscous dissipation prevents drop ejecting and at high values of Z , the primary droplet is followed by multiple satellite droplets [41]. Satellite drops are undesirable because they are detrimental to precision of drop deposition [39].

$$Z = 1/Oh \quad \text{Eq. 2.4}$$

The Weber number relates the fluid's inertia to its surface tension. There is a minimum Weber number before which drop breakup does not occur because a drop must have sufficient energy to overcome the fluid/air surface tension at the nozzle exit [24]. After the drop is deposited, it should leave a single isolated spread drop. The mechanisms that lead to splashing are still subject to research but there is an experimental threshold presented in Equation 2.5, where $f(R)$ is a function of surface roughness [42].

$$We^{1/2} Re^{1/4} > f(R) \quad \text{Eq. 2.5}$$

Operating limits on the dimensionless numbers for stable drop formation have been determined for Newtonian fluids [24]. Figure 2.6, is established with the use of equations 2.1 through 2.5.

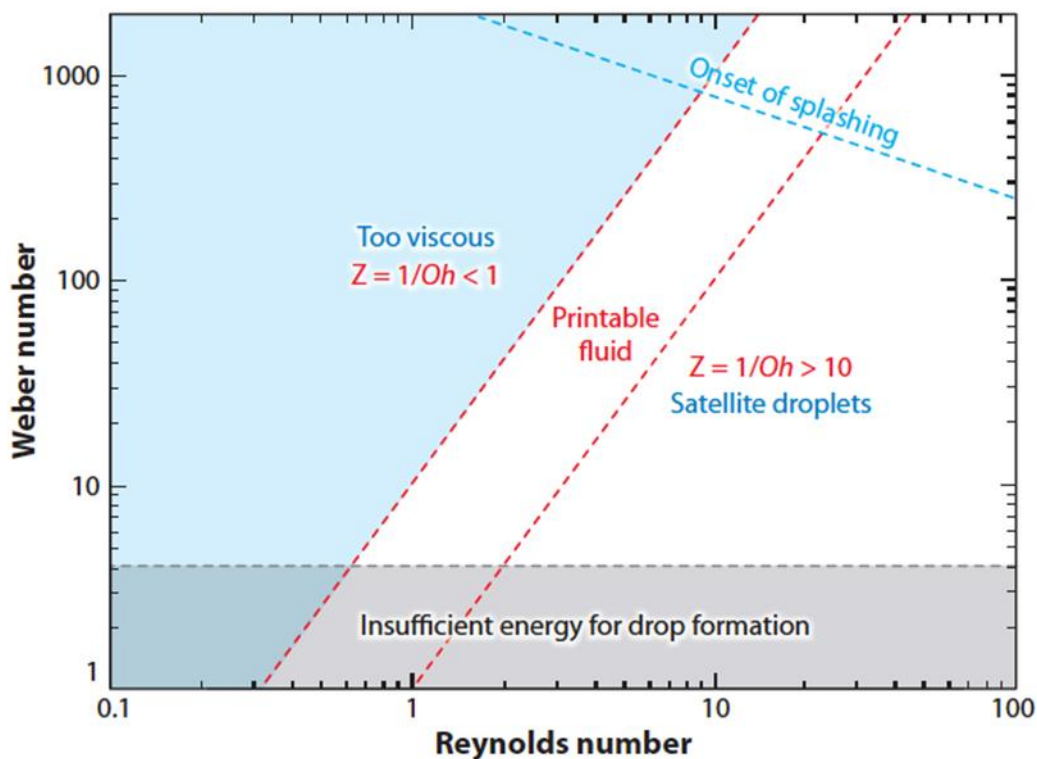


Figure 2.6 Printable fluid properties for Newtonian fluids [24]

However additional research is required for establishing such operating regimes for viscoelastic fluids [38], such as solutions or melts of polymer and API and such work is ongoing in our research team. Preliminary studies to determine the operating region for solvents is presented in Chapter 4. The operation region has to be chosen carefully to ensure the integrity of the drop until it deposits to the substrate. After ejection, a drop may separate into a primary and one or more secondary drops, which are called satellite drops [41]. Satellite drops are undesirable because they are detrimental to precision of drop deposition [39]. If the primary and the satellite drops do not combine to a single drop after ejection, they might land on a different area on the substrate and affect the final API loading of the form.

After passing through the pump, the drug material ejects through a nozzle onto the substrate placed on the xy staging. The tubing connected to the inlet and outlet of the pump is Teflon tubing with 1/8" O.D. and 1/16" I.D. with corresponding Teflon ferrules and fittings. In the DAMPP system, nozzles with different diameter sizes can be used: typical sizes used in our work are listed in Table 2.1. In order to adjust the drop size, nozzle diameters can be changed along with the printing parameters, such as RPM, volume strokes and pump displacement.

Table 2.1 Nozzle sizes

Nozzle #	1	2	3	4	5	6
Standard Wire Gauge Size	13 AWG	14 AWG	15 AWG	17 AWG	19 AWG	20 AWG
Inner Diameter	1.83 mm	1.63 mm	1.45 mm	1.15 mm	0.91 mm	0.81mm

2.2.4 Drop Monitoring and Deposition

For pharmaceutical applications, it is very important for the dosage to have the proper API loading. Therefore, the process conditions must be chosen carefully so that the potential for satellite drop formation is minimized. In order to ensure consistent drop formation without satellite drops, the drop formation is monitored using a moderate speed Manta camera based imaging system. With the help of motion sensors, an image of each drop is taken after it is ejected from the nozzle and before it is deposited on the substrate. If satellite drops are detected, printing settings can be adjusted online to obtain stable drop formation. The captured drop image is converted to drop volume using pixel counts within a shape model that can accommodate arbitrary rotational symmetry [43]. To

demonstrate the reproducibility of the drops, a melt of PEG 3350 is printed using the 15 AWG nozzle, 2.5 displacement, 1200 RPM and volume strokes of 1. Drop images captured with the imaging system are shown in Figure 2.7. The average volume of the drops printed with this formulation and printing settings is 13.70 μL with a relative standard deviation of 1.59 %. The details of the automation system including the imaging system and the volume calculation are presented in Chapter 3.

Drop positioning is accomplished by locating the printer nozzle above the desired location on the substrate before ejection. The xy-staging and synchronization logic allows creating precise drop positioning on the substrate while printing and enables layering of different drugs. The drops are deposited in a grid structure using the DAMPP system, as shown in Figures 2.2 and 2.3. The behavior of a drop on impacting a solid surface is controlled by a number of physical processes including the drop velocity, size, drop material properties, distance from the surface and surface properties [24], [44]. Upon impinging the drop can splash, spread or even rebound [44]. In order to achieve a single isolated drop without splashing or spreading, the physical process parameters must be suitably selected. Since solidification of drops occurs post-deposition, melt-based formulations must retain some stability in the liquid state prior to solidification.

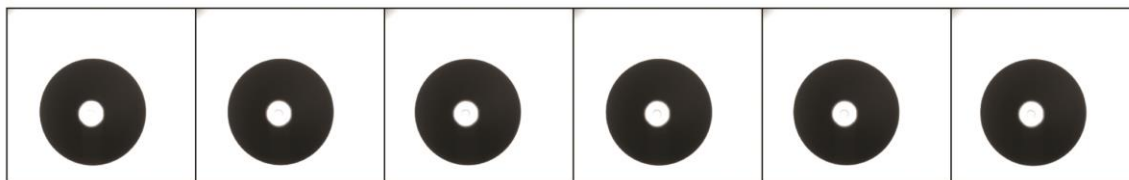


Figure 2.7 Images of PEG 3350 drops printed with DAMPP

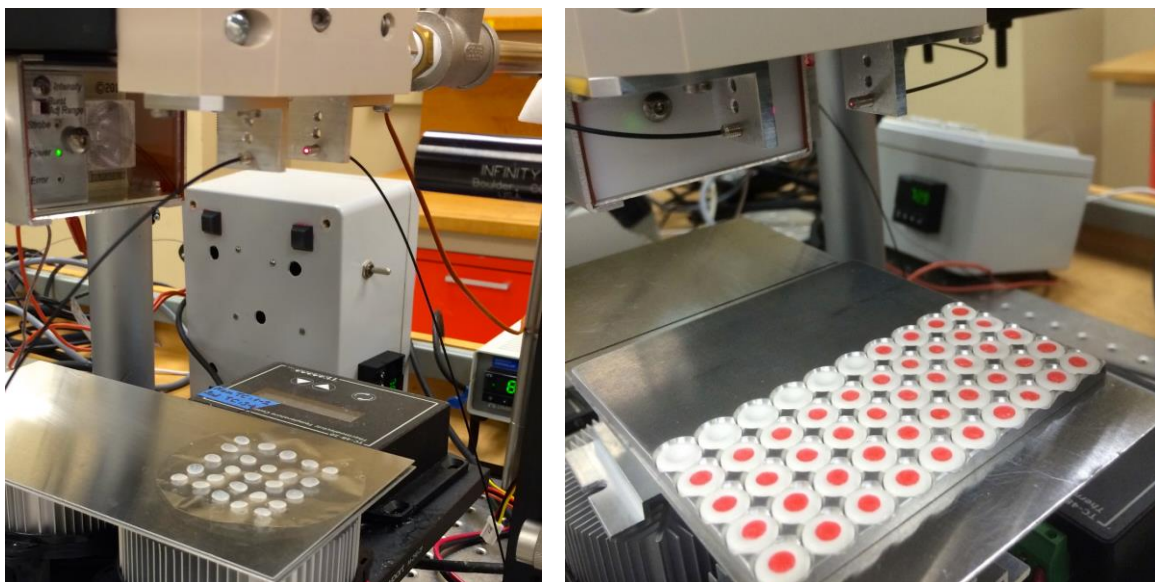


Figure 2.8 Melt-based formulations during deposition on a. polymeric films b. placebo tablets

2.2.5 Substrate Selection

Using this process, the formulations can be printed on a variety of substrates including polymeric films and placebo tablets or into capsules. Printing melt-based formulations on edible polymeric films and on placebo inert tablets are shown in Figure 2.8. Surface properties of the substrate onto which the drops are deposited have an effect on drop deposition characteristics as well as on the solid state of the drug. The use of polymeric films or inert tablets of different porosities can have an effect on the crystallization and dissolutions profiles of the formulations. It has been shown that by printing on films containing HPMC or chitosan, the microstructure, crystallinity and even the dissolution of drug deposits can be controlled [45]. The surface chemistry of chitosan films, such as its capability of forming H-bonds with the drug, also effects the crystallization of drugs [46]. The surface properties of the substrate, such as roughness, also can have an effect

on product morphology [26], [47]. Therefore the substrate should be selected by considering the desired end product.

2.2.6 Control of Substrate Conditions

The temperature of the deposited drops are controlled via the Peltier device with PID controller placed on the xy staging underneath the substrate. This allows control of the rate of solidification of melts and thus control of nucleation and crystallization phenomena. Since crystallization temperature will have an effect on product solid state characteristics, influencing the dissolution properties and hence the bioavailability of the drug, precise control of the drop solidification process once the drop is deposited on the substrate is essential [48]. This is achieved indirectly by manipulating the substrate temperature profile using controlled temperature gradients [28]. Using the substrate temperature control strategy explained in Chapter 5, the crystallization behavior can be tailored and consistent drug properties achieved [28].

2.2.7 Confirmation of Solid-State Form

After the dosage forms solidify, the solid state form of the drug substance should be verified by an online or offline technique such as X-ray diffraction, microscopy or a spectroscopic technique. The noninvasive nature of spectroscopic techniques, including Raman and Near Infrared (NIR) spectroscopies, allows continuous real-time measurements of critical product properties without sample preparations [49]. For instance, they can also be used to distinguish different polymorphic forms [50]. The best

technique to verify the crystallinity or drug polymorphic form in the dosage forms can be selected based on the drug formulation.

2.2.8 Postprocessing

After the dosage forms are produced, a number of different post-processing steps can be applied, including coating of dosage forms to insure adhesion of deposit on the substrate, to shield the API from moisture, to alter the dissolution profile of the drug, or for taste-masking. For multilayered drug production, another layer of the same drug or another drug could be printed to adjust the dosing or to produce a drug cocktail for a specific treatment.

2.3 Materials and Methods for the Analysis of Melt Based Drug Products

DAMPP is used to produce solid oral dosage forms from hot-melts of an active pharmaceutical ingredient and a polymer. The dosage forms are analyzed to show the reproducibility of dosing and the dissolution behavior of different formulations. In this section the materials used in the formulation of the drug products and the methods used to analyze those products are demonstrated.

2.3.1 Materials and Formulation Preparation

In this study, naproxen is chosen as the model API to form melt formulations either with the polymer, polyethylene glycol with a molecular weight of 3350 or with the block copolymer Pluronic F38 with a molecular weight of 4700. Naproxen (NAP) was purchased from Attix Pharmaceuticals (Montreal, QC, Canada). PEG 3350 and Pluronic

F38 were provided by The Dow Chemical Co. (Midland, Michigan) and BASF (Florham Park, New Jersey), respectively. Naproxen and the polymer (PEG 3350 or Pluronic F38) were mixed in (15:85) weight ratio. The mixture is comelted at 65 °C until completely melted. The melt formulation is printed on polymeric films prepared with hydroxypropyl methylcellulose (HPMC) (E50) and PEG 400. HPMC (E50) is purchased from Sigma Aldrich Corporation (St. Louis, Missouri). PEG 400 likewise was provided by The Dow Chemical Co. (Midland, Michigan).

2.3.1.1 Film Preparation

In order to make a 5% (w/v) polymer solution, 0.6 gr HPMC powder (E50) and 0.4 gr PEG 400 were dissolved in 20 ml water at 90 °C. The 5% (w/v) HPMC-PEG 400 solution was stirred at room temperature overnight to ensure that the polymeric chains were homogeneously dispersed in the solution and cast onto a Petri glass. After drying was completed, the film was peeled off.

2.3.2 Methodology

After deposition of the drops onto the film, the resulting dosage forms were analyzed to determine whether the different formulations would affect the dissolution behavior of the API. The dosage forms were created and analyzed at the same time and thus varying ambient conditions, such as relative humidity, were not impactful on the results.

2.3.2.1 Hot Stage Microscopy Experiments

Formulation consisting of naproxen and polymer were prepared as described in Section 2.3.1. After the solid dispersions solidified, they were ground using a mortar and pestle. The resultant powder was evaluated using a Nikon Eclipse E600 polarized light microscope (Nikon Inc., Melville, New York) equipped with a Linkam THMS 600 hot-stage (Linkam Scientific Instruments Ltd., Surrey, UK). The samples were heated at 1 °C/min until completely melted. The temperature where the last crystal melted was recorded and was used to construct the phase diagram.

2.3.2.2 High Performance Liquid Chromatography Experiments

Quantification of the drug in the dosage forms was done using an Agilent 1260 infinity high performance liquid chromatography (HPLC) system using an Agilent plus C₁₈ 5µm, 2.1x150 mm column (Agilent Technologies, Santa Clara, California). The mobile phase consisted of acetonitrile (ACN) as the organic phase and pH 2.5 phosphate buffer as the aqueous phase. Isocratic elution was performed on the samples at a flow rate of 0.5 mL/min with the mobile phase consisting of 60% aqueous phase and 40% ACN. Naproxen was detected at a wavelength of 210 nm using an ultraviolet detector. The retention time of naproxen was 4.5 min using the method listed above. A calibration curve was plotted from 1µg/mL to 100 µg/mL with a R² value of 0.9999. For analysis of the dosage forms, individual drops of naproxen-PEG 3350 and naproxen-Pluronic F38 were dissolved in ACN and diluted appropriately to obtain the concentration in the range of the calibration curve.

2.3.2.3 Reproducibility of Dosage Amounts

Different drop sizes are used to produce the dosage forms with target dosage of 15 mg of API. The different drop sizes are obtained by changing the pump and printing operating parameters such as nozzle diameter, displacement, volume strokes and rate. The number of drops needed to reach the target amount varied for each printing setting and was determined experimentally before producing the dosage forms. To analyze reproducibility, HPMC-PEG 400 film measuring 2 cm by 2 cm was weighed on an Omega AL-201s balance. Next, a specific number of drops were deposited on the film to reach the target dosage amount. The films were then subjected to room temperature until the deposits solidify. After solidification of the drops, the films were weighed again to determine the total mass of the deposits on the film. The amount of drug was determined by multiplying this mass of solids by the composition of drug in the solution (15%). These results were then used to analyze how consistently and accurately the dosage forms are created.

2.3.2.4 Dissolution Testing

The dissolution test was conducted using USP-I apparatus (Agilent Varian VK 7010) at 100 rpm. The dissolution media consisted of the USP phosphate buffer solution of pH 7.4, which was maintained at 37 °C. The experiments were performed in sink conditions to prevent the drug from saturating the dissolution media. The experiments were run for 90 minutes, and aliquots of the dissolution medium were collected at intervals of 3 minutes through 35 micron full flow filters (Agilent filters) by a peristaltic pump. Sample

absorbance was measured by a UV spectrophotometer (Cary 50) at 243 nm. Absorbance values from the spectrophotometer were used to calculate the percent release of the API from the films. Each experiment was performed in three replicates.

2.3.2.5 X-ray Diffraction

X-ray diffraction was performed on the dosage forms to confirm the physical nature of naproxen. The drops were loaded onto glass sample holders and data collection was performed using $\text{CuK}\alpha$ radiation from a Rigaku SmartLab diffractometer (The Woodlands, Texas) at 40kV and 20mA. Measurements were performed in the range of $5-35^\circ 2\theta$ with a scan rate of $4^\circ 2\theta/\text{min}$ and a step size of 0.04° using Bragg-Bretano mode. Si peak was used as an external reference standard. Diffractograms of the crystalline drug, PEG 3350, Pluronic F38 and physical mixture of the drug with the polymers were collected as reference.

2.4 Analysis of Melt-Based Dosage Forms

In order to demonstrate the performance of DAMPP system, dosage forms of melts are produced using different formulations. The first formulation consists of 15% naproxen and 85% polyethylene glycol 3350 (PEG 3350) by weight. This formulation is selected based on the studies done by Zhu et al., which shows that naproxen and PEG 3350 form a eutectic system with a eutectic composition of around 15% naproxen [51]. The dosage forms are shown in Figure 2.9.

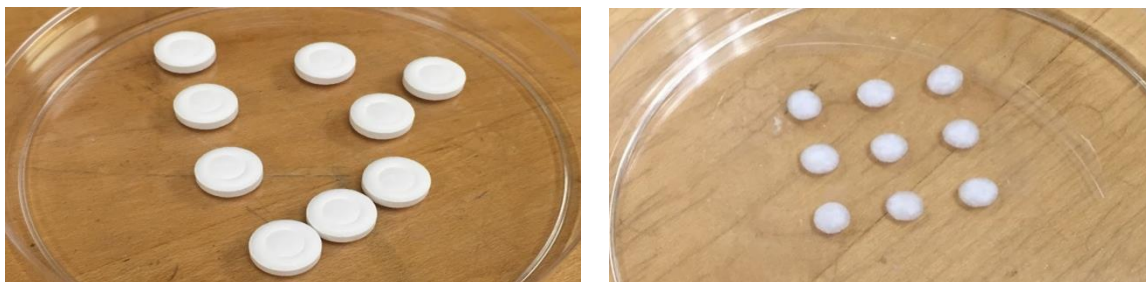


Figure 2.9 Dosage forms containing Naproxen/PEG 3350 formulation deposited on a. inert tablets b. HPMC film

The second formulation consists of 15% naproxen and 85% Pluronic F38 by weight. The phase diagram for naproxen/Pluronic F38 solid dispersions is constructed using optical microscopy to determine the melting point depression of mixtures of various compositions and is shown in Figure 2.10. The liquidus temperature refers to the temperature at which the mixture is entirely liquid. The eutectic composition of Pluronic F38 and naproxen is determined between 10% and 15% of naproxen by weight. Therefore both formulations are prepared with 15% naproxen and 85% polymer.

The formulations were comelted at 65 °C and the temperature of the system was controlled at 70 °C throughout the process. The molten formulations were subject to the operating temperature of 70 °C during the maximum residence time of 5.4 minutes which is determined for the smallest drop size of 9 μL . For larger drop sizes the residence time is shorter as the number of drops deposited per time is fixed. In order to check the chemical stability of naproxen under production, we performed HPLC experiments on the dosage forms, which were intentionally subjected to 70 °C for 15 min during production. The HPLC experiments showed that naproxen found in the dosage forms is stable. The

amount recovered is the same of the amount present in the dosage forms and no degradation peaks were observed.

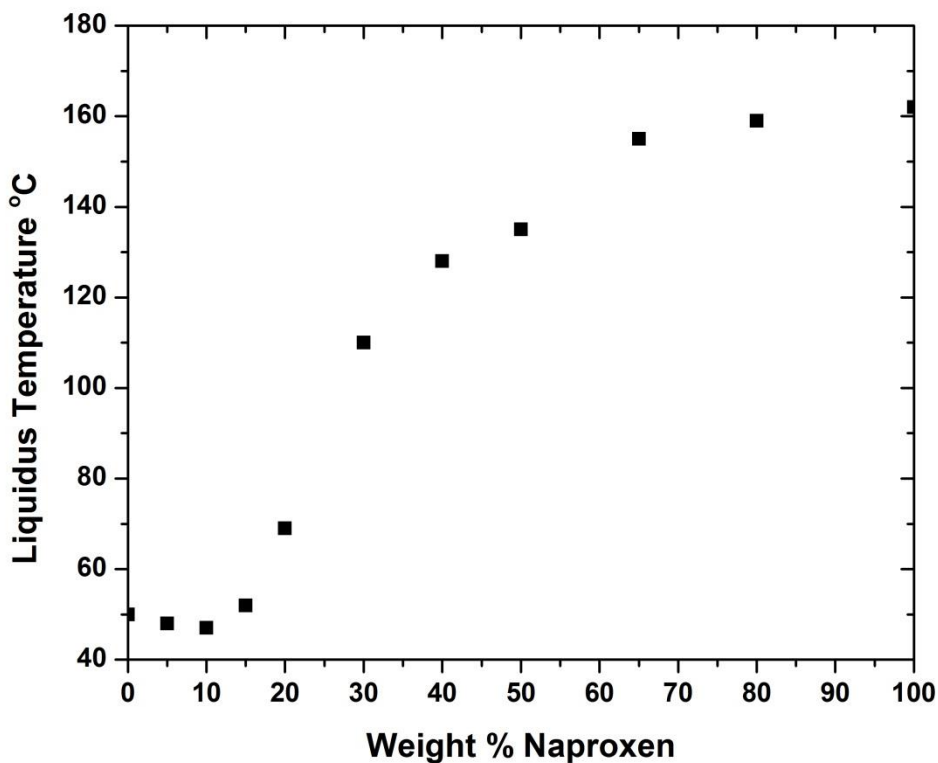


Figure 2.10 Phase Diagram of Naproxen / Pluronic F38

2.4.1 Reproducibility of Dosage Forms

To demonstrate different drop sizes, two intermediate sizes of nozzles (i.e. with internal diameters of 15AWG and 17AWG) are used. The pump settings are determined to achieve consistent drop formation for both formulations using these nozzle sizes. Using the DAMPP system, dosage forms are produced by printing different sizes of drops on HPMC-PEG films as the substrate. The reproducibility of the dosage forms so produced is shown in Table 2.2. The relative standard deviation (RSD) is less than 1% for most

cases and up to 2% for others. These RSD values are well within the 5% RSD limit required by the FDA.

Table 2.2 Reproducibility analysis of dosage forms

Formulation	Number of drops printed	Average dosage amount (mg)	RSD (%)
15% Naproxen 85% PEG 3350	10	14.32	0.56%
	9	15.69	0.18%
	7	16.13	0.05%
	6	15.53	1.30%
15% Naproxen 85% Pluronic F38	10	15.76	0.69%
	9	16.11	2.05%
	7	15.12	0.08%
	6	13.77	0.17%

2.4.2 Dissolution Testing

Dissolution testing was performed on the dosage forms produced with different sizes of drops and different formulations. In Figure 2.11, the dissolution profiles of the dosage forms with the first formulation, i.e. containing 15% naproxen and 85% PEG 3350 are shown. Dissolution of 98% was achieved in one hour and 85% within 20 minutes. In Figure 2.12, the dissolution profiles of the dosage forms with the second formulation, i.e. containing 15% naproxen and 85% Pluronic F38 are shown. Dissolution of 99% dissolution was achieved in one hour and 85% in 33 minutes.

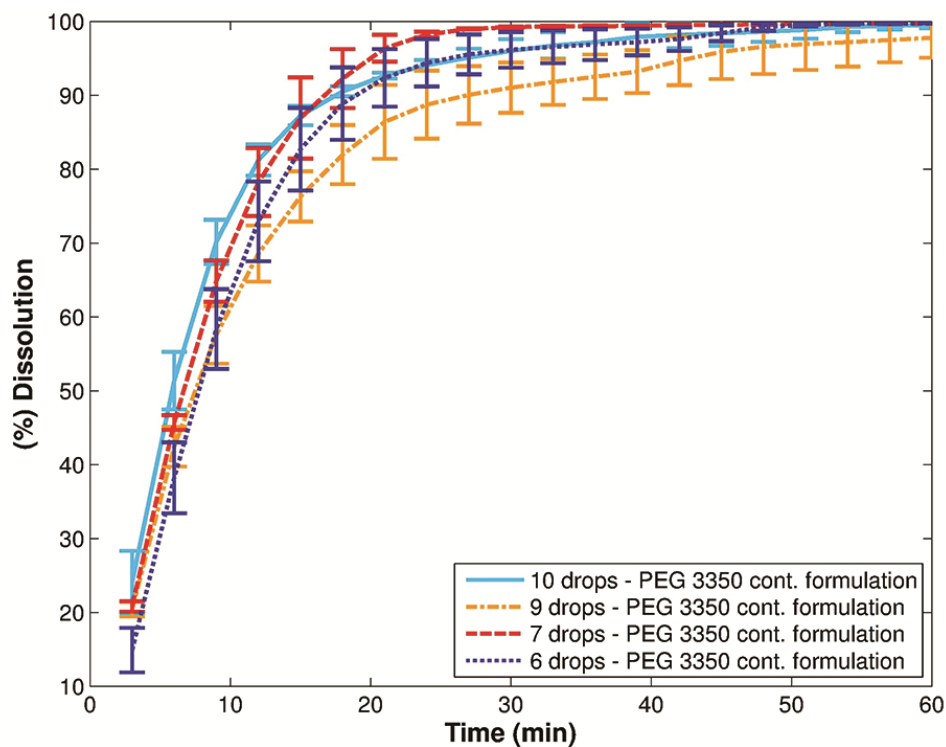


Figure 2.11 Dissolution profiles of dosage forms created with different number of drops of the formulation containing PEG 3350.

For both formulations, there are slight differences in the dissolution profiles of the dosage forms printed using different drop sizes. This is due to the effect of the cooling temperature gradient within the drops as they are solidifying which can lead to morphology changes. By applying temperature control on the substrate, one can overcome the effect of temperature gradients due to different drop sizes and tailor the dissolution behavior [28]. The effect of temperature is discussed in Chapter 5.

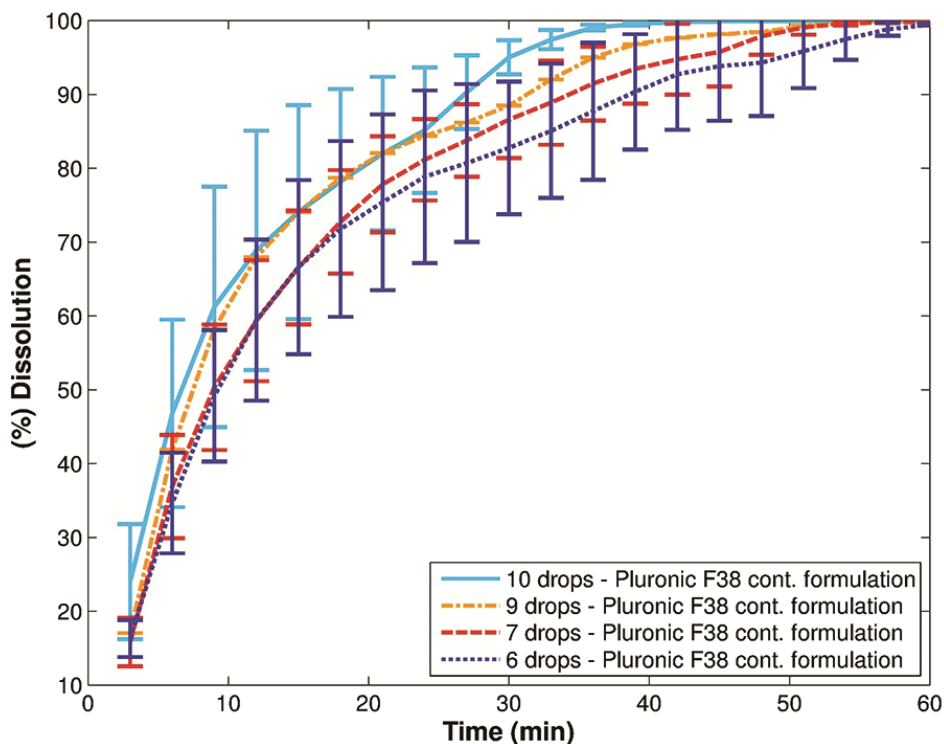


Figure 2.12 Dissolution profiles of dosage forms created with different number of drops of the formulation containing Pluronic F38.

2.4.3 Effect of Formulation on Dissolution

The effect of formulation on the dissolution profile is shown in Figures 2.13 and 2.14. Here, the dosage forms created with 6 drops of large size and 10 drops of small size are compared for the PEG 3350 and Pluronic F38 containing formulations. Dosage forms with PEG 3350 formulation have a faster dissolution than the dosage forms containing Pluronics F38. This is a result of the structural differences between the two polymers.

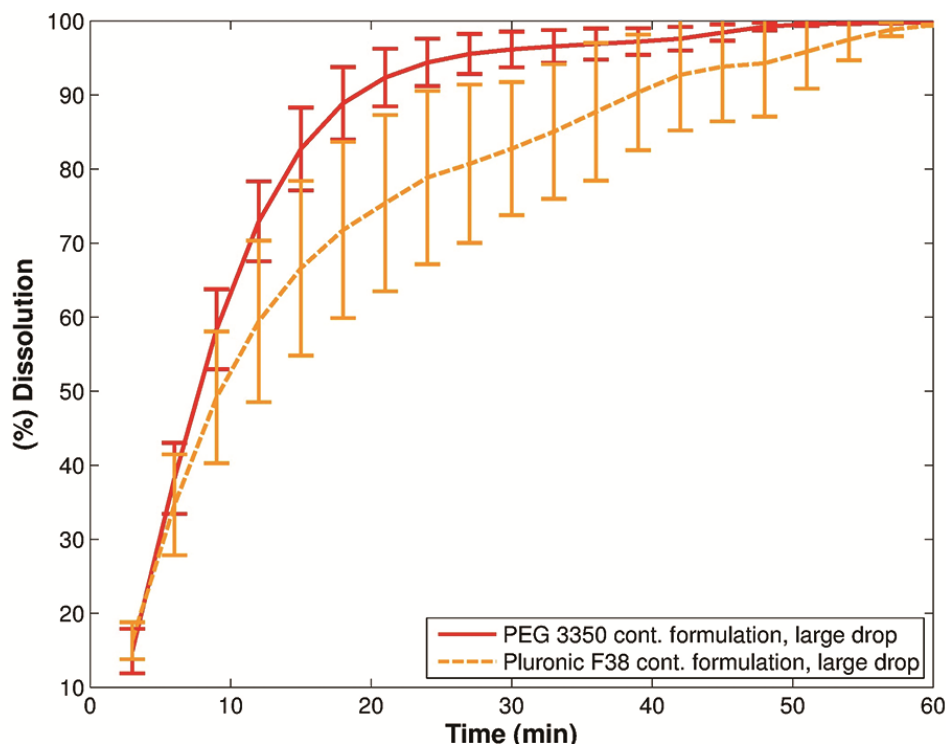


Figure 2.13 Effect of formulation (PEG 3350 vs Pluronic F38) on the dissolution of dosage forms consisting of large drops.

PEG is a polymer of ethylene oxide (EO) and is hydrophilic with a good solubility in water [34]. It is known to enhance dissolution of many drugs that have poor solubility [34], [36]. Pluronic is a triblock copolymer which consists of repeating chains of EO and propylene oxide (PO) in the structure of $EO_x-PO_y-EO_x$, where x and y are the average number of EO and PO units respectively [52], [53]. Pluronic F38 consists of 80% EO with a structure of $EO_{43}-PO_{16}-EO_{43}$. Although Pluronic type polymers are amphiphilic with hydrophilic EO and hydrophobic PO units, those with 80% PEO blocks are considered as very hydrophilic block copolymers with high solubility [53]. However the presence of PPO blocks in the Pluronic F38 containing formulation results in a slower release of the drug compared to PEG 3350 containing formulation. Another difference in

the dissolution profiles are the larger error bars observed for the Pluronic F38 containing formulation compared to the PEG 3350 containing formulation. This can also be related to the differences in the structures of the two polymers, where amphiphilic Pluronic units could potentially cause varying release profiles.

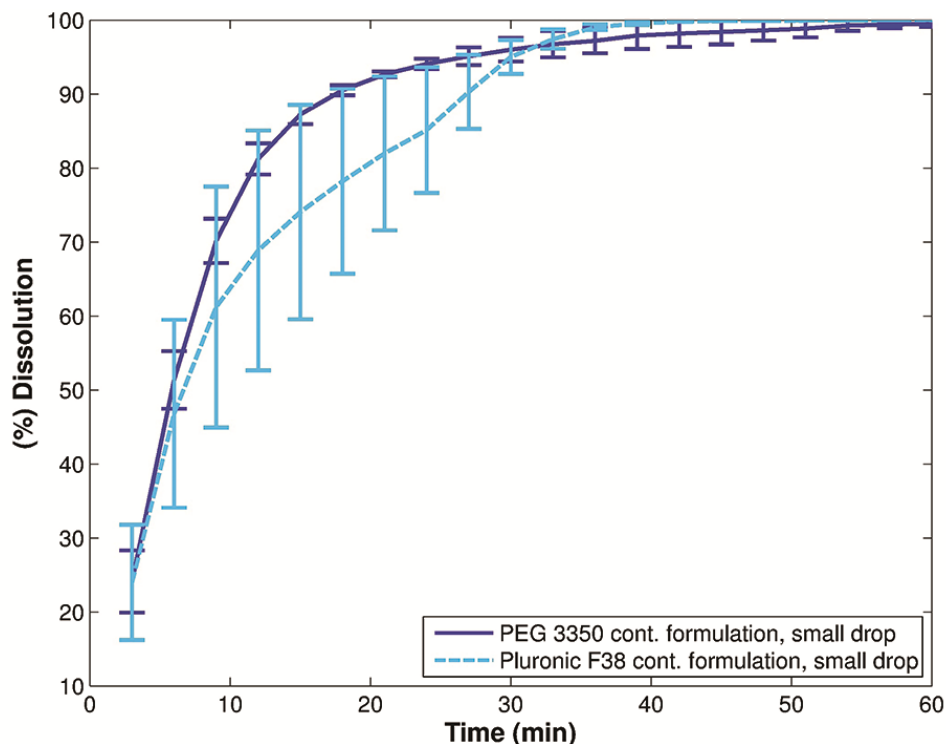


Figure 2.14 Effect of formulation (PEG 3350 vs Pluronic F38) on the dissolution of dosage forms consisting of small drops.

For the model drug used, the first formulation which leads to faster dissolution is favorable but the use of the Pluronic type polymers might be favorable for some other drugs. Pluronic not only increases oral solubility of poorly soluble drugs by its hydrophilic EO side but it can also enhance the oral absorption of selected drugs with its ability to form unimers or micelles [52]. Pluronic type polymers with large PPO blocks

can self-assemble into micelles in aqueous environments and the PO core can serve as a ‘cargo’ for the incorporation of various hydrophobic compounds that exhibit poor solubility, undesired pharmacokinetics and low stability in physiological environment [52], [54]. Unimers of Pluronic block copolymers increase membrane transport and transcellular permeability in intestinal epithelium cells thus inhibit drug efflux systems in intestinal epithelial cells [52], [55], [56]. Overall, Pluronic block copolymers may be useful in designing formulations to increase bioavailability of select drugs.

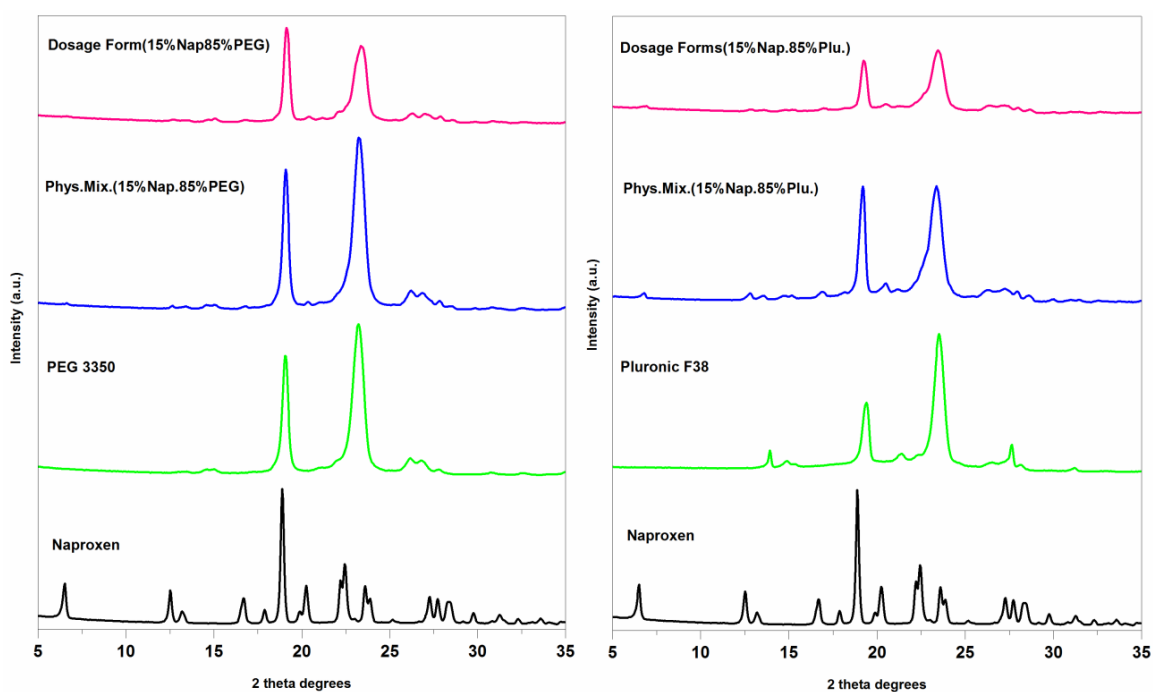


Figure 2.15 XRD spectra of crystalline naproxen, PEG 3350, Pluronic F38, and physical mixtures of both formulations and resulting dosage forms.

With the model formulations used in this study, the amorphous form of naproxen is not observed in the presence of PEO, which promotes crystallization of naproxen [51]. X-ray diffraction studies showed that the naproxen present in the dosage forms is crystalline

and present in the same polymorphic form as the material used in the formulations both in the presence of PEG 3350 and Pluronic F38 which is shown in Figure 2.15. However amorphous forms can be potentially produced with alternative choices of operating conditions and polymers, which inhibit crystallization. Amorphous drug forms can offer improved dissolution performance thus higher bioavailability. However, since the amorphous API is a metastable state, precise temperature control and design of crystallization temperature profile are required in order to achieve the desired solid state form.

2.5 Conclusions

A dropwise additive manufacturing system of pharmaceutical products (DAMPP) for melt-based dosage forms is developed which takes various scientific and engineering principles into account. The temperature controlled process enables the production of melt-based pharmaceuticals reproducibly and consistently. Using the DAMPP system, different polymer containing formulations are used to enhance the bioavailability of the model drug: naproxen. Alternative formulations based on other active ingredients and on other carriers such as other low-melting point polymers, lipids or surfactants can be used, as well.

The imaging system enables monitoring the drop sizes and therefore the dosage amounts. The dosage amount can be adjusted according to patients needs by simply changing the drop size and/or the number of drops in each dose. For the formulations studied in this chapter, differences are observed in the dissolution profiles of the dosage forms printed

using different drop sizes. This is because of the cooling temperature gradient observed within the drops during solidification which can lead to morphology changes. By applying temperature control on the substrate, one can overcome the effect of temperature gradients due to different drop sizes and tailor the dissolution behavior. Achieving the same dissolution behavior for each dose regardless of the drop size enables the application of the DoD system for the production of individualized dosage regimens for adaptive clinical trials and personalized treatments. The effect of temperature control is discussed in the subsequent chapters. The prototype system offers great promise as a tool for advancing personalized therapies by allowing the precise production of convenient solid oral dosages tailored to the patient on site at hospitals, clinics and even pharmacies.

CHAPTER 3. REAL TIME PROCESS MANAGEMENT STRATEGY FOR DROPWISE ADDITIVE MANUFACTURING OF PHARMACEUTICALS[†]

3.1 Introduction

To address the challenges associated with producing high quality pharmaceutical products, the DAMPP process allows the application of process control, on-line monitoring and fault diagnosis systems. Since the process is small-scale, consists of simple unit operations, and involves fluid processing, as opposed to the solids processing used in conventional processes for pharmaceutical solid oral dosage products, the implementation of automation and low-level control for DoD systems is comparatively simpler [57], [58]. There are some complexities involved with controlling drop dynamics which require attention and a unique control and monitoring strategy. The formation and behavior of drops is affected greatly by material properties; the surface tension and viscosity of the fluid, in particular, are important to consider in relation to the pressure that is applied to the nozzle [59]. The viscosity of the drop should be low enough to ensure that a drop will actually eject from the nozzle but high enough that the fluid does not splash out of the nozzle [38]. The surface tension must be high enough so the fluid does not leak from the nozzle at rest and to ensure the drops form uniformly [38]. It has

[†] This chapter is based on: L. Hirshfield, E. Içten, A. Giridhar, Z. K. Nagy, and G. V. Reklaitis, “Real-Time Process Management Strategy for Dropwise Additive Manufacturing of Pharmaceutical Products,” *J. Pharm. Innov.*, vol. 10, no. 2, pp. 140–155, 2015.

been said that the “only way to check the quality of a printing process is by checking the result, as the process itself does not give any direct feedback [60];” so in addition to traditional process control, there must be a careful automation strategy and sufficient on-line monitoring to ensure a quality product. Therefore, DAMPP necessitates an advanced real-time process management (RTPM) strategy, encompassing automation of each unit operation, careful control of process parameters, monitoring of the process and product quality and an exceptional events management system that detects and diagnoses process faults that are outside of regulatory control.

This chapter presents the RTPM strategy developed for the DAMPP system [30]. An automation program makes the unit operations run synchronously, while maintaining the control of equipment and recording the various monitored parameters. The printing material and process temperatures are carefully controlled to maintain consistent material properties and thus predictable drop dynamics, while the process temperature is manipulated to control the product's final dosage form morphology. Each drop is monitored with a vision system, allowing for the calculation of drop size, storage of the process parameters, drop images and drop characteristics for each deposited drop. Image capture of each drop also allows for the management of exceptional events. With careful selection of process parameters and printing materials and a successful RTPM strategy, DAMPP allows for precise and accurate control of the dosage amount, composition, phase, morphology, and release profile of the drug, all through monitoring and controlling critical process parameters and critical product quality attributes. Moreover,

since each dosage is tracked as it is formed, deviations can be identified and eliminated as they are produced, providing real time release functionality.

3.2 Development of a Real Time Process Management Strategy

For pharmaceutical processes, the performance of a drug product is defined in terms of its critical quality attributes (CQA), which are its essential physical, chemical and biological characteristics [61]. For the dropwise additive manufacturing system, the desired critical quality attributes (CQA) of the dosage forms that should be kept within the appropriate limits are the dosage amount and drug morphology. The CQAs were determined by identifying the key characteristics of a quality dosage form: the API should be deposited in the proper amount for the patient (dosage amount) and in the desired form: amorphous or crystalline (drug morphology). The critical process parameters (CPP) that have a direct impact on the CQA's, are the drop size, product and process temperatures, as shown in Table 3.1.

Table 3.1 Critical quality attributes and critical process parameters

Critical Quality Attributes (CQA)	Critical Process Parameters (CPP)
Dosage amount	Drop volume
Dosage form morphology	Process temperature
	Product temperature

By knowing the concentration of the API in the printing fluid, the dosage amount can be determined from the drop volume. It is important to monitor the drop via imaging, not only to calculate the drop volume, but to track the drop's trajectory and detect any

possible faults in the drop formation system. On-line Raman or NIR measurements can also be used to confirm API concentration in the solid dosage. For a given formulation, the drug morphology can be ensured by controlling the process temperature and the temperature of the product after the drops have been deposited. Temperature control of the process maintains material properties and ensures printability of the fluid, while temperature control of the product affects rate of solidification of melts or evaporation of solvents and thus control over crystallization phenomena. The dosage form morphology and drug's solid state behavior can be monitored on-line using a spectroscopic method such as NIR or Raman [49]. The RTPM strategy developed for DAMPP consists of four main steps and is shown in Figure 3.1.

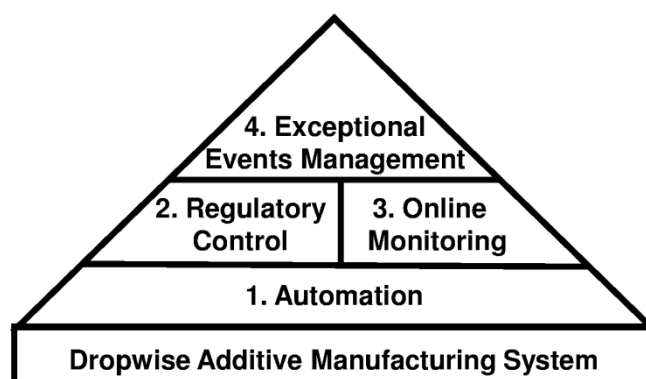


Figure 3.1 RTPM strategy for DAMPP

1. **Automation** consists of logic programming to drive synchronous execution of all unit operations, including controllers and instruments, and to ensure automatic completion of the entire drop deposition process.

2. **Regulatory control** is used to maintain the CPPs within a normal operating regime in the presence of common cause variations.
3. An **online monitoring strategy** is needed to ensure that the CQAs of the product are within specifications. It consists of various sensors, on-line spectroscopy, and imaging equipment.
4. **Exceptional events management (EEM)** helps to detect and mitigate infrequent failures that may arise during process operations due to special causes. In the context of pharmaceutical dosage manufacturing, this capability insures that production of noncompliant dosage is minimized and any such production immediately isolated.

The components of RTPM strategy is discussed in the following sections. The Exceptional Events Management is explained in Hirshfield et al.(2015) and is the subject of Dr. Hirshfield's dissertation [30], [62].

3.3 Automation

A LabVIEW program has been developed for synchronous execution of the pump, staging and camera and also incorporates the control and monitoring methods discussed previously. The user interface of the automation program is shown in Figure 3.2. This section describes the automation program in detail, including the input variables the user must define, the steps that the program executes, and the outputs of the program. The performance of the automation program is also presented; specifically, what manufacturing throughput can be achieved with the use of the program.

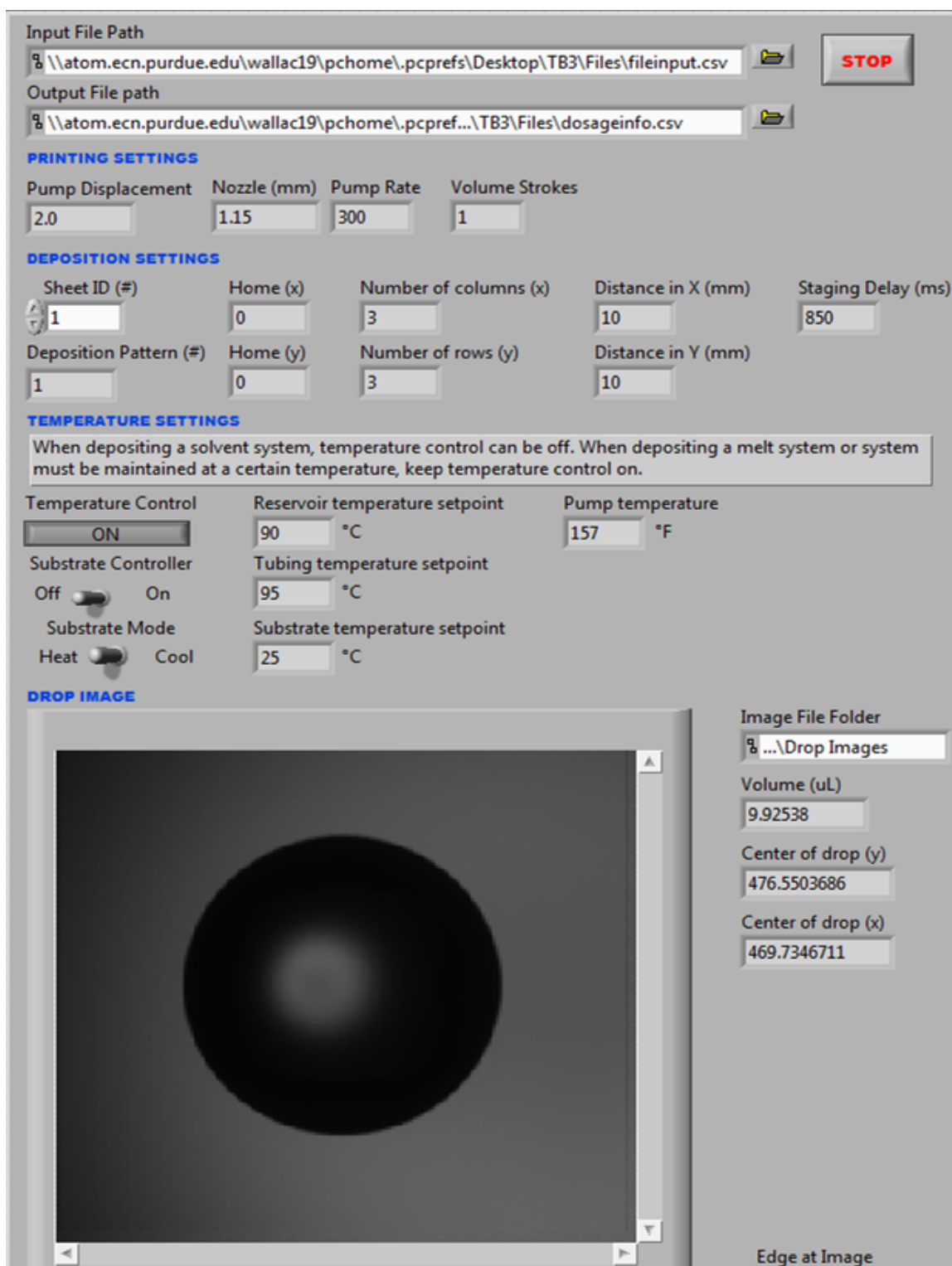


Figure 3.2 The user interface of the LabVIEW-based automation program

The automation system is integrated with the knowledge management system (KMS) designed for DAMPP. In the knowledge management system, all the input data are saved to a file, which needs to be uploaded to the LabVIEW automation program. After the process run, automation program generates an output file containing all the output data. The integration of the automation program with the knowledge management program is discussed in Chapter 4.

3.3.1 Program Inputs

First, the user must define the inputs through the KMS system.

- Printing Settings
 - Pump displacement – The setting of the pump displacement. It can have a value between 1 and 4.
 - Nozzle diameter – The diameter of the nozzle used in millimeters.
 - Pump rate – The setting of pump rate. Has a value between 0-999 corresponding to % RPM.
 - Volume stroke – This setting corresponds to how many times the piston rotates within the cylinder in the pump per trigger. Preferably, it has a value of 1 or 2.
- Deposition Settings
 - Sheet ID – The number of sheet, which is used as the substrate.

- Deposition pattern – The number of selected deposition pattern. It can be a grid pattern with boustrophedonic movement (#1) or row by row deposition (#2).
- Home position (x) and (y) – The starting position of the drop grid pattern. This is variable depending on the substrate's position on the staging and where the grid pattern will be deposited over the substrate.
- Number of columns (x) – The program executes a grid pattern of drops. This parameter refers to the number of columns, or number of drops in the x direction.
- Number of rows (y) – Similarly, this parameter is the number of rows, or number of drops that deposit in the y direction.
- Distance in X and Y – The distance, in millimeters, between each drop space on the grid in x and y directions. The distance must be sufficient so that drops do not coalesce together. In case of the deposition on tablets, the distance should be same as the distance between tablets on the tablet holder.
- Staging delay – The delay, in milliseconds, for staging to move to the following deposition position. The delay should be sufficient enough for the staging to move to the next drop position in order to avoid coalesce.
- Temperature Settings
 - Temperature control – This switch turns the temperature control on or off. For solvent systems, the temperature control may be turned off and then the process will proceed at ambient conditions. For melt systems the

temperature control should be turned on so that the reservoir, tubing, and substrate temperatures are controlled. If the temperature control is turned off, a “0” is saved and if it is on, a “1” is saved.

- Substrate control – This turns the substrate control off or on.(0/1)
- Substrate mode – This switches the Peltier devices from being used as either a heating device (“0”) or a cooling device (“1”).
- Reservoir temperature setpoint – The temperature, in °C, of the material within the reservoir. This is important for melt systems so the polymer solid will liquefy and become printable.
- Tubing temperature setpoint – The temperature, in °C, of the tubing and nozzle.
- Substrate temperature setpoint – The temperature, in °C, of the substrate during the drop deposition pattern.
- Pump temperature – – The temperature, in °F, of the pump during the drop deposition pattern.

The input file containing all the program input data is generated through the KMS system.

The input file is shown in Figure 3.3.

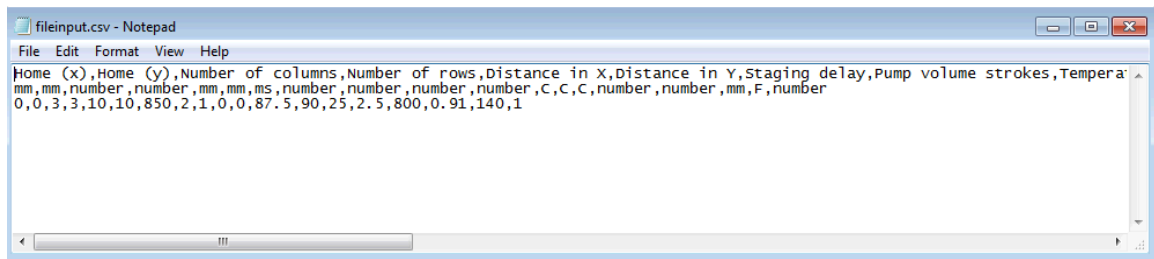


Figure 3.3 Input file in CSV format

Before starting the DAMPP program, the user must define the file paths through the automation program.

- Input file path – This refers to the file name where the comma separated values (CSV) input file containing each of the program inputs is saved. Automation program will read the inputs from this file automatically and display on the user interface shown in Figure 3.2.
- Output file path – This refers to the file name where the comma separated values (CSV) output file containing each of the program outputs will be saved after the program run finishes.
- Image file folder – The folder where the drop images will be saved.

After the user defines the file locations and starts the program, it proceeds as shown in Figure 3.4.

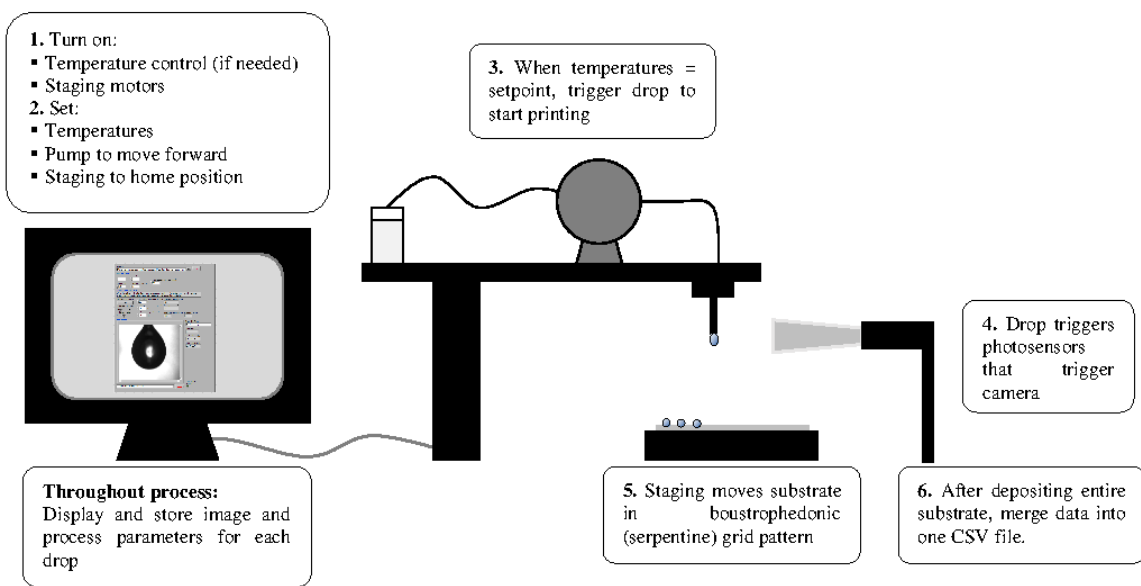


Figure 3.4 Automation process of DAMPP

3.3.2 Program Outputs

Various process parameters, a drop image and image analysis are saved for each drop. The drop data and image analysis data are written to two separate CSV files. The image analysis methods are discussed in a following section. At the conclusion of the drop deposition process, the output files are merged into one data file. This section details the data that is saved for each drop.

- Drop data
 - Time at which the drop deposited
 - Sheet ID, showing on which substrate sheet the drop is deposited.
 - Drop number, calculated by $1+xi+j$ where i is the row the drop is located (in the y direction) and j is the column (in the x direction)

- The location of the drop on the stage in the x-direction (mm)
- The location of the drop on the stage in the y-direction (mm)
- The temperature of the reservoir (°C) at the time of deposition. If the temperature control is turned off, the temperature is recorded as the absolute zero “-273.”
- The temperature of the tubing (°C) at the time of deposition. If the temperature control is turned off, the temperature is recorded as the absolute zero “-273”.
- The temperature of the substrate (°C) at the time of deposition. If the temperature control is turned off, the temperature is recorded as the absolute zero “-273”.
- The power output of the substrate heating devices (as a percentage)
- Pump displacement – The setting of the pump displacement.
- Nozzle diameter – The diameter of the nozzle used in millimeters.
- Pump rate – The setting of pump rate (% RPM).
- Volume stroke – Number of piston rotations within the cylinder in the pump per trigger.
- The temperature of the pump in (°F).
- Image analysis data
 - Drop volume (μL)
 - X coordinate of the center of the drop in the image (pixels)
 - Y coordinate of the center of the drop in the image (pixels)
 - File path of the drop image

An example of the written outputs in a CSV file is shown below in Figure 3.5.

```
dosageinfo.csv - Notepad
File Edit Format View Help
[timestamp,Sheet ID,Drop number,Location on stage (x),Location on stage (y),Reservoir temperature,Tubing temperature,Substrate temperature,Subs
MM-DD-YYYY HH:MM:SS #,#,mm,mm,"C","C","C",%,#,%,RPM,"F",mm,ul,pixels,pixels,path
7/27/2015 12:45:18 PM,1,1,0,0,88.1,90.1,-273,-100,2,2.5,800,140,0.91,14.557784,514.571429,421.309342,20150727_124507.52_drop1.jpg
7/27/2015 12:45:21 PM,1,2,10,0,88.2,90.1,-273,-100,2,2.5,800,140,0.91,12.562040,501.290822,438.627866,20150727_124516.24_drop2.jpg
7/27/2015 12:45:24 PM,1,3,20,0,88.1,90.1,-273,-100,2,2.5,800,140,0.91,13.554068,495.352732,428.899648,20150727_124519.11_drop3.jpg
7/27/2015 12:45:27 PM,1,4,20,10,88.1,90.0,-273,-100,2,2.5,800,140,0.91,15.247948,493.778436,423.155143,20150727_124522.01_drop4.jpg
7/27/2015 12:45:30 PM,1,5,10,10,88.1,89.9,-273,-100,2,2.5,800,140,0.91,18.158223,498.668263,416.759232,20150727_124524.89_drop5.jpg
7/27/2015 12:45:33 PM,1,6,0,10,88.1,90.0,-273,-100,2,2.5,800,140,0.91,14.917058,458.187886,430.133244,20150727_124527.78_drop6.jpg
7/27/2015 12:45:36 PM,1,7,0,20,88.1,90.1,-273,-100,2,2.5,800,140,0.91,13.685235,448.385482,439.137363,20150727_124530.82_drop7.jpg
7/27/2015 12:45:39 PM,1,8,10,20,88.1,90.0,-273,-100,2,2.5,800,140,0.91,14.545803,456.724907,429.986577,20150727_124535.73_drop8.jpg
7/27/2015 12:45:41 PM,1,9,20,20,88.1,90.0,-273,-100,2,2.5,800,140,0.91,14.914184,457.944376,432.830417,20150727_124536.87_drop9.jpg
```

Figure 3.5 Output file in CSV format

3.3.3 System Performance

The automation code is designed to reach an optimal production rate with the current equipment. The fastest possible communication with the temperature, pump and staging controllers is established by operating with the minimum communication times required by the individual controllers.

In order to eliminate the first drop effect in the beginning of each row, the time spent between the deposition of each drop is fixed [39]. After printing a row in the positive x direction, the staging moves so the nozzle is positioned over the next row and the system continues printing in the negative x direction. This boustrophedon movement, shown in Figure 3.6, allows minimizing the time required for the stage movement.

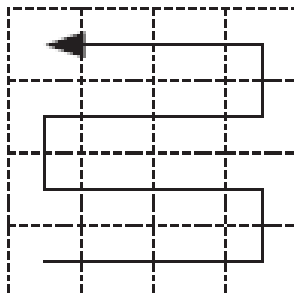


Figure 3.6 Boustrophedon movement path

The performance of DAMPP using the LabVIEW automation system is summarized in Table 3.2. The time required to initialize the process refers to the time spent before the ejection of the first drop communicating with the controllers and setting the process input parameters by the user. The time is longer for melt-based systems than the solvent-based systems due to the added communication time with the temperature controllers. The time spent for the deposition of one drop and recording the data is also shorter for solvent-based systems, which do not require as much temperature control.

Table 3.2 Process performance for different formulations

Time Spent	Solvent-Based Drop Deposition	Melt-Based Drop Deposition
For initialization	5.74 sec	9.55 sec
Per drop	2.24 sec per drop	2.64 sec per drop

3.4 Feedback Control

Although regulatory control is relatively simple to implement on drop-on-demand systems like DAMPP, there are nonetheless challenges that arise [57], [58]. Feedback

control is based on applying a correction that depends on the deviation between the current measurement of a critical attribute and the desired or setpoint value of that attribute. Given the fast dynamics of drop formation, the control system is unable to correct for the deviations observed during the drop formation but instead can only apply those corrections to the next drop to be generated. However, by carefully tuning of process parameters to achieve robust operation, it is possible to limit feedback control action to maintain critical attributes within acceptable ranges and reduce the possibility of off-specification product. One aspect of the process that is readily controllable is the environment of the printing process; specifically, the temperature at each point in the process.

In DAMPP, we are controlling the temperature at four locations. We can control the temperature of the process at three points: (1) in the printing material reservoir, (2) in the pump and (3) throughout the tubing and nozzle in order to control the temperature of the printing material during deposition. We control the temperature of the product at point (4) underneath the substrate to control the product after it has been deposited. Figure 3.7 shows the points of temperature control in the system. Controlling the temperature at points (1)-(3) allows for control of the process temperature while controlling the temperature at point (4) allows for direct control of the resulting dosage form product, by controlling the temperature of the substrate during and after the drops have been deposited.

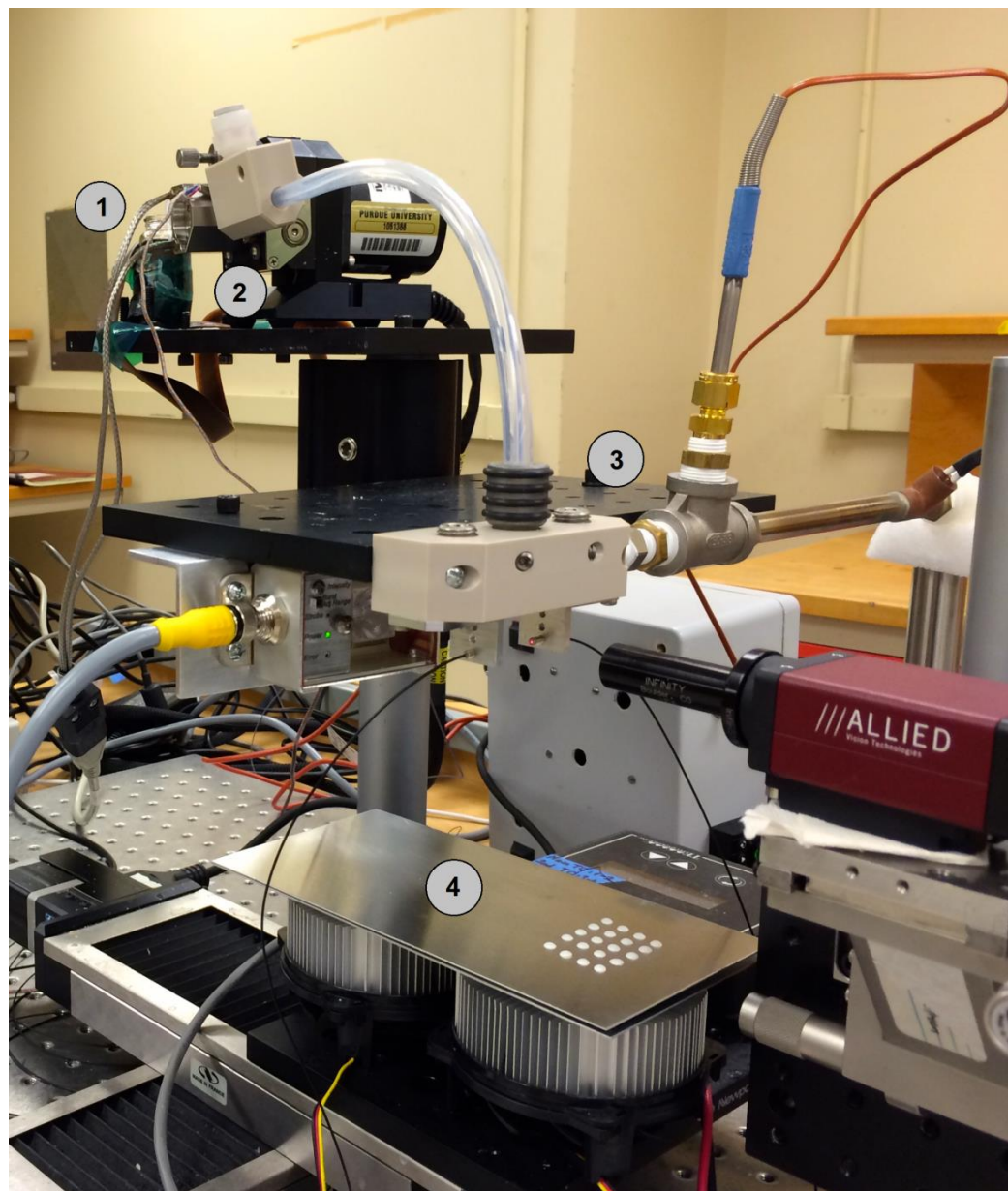


Figure 3.7 Points of temperature control in DAMPP process

3.4.1 Process Temperature Control

While depositing solvent-based systems, temperature control is not necessary but it can be beneficial to minimize temperature effects on fluid properties. It is best to maintain the process at ambient or lower temperatures in order to control solvent evaporation.

However, when depositing melts, controlling the temperature of the process is essential for three reasons. First, the polymer must be melted and liquefied so it is printable. Second, since material properties (specifically, surface tension and viscosity) affect the drop dynamics so greatly, it is important to ensure that the predicted material properties are maintained throughout the process [60]. Third, temperature of the material needs to be regulated throughout the process to maintain the concentration (mass per volume) of drug within the fluid, as the calculation of the amount of API per drop volume uses this parameter.

The process temperature is currently controlled at three points: the reservoir, the pump and the tubing.

3.4.1.1 Reservoir Temperature Control:

It is important to have a heated fluid reservoir when depositing melt systems in order to melt and hold the polymer system as a liquid. The temperature must be controlled carefully to maintain constant fluid properties and thus have predictable drop dynamics. The temperature of the reservoir at point (1) is controlled using heating tape and a PID controller. The LabVIEW program allows the user to input the temperature setpoint, and then the program calculates and sets the high and low alarms for the controller based on a user-specified range of acceptable temperatures around the setpoint. The PID controller can be tuned automatically; this involves the controller cycling the output, measuring the process response, and then calculating and storing the optimal PID values.

3.4.1.2 Pump Temperature Control:

It is most important to control the temperature in the pump in order to maintain the printing fluid's material properties and to ensure that no polymer melt solidifies in the pump. The temperature of the pump at point (2) is controlled via an IVEK-assembled PID controller. This PID controller is also tuned automatically. The temperature setpoint of this controller is entered manually and is not currently adjusted from LabVIEW.

3.4.1.3 Tubing and Nozzle Temperature Control:

The temperature of the tubing and nozzle must be controlled in order to maintain material properties and also to prevent the material from solidifying and causing clogging within the tubing. The temperature of the tubing and nozzle at point (3) is controlled using a custom air heater and a PID controller. The control of the tubing is similar to that of the reservoir: the LabVIEW program allows the user to input the temperature setpoint, and then the program calculates and sets the alarms for the controller. This PID controller is also tuned automatically.

3.4.2 Product Temperature Control

As discussed previously, the printing material, drop size and substrate all have an effect over the dosage form morphology. Controlling the substrate conditions during and after deposition at point (4) is an additional way to affect the solid's crystallization and thus ultimately dissolution behavior after it is deposited onto the substrate [28]. As in traditional crystallization processes, temperature directly influences the crystallization of

the API, by affecting both the nucleation rate and crystal growth rate [48]. When printing solvent formulations, the cooling or heating rate of the dosage form after deposition also affects the evaporation of the solvent. The evaporation of the solvent then affects the liquid composition and thus the nucleation and crystallization rates as well. Therefore, the crystallization behavior of the drug is dependent not only on the melting temperature and glass transition temperature of the API, but on the solvent formulation properties as well: more specifically, the concentration, temperature and solubility properties of the API in the solvent [48]. When printing melt formulations, it may be preferable to cool the substrate in order to solidify the drops more rapidly, but the morphology may need to be controlled by reheating the dosage form, possibly in heating/cooling cycle. Therefore, when depositing either solvent-based formulations or melt-based formulations, the temperature of the substrate must be optimized to balance the needs to decrease production time by cooling or heating of the substrate to affect evaporation rate or solidification rate and also heating the substrate to control the drug morphology.

The temperature of the deposited drops are controlled via the Peltier devices with PID controller placed on the xy staging underneath the substrate. In order to achieve the desired response characteristics, the temperature controller had to be tuned. An online controller tuning approach has been used and the control parameters have been supported with Ziegler-Nichols method.

The user interface of the program can be seen in Figure 3.8. Using the program, the user can:

- enable or disable the output action of the controller,
- set the desired temperature set point,
- read the actual temperature,
- read the power output of the controller.

The controller is operating in heating-only mode and the control requirements are handled by the program. These include:

- defining the high and low temperature values for the operating temperature range (The maximum temperature the current Peltier devices can handle is 80 °C),
- enabling or disable the alarm (In future, two alarms can be used with two thermistors while monitoring two different actual temperatures in the system.),
- defining the high and low temperature values for the low and high alarm temperatures.

The LabVIEW program for product temperature controller has been combined with the main LabVIEW automation program for simultaneous execution of the pump, staging and camera. Initial substrate temperature is set using the user interface of the LabVIEW-based automation program. This allows maintaining the temperature of each deposited drop at the same initial temperature. For example, during the deposition of a melt-based formulation the temperature can be set at 60 °C and the substrate is maintained at this temperature during deposition. After the last drop is deposited and the run is finished, the LabVIEW program for product temperature control starts to run. It also enables to

visually design the temperature profile using the interface shown in Figure 3.9. The initial and final temperatures, rate of cooling and duration are specified and the input temperature profile is generated.

During process execution, the real time temperature setpoint and actual temperature are displayed on the user interface as shown in Figure 3.8. The power output is also displayed, which helps the user track the Peltier operation. The times series measurements of set point and actual temperatures and power output are saved in the file specified by the user.

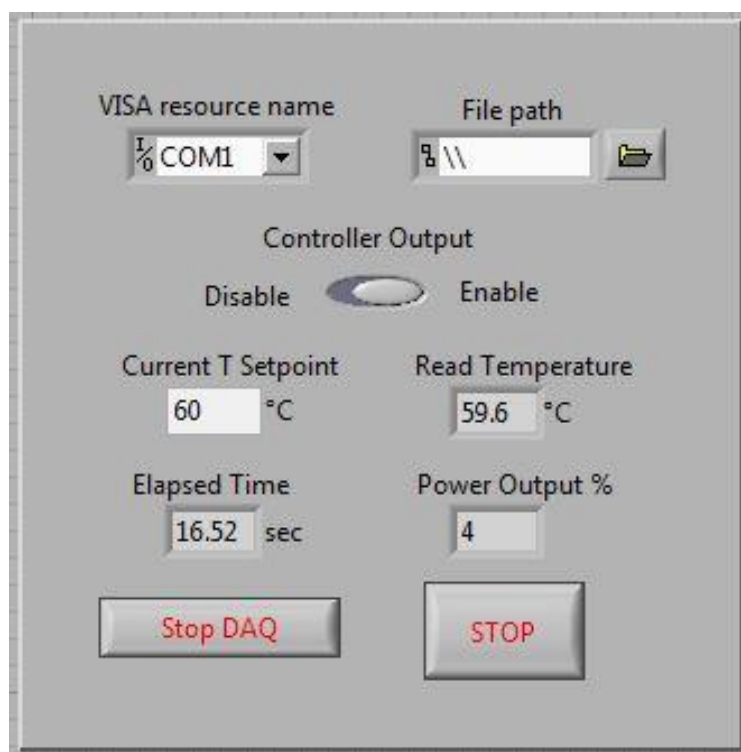


Figure 3.8 Labview program for product temperature control

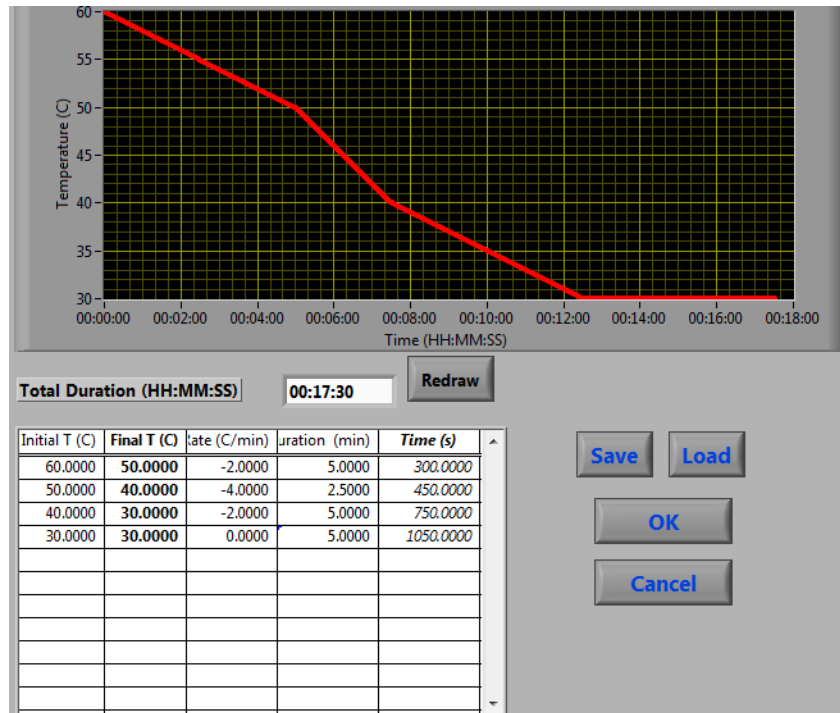


Figure 3.9 Design program for product temperature setpoint profile

3.5 Online Monitoring Strategy

As mentioned previously, feedback control on a given drop is not possible given the fast dynamics of the printing process. Feedback control can only be applied to subsequent drops. Therefore, it is important to have several methods of monitoring in order to ensure product quality. One way to monitor drops is with imaging.

The ejected drops are monitored using a Manta G-146B camera-based imaging system with a Banner D10 photoelectric sensor and an XS40-WHI backlight from Spectrum Illumination. Imaging each drop that is formed via LabVIEW allows for the monitoring of several aspects of the process. First, it allows the user to closely see each drop throughout the process. Second, it is possible to make several conclusions about the

process or product just from an analysis of the drop image. Using the LabVIEW program, the drop volume, and thus amount of drug per drop, can be calculated. The program also calculates the center of the drop within the image so it is possible to track the drop trajectory. Although this information cannot be used to remedy anything that happened within that drop, the information can then be used in a form of feedback control to adjust future drops to return the process to within desired operating bounds.

The automation program, discussed previously, includes an imaging strategy. First, the image is acquired and saved. Using the acquired image, the volume of the drop is calculated to determine the amount of API depositing onto the substrate. The image can then be analyzed to detect certain process faults, or exceptional events, that may be occurring.

3.5.1 Image Acquisition

A photosensor is used to trigger both the backlight and the camera, so the camera captures an image at the same point in the trajectory for each drop. This allows for a consistent view of the drop, and also for comparison between sequential drop images. The triggering of the camera via the photosensors also allows for the camera code to be incorporated into the overall LabVIEW code, but to still run independently of the drop deposition and control codes.

After LabVIEW acquires an image, it displays the image on the program interface and also saves each image file to a user-defined folder. The image is saved with the file name *date_time_dropX.jpg*, where date and time correspond to date and time of image capture

and X corresponds to the number iteration of the loop that contains the camera capture code. Essentially, X gives the number of drop in the order of deposition.

3.5.2 Volume Calculation

By calculating each drop volume and knowing the concentration of the printing solution, we can calculate the amount of API in each drop. The volume is found using a “arbitrary rotational symmetric shape model” [43]. This method generally works well for calculating volumes of drops in flight, as we cannot assume that the drop is a sphere but we can normally assume axial symmetry, as seen in Figure 3.10. However, this method may be inaccurate if the drop is not circular around its axis but is of a different shape, such as ellipsoidal, instead. This can arise with certain types of process faults, such as irregular material deposits at the nozzle tip.

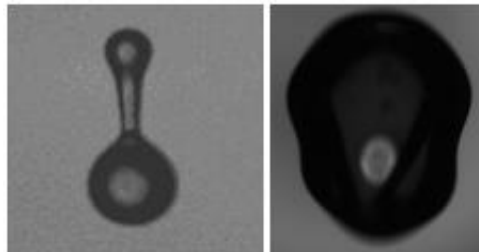


Figure 3.10 Images of non-uniform drops

This method is based on calculating the diameter in each row or column of pixels in the image and then integrating over the entire drop length to find the volume of the drop in voxels. Essentially, the method assumes that the drop is a stack of several cylinders with different diameters and adds the volume of these cylinders together to find the volume of

the whole drop. Then, using a ratio of voxels to volume units, such as microliters or picoliters, for the specific camera system, it is possible to calculate the actual volume of the drop. The detailed methodology of volume calculation can be accessed in Hirshfield et al.(2015) [30]. It is important to note that the volume calculation method was verified with both calibration slides and real droplets. The calculated volumes vs known volumes (for calibration slides) or gravimetrically determined volumes (for real drops) were within 0.33% and 4% error, respectively [30].

The volume calculated for each drop is recorded in the comma separated values (CSV) file and also displayed to the user. Besides being able to use the volume calculations to analyze the consistency of drops throughout the process, it is also possible to keep a running total of the total volume deposited. For melt-based formulations, this is equivalent to knowing the total amount of solids deposited on the dosage form, and thus, with the known concentration, it is possible to keep a running total of the amount of drug on the form. However, for solvent-based formulations, it is also necessary to know the density of the printing material in order to deduce the mass of each drop and thus the mass of the solids within the drop.

3.6 Conclusions

Dropwise Additive Manufacturing for Pharmaceutical Products (DAMPP) is a viable system for flexible, on-demand production of dosage forms. The simple unit operations and small scale of the prototype allow for more extensive on-line monitoring and real time control than can be provided by the traditional batch large-scale pharmaceutical

manufacturing methods. However, the drop-on-demand technology does require the engineering of specific control strategies to ensure a quality product. The real-time process management strategy as described in this chapter encompasses temperature control on the reservoir, tubing, pump and substrate and an image monitoring strategy that allows for imaging of each drop, calculation of drop volume, and determination of the center of drop within the image. The entire process is controlled and automated via LabVIEW, allowing for the recording of the complete set of data that corresponds to each drop deposited. It bears re-emphasizing that the additional benefit of the real time process monitoring system is that not only can deviations be observed but they can be directly associated with individual dosages through the Labview data recording system. The details of the knowledge management system to complete the data provenance are discussed in the next chapter. Consequently tablets deviating from required specifications can be tracked, isolated and rejected, providing a form of real time release. In this manner the system provides the full provenance of each discrete deposit, and allows for creation of a precise final dosage form by controlling and monitoring each drop.

CHAPTER 4. A KNOWLEDGE PROVENANCE MANAGEMENT SYSTEM FOR DAMPP

4.1 Introduction

The feasibility of dropwise additive manufacturing of pharmaceutical products has been successfully demonstrated both for melt-based and solvent-based formulations, as presented in previous chapters [18], [19]. These feasibility studies included a variety of solvents and polymers as carriers, active pharmaceutical ingredients (API) and substrates such as polymeric films and placebo tablets.

If the DAMPP facility were used to manufacture drug products at a commercial scale then the US Food and Drug Administration (FDA), would require detailed information about the manufacturing process to support a filing for FDA approval as well as for reporting on quality compliance during the actual manufacturing of specific products. For example, if one set of drops constitutes one dose, then data would be required to prove, if so required by the FDA, that the amount of active in the deposited set of drops is indeed within the allowable limits of the prescribed dose for that person. In addition, data for other critical quality attributes, such as dissolution rates, would also be required. If the facility were used by a compounding pharmacy or clinic for production of a dosage for immediate use by patients then too a record of the production to the dosage would be needed in order to document that the dosage produced met specifications. In either case, a

system is required to record and make accessible the data provenance of each and every dosage produced.

To address this need, the DAMPP test bed has the instrumentation to collect a wide range of process variables for process monitoring and control as described in Chapter 3. Additionally, the test bed was integrated with the Knowledge Provenance Management System, KProMS, [63] for the purpose of managing all information generated during a run. For a typical run, KProMS is used to set up each production run and store the data generated during that run, thereby providing a single point of information access. In this chapter, the use of KProMS in managing all aspects of running a DAMPP test bed is demonstrated. First, the important parameters for operating a DAMPP test bed is briefly described, which is followed by the description of the steps in creating an integrated application with KProMS. Then the use of the integrated system for data retrieval and analysis is described.

4.2 DAMPP Test Bed Operation

As a drug product manufacturing system, the DAMPP process must be operated so as to assure and document that critical product quality specifications are met. Thus it requires precise monitoring and control of the manufacturing operations as well as capture and organization of all of the information associated with these operations. The use of DAMPP for a new product formulation generally requires execution of two experimental phases: determining the range of conditions under which good quality drops are formed consistently for that formulation, followed by operation of the manufacturing system

under the most desirable operating conditions in that range. In the case study reported here the use of KProMS to support both phases are addressed.

During the DAMPP test bed operation, the input settings associated with all process units are specified, which is presented in Section 3.3. The input file contains all the input parameter settings, which are required to run the automation program; and it is shown in Figure 3.3. The automation program developed in the LabVIEW environment allows synchronized execution of the process units. As the first step, a selected drug formulation is placed in the materials reservoir. The second step is the IVEK pump, where the previously determined best operating conditions are specified: pump rate (RPM), pump displacement and volume strokes. Using the precision IVEK pump, the material is ejected through the nozzle and deposited on the substrate. The motion sensors detect the drop and the camera automatically captures an image of the falling drop. Using real-time image analysis, the volume is calculated for each drop and the corresponding dosage amount is calculated from the known formulation density and drug concentration. The synchronization logic enables the deposition of the drops on the substrate with pre-defined x - y coordinates, which allows creating a grid-like deposition pattern as well as multi-layered drug formulations. After deposition, the substrate temperature controller is used to control the cooling temperature profile of the drug deposits, with an Infra-Red (IR) camera used to monitor the spatial temperature distribution within the deposit. Both the solidification temperature profile and the formulation properties can have an effect on the bioavailability of the drug products. Therefore post-processing steps can include different quality control tests such as crystallinity measurement or dissolution testing. At the end

of a run, the LabVIEW program generates an output file, which is shown in Figure 3.5, containing all the process monitoring and control parameters for each drop deposited. This includes x - y coordinates, image file name for each drop, drop volume, drop center, actual temperature values. Also the drop images, IR images and quality control results are saved for each run.

4.3 KProMS System

A workflow based Knowledge Provenance Management System, KProMS, that functions as a HUBzero [64] component has been developed at Purdue University. It captures the complete provenance of knowledge by modeling the details of the associated knowledge generation steps as a set of hierarchical workflows. Its unique workflow representation captures relationships between the steps as a network of nodes connected by material and/or information flows. Each data input or output step is represented as a node connected by an information flow to the step processing or generating the data. The general framework can be used for experimental, scientific and business workflows and manufacturing recipes [63].

4.3.1 Using KProMS

The use of the KProMS system broadly consists of two steps: the creation of a workflow(s) to represent the knowledge generation steps and exercising the workflow(s) to create knowledge. A graphical Workflow Builder is used for creating a workflow using the following workflow building blocks: workflow; task; subtask; material source, sink, input, output and flow; and information input, output and flow. For example, the

workflow, named *TB3Basic*, for modeling the DAMPP system is shown in Figure 4.1.a.

The icons used in the workflow are explained here:

- a. Through the blue *TB3Basic* workflow icon, the data entry form can be accessed. This allows the user to specify necessary information about the run. The data entry form is shown in Figure 4.1.b.
- b. The material sources (yellow pentagon: *RI* and *Subs*) represent the formulation and substrate used. The data entry form for formulation material source *RI* is shown in Figure 4.1.c.
- c. A yellow triangle represents material produced.
- d. The workflow consists of the five tasks (green rectangles: *Reservoir*, *IVEK*, *Nozzle*, *Staging* and *Cryst*) which are described in Section 4.2. The data entry form for *IVEK* pump setup task is shown in Figure 4.1.d.
- e. A camera captures the image of each drop released from the nozzle and an IR camera captures the image of drops solidifying on the substrate. The data nodes named *LabviewData*, *IRData* and *CrystData* represent the data created by Labview, IR camera image files and crystallinity data for the dosage forms, respectively.

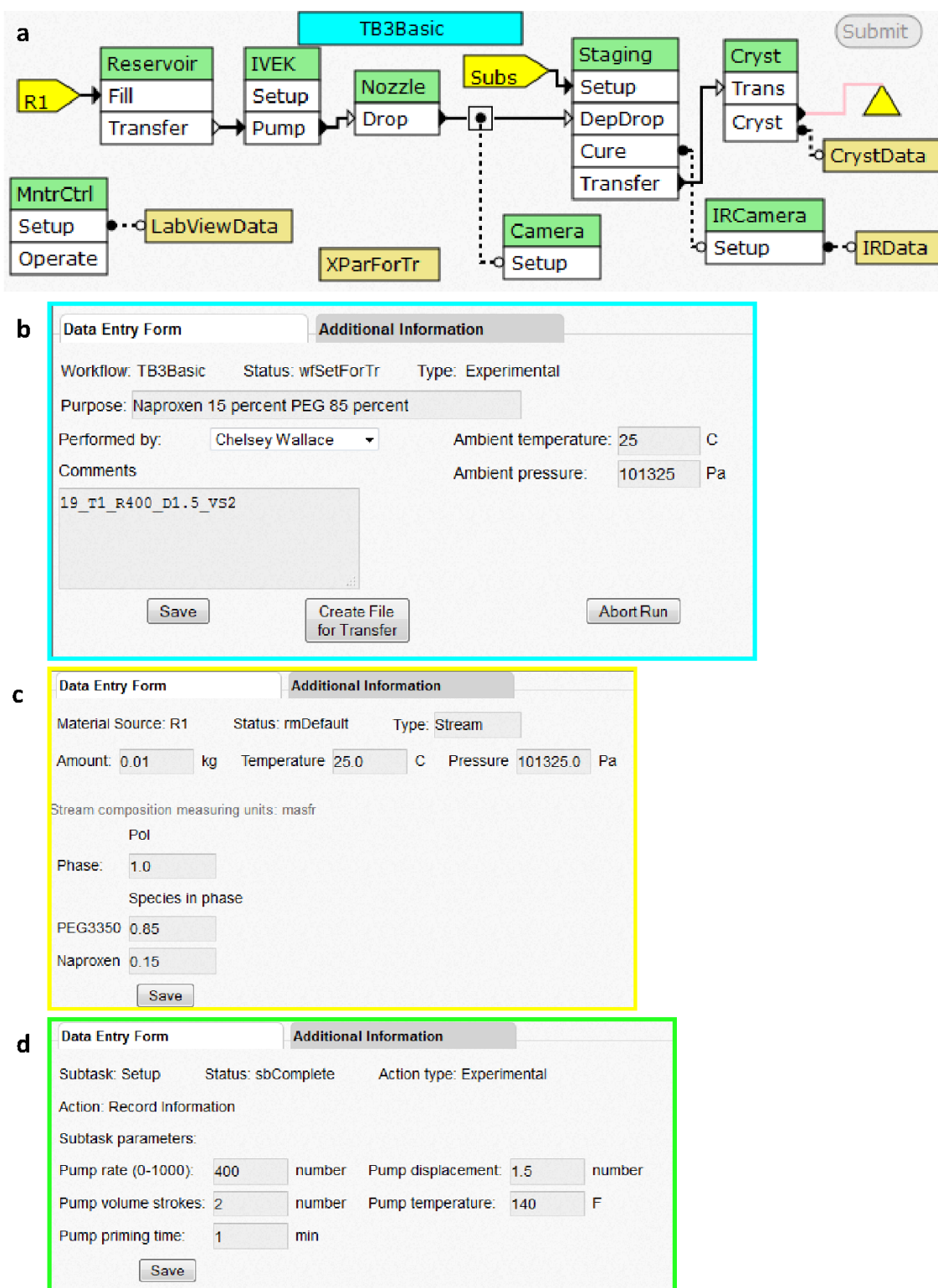


Figure 4.1 a DAMPP system workflow, b. Data entry form for TB3Basic workflow, c. Data entry form for Material Source R1, d. Data entry form for IVEK pump setup task

4.3.2 Management of the DAMPP Test Bed

The first step in managing the information related to the DAMPP test bed is to create the workflow for the associated processing step as shown in Figure 4.1.a. Each production run of the test bed is one instance of the workflow. A production run is associated with the set of drops on substrate strips/tablets produced under given set of fixed operating conditions. A total of 29 task and subtask parameters define the operating conditions for a run, including the set points for pump rpm, number of volume strokes, four temperature settings (reservoir, pump, material line and substrate). The set points are used by the LabVIEW system, which controls the operation of the system.

The steps in executing a run are shown in Figure 4.2. The PC that runs the system via LabVIEW also runs KProMS GUI on the FireFox web browser. After setting up an instance using the KProMS GUI, an intermediate text file consisting of the parameters defined in the *XParForTr* data node shown in Figure 4.1.a is downloaded on the PC in a specific folder. The Virtual Instrument (VI) created for the system is started and the intermediate file is loaded into the VI. The operator confirms that the loaded parameter values are correct by observing the user interface of the LabVIEW automation program shown in Figure 3.2 and starts the run. The run is executed by LabVIEW via communication with the process equipment through the serial and USB ports on the PC according to the design of the VI. During the run, LabVIEW creates a tabular text file consisting of fixed set of columns. Each row in the file has the following key pieces of information about each drop deposited on the substrate: drop volume computed from the

processing the drop image captured by the camera, the name of the .png file which has the drop image, the x and y coordinates of the drop on the substrate.

At the end of the run, the LabVIEW output file and a compressed file consisting of all drop image files are uploaded into the LabViewData data node of the workflow using the KProMS GUI. Similarly, crystallinity data and the IR data about a preselected set of drops, if applicable, are loaded in the *CryData* and *IRData* data nodes of the workflow. Thus, a completed run that is stored in the repository has the complete provenance of the associated run, including all process parameters and outputs along with the relationships defined by the graphical network of the workflow.

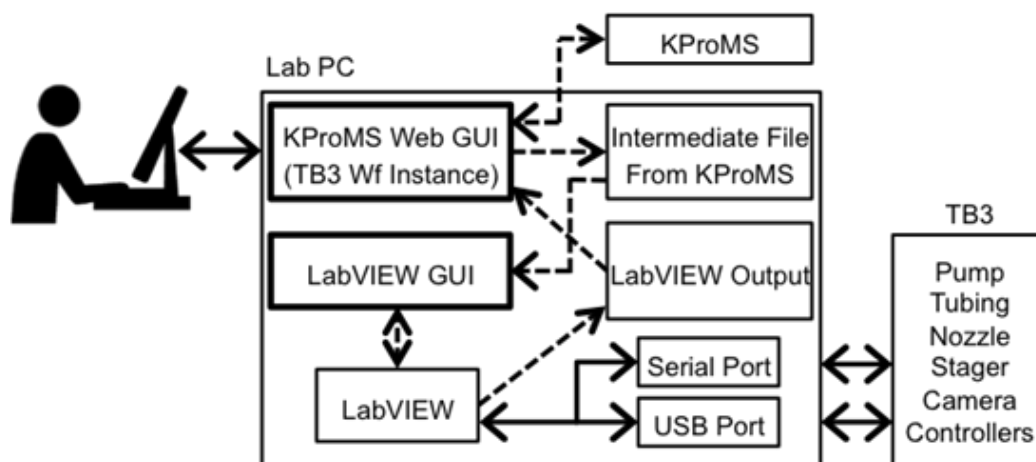


Figure 4.2 Integration of KProMS and the DAMPP test bed

4.4 Data Extraction and Analysis

In order to generate useful knowledge from the execution of the process workflow, data recorded through the KProMS is extracted and analyzed. A data node in a workflow can

have any number of parameters. Each parameter has the following key attributes: name of the file in which the associated data is stored and metadata for the data. The metadata can be predefined or derived from the file structure. In addition, each piece of information stored in the repository using KProMS is accessible with a unique tuple. For example, a task parameter is identified by the triplet (Workflow name, task name, parameter keyword), a subtask parameter identified by the 4-tuple (Workflow name, task name, subtask name, parameter keyword), a column in a data file by the 4-tuple (Workflow name, data node name, parameter keyword, column name) and so on.

The knowledge of metadata and a unique identity for each piece of information facilitate extraction of data using context sensitive menus. A data node of type *Extract Data* can be incorporated into a workflow to represent data extraction step, which could be part of a scientific workflow for analyzing data. An example of a general purpose workflow to draw x-y plots is shown in Figure 4.3.

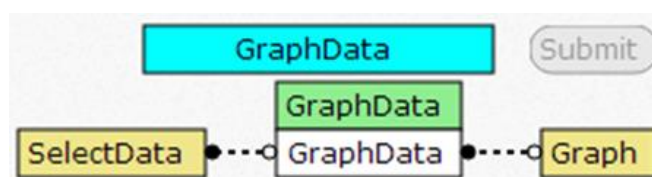


Figure 4.3 Scientific workflow for drawing plots

The *SelectData* node allows specification of the sets of x - y data to extract, for single or multiple runs. The data selection process is shown in Figure 4.4. First a template is selected, such as *TB3Basic:Experimental*. Then instances of that template are selected. In

this case 6 different process runs, 255 through 260, are selected. Next, the data to be extracted is selected. The variables are selected from context sensitive menus to identify the 4-tuple associated with it. Here, the columns in a data file are generated from the metadata. In Figure 4.4, drop number and drop volume are selected for use in *GraphData* workflow.

	Workflow	WfObjLvl1	WfObjLvl2	Parameter	Unit
<input checked="" type="checkbox"/>	TB3Basic	dn:LabView	pa:Drop ser	co:Drop Nur	Numbe
<input checked="" type="checkbox"/>	TB3Basic	dn:LabView	pa:Drop ser	co:Drop volt	ul
<input type="checkbox"/>	TB3Basic	dn:LabViewData	Drop series data	Select One	

- Select One
- co:Time stamp
- co:SheetID
- co:Drop Number
- co:Location on stage (X)
- co:Location on stage (Y)
- co:Reservoir temperature
- co:Tubing temperature
- co:Substrate temperature
- co:Substrate power ouput
- co:Pump volume strokes
- co:Pump Displacement
- co:Pump rate
- co:Pump temperature
- co:Nozzle size

Figure 4.4 Data selection through SelectData node

The *GraphData* program of KProMS draws a plot. An example plot is shown in Figure 4.5.a, where the drop volume vs the drop number is plotted for six different DAMPP production runs 255-260. This plot corresponds to the data selection process shown in Figure 4.4. Runs 255-257 were performed with a pump rate of 400, pump displacement

of 2.5 and volume strokes of 1. These conditions yield an average drop volume of 14.24 μl . For the runs 258-260, the displacement is 1.5, which decreases the average drop size to 9.88 μl .

The KProMS system has a library of programs written in PHP to perform specific computational tasks, including: full factorial DOE, linear multiple regression, and basic statistics for columns of data such as mean, average, standard deviation and relative standard deviation. For the DAMPP run instances the average drop volumes, standard deviation and relative standard deviation within each instance and between different instances are calculated. The reproducibility of drop sizes is crucial for this process, since it directly correlates with the dosage amount. For instances 255-260, the statistics calculations are shown in Figures 4.5.b and 4.5.c.

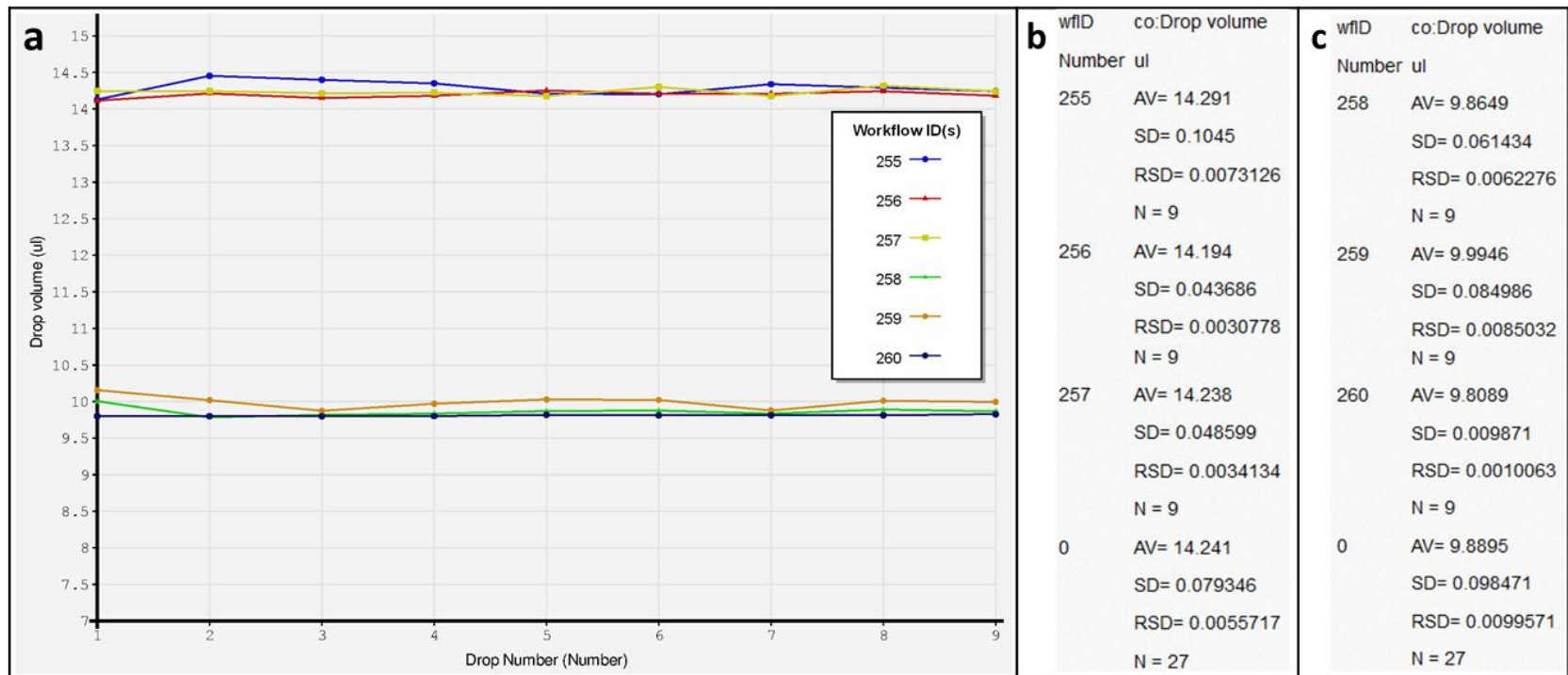


Figure 4.5 a. Drop number vs drop volume for instances 255-260, Basic statistics results for instances b. 255-257 and c. 258-260

4.4.1 Operating Regime Determination

Drop quality depends on the drop dynamics which is affected by fluid properties and operating conditions. For stable drop formation of a selected formulation, the operating regimes should be characterized. For a selected drug formulation, the best operating conditions can be determined either using dimensionless numbers as described in Section 2.2.3 or it can be based on the printing parameters.

4.4.1.1 Operating Regime Based on Dimensionless Numbers

In order to illustrate the regime of fluid properties where successful drop on demand printing can be achieved, the dimensionless numbers such as Re , We and Oh are calculated. First, the fluid parameters are measured for two solvent-based formulations which either consisting of 30% naproxen and 70% PVP K90, or 70% naproxen and 30% PVP K90 dissolved in ethanol. Measured parameters including the density, surface tension and viscosity are listed in Table 4.1. The density is calculated by measuring the weight of solution per unit volume. The surface tension is measured with pendant drop method and viscosity is measured with a rotating cylinder rheometer (Brookfield Engineering Laboratories, Inc., Massachusetts).

Table 4.1 Fluid properties for solvent-based formulations

	30NAP70PVP	70NAP30PVP
Density (g/ml)	0.83	0.83
Interfacial surface tension (mN/m)	24.48	24.14
Viscosity (mPa.s)	73.90	16.37

The fluid velocity is also measured experimentally. At each printing setting, the pump is primed for 30 seconds and the volume of the printed drops is measured with a graduated cylinder. Three measurements are recorded for each setting and the average value is used in the calculations. With the known nozzle diameter and cross sectional area, the fluid velocity is calculated.

Next, the Reynolds, Weber and Ohnesorge numbers are calculated using Equations 2.1 to 2.3 and measured values of velocity, density, nozzle diameter, viscosity and surface tension. The drop formation quality information of solvent-based formulation 30NAP70PVP at various printing settings is presented in Table 4.2 along with the measured velocity values and calculated Re, We and Oh numbers. An operating region graph using Weber and Reynolds numbers is plotted in Figure 4.6. Although a clear distinction between different regions could not be observed, the black arrow demonstrates the transition from printable region to the region, where tail and satellite drop formation is observed, followed by the region, where there is insufficient energy for drop formation. The outlier points shown in Figure 4.6, might be due to experimental errors while measuring various parameters. Similar studies to determine the operating regime using the dimensionless numbers has been done for Newtonian fluids [24]. This preliminary study demonstrates that a similar operating region can be determined for non-Newtonian fluids. However it requires extensive experimental measurement done for each formulation at each printing setting. When the operating region is ready for using in the DAMPP process, it will be incorporated with the KProMS system.

Table 4.2 Dimensionless number calculations for solvent-based formulation Naproxen-PVPK90 (30:70)

Drop Quality	Printing Settings	Nozzle diameter (mm)	Velocity (m/s)	Re	We	Oh
Printable	N17 D2.0 R400	1.15	0.193	2.490	1.449	0.483
Printable	N19 D1.5 R400	0.91	0.281	2.884	2.450	0.543
Printable	N19 D1.5 R500	0.91	0.284	2.915	2.503	0.543
Tail	N17 D2.5 R800	1.15	0.215	2.781	1.807	0.483
Tail	N17 D2.5 R900	1.15	0.208	2.685	1.685	0.483
Tail	N17 D2.0 R800	1.15	0.209	2.698	1.700	0.483
Tail	N17 D2.0 R900	1.15	0.209	2.698	1.700	0.483
Tail	N15 D2.0 R600	1.45	0.126	2.057	0.784	0.430
Satellite	N17 D2.0 R500	1.15	0.192	2.478	1.434	0.483
Satellite	N17 D2.0 R600	1.15	0.197	2.544	1.512	0.483
Satellite	N17 D2.0 R700	1.15	0.206	2.656	1.649	0.483
Not enough energy	N17 D1.5 R400	1.15	0.173	2.241	1.174	0.483
Not enough energy	N17 D1.5 R500	1.15	0.178	2.295	1.231	0.483
Not enough energy	N17 D1.5 R600	1.15	0.178	2.295	1.231	0.483
Not enough energy	N17 D1.5 R700	1.15	0.181	2.337	1.276	0.483
Not enough energy	N17 D1.5 R800	1.15	0.181	2.337	1.276	0.483
Not enough energy	N17 D1.5 R900	1.15	0.178	2.295	1.231	0.483

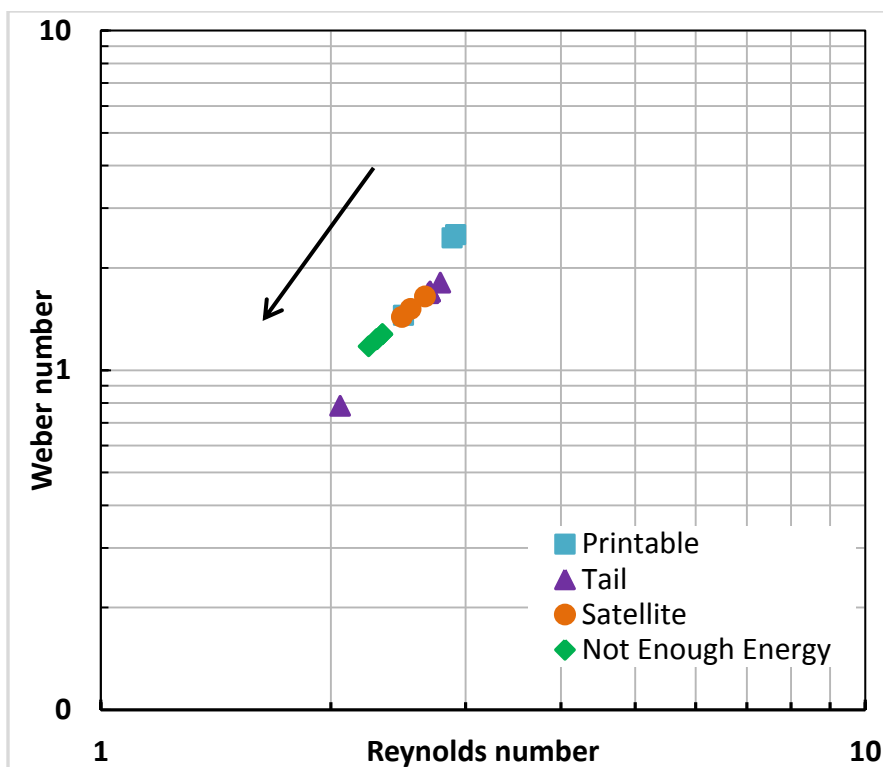


Figure 4.6 Operating regime graph for solvent formulation Naproxen-PVPK90 (30:70)

4.4.1.2 Operating Regime Based on Printing Parameters

For a selected drug formulation the best operating conditions can be determined experimentally. A combination of operating variable values is acceptable if it produces good quality drops where good quality drop formation constitutes reproducible formation of single primary drop with no tail, satellite drops or spraying. Drop specification criteria are demonstrated in Figure 4.7 along with examples of on and off specification drops. The images are taken during operating regime determination of various melt-based formulations.

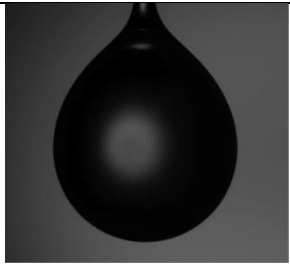
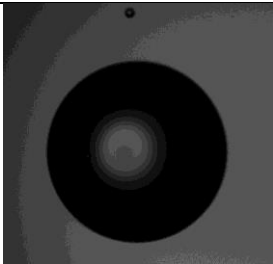
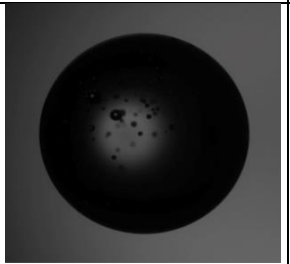
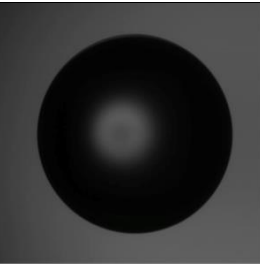
Drop not within specification due to			Drop within specification
tail	satellite drop	spraying	
			

Figure 4.7 Drop specification criteria

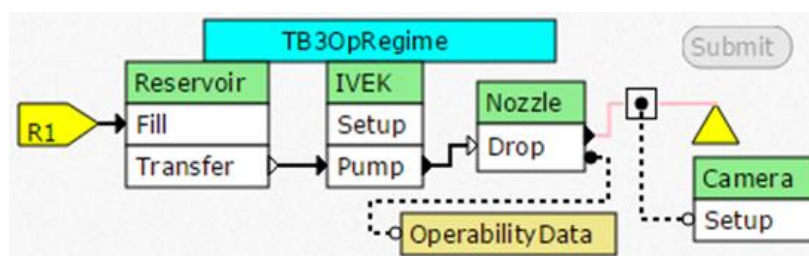


Figure 4.8 Workflow for determining the operating regime

The workflow, named *TB3OpRegime*, for determining the operating regime for a given formulation shown in Figure 4.8. The data node named *OperabilityData* represents the operating regime data created for one combination of nozzle and formulation. An instance of this workflow represents an experiment performed to determine the operating regime for one combination of formulation, nozzle size and operating temperature. The test bed is operated at different settings for pump displacement, pump rate and number of volume strokes. The data file associated with the data node has the following four columns: Pump rate (RPM), pump displacement, number of volume strokes, drop quality. The first three values in each row in the file represent one set of operating conditions, and

the last value represents the quality of drops generated (0 for bad drops, 1 for good drops) under those operating conditions.

The operating regime data corresponding to the experiment with workflow ID: 382 is shown in Table 4.3. The experiment is performed with melt-based formulation consisting of 85% PEG3350 and 15% naproxen, and with reservoir, tubing and pump temperatures controlled at 87.5 °C, 90°C and 140 °F, respectively. The nozzle N19 is used which has an inner diameter of 0.912 mm (19 AWG). In Table 4.3, operating regime data is shown only for pump volume strokes of 2. For melt-based formulations containing polymers as the carrier, volume strokes 2 is the optimum operating region. However, volume strokes 1 and 3 are also tested and good drop quality could not be achieved. The data for all volume strokes is saved in the *OperabilityData* node, but it is not shown here.

Table 4.3 Operating regime data for PEG:NAP (85:15) with nozzle N19 and workflow ID: 382

Pump rate (0-1000)	Pump volume strokes	Pump displacement	Drop quality
Number	Number	Number	Number
300	2	1	0
400	2	1	0
500	2	1	0
600	2	1	0
700	2	1	0
800	2	1	0
900	2	1	0
1000	2	1	0
300	2	1.5	0
400	2	1.5	1
500	2	1.5	1
600	2	1.5	0

Table 4.3 continued

700	2	1.5	0
800	2	1.5	0
900	2	1.5	0
1000	2	1.5	0
300	2	2	0
400	2	2	1
500	2	2	1
600	2	2	1
700	2	2	0
800	2	2	0
900	2	2	0
1000	2	2	0
300	2	2.5	0
400	2	2.5	0
500	2	2.5	1
600	2	2.5	1
700	2	2.5	0
800	2	2.5	0
900	2	2.5	0
1000	2	2.5	0
300	2	3	0
400	2	3	0
500	2	3	0
600	2	3	0
700	2	3	1
800	2	3	0
900	2	3	0
1000	2	3	0

Next, the *GraphData* workflow is used to generate a visual operating region for each formulation. In Figure 4.9, for the same experiment with workflow ID: 382, the operating region is plotted as a combination of pump displacement and pump rate. With the help of this plot, the user can choose from the pump displacement and rates to generate good drops at pump volume strokes 2.

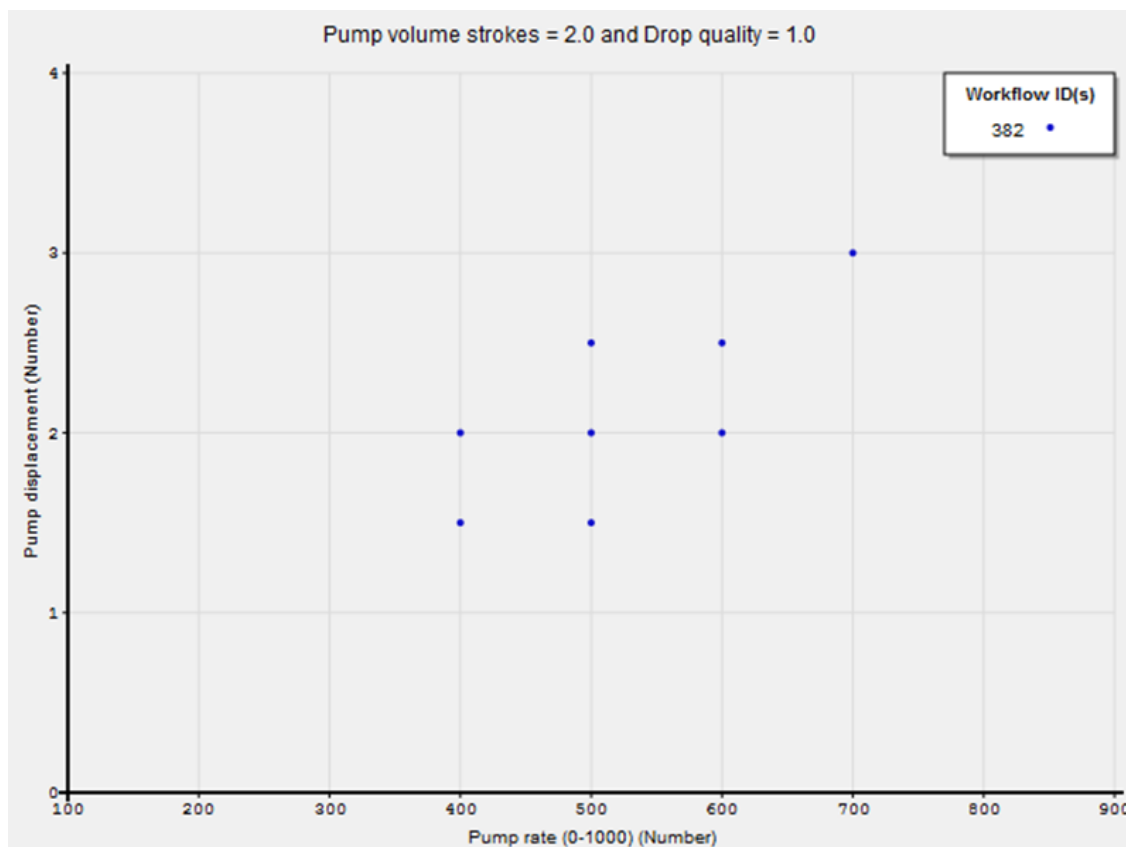


Figure 4.9 Operating region plot

4.5 Conclusions

A knowledge management system is essential to record and make accessible the data provenance of each and every dosage produced via DAMPP. Therefore, the processing steps in the DAMPP system were modelled in the workflow based Knowledge Provenance Management System, KProMS. The integration of the automation program and KProMS allows inputting all process settings data only once through KProMS and successfully running the automation program to execute the process operation. The ability to save the output data file, drop images, IR images and crystallinity data after each process run allows easy access to all process related online or offline generated data.

KProMS is readily and effectively used for managing the data associated with the experimental studies. Through statistical analysis of production runs, the experiments are compared and the best process conditions are determined for the desired outcome, i.e. dosage amount.

Using KProMS, operating regions based on printing parameters are generated for various formulations and this knowledge is later used to execute the process workflow with the best operating conditions. Operating region can also be presented as a printability region based on the dimensionless numbers. In order to develop the printability region accurately, extensive experimental data is needed and the fluid parameters should be determined for each formulations. Preliminary studies of the printability region are presented for solvent-based formulations and in the future it can be extended to melt-based formulations.

KProMS was used by a group of undergraduate researchers to run DAMPP process during their summer internships. It enables the users to build a consensus during their experimental studies by providing a logical structure to organize, store and retrieve data and by allowing easy access to the generated knowledge.

CHAPTER 5. SUPERVISORY CONTROL OF DAMPP: EFFECT OF CRITICAL PROCESS PARAMETERS ON PRODUCT QUALITY OF MELT-BASED SOLID ORAL DOSAGES[‡]

5.1 Introduction

For the dropwise additive manufacturing system, the desired critical quality attributes (CQA) of the dosage forms that should be kept within the appropriate limits are the dosage amount and drug morphology. The critical process parameters (CPP) that have a direct impact on the CQA's are the drop size, product and process temperatures. This chapter presents a supervisory control system implemented on the drop on demand manufacturing process which manipulates these CPP's with the goal of ensuring that the CQA's are maintained within specified limits. This control system is based on the RTPM strategy discussed in Chapter 3, which consists of on-line monitoring, automation and regulatory control. These principles are essential for producing individual dosage forms with the desired critical quality attributes.

First, the supervisory control framework is presented which serves to control critical process parameters such as product temperature and drop size. Then, the effects of process parameters on the final product quality are investigated and the resulting melt-

[‡] This chapter is based on: E. İçten, A. Giridhar, Z. K. Nagy, and G. V Reklaitis, "Drop-on-Demand System for Manufacturing of Melt-based Solid Oral Dosage: Effect of Critical Process Parameters on Product Quality," AAPS PharmSciTech, doi: 10.1208/s12249-015-0348-3, 2015.

based pharmaceutical dosage forms are characterized using various techniques, including Raman spectroscopy, optical microscopy with a hot stage and dissolution testing.

5.2 Supervisory Control Framework

The supervisory control framework applied to the DAMPP is shown in Figure 5.1. It consists of a network of PID loops controlling the process and product temperatures while executing camera, pump and staging simultaneously. This framework enables control of the CPP's to achieve the desired CQA's, which are listed in Table 3.1. The dosage amount is determined from the drop size and the known formulation composition. The product solid state depends on the formulation composition, on the selection of the substrate and on the CPP's, i.e. product temperature and drop size. The selection of the polymer used in the formulation can change the morphology by promoting or inhibiting crystallization of the drug [32].

The product temperature corresponds to the crystallization temperature of the deposited drops. The crystallization temperature profile has a strong effect on product solid state and morphology, which influence the dissolution properties and hence the bioavailability of the drug. In bulk crystallization, a controlled temperature profile followed through the crystallization process can affect the final product properties [27], [48], [65]. Similarly, by manipulating the substrate temperature profile using varying temperature gradients, the drop solidification process can be controlled [28]. Since the drop size also affects the drop solidification process by changing the heat transfer dynamics, precise control of the drop solidification process occurring on the substrate is critical. In the DAMPP process,

the crystallization temperature of the deposited drops is controlled via the Peltier devices placed underneath the substrate on the xy-staging. The substrate temperature control via Peltiers is implemented through a PID loop. Programmed temperature gradients, including step changes, ramping heating or cooling, cycling or any combination of these temperature profiles, can be applied to the drug deposits using the LabVIEW based automation of the substrate temperature control system. As in the case of bulk crystallization processes, cycling of temperature also can be an effective mechanism for control of crystal size, thus controlling feature granularity [66], [67].

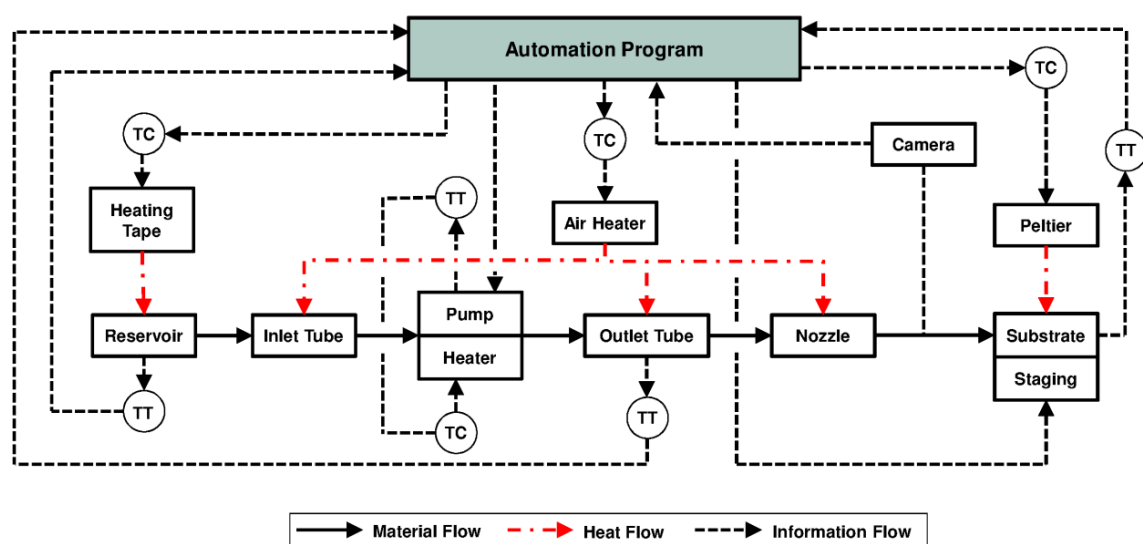


Figure 5.1 Supervisory control framework for DAMPP. TC: temperature controller, TT: temperature transmitter.

5.3 Production of Dosage Forms with Different Critical Process Parameters

In order to study the effects of critical process parameters on the product solid state and morphology, dosage forms of melts were produced using two different drop sizes by

applying different substrate temperature profiles. In this study, naproxen and PEG 3350 were chosen as the model API and polymer. The preparation of the formulation and substrate films were explained in Chapter 2. The dosage forms consisted of 15% naproxen and 85% PEG 3350 by weight. The formulation was co-melted at 65°C, at which temperature the polymer melts and the drug dissolved in the molten polymer. The temperature of the system was controlled at 70°C throughout the process. The molten formulation was subjected to the operating temperature of 70°C during the maximum residence time of 5.4 min, which was achieved with the slowest production rate. In Chapter 2, the chemical stability of naproxen during production was investigated via HPLC experiments, which showed that the drug found in the dosage forms was stable for at least 15 min under the same operating conditions. Since the dosage forms were created and analyzed within a matter of minutes, varying ambient conditions, such as relative humidity, were not impactful on the results.

Two different drop sizes are used to produce the dosage forms with target dosage of 15 mg of API. The different drop sizes are obtained by changing the pump settings such as displacement, volume strokes, and rate as well as nozzle size. For simplicity, the drops with different sizes will be referred as ‘small’ and ‘large’ drops. The reproducibility of the dosage forms are analyzed gravimetrically as described in Chapter 2. The reproducibility results are shown in Table 5.1. A relative standard deviation (RSD) of less than 6% is achieved for melt-based dosage forms produced for this study. These dosage forms were produced before the nozzle holder and the air heating system has been built. Therefore, a single diameter of 1.65 mm was used as the nozzle and the different drop

sizes were achieved by changing the pump printing parameters. In Chapter 2, lower RSD values (less than 2% for most cases) has been reported, where the new nozzle holder and air heating system was used. The number of drops to be printed on the HPMC-PEG films was adjusted depending on the drop size to reach the proper dosage amount. Dosage forms were produced by printing either ‘large’ drops of size 23.4 mg with a standard deviation of 1.4 mg or ‘small’ drops of size 19.4 mg with a standard deviation of 0.3 mg on HPMC-PEG films as the substrate.

Table 5.1 Reproducibility analysis of dosage forms

Drop Size	Average Dosage Amount (mg)	RSD (%)
Small	14.56	1.71
Large	14.27	5.74

5.4 Analysis of Melt Based Solid Oral Dosages

5.4.1 Raman Microscopy: Crystallinity Study

The crystallinity of the melt formulations consisting of 15% naproxen and 85% PEG 3350 was studied using Raman microscopy: Raman RXN1 Microprobe (Kaiser Optical Systems, Michigan). First the spectra of pure naproxen and PEG 3350 solid dispersions were obtained. Naproxen and PEG 3350 powders were heated above their melting temperatures, to 160 °C and 60 °C, respectively. The melts of pure naproxen and pure PEG 3350 were solidified at room temperature and then analyzed to obtain the spectra of pure compounds. The spectra of the melt formulation consisting of 15% naproxen and 85% PEG 3350 were obtained by analyzing the drops of the melt formulation deposited using the dropwise additive manufacturing process.

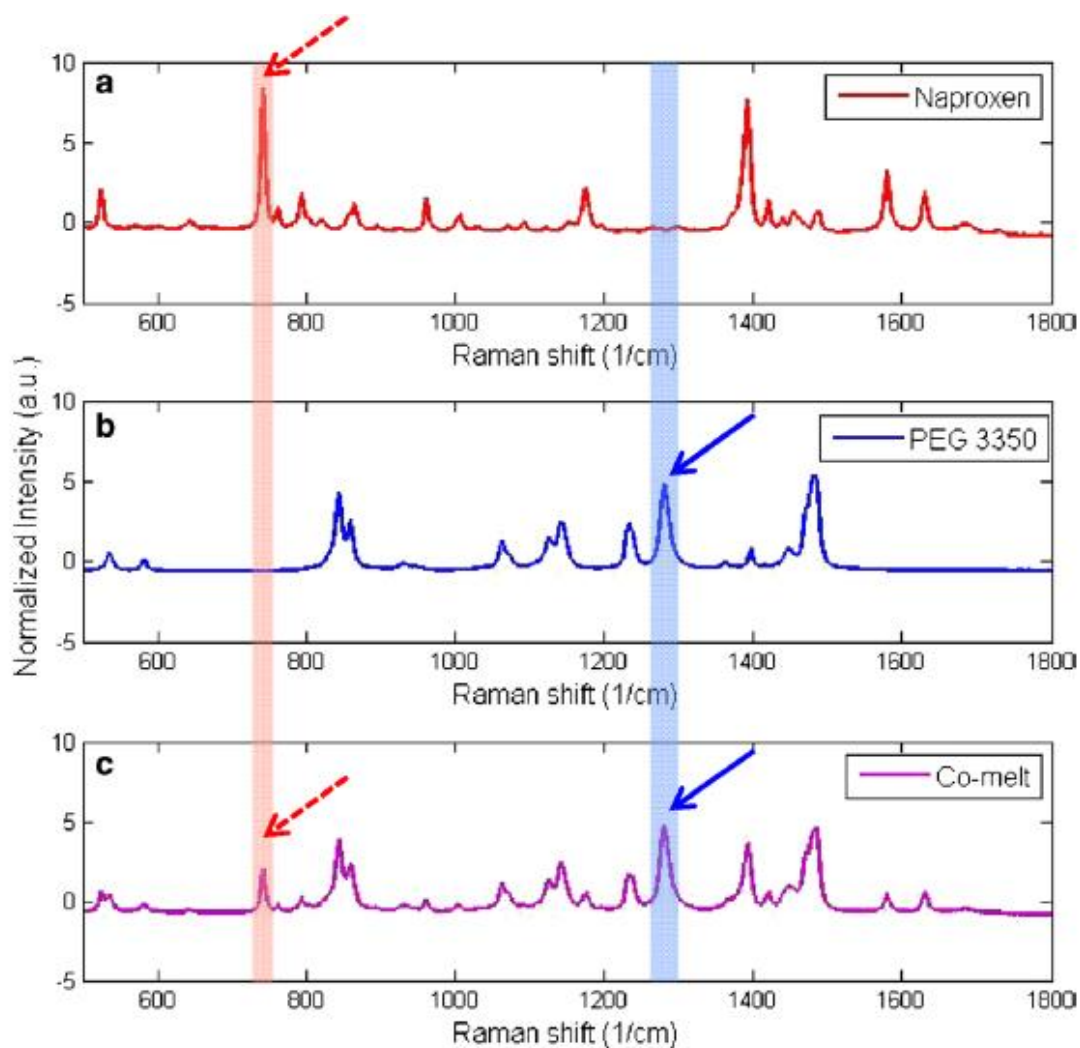


Figure 5.2 Raman spectra of a. pure NAP, b. pure PEG 3350, c. co-melt of NAP-PEG 3350 (15:85). Characteristic peaks at 760 and 1280 cm^{-1} are shown with red and blue arrows, respectively.

Raman spectra of pure naproxen melt, pure PEG 3350 melt and melt-based drug deposits of NAP-PEG 3350 (15:85) are presented in Figures 5.2.a, 5.2.b and 5.2.c, respectively. The characteristic peaks of pure naproxen and pure PEG 3350 at 760 cm^{-1} and 1280 cm^{-1} are used for the analysis. Raman spectra of the dosage forms confirm that naproxen

present in the dosage forms is crystalline, which is in accordance with x-ray diffraction analysis of the same formulation reported in Chapter 2 and by [19].

5.4.2 Raman Mapping: Distribution of API throughout the Drop

The drug distribution throughout the deposited drop is analyzed using Raman mapping employed for the dosage forms. Different areas throughout the drop deposits were analyzed (data not shown). A color intensity Raman map was built based on the ratio of the characteristic peaks of naproxen and PEG 3350. In Figure 5.3, a representative area ($660 \mu\text{m} \times 1000 \mu\text{m}$) of the drop deposits is mapped with $100 \mu\text{m}$ step sizes. The scale on the right hand side represents the ratio of the characteristic peaks of naproxen and PEG 3350 at 760 cm^{-1} and 1280 cm^{-1} , respectively. The small relative intensity differences confirm that naproxen has an even distribution throughout the drop. This finding is in accordance with HPLC analysis conducted on the melt-based formulations, which suggested that the amount of drug recovered from each drop was the same as the amount present in the drug formulation [19]. Here it is shown that in a sample area of the drop, the drug is distributed well within the polymer matrix. Raman measurements performed over different areas of the droplet indicated similarly homogenous drug distribution.

5.5 Effect of Crystallization Temperature Control on Product Solid State

Since the crystallization temperature of the drug deposits has an effect on the product solid state and morphology, precise control of the drop crystallization and solidification processes is crucial to reach the desired product quality. In the DOD system, different programmed cooling temperature profiles were applied to the substrates containing the

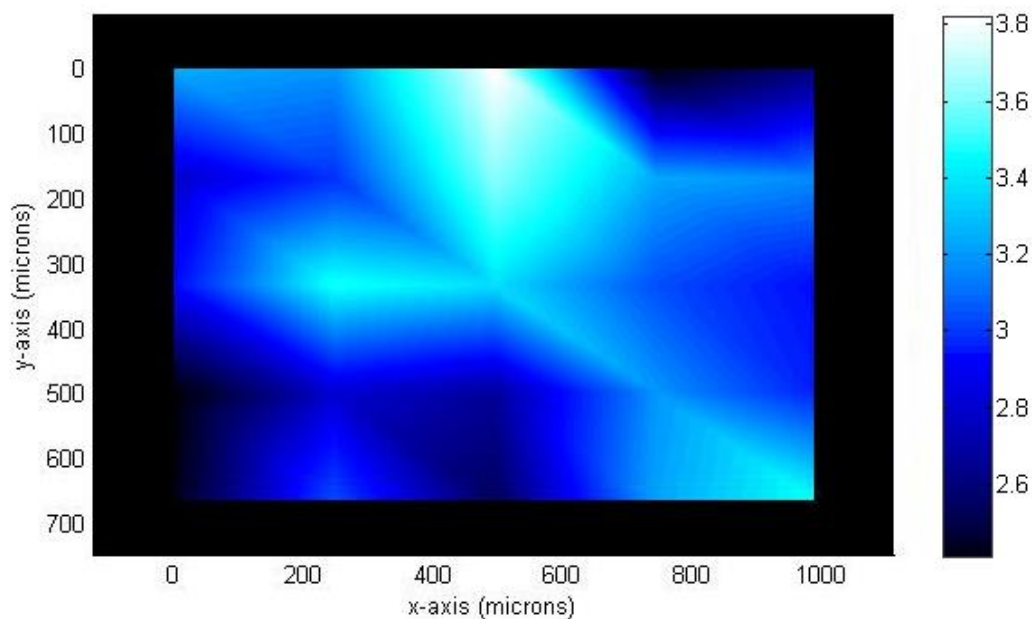


Figure 5.3 Raman map of melt-based deposits of NAP-PEG 3350 (15:85). Map Area 600 μm x 1000 μm .

drug deposits. Specifically, in this study four different temperature profiles were designed and applied via the Peltier devices placed underneath the substrate. The molten deposits were cooled from 60 $^{\circ}\text{C}$ down to 30 $^{\circ}\text{C}$ using different temperature profiles, which are shown in Figure 5.4. A constant temperature profile is achieved by printing the drops onto films maintained at 30 $^{\circ}\text{C}$ and by controlling its temperature at 30 $^{\circ}\text{C}$ until the drops are solidified. The other dosage forms were printed onto films maintained at 60 $^{\circ}\text{C}$ and cooled down to 30 $^{\circ}\text{C}$ using: a fast cooling rate of 10 $^{\circ}\text{C}/\text{min}$; or a slow cooling rate of 1 $^{\circ}\text{C}/\text{min}$; or by applying heating/cooling cycles where the dosage forms were cooled with repeated cycles of cooling with a rate of 10 $^{\circ}\text{C}/\text{min}$ for one minute followed by heating with a rate of 1 $^{\circ}\text{C}/\text{min}$ for one minute until the deposit reached 30 $^{\circ}\text{C}$.

In order to study the crystallization of the drug within the dosage forms under different temperature profiles, optical microscopy experiments are performed with a hot stage following the cooling temperature profiles shown on Figure 5.4. A Zeiss Axio Imager A2m polarized light microscope (Carl Zeiss Microscopy, LLC, NY) equipped with a Linkam THMS 600 hot-stage (Linkam Scientific Instruments Ltd., Surrey, UK) was used for this study. The naproxen and PEG 3350 were physically mixed in (15:85) weight ratio and heated to 65 °C until completely melted. After a homogeneous melt was formed, it was cooled down to 30 °C with the different cooling rates shown in Figure 5.4.

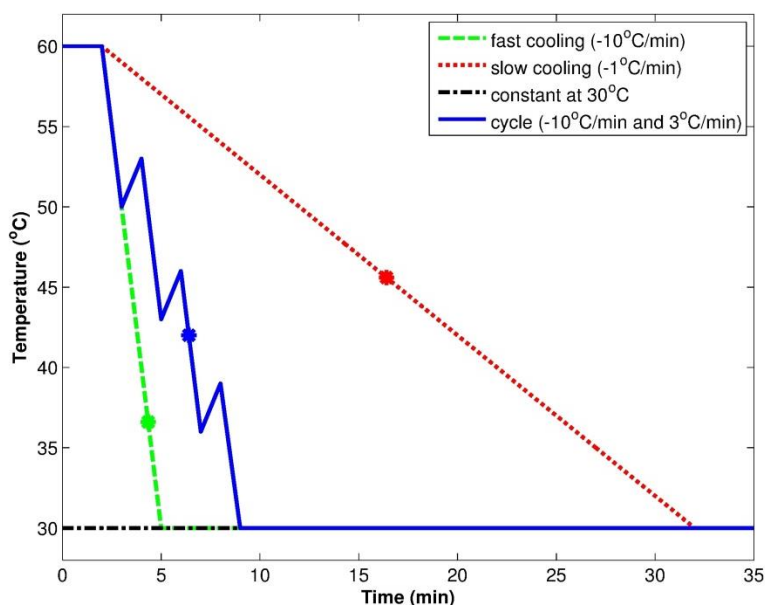


Figure 5.4 Temperature profiles applied on the substrate

Although there were no differences observed in the crystallinity of the dosage forms, the application of different temperature profiles did in fact change the crystallization behavior and morphology. The induction times for crystal formation showed differences

based on the temperature profile applied. Using the images recorded via hot-stage microscopy, the induction time and temperatures corresponding to the first nucleus formation were determined. In Figure 5.4, the induction times are shown with the points marked on the fast cooling, slow cooling and cycling temperature profile curves. The measurements were taken in replicates to determine the mean induction temperatures and times, and the corresponding standard deviations are listed in Table 5.2. Under the fast cooling profile, the induction occurs at 36.6 °C in 4.3 min. Under cycling and slow cooling temperature profiles, the average induction temperatures are 42.0 °C and 45.6 °C occurring in 6.4 min and 16.4 min, respectively. These results indicated that instead of applying slow cooling for 16.4 min, a designed temperature cycle can be applied to shorten the induction time by keeping the induction temperature, hence crystallization behavior, similar.

Table 5.2 Induction points when different temperature profiles are applied

	Fast Cooling	Cycling	Slow Cooling
Induction Temperature (°C)	36.6 ± 1.5	42.0 ± 0.8	45.6 ± 1.5
Induction Time(min)	4.3	6.4	16.4

In addition to the differences observed in the crystallization behavior, morphological differences are also observed between the dosages solidified under different temperature profiles using optical microscopy with a hot stage. When the melts are cooled down with the fast cooling rate of 10 °C/min, surface defects are observed, which are shown in Figure 5.5.a. This is mainly due to the fact that fast cooling resulted in more nucleation sites during crystallization, thus producing higher surface area of crystals.



Figure 5.5 Optical microscopy images of melt-based deposits (Naproxen-PEG 3350) after a. fast cooling, b. slow cooling, c. cycling.

When the melts are cooled down with the slow cooling rate of 1 °C/min, surface defects were reduced, however they were still observed as shown in Figure 5.5.b. When the melts were subjected to the cycling temperature profile, the surface defects were eliminated, as shown in Figure 5.5.c. With designed cycles and through repeated partial re-melting and solidifying the dosage forms, alternative morphology changes can be obtained.

5.6 Effect of Critical Process Parameters on the Dissolution of Dosage Forms

The crystallization temperature profile applied to the drug deposits affects both the crystallization behavior and the morphology of the drug, which are known to influence both the dissolution behavior and bioavailability of the drug. Therefore, dissolution testing was performed to study the effect of the substrate temperature profile and also the effect of the drop size on the dissolution properties of the drug. Dissolution testing is performed as described in Chapter 2. Dosage forms of melts containing 15% naproxen and 85% PEG 3350 were produced using small and large drop sizes by applying different substrate temperature profiles.

First, the effect of substrate temperature profile was studied and the dissolution behaviors of the dosage forms produced with the same drop size and following different cooling profiles were compared. The dissolution profiles of the dosage forms, which are produced with small drop size and solidified using fast or slow cooling rates, are compared in Figure 5.6. When the fast cooling rate of 10 °C/min is applied to the dosage forms containing small drops, faster dissolution is observed than is seen with samples produced with the slower cooling rate of 1 °C/min. The dissolution profiles of the dosage forms,

which are produced with large drop size and solidified using fast or slow cooling rates, are compared in Figure 5.7. Similar to the behavior of the dosage forms containing small drops, faster dissolution is observed when the fast cooling rate of 10 °C/min is applied to the dosage forms containing large drops. During fast cooling, more nucleation sites are created that result in higher surface area, which was also observed with hot-stage microscopy experiments, and therefore in faster dissolution of the dosage forms.

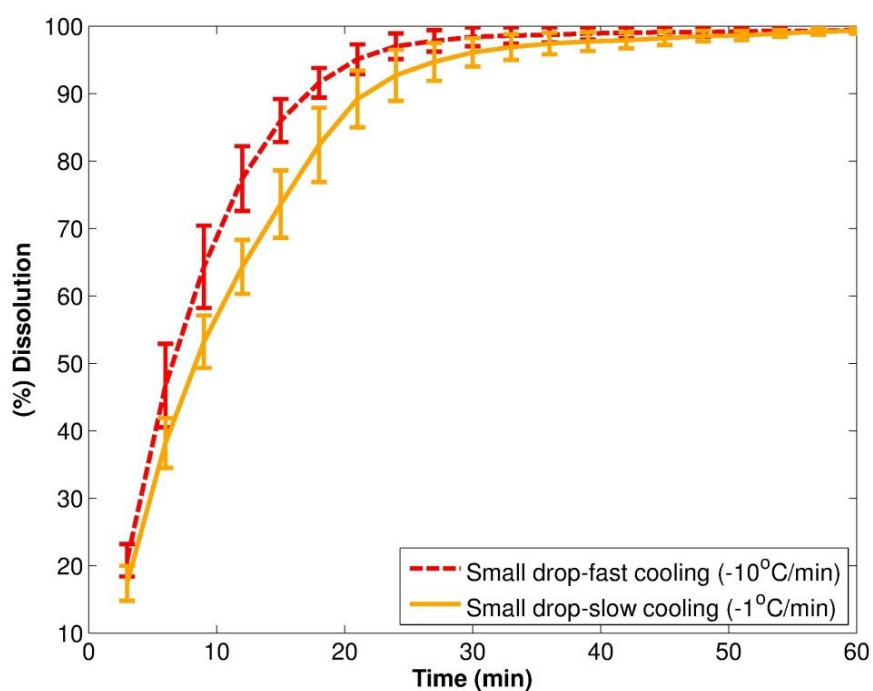


Figure 5.6 Effect of different cooling profiles on the dissolution of the dosage forms created with small drops.

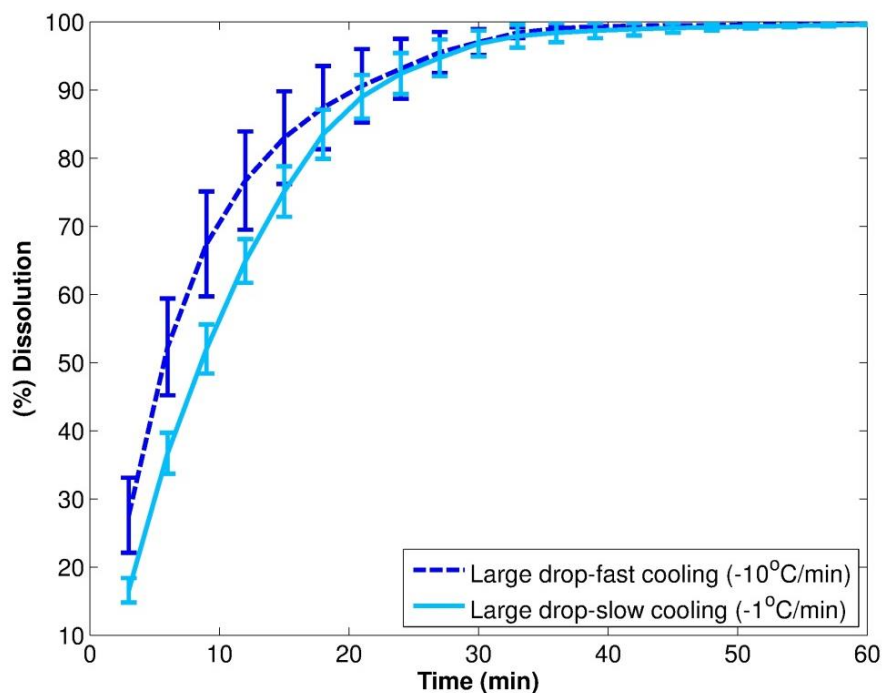


Figure 5.7 Effect of different cooling profiles on the dissolution of the dosage forms created with small drops.

The effect of the drop size was further investigated and the dissolution behavior were compared for the dosage forms containing either large or small drops under the same crystallization temperature profiles. When the temperature of the drug deposits containing either small or large drops are controlled at a constant temperature of 30 °C, significant variation of the dissolution profiles are observed both within the dosage forms of the same drop size and between the dosage forms containing different drop sizes. This variation is evident from the error bars shown in Figure 5.8.a. When the substrate temperature is held constant, then the cooling profile within the droplets is influenced by their volume, which can result in significant variations in the crystallization conditions. While control of the temperature of the deposits was exercised by manipulating the temperature of the surface of the Peltier, the temperature within a deposit is non-uniform.

Indeed infra-red camera images of melt-deposits solidifying at room temperature, shown in Figure 5.9, indicate that there are temperature gradients present within the drops.

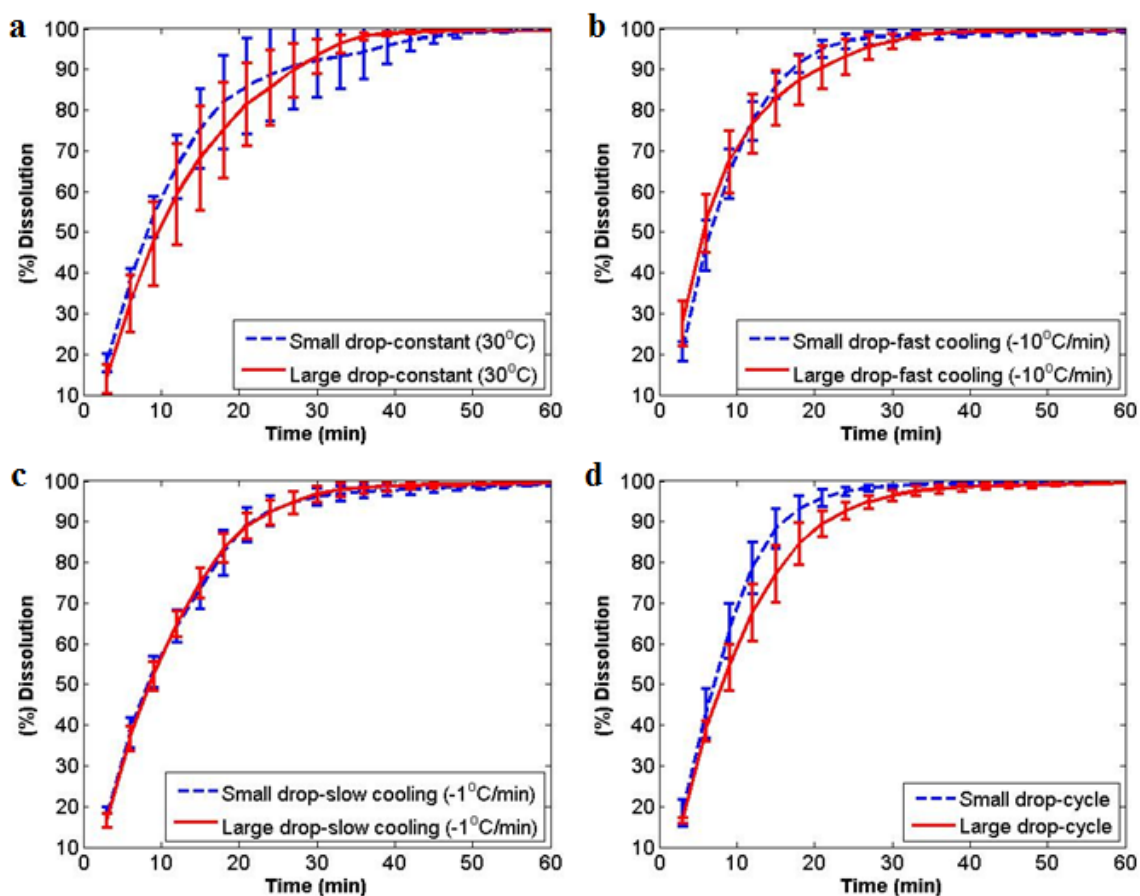


Figure 5.8 Dissolution profiles of the dosage forms created with two different drop sizes and solidified at different temperature profiles: a. constant temperature, b. fast cooling, c. slow cooling, d. cycling.

However, when the drug deposits are solidified by applying a fast cooling rate of 10 °C/min; the temperature gradient within the dosages containing the same drop size decreases significantly. Thus, this results in smaller variation in the dissolution profile for the dosage forms containing the same size of droplets, which reflected in the reduced

error bars shown in Figure 5.8.b. In the case of solidification of dosage forms by applying a slow cooling rate of 1 °C/min, the differences in the dissolution profile of the dosages containing both the same drop size and different drop sizes decrease further, as shown in Figure 5.8.c. The use of the slow cooling profile minimizes the differences due to drop size by enabling better heat transfer and thus minimizes the spatial distribution of temperature differences.

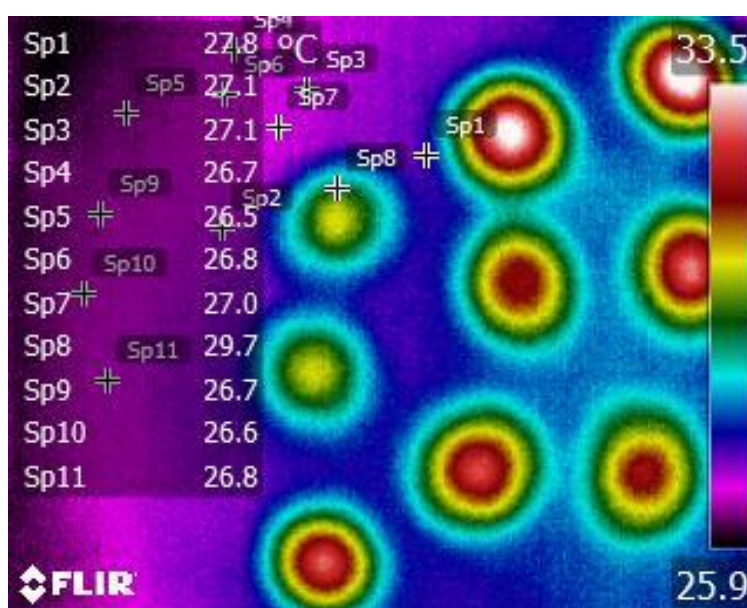


Figure 5.9 Infrared camera image of melt-based deposits solidifying at room temperature

Finally, the effect of cycling of the substrate temperature on the dissolution profile was studied. The effect of the drop sizes used can be seen in terms of the different dissolution rates. There are small variations in the dissolution of the dosages produced with the same drop size as represented by reduced error bars in Figure 5.8.d. Cycling of temperature is also an effective mechanism for the control of crystal morphology as further discussed in

the previous section. Designed cycles can be used to eliminate surface defect and achieve morphological changes by repeated partial re-melting and solidifying the dosage forms. It can also be used to reduce the time for crystallization and achieve a similar crystallization behavior.

Since pharmaceutical products must meet the target bioavailability regardless of their dosage amount, knowledge of the effect of the process conditions on the dissolution of the drug is of utmost importance. Thus by applying an appropriate cooling profile the differences due to drop sizes can be minimized and a desired dissolution rate can be achieved for dosages with different drop sizes.

With the model formulation used in this study, the amorphous form of naproxen is not produced in the presence of PEG 3350, since it actually promotes crystallization of naproxen. However amorphous forms can be produced with alternative choice of polymers, which inhibit crystallization, along with suitable choice of operating conditions. It is well known that the dissolution of low-solubility drugs can be enhanced, by producing product forms in which the active is in amorphous forms. However since stability of amorphous drug forms can be challenging, design of crystallization temperature profile and precise control of substrate temperature profile are even more important than in the case of crystalline API formulations.

5.7 Conclusions

In this chapter, a supervisory control system implemented for the dropwise additive manufacturing process is reported which has as its goal ensuring reproducible production and final product quality. The effect of the critical process parameters, such as drop size and product and process temperatures, on the final product quality, namely dosage amount and drug morphology, is investigated and the produced melt-based pharmaceutical dosage forms are analyzed. Dosage forms of melts containing the model formulation of naproxen and PEG were produced using small and large drop sizes by following selected substrate temperature profiles, including cooling ramping profiles, constant temperature and temperature cycling. The presented crystallization temperature control strategy is used to tailor the crystallization behavior of drug deposits and to achieve consistent drug morphology. Hot-stage microscopy studies prove that the different product morphologies can be achieved by controlling the cooling profile. The results indicate that by applying controlled temperature cycles on the deposits, the desired drug morphology and crystallization behavior can be achieved. Moreover, melt-based dosages of smaller drops have faster dissolution compared to melt-based dosages of larger drops with the same dosage amount. Thus, the supervisory control strategy can be used to monitor the drop size online and to predict a crystallization temperature profile for the monitored drop size such that the desired bioavailability of the drug is achieved and variations in the dissolution profiles due to variable dosage amount are mitigated. Such a process control strategy is developed and presented in the next chapter. Hence, it enables the application of the drop on demand system for the production of individualized dosage regimens for personalized treatments.

Although the use of PEG in the formulation enhances the dissolution of naproxen, the API present in the melt-based formulation is in crystalline form. Solubility of APIs can be enhanced further by using the active ingredient in the amorphous form which is discussed in Chapter 8. Amorphous forms can be stabilized through designed temperature profiles, which can be then controlled and applied with the supervisory control system.

CHAPTER 6. PROCESS CONTROL OF THE DROPWISE ADDITIVE
MANUFACTURING SYSTEM USING POLYNOMIAL CHAOS EXPANSION
BASED SURROGATE MODEL[§]

6.1 Introduction

The development of a supervisory control framework on DAMPP, including on-line monitoring, automation and closed-loop control, is presented in the previous chapter. The effect of the critical process parameters on the final drug property is investigated and it is shown that implementation of a supervisory control system on the process is essential for producing individual dosage forms with the desired critical quality attributes. This chapter presents an improved process control framework, which assures precise control of formulation composition, drop size, deposit morphology and drug dissolution [68].

In order to achieve proper product morphology, a data driven approach based on polynomial chaos expansion (PCE) is used to relate the critical process parameters to deposit morphology using dissolution data of the active pharmaceutical ingredient. The dissolution testing is a standardized off-line laboratory procedure widely used as indicator of bioavailability. The PCE-based surrogate model is then used in an optimal control framework to determine the required temperature profile to achieve a desired

[§] This chapter is based on: E. Içten, Z. K. Nagy, and G. V. Reklaitis, “Process control of a dropwise additive manufacturing system for pharmaceuticals using polynomial chaos expansion based surrogate model,” *Computers & Chemical Engineering*, vol. 83, pp. 221–231, 2015.

bioavailability. In pharmaceutical manufacture, the preferred product quality targets are those closer to reflecting the performance of the product in the patient, such as dissolution, than are traditional quality metrics, such as composition. As noted in recent FDA publications [69], the ultimate goal is real time release of product, that is, by passing of the traditional laboratory-based quality control step, such as dissolution testing, through use of measurement and advanced control methods during manufacture so as to allow product to be ready for release to the market immediately upon manufacture. The process control strategy reported in this chapter is novel not only in providing effective control of the drop on demand manufacturing process but also is one of the first efforts in the literature demonstrating elements of model-based real time release (MBRTR) and the concept of quality-by-control (QbC), whereby product performance and consistent quality are achieved by the design of suitable control strategies.

6.2 Process Control Strategy

The process control strategy for the dropwise additive manufacturing process is shown in Figure 6.1. The control strategy consists of two main parts: a supervisory control system and a surrogate model based hierarchical control layer. The supervisory control system is described in Chapter 5 along with the effect of CPP's on the quality attributes of drug products. The supervisory control system provides effective control of the drop on demand manufacturing process, whereas the surrogate model based hierarchical control layer demonstrates the indirect control of drug dissolution online and enables model-based real time release of solid oral dosages.

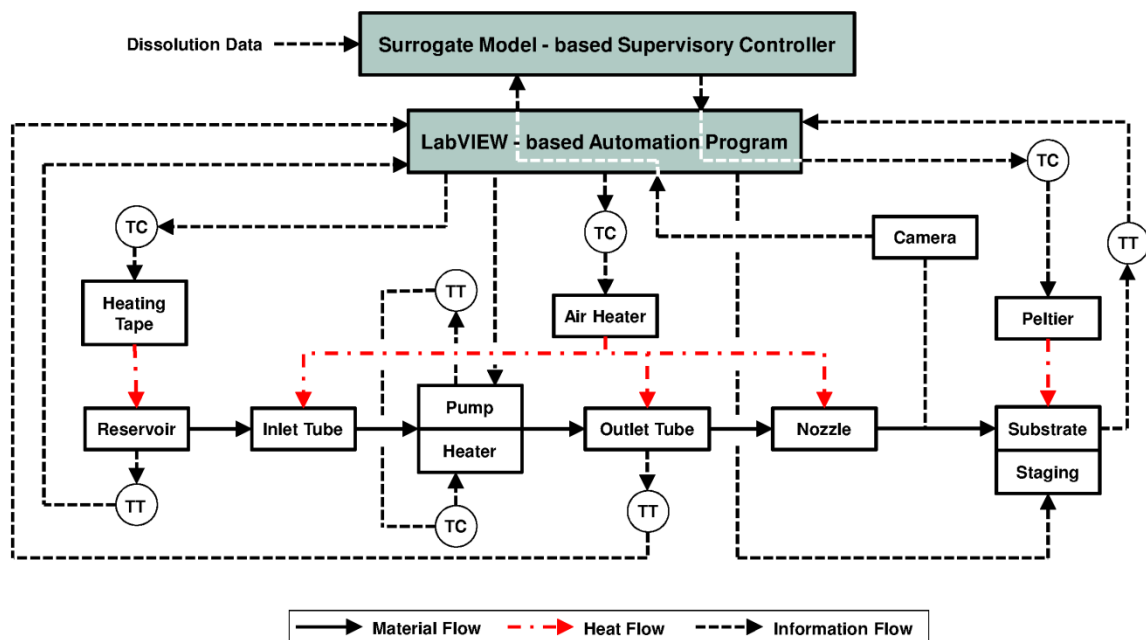


Figure 6.1 Process control strategy for DAMPP

6.2.1 Surrogate Model-based Hierarchical Control System

A surrogate model-based hierarchical control system is implemented on top of the low-level control system to ensure that the drug products have the desired product morphology regardless of their dosage amount, i.e. drop size. This can be achieved by monitoring the drop size via the online imaging system and manipulating the temperature profile applied on the substrate for the measured drop size to ensure consistent quality attributes. The crystallization temperature profile has a strong effect on product solid state and morphology, which influence the dissolution performance of the drug.

In the pharmaceutical industry, drug dissolution testing is performed as a standard requirement to provide critical in vitro drug release information for quality control

purposes of solid oral dosage forms. The effectiveness of solid oral dosage forms relies on the drug dissolving in the fluids of the gastrointestinal tract prior to absorption into the systemic circulation. The rate of dissolution of a dosage form therefore influences the amount of drug available to the body, i.e. its bioavailability. Since inadequacies in bioavailability can result in ineffective or excessive treatment, precise control of the drop solidification process occurring on the substrate is critical.

In order to optimize the temperature profile applied on the substrate, a data driven modelling approach is used which relates the temperature profiles to the dissolution properties of the drug as a measure of product quality. With this approach, consistent dissolution profile can be achieved for drug products containing different drop sizes. The effect of critical process parameters on product quality is investigated in Chapter 5. It is shown that the differences in the drop size create a cooling temperature gradient within the drop deposits, which affects the dissolution properties of the drug. This knowledge is used to build a surrogate model-based control system, which is described in Section 6.3, and to optimize the temperature profiles as outlined in Section 6.4.

6.3 Polynomial Chaos Expansion Based Surrogate Model Development

Due to the nonlinear behavior of the solidification and crystallization processes occurring within the melt drops and due to the presence of disturbances, the typical linear data driven modeling approaches may be challenged in relating the crystallization temperature profiles to the dissolution profile with acceptable accuracy. A methodology based on nonlinear data driven modelling approaches such as artificial neural networks (ANN) or

polynomial chaos expansions (PCE) can be used to develop a surrogate model describing this system. A surrogate model can be thought of as a “regression” to a set of data, where the data is a set of input–output pairings obtained by evaluating a black-box model of the complex system [70], [71]. Maintaining fidelity while being computationally economical are the main aspects to consider while choosing a surrogate model for a certain application [72].

ANNs are mathematical models consisting of interconnected simple processing units, known as neurons, represented in input-output layers along with hidden layer(s) [73]. The parameters of a network include weights and biases, and the operation performed at each neuron. The problem of fitting these parameters is known as training the network. One disadvantage of ANNs is the need for selecting the number of neurons, which must be sufficiently high to capture functional behavior but not so high as to cause overfitting [71]. In the case of a limited number of experimental data, capturing functional behavior can be a challenge. Another disadvantage of ANNs is that there are no mechanisms for taking into account the nature of the distribution functions of the uncertainties in the data.

Polynomial chaos is a type of spectral method with useful properties that can be exploited for the computations of surrogate model generation and parameter determination [74]. Polynomial chaos expansion was introduced by (Wiener, 1938) for turbulence modeling [75] and it became popular only in the last few decades after the surge of fast computers with parallel computing ability [74]. The implementation of PCEs in terms of Hermite polynomials for linear elastic problems [76] started broadening the application area of

this method. More recently, since the discovery of the possible uses of PCE to define the uncertain model as a deterministic model with an extended number of variables, PCE has been applied in a large variety of disciplines [77]. Its application areas include computational fluid dynamics [78], robust design problems [79] and chemical processes [77], [80].

In this work, a methodology based on polynomial chaos expansion (PCE) containing orthogonal basis with respect to the Gaussian probability measure is used to develop a surrogate model [74]. PCE can be used to replace a nonlinear system with a surrogate model that adequately describes the input to state and input to output behavior [80]. PCE offers three main advantages: small number of parameters hence efficiency in using experimental data, ability to incorporate information about parameter uncertainty and an expansion structure which allows convenience incorporation of additional nonlinear terms if the data requires it. If the parameter uncertainties are described in terms of standard normal random variables, the PCE can describe the model output ψ as an expansion of multidimensional Hermite polynomial functions of the uncertain parameters θ [80]. Using the Hermite bases in the PCE, the output can be expressed in terms of the standard random normal variables θ_i using an expansion of order d :

$$\psi^{(d)} = \underbrace{a_o^{(d)} \Gamma_o}_{\text{constant}} + \underbrace{\sum_{i_1=1}^{n_\theta} a_{i_1}^{(d)} \Gamma_1(\theta_{i_1})}_{\text{firstorderterms}} + \underbrace{\sum_{i_1=1}^{n_\theta} \sum_{i_2=1}^{i_1} a_{i_1 i_2}^{(d)} \Gamma_2(\theta_{i_1}, \theta_{i_2})}_{\text{secondorderterms}} + \underbrace{\sum_{i_1=1}^{n_\theta} \sum_{i_2=1}^{i_1} \sum_{i_3=1}^{i_2} a_{i_1 i_2 i_3}^{(d)} \Gamma_3(\theta_{i_1}, \theta_{i_2}, \theta_{i_3})}_{\text{thirdorderterms}} + \dots \quad \text{Eq. 6.1}$$

where n_θ is the number of parameters and $a_{i_1}^{(d)}, a_{i_2}^{(d)}, a_{i_2 i_3}^{(d)}, \dots$ are deterministic coefficients in \mathbb{R} to be estimated [80]. The multidimensional Hermite polynomials of degree $m = i_1, i_2, \dots, i_{n_\theta}$, $\Gamma_m(\theta_{i_1}, \dots, \theta_{i_m})$ are

$$\Gamma_m(\theta_{i_1}, \dots, \theta_{i_m}) = (-1)^m e^{1/2\theta^T \theta} \frac{\partial^m e^{-1/2\theta^T \theta}}{\partial \theta_{i_1} \dots \partial \theta_{i_m}} \quad \text{Eq. 6.2}$$

The number of coefficients N in the PCE depends on the number of uncertain parameters and the order of expansion. It can be calculated as

$$N = 1 + \frac{n_\theta!}{(n_\theta - 1)!1!} + \frac{(n_\theta + 1)!}{(n_\theta - 1)!2!} + \frac{(n_\theta + 2)!}{(n_\theta - 1)!3!} + \dots + \frac{(n_\theta + m - 1)!}{(n_\theta - 1)!m!} \quad \text{Eq. 6.3}$$

For most engineering applications, the use of third or fourth order expansion is sufficient. However, the determination of the most appropriate number of terms to be used in the expansion needs to be made for each application. For instance Nagy and Braatz (2007) reported that a second order model was sufficient in the case of a batch crystallization process application and thus that the use of third order PCE model was not required [80]. The use of high order expansion increase the number of coefficients required for the model development. In the case of limited number of experimental data available, lower order PCE models are preferred.

The polynomial chaos expansion is convergent in the mean-square sense [76]. Therefore the coefficients in the PCE $a_{i_1}^{(d)}, a_{i_2}^{(d)}, a_{i_2 i_3}^{(d)}, \dots$ can be calculated using least square

minimization by considering sample input-output pairs from the model to achieve the best fit between the surrogate PCE model and the experimental data [80]. The initial coefficients in the PCE are selected randomly. Since the initial coefficients affect the accuracy of the calculations, the coefficients from the previous solution are used to perform the least square minimization iteratively until there is no significant difference between the predicted outputs. In this manner, the best PCE parameters can be determined. The steps of the surrogate model development using PCE are shown in the flowchart in Figure 6.2.

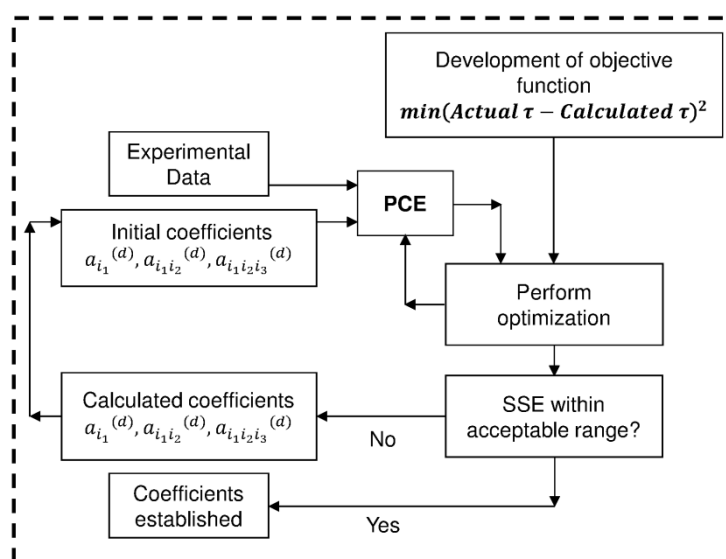


Figure 6.2 PCE based surrogate model development

This computationally efficient method is used to generate a data driven input-output model relating temperature control profiles and the dissolution profiles of the dosage forms produced with the dropwise additive manufacturing process. In the pharmaceutical industry, it is common practice to treat the uncertainties in dissolution data as normally

distributed [81]. Moreover, uncertainties in temperature measurements via thermocouples are generally accepted to have normal distributions. Consequently, normal distribution on the model input data is assumed and therefore orthogonal Hermite polynomials are used in the PCE model. However if the uncertainties are not normally distributed, then different orthogonal polynomials with different distribution types can be used in PCE model development, including Jacobi, Legendre, Laguerre and Chebyshev polynomials [74].

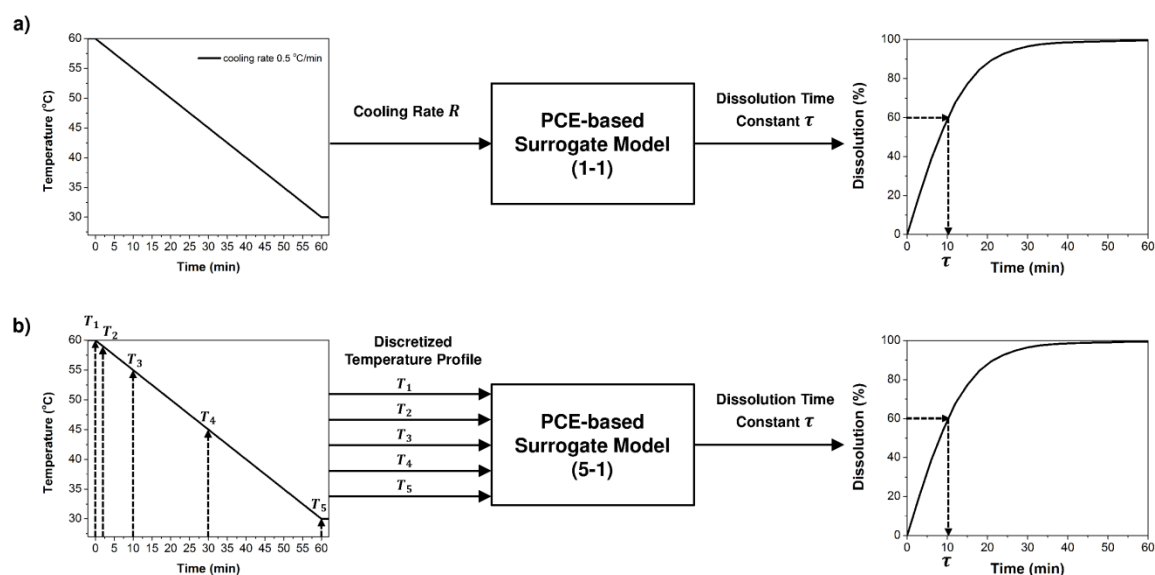


Figure 6.3 Input-output pairs for (1-1) and (5-1) PCE-based surrogate models

In Figure 6.3, two different representations of the model inputs, i.e. temperature profiles, and the model outputs, i.e. dissolution profiles, are shown. Different PCE models can be developed with different numbers of input data, which are required to describe the system accurately. In Figure 6.3.a, (1-1) PCE model representing single input-single output case

is shown. For (1-1) PCE model, the temperature control profiles are described with a single input data representing the linear cooling rate applied to the drops. In Figure 6.3.b, (5-1) PCE model representing multiple input-single output case is shown. For (5-1) PCE model, the temperature control profiles are represented as the temperature values corresponding to discrete times. These time values are selected to ensure distinct discretization between different temperature profiles.

In addition to better accuracy, another advantage of the (5-1) PCE model is that more complex temperature trajectories can be included in the hierarchical control scheme, not only linear cooling, enabling better control of the dissolution profile. The output data is calculated as the characteristic time constant τ corresponding to time to reach 60 % of total dissolution, which would be an approximation of the time constant of the dissolution profile, approximating the dissolution process with first order dynamics. Eq. 6.4 gives the functional input-output representation for the (1-1) PCE model,

$$\begin{aligned}\tau_{PCE}^{(1-1)} &= f_{PCE}^{(1-1)}(R) \\ \tau_{PCE}^{(1-1)} &= a_0 \Gamma_0 + \sum_{i=1}^{n_\theta} a_i \Gamma_1(\theta_i), \quad n_\theta = 1 \\ R &= \Gamma_1(\theta_i), \quad i = 1\end{aligned}\tag{Eq. 6.4}$$

where a_i are the PCE coefficients, $\Gamma_1(\theta_i)$ are the first degree Hermite polynomials, and R is the linear cooling rate applied to the drops. Eq. 6.5 gives the functional input-output representation for the (5-1) PCE model,

$$\begin{aligned}\tau_{PCE}^{(5-1)} &= f_{PCE}^{(5-1)}(T_i |_{i=1,2,\dots,5}) \\ \tau_{PCE}^{(5-1)} &= a_0 \Gamma_0 + \sum_{i=1}^{n_\theta} a_i \Gamma_1(\theta_i), \quad n_\theta = 5 \\ T_i &= \Gamma_1(\theta_i), \quad i = 1, \dots, 5\end{aligned}\tag{Eq. 6.5}$$

where a_i are the PCE coefficients, $\Gamma_1(\theta_i)$ are the first degree Hermite polynomials, and T_{n_θ} are the discretized temperature values.

As a case study, dosage forms of melts containing 15 mg of API were produced by depositing 5 drops with the average size of 18.6 mg with a standard deviation of 0.6 mg. The average drop sizes and the corresponding standard deviations are calculated based on 21 replicates of dosage forms. The same model formulation, substrate and process temperatures are used throughout the process as described in Chapter 5. After the deposition, different controlled cooling profiles, which are shown in Figure 6.4, are applied to the dosage forms with 3 replicates at each condition.

The corresponding dissolution profiles are used to test a 1st order PCE with different number of input parameters. Single value cooling rates are used as the single input parameters for (1-1) PCE model. Discretized cooling profiles are obtained by using the temperature values corresponding to 0, 2, 10, 30, 60 minutes during cooling and are used as multiple input parameters for (5-1) PCE model. Depending on the number of input parameters, different numbers of coefficients are required to build the model. In this case study, $N = 2$ and $N = 6$ coefficients are used for the PCE models with single input (1-1)

and with multiple input (5-1), respectively. The single input, i.e. cooling rates, and multiple input, i.e. discretized temperature profiles, along with the output data, i.e. the time constants of the dissolution profiles, used in the model development are listed in Table 6.1.

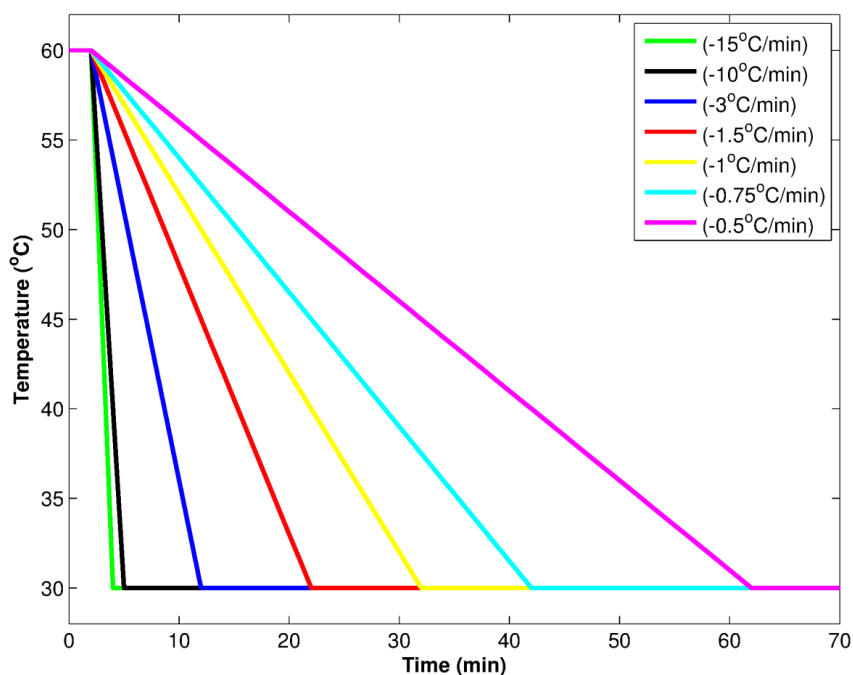


Figure 6.4 Crystallization temperature profiles used in the PCE model development

Next, the PCE models are subjected to leave-one-out cross-validation and resampling to get a better comparison on the prediction capability of the single input (1-1) and 5 input (5-1) PCE models. Here validation data both within and outside the range of training data are used. For both models, the mean square error of estimation (MSEE) and mean square error of prediction (MSEP) are calculated and shown in Table 6.2. The model fit and prediction capabilities of the (1-1) PCE model and the (5-1) PCE model are shown in

Figure 6.5.a and 6.5.b, respectively. The average residuals of (1-1) and (5-1) models are 15.0% and 4.4%, respectively. The (5-1) PCE model provides better prediction than the (1-1) PCE model both with lower residuals and with lower MSEE and MSEP values.

Table 6.1 Single input, multiple input, single output parameters for PCE based model development

Cooling Rates	Discretized Temperature Profiles	Dissolution Time Constants τ
15 °C/min	[60 30 30 30 30]	8 min
10 °C/min	[60 40 30 30 30]	8.8 min
3 °C/min	[60 54 30 30 30]	9.6 min
1.5 °C/min	[60 57 45 30 30]	10.2 min
1 °C/min	[60 58 50 30 30]	10.7 min
0.75 °C/min	[60 58.5 52.5 37.5 30]	11.5 min
0.5 °C/min	[60 59 55 45 30]	18.4 min

Table 6.2 Mean square error of estimation (MSEE) and prediction (MSEP) values for single input (1-1) and multiple input (5-1) PCE based models

	1-1 PCE Model	5-1 PCE Model
Mean Square Error of Estimation	6.33	0.72
Mean Square Error of Prediction	11.62	7.05

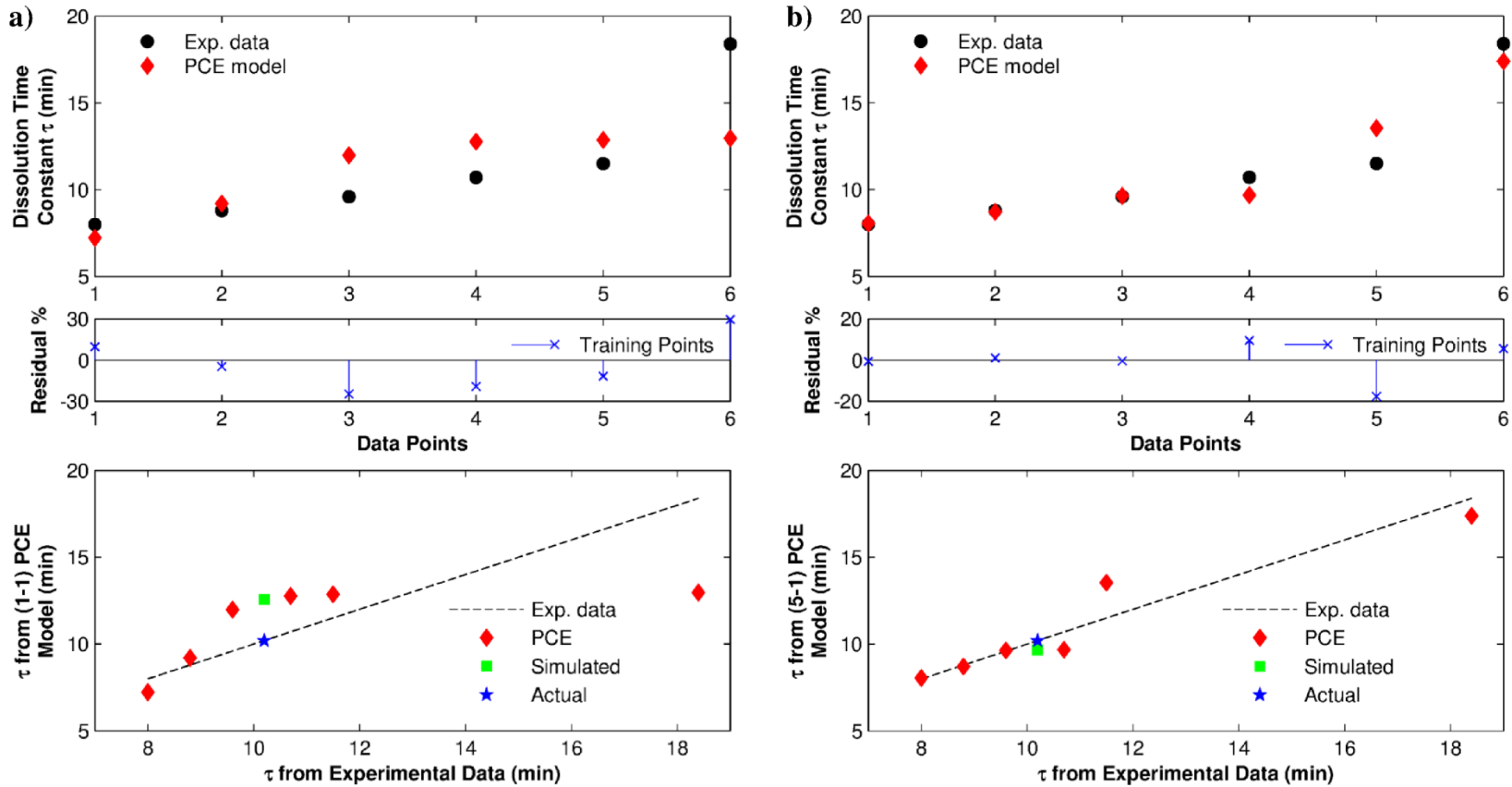


Figure 6.5 Performance of 1st order PCE model with validation and prediction for a. single input single output (1-1), b. multiple input single output (5-1) cases. Exp data: experimental data points used in PCE development, PCE: model validation points, Actual: the experimental time constant, which is predicted using the PCE model, Simulated: the model prediction

6.4 Surrogate Model Based Optimization of Temperature Profiles

After validation, both of the PCE models, i.e. (1-1) and (5-1) PCE models, are used to determine the optimal temperature profiles needed to reach the desired process outcome, i.e. time constant τ of the dissolution profile. The predicted temperature profiles using different models are compared qualitatively. The data points which are left out for cross validation are used in the prediction of the temperature profiles.

The optimal control formulation based on the (1-1) PCE model used in the higher level supervisory controller is given by Eq. 6.6. The minimum and maximum temperature cooling rates are $R_{\min} = 0.5^\circ\text{C}/\text{min}$ and $R_{\max} = 15^\circ\text{C}/\text{min}$, respectively. The average of the seven cooling rates, shown in Figure 6.4, is used to initialize the optimization problem.

$$\begin{aligned}
 & \min_R \left(\tau_{desired} - \tau_{PCE}^{(1-1)} \right)^2 \\
 & s.t. \quad \tau_{PCE}^{(1-1)} = a_0 \Gamma_0 + \sum_{i=1}^{n_\theta} a_i \Gamma_1(\theta_i), \quad n_\theta = 1 \\
 & \quad \quad R = \Gamma_1(\theta_i), \quad i = 1 \\
 & \quad \quad R_{\min} \leq R \leq R_{\max}
 \end{aligned} \tag{Eq. 6.6}$$

The optimal control formulation used in the supervisory control in the case of the (5-1) PCE model is given by Eq. 6.7. The initial and final temperatures are fixed at $T_{initial} = 60^\circ\text{C}$ and $T_{final} = 30^\circ\text{C}$, respectively. The average of the seven cooling rates, shown in Figure 6.4, is discretized at the same time points that are used for the

discretization during (5-1) PCE model development. Then this discretized average cooling profile is used to initialize the optimization problem.

$$\begin{aligned}
 & \min_T \left(\tau_{desired} - \tau_{PCE}^{(5-1)} \right)^2 \\
 & s.t. \quad \tau_{PCE}^{(5-1)} = a_0 \Gamma_0 + \sum_{i=1}^{n_\theta} a_i \Gamma_1(\theta_i), \quad n_\theta = 5 \\
 & \quad T = [T_1, T_2, \dots, T_5] \\
 & \quad T_i = \Gamma_1(\theta_i), \quad i = 1, 2, \dots, 5 \\
 & \quad T_i \geq T_{i+1}, \quad i = 1, 2, \dots, 4 \\
 & \quad T_1 = T_{initial} \\
 & \quad T_5 = T_{final}
 \end{aligned} \tag{Eq. 6.7}$$

The optimal temperature profiles are shown in Figure 6.6. Using both the (1-1) and (5-1) models, for faster cooling rates of 15 °C/min and 10 °C/min, the predicted temperature profiles to reach the desired dissolution profiles compare well with the actual temperature profiles applied to the dosage forms. However for a cooling rate of 1 °C/min, the (5-1) model gives a better prediction compared to (1-1) model. The prediction capabilities of the models show that the (5-1) PCE model captures the behavior of the system better.

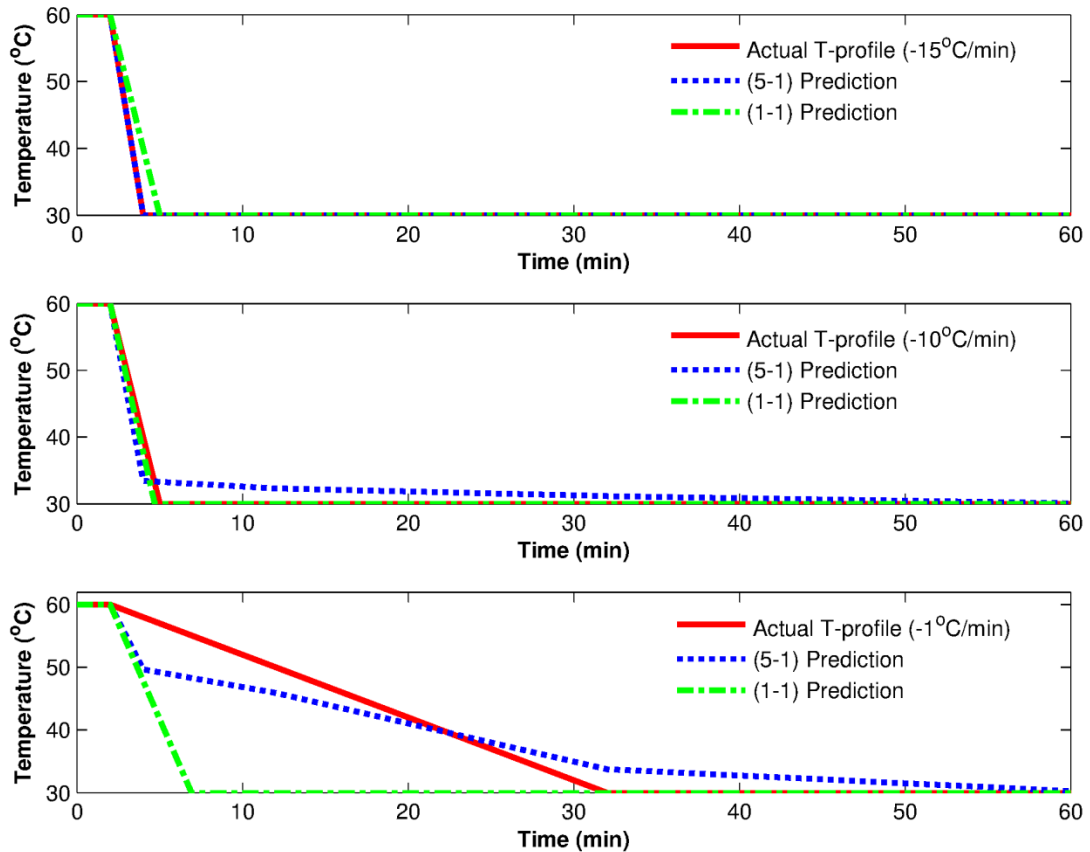


Figure 6.6 Optimized temperature profiles using (1-1) and (5-1) PCE models vs. the actual temperature profiles

Using discretized temperature profiles also allows the use of optimized temperature cycles with variable cooling and/or heating rates. In chapter 5, it is shown that cycling temperature profile can be used to reduce the solidification times compared to a slow constant cooling rate. Different cycles can be designed to achieve differences in the dissolution times. They can be also accommodated in the PCE model to achieve a desired dissolution property in shorter time. First, as explained in section 6.3, a PCE model would be developed with model input temperature profiles, which correspond to the cycling profile. In this case a single input single output (1-1) PCE model cannot be used,

since the cycling temperature profiles cannot be represented with a single cooling rate. A multiple input single output PCE model, which captures the cycling profile, should be developed. This would require a higher number of inputs and thus a higher number of data points to build the PCE model. Since the cycling profiles are not monotonic, a higher order PCE model could be necessary to capture the experimental data. Next, the model would be used in an optimal control framework with a formulation, similar to Eq. 6.7, except the constraints on temperatures would allow a cooling and heating cycle.

By using more experimental data points, the PCE based surrogate model can be improved to have better model fit and also better prediction. A higher order PCE model can also be developed with more data points. Moreover, using a different pharmaceutical formulation, which would undergo not only morphological but also crystallinity changes depending on the applied control strategies, can result in more diverse dissolution profiles.

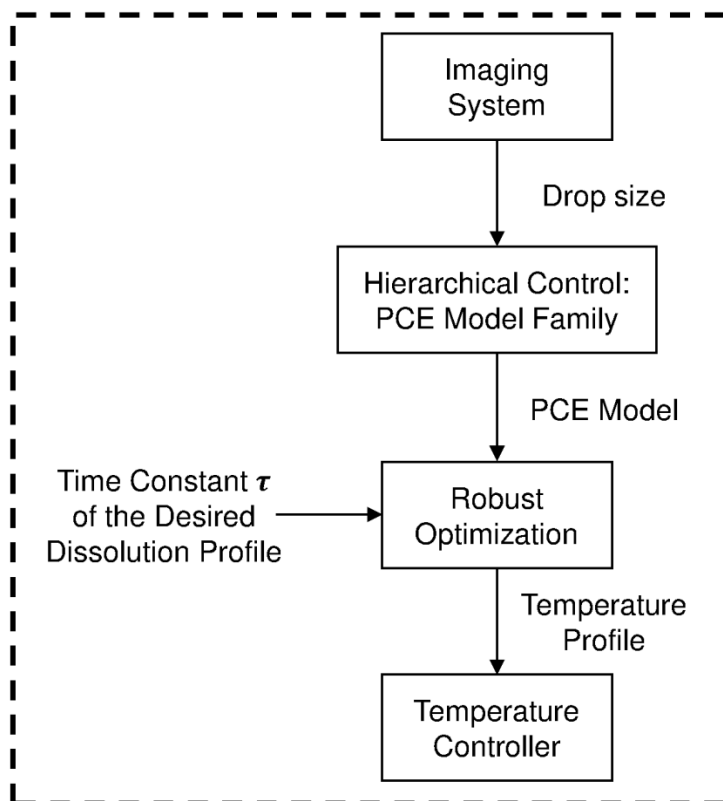


Figure 6.7 Hierarchical temperature control strategy

A hierarchical control strategy can be implemented on the dropwise additive manufacturing process by monitoring the drop size on-line, and selecting a PCE model from the PCE model family developed for different drop sizes. One such hierarchical control strategy is shown in the flowchart in Figure 6.7. Using the proposed hierarchical control strategy, for a measured drop size, the temperature profiles can be optimized to reach the desired process outcome, in this case, a desired dissolution profile.

6.5 Conclusions

In this work, a process control strategy for the dropwise additive manufacturing system is reported. Using the imaging system, the drop sizes and therefore the dosage amounts are monitored. Using the proposed substrate temperature control strategy, the crystallization behavior can be tailored and consistent drug morphology can be achieved. A PCE based surrogate model is developed to predict the dissolution profile of the solidified drug deposition given the temperature profile applied on the substrate. Using this model, a hierarchical control system is implemented by monitoring the drop size on-line and predicting a temperature profile to achieve the desired dissolution profile for the dosage forms created. The process control strategy reported in this chapter is novel not only in providing effective control of the drop on demand manufacturing process but also is one of the first efforts in the literature demonstrating elements of model-based real time release and the concept of quality-by-control, whereby product performance and consistent quality are achieved by the design of suitable control strategies.

The reported process control strategy can effectively mitigate variations in the dissolution profiles due to variable dosage amounts, hence enabling the application of the DoD system for the production of individualized dosage regimens for adaptive clinical trials and personalized treatments. The prototype system offers great promise as a tool for advancing personalized medicine by allowing the precise production of convenient solid oral dosages tailored to the patient on site at hospitals, clinics and even pharmacies.

CHAPTER 7. MODELLING OF CRYSTALLIZATION OF MELT-BASED SOLID ORAL DRUG FORMS **

7.1 Introduction

Melt-based solid oral drug forms are produced using a dropwise additive manufacturing process for pharmaceuticals. In Chapters 3, 5 and 6, both the effects of critical process parameters on the quality of the individual dosage forms and the process control strategies to control those CPP's are discussed. It is shown that the crystallization temperature affects product solid state characteristics, e.g. morphology and crystal size, and thus the dissolution properties and bioavailability of the drug. Therefore the drop solidification process following the drop deposition on the substrate should be controlled. With this purpose, in Chapter 6 a surrogate model based on polynomial chaos expansion was developed to relate the crystallization temperature profile to the final drug property: dissolution profile.

This chapter presents a different approach to investigate the solidification and crystallization processes of the drug deposits using temperature dependent crystallization kinetics and cooling profiles [82]. A model is developed based on the non-isothermal

** This chapter is based on: E. Içten, Z. K. Nagy, and G. V. Reklaitis, "Modelling of Crystallization of Solid Oral Drug Forms in a Dropwise Additive Manufacturing System," in 12th International Symposium on Process Systems Engineering and 25th European Symposium on Computer Aided Process Engineering, vol. 37, pp. 2195–2200, 2015.

Avrami kinetic equation and it incorporates the crystallization kinetics monitored via an optical microscopy with a hot stage. This model increases the understanding of solidification and crystallization processes from undercooled melts. Using the proposed model, the effect of temperature profiles leading to differences in solid-state parameters such as the mean size can be investigated.

7.2 Crystallization Model Development

The solid-state transformation of the melt-based solid oral dosages produced using the dropwise additive manufacturing process are modelled based on the modified Avrami (1939) kinetic equation [83]. The formulation used for the model development consists of 15 % drug, naproxen, and 85 % polymer, PEG 3350. The drops are deposited at 60 °C and cooled to 20 °C using two different controlled cooling rates, 1 °C/min and 10 °C/min. The temperature of the deposited drops is controlled indirectly by controlling the temperature of the substrate using a Peltier device placed beneath the substrate on the xy-stage. The controlled cooling rates are applied through the Labview based automation program. This allows control of the rate of solidification of melts and thus control of nucleation and crystallization phenomena. Precise control of the drop solidification process occurring on the substrate is very important since the crystallization temperature profile has a direct effect on product solid-state characteristics. In Chapter 5, it is reported that applying a fast cooling rate of 10 °C/min to the deposits containing naproxen results in faster dissolution profiles compared to a slow cooling rate of 1 °C/min. Controlling crystallization temperature profiles can be used to enhance the solubility of dissolution limited drugs such as naproxen.

In order to determine the nucleation and growth kinetics experimentally, the solidification process under the same conditions are monitored using optical microscopy with a hot stage. It is observed that the model formulation undergoes sporadic nucleation and spherical crystal growth. Determination of kinetic parameters is described in Section 7.3.

The Avrami equation describes isothermal solid-state transformation reactions based on nucleation and growth kinetics, which is widely used for various processes including metal, fat and polymer crystallization. The Avrami model equation for different growth geometries and types of nucleation is given by Eq. 7.1, where m_s is total mass of solids present in the system at a particular time, m_{max} is maximum total mass of solid at infinity, $(m_{max} - m_s)$ is mass of supercooled material that has not crystallized yet, t is crystallization time (min), s is the geometrical shape factor, I_c is the number of crystals per unit volume in the system (cm^{-3}), A_g is the area of crystal involved in growth (cm^2).

$$\frac{\partial m_s}{\partial t} = (m_{max} - m_s) \cdot s \cdot I_c \cdot A_g \quad \text{Eq. 7.1}$$

For spherical crystal growth, the geometrical shape factor is $s = 4\pi/3$ and crystal growth A_g is described by Eq. 7.2, where r is linear growth rate of crystal radius in time (cm) and g is growth rate constant for crystals radius per time (cm min^{-1}).

$$A_g = r^2 = g^2 \cdot t^2 \quad \text{Eq. 7.2}$$

For sporadic nucleation, the change in the number of nuclei as a function of time, I_c is described by Eq. 7.3 where j is nucleation rate constant ($\text{cm}^{-3} \text{s}^{-1}$).

$$I_c = j \cdot t \quad \text{Eq. 7.3}$$

In the dropwise additive manufacturing process, different controlled temperature cooling profiles are applied to the deposited drops in order to achieve the targeted dissolution behavior. Temperature profiles applied to the drug deposits as a function of time and cooling rate are shown in Eq. 7.4, where the induction time is defined as a function of cooling rate $t_{ind} = t_{ind}(r_{cool})$.

$$T(t) = T_i - r_{cool} \cdot (t + t_{ind}) \quad \text{Eq. 7.4}$$

In order to capture the effect of temperature on crystallization kinetics the modified Avrami equation is used, which is extended for non-isothermal kinetics by using temperature dependent nucleation and growth rates [84]. Since the cooling profiles are represented as a function of time, the crystallization model can be expressed as in Eq. 7.5, where both $j(T)$ and $g(T)$ are temperature and therefore time and cooling rate dependent.

$$\frac{\partial m_s}{\partial t} = (m_{\max} - m_s) \cdot \frac{4}{3} \pi \cdot j(T) \cdot g(T)^2 \cdot t^3 \quad \text{Eq. 7.5}$$

The growth rate constant is described as $g(T) = \alpha_1 \cdot T + \alpha_2$. The parameters α_1 and α_2 are a function of cooling rate which are determined experimentally as described in Section 7.3. The nucleation rate constant is described as $j(T) = \beta_1 \cdot T + \beta_2$. The parameters β_1 and β_2 are a function of cooling rate which are also determined experimentally as described in Section 7.3.

7.3 Determination of Kinetic Parameters

The kinetic parameters of the model formulation consisting of 15 % naproxen and 85 % PEG 3350 are determined experimentally, based on the crystallization behavior observed using an optical microscopy with a hot stage when a particular cooling profile is applied. The two cooling rates used in this study are 10 °C/min and 1 °C/min.

7.3.1 Induction Time

The cooling rates applied to the deposits effect the induction time. Induction times corresponding to 10 °C/min and 1 °C/min are determined experimentally as 2.2 min and 12 min, respectively. In the model development, it is assumed that the changes in the induction times are linearly proportional to the change in the cooling rates.

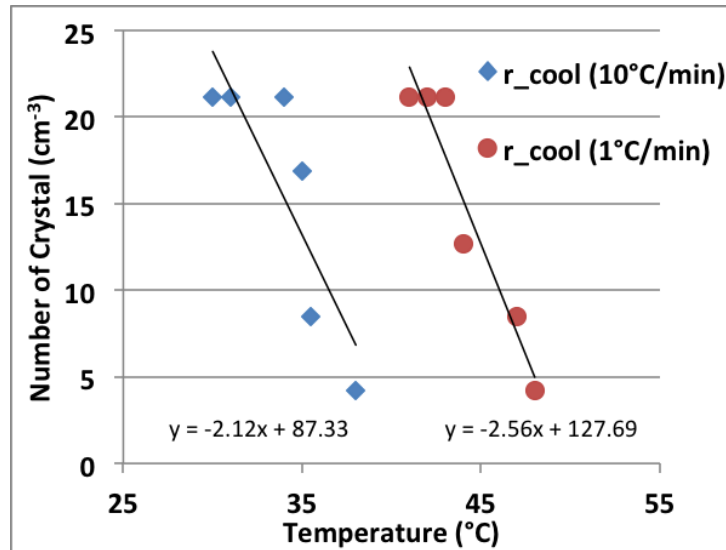


Figure 7.1 Nucleation kinetics for different cooling rates

7.3.2 Nucleation Rate

For a cooling rate, the change in the number of nuclei per volume as a function of time is determined from the images captured using optical microscopy at different times during the whole cooling duration. For the same cooling rate, the parameters β_1 and β_2 are determined by fitting a linear relation to experimental data points. Here, the data fit can be improved by excluding the data points after the number of crystals reaches a constant value. The nucleation rate parameters determined for the two cooling rates used in the experiments are shown in Figure 7.1. Next, these parameters are used to calculate the nucleation rate parameters β_1 and β_2 when cooling rates $10 \text{ }^\circ\text{C}/\text{min} \geq r_{cool} \geq 1 \text{ }^\circ\text{C}/\text{min}$ are applied to the deposits. Here it is again assumed that the changes in the parameters are linearly proportional to the change in the cooling rates.

7.3.3 Growth Rate

For a particular cooling rate, the linear growth rate constants of crystal radius as a function of time is determined from the images captured through optical microscopy. The calculation of linear growth rate of crystal radius are depicted for fast cooling rate of 1 °C/min and slow cooling rate of 10 °C/min in Figures 7.2 and 7.3.

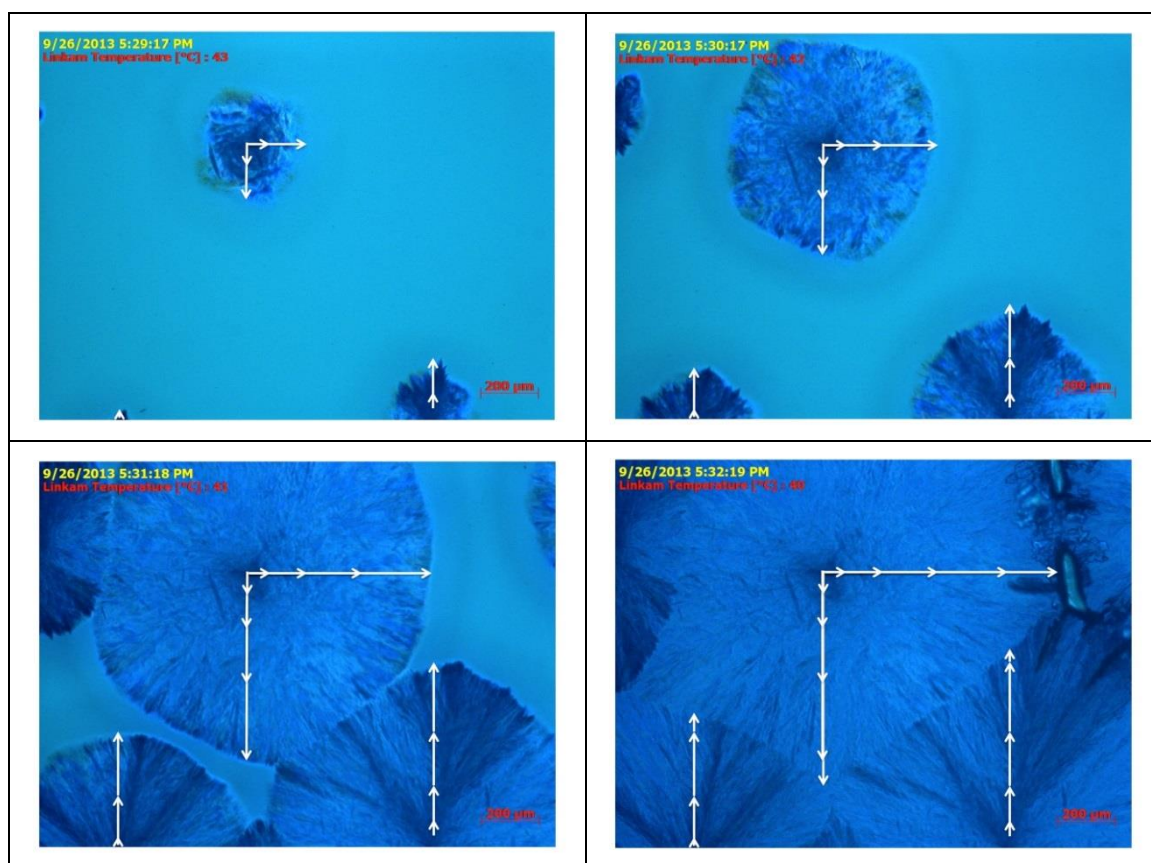


Figure 7.2 Optical microscopy images used for growth rate estimation with cooling rate 1°C/min

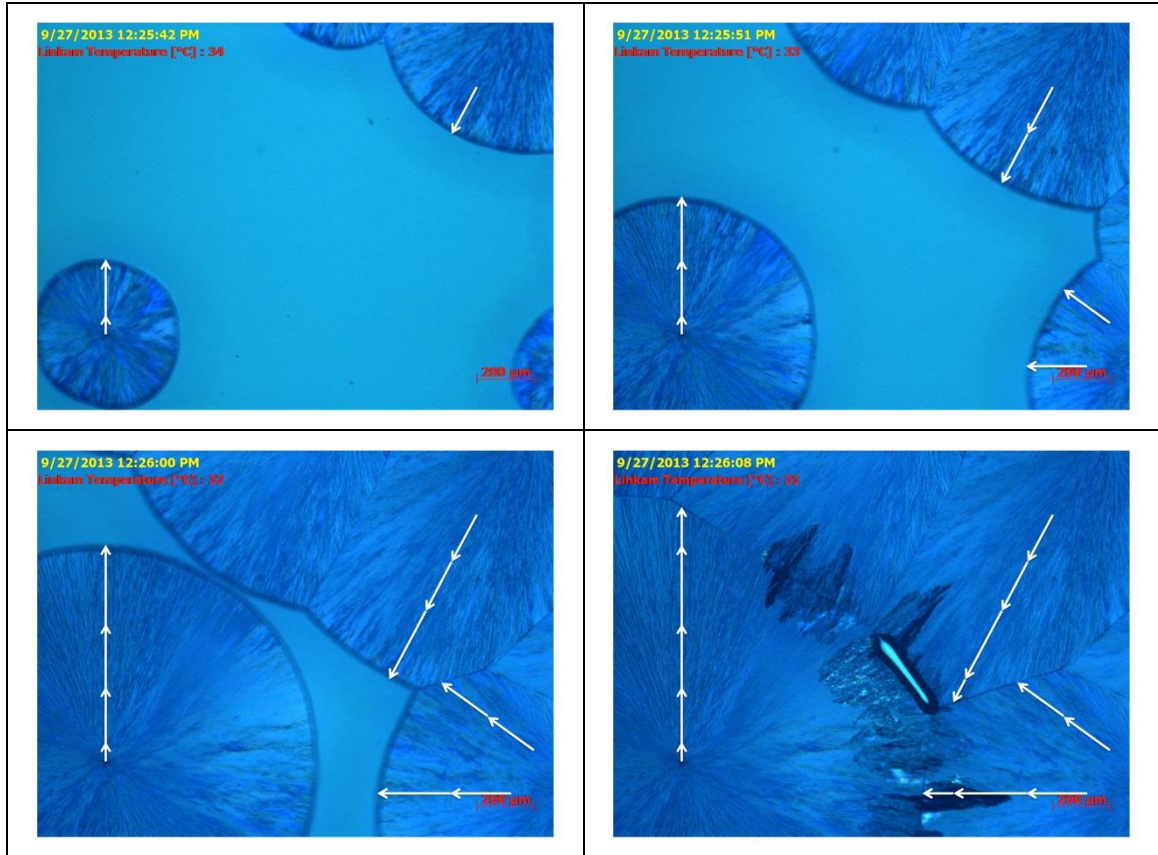


Figure 7.3 Optical microscopy images used for growth rate estimation with cooling rate $10^{\circ}\text{C}/\text{min}$

White arrows represent the dynamic changes in the linear growth rate of crystal radius in consecutive images, when either of the cooling rates is applied to the deposits. By measuring the changes in the growth front throughout different cooling profiles, the dynamic growth rate constants parameters α_1 and α_2 are determined. The growth rates determined for the two cooling rates used in the experiments are shown in Figure 7.4. These parameters are used to calculate the growth parameters α_1 and α_2 when cooling rates $10^{\circ}\text{C}/\text{min} \geq r_{cool} \geq 1^{\circ}\text{C}/\text{min}$ are applied to the deposits. Here, it is again

assumed that the changes in the crystallization parameters are linearly proportional to the change in the cooling rates.

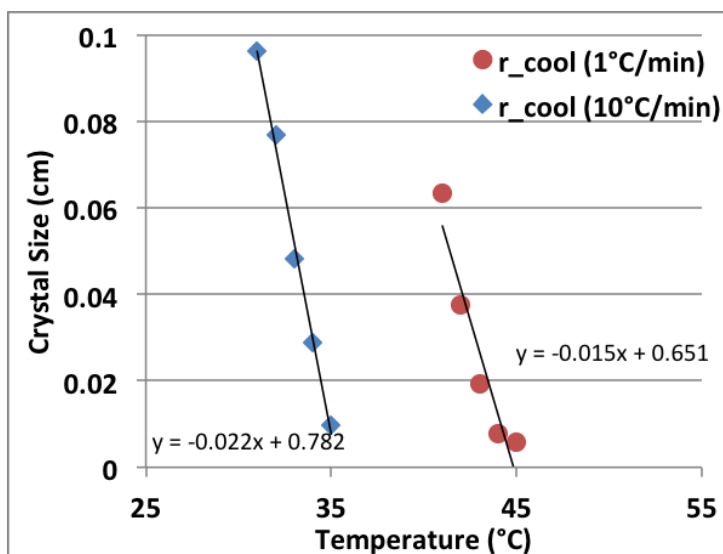


Figure 7.4 Growth kinetics for different cooling rates

7.4 Crystallization Modelling Results and Discussion

Using the modified Avrami model, the solid fraction of the dosage forms produced of the model melt-based formulation by the dropwise additive manufacturing process with different cooling rates is calculated as a function of time. The differential equation, Eq.5, is solved numerically. The time and cooling rate dependence of kinetic parameters are taken into account as explained in Section 7.2. The nucleation and growth kinetic parameters presented in Section 7.3 are used in the model. The solidification rates of the dosage forms solidified with cooling rates of 1 °C/min and 10 °C/min is shown in Figure 7.5. For both cooling rates, the experimentally determined and calculated times to reach 100% solidification are compared in Table 7.1.

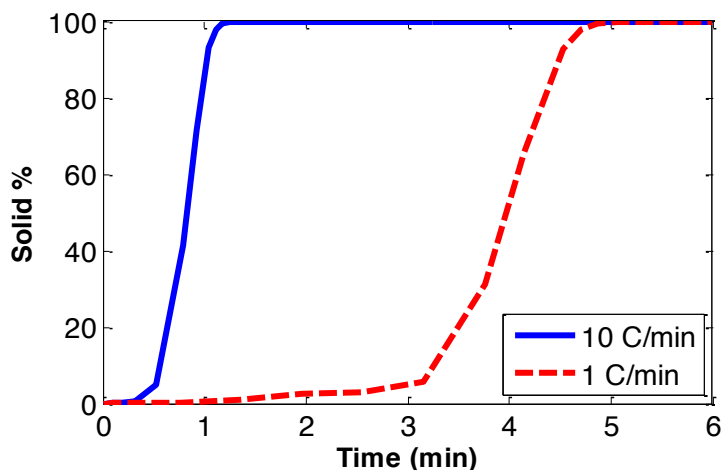


Figure 7.5 Solid percentages of the dosage forms using the developed crystallization model

Table 7.1 Calculated and experimental solidification times under different cooling rates

Cooling Rate	1 °C/min	10 °C/min
Experimental Solidification Time	5 min	1.1 min
Calculated Solidification Time	7 min	0.8 min

For 10 °C/min, complete solidification occurs after 1.1 min, whereas in experiments this time was observed as 0.8 min. For 1 °C/min, complete solidification occurs after 5 min, whereas in experiments this time was 7 min. The mismatch between the experimentally observed and modeled solidification times could potentially be reduced by using experimental data points corresponding to intermediate cooling rates and checking the validity of the linearity assumptions made during the kinetic parameter estimation. The kinetic parameters can be estimated more accurately through monitoring a larger area. This would allow both detecting more nucleation points and detecting growth rates more accurately through monitoring the complete area of spherical crystals.

The developed model is used to determine the mean size of crystals when different cooling rates are applied. For different cooling rates, the time, t^* , to reach 100 % solidification is calculated. The number of nuclei formed per image area at t^* is calculated and mean crystal radius is calculated, which are plotted in Figure 7.6 for cooling rates from 1 to 10 °C/min. By increasing the cooling rate from 1 to 10 °C/min, the mean size is decreased from 434 to 307 μm , which is in accordance with the increase in the dissolution rate observed in Chapter 5 when fast cooling rate of 10 °C/min is applied to the same model formulation containing 15 % naproxen and 85 % PEG 3350. According to model results, the minimum radius of 217 μm can be achieved with a cooling rate of 5.5 °C/min. This can be used to further increase the dissolution rate of naproxen for which dissolution is limiting.

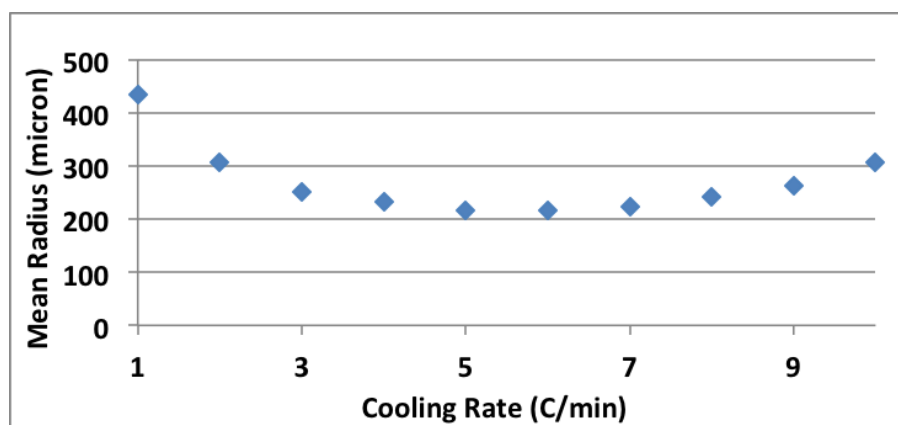


Figure 7.6 Crystallization model results for mean crystal radius vs cooling rate

7.5 Conclusions

In this chapter, a crystallization model based on non-isothermal Avrami kinetic equation is presented. The model is developed for the cooling temperature dependent solid-state transformation of the melt-based solid oral dosages produced using the dropwise additive manufacturing process. The kinetic parameters of the model formulation are determined experimentally, based on the crystallization behavior observed using an optical microscopy with a hot stage when either a fast or slow cooling profile is applied. For induction time, nucleation and growth kinetics, it is assumed that the changes in the crystallization parameters are linearly proportional to the change in the cooling rates for intermediate cooling rates.

The model is used to calculate the solidification times of the dosage forms and their mean crystal sizes under two different cooling profiles. The experimentally observed and modeled solidification times have the same trend. The accuracy of the model can be improved by using experimental data points corresponding to intermediate cooling rates and by validating the linearity assumptions made during the kinetic parameter estimation.

CHAPTER 8. AMORPHOUS AND SELF-EMULSIFYING MELT-BASED SOLID ORAL DOSAGE FORMS

8.1 Introduction

Although oral drug delivery is the major route for the administration of many drugs, increasing the oral bioavailability of most compounds is still a challenge. It has been suggested that more than 40% of new chemical entities (NCE) have low aqueous solubility, which leads to poor oral bioavailability, high intra- and inter-subject variability and lack of dose proportionality [85], [86]. In recent years, several delivery methods are being investigated to eliminate these disadvantages. These methods include use of solution or emulsion based formulations, nanocrystals, solid dispersions, amorphous formulations and lipid based formulations among others [33], [85]–[87]. It is demonstrated that via the DAMPP process, bioavailability of poorly water soluble drugs can be enhanced by using solvent-based amorphous or crystalline formulations [18] and melt-based crystalline formulations [19].

The main goal of this study is to developing alternative dosage forms to increase the bioavailability of poorly water soluble drugs that can be used in the DoD manufacturing system. Therefore both amorphous and lipid-based formulations are investigated. Lipids with low-melting temperatures can be used in the DAMPP process developed for melts-based formulations.

8.1.1 Amorphous Drug Formulations

The solubility of active ingredients can be increased by formulating the drug in the amorphous form. The drawback of amorphous drug formulations is their high instability. In comparison to amorphous forms, crystalline forms have lower energy states and are thermodynamically favored. Although stability is a critical issue in amorphous drug formulation, in some cases it can be overcome with the use of polymer additives that inhibit crystallization [33] or with a process control strategy that slows down or prevents crystallization of the compound. Performing a thorough stability analysis is common practice to assure that the final drug product contains the desired API form during the shelf-life of the products. On-demand production systems, such as DAMPP, have a great advantage for the manufacturing of amorphous drug products, because the dosage forms is produced following the prescription of the medicine by the physician and consumed within the prescription time. Thus, using DAMPP process, the long-term shelf-life constraints would be eliminated.

8.1.2 Self-Emulsifying Drug Delivery Systems

The solubility of poorly water soluble and highly lipophilic drugs can be increased using lipid-based formulations, which can be achieved by incorporating the drug into inert lipid vehicles such as oils, surfactants, emulsions and self-emulsifying drug delivery systems (SEDDS) [87], [88]. SEDDS are defined as isotropic mixtures of oils, solid or liquid surfactants, or alternatively, one or more hydrophilic solvents and co-solvents/surfactants [87]. The most frequently used excipients for lipid based formulations are reported as dietary oils and various pharmaceutically-acceptable surfactants [86]. Self-emulsifying

drug delivery systems form oil in water (o/w) emulsions upon dilution and mild agitation in aqueous environment. After the drug products enter the GI track, emulsion is achieved by chemical rather than mechanical means. This makes SEDDS easy to manufacture and stabilize compared to emulsions. Consequently, for lipophilic drug compounds displaying dissolution rate-limited absorption, SEDDS systems can improve the rate and extent of absorption and result in more reproducible blood time profiles [87].

8.2 Investigation of Amorphous and Self-Emulsifying Drug Delivery Systems for DAMPP

The two aims of this study are creating an amorphous drug product and also investigating self-emulsifying drug delivery systems. For this purpose, celecoxib is chosen as the model API which exhibits lipophilic properties and low solubility in aqueous environment. Several lipids and surfactants are investigated for the use with the DAMPP process. While selecting the lipid and surfactants used in the formulations, material properties that affect the printability of the formulations, such as the melting temperature and viscosity, are taken into account.

The excipients that are investigated for the use in the DAMPP process are shown in Table 8.1. All materials are provided by Gattefosse (Paramus, New Jersey). The main reason for selecting these excipients was their relatively low melting points. The current DAMPP prototype system is best suitable for formulations with melting temperatures of less than 70 °C, which can be increased by suitable design of the temperature control

system. For increased operating temperatures, assuring stability of the API would present another limitation on formulation selection.

Table 8.1 Lipid-based excipients used in DAMPP system and their properties

Excipient	Type	Physical Form	Average Melting Temperature	Solubility / HLB
Compritol 888ATO	Lipid	Powder	70 °C	Insoluble in water
Precirol ATO 5	Lipid	Powder	56 °C	Insoluble in water / 2
Gelucire 44/14	Surfactant	Semi solid block	44 °C	14
Labrasol	Surfactant	Liquid	undetermined	12

In addition to material rheological properties, chemical properties of the excipients also play an important role in the final drug product since their nature and amount determine the overall quality of the emulsions obtained. Non-ionic surfactants with relatively high hydrophilic-lipophilic balance (HLB) are recommended to be used with or without lipid excipients to promote self-emulsification or micro emulsification. Due to their relatively low toxicity, the acceptable quantities are limited primarily by their physical stability in the final dosage form [86]. HLB reflects the proportion of water soluble to lipid soluble moieties in each material. The classification of surfactant function based on their HLB values is shown in Figure 8.1.

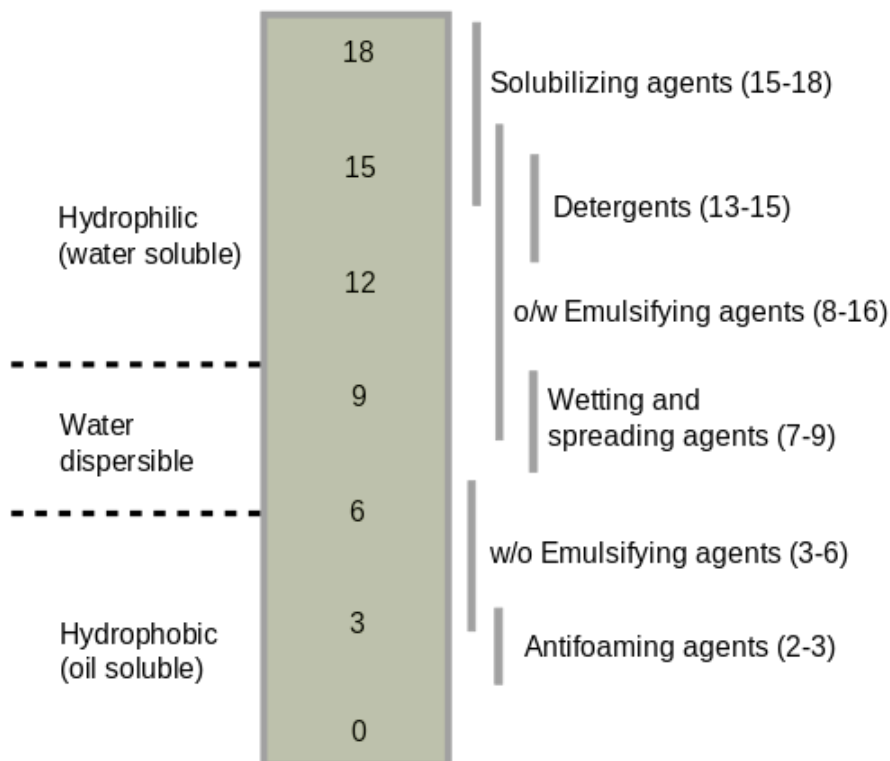


Figure 8.1 Hydrophilic – Lipophilic Balance (HLB) scale [89]

For initial formulation study, a US patent for solid solution beadlet (US 6,692,767) is followed [90]. For a self-emulsifying formulation, lipid and surfactant amounts are suggested to have between 20 to 97% and 3 to 40% by weight, respectively.

- a. **The first formulation** consists of 60% compritol, 30% labrasol and 10% celecoxib. In the DAMPP process, the temperatures of the reservoir, tubing and pump temperature controllers are set at 90 °C, 95 °C and 157 °F, respectively. Although the operating temperature is increased to the highest operating limit, this didn't prevent the formulation from solidifying within the tubing. Due to its high

melting temperature, Compritol is found not suitable for the use in the current prototype DAMPP system. Also, high hydrophobicity of the formulation creates a problem while cleaning the processing line. Cleaning solutions, including soap, soap-water and ethanol, could not be pumped through the processing line after running this formulation. Compritol is soluble in chloroform and methylene chloride under heating conditions, but these solvents are avoided for use with DAMPP due to safety concerns.

- b. **Second formulation** consists of 60% precirol, 30% labrasol and 10% celecoxib. This formulation was printed successfully with the DAMPP process and the reproducibility of the drops was within the desired 5% range. The temperatures of the reservoir, tubing and pump temperature controllers were set at 90 °C, 95 °C and 157 °F, respectively. However, cleaning the system after operation was a challenging task because the formulation is very hydrophobic. The processing line could not be cleaned with cleaning solutions, including soap-water and ethanol, after running this formulation. Therefore tubes should be replaced after each operation. This is also an indicator of the poor solubility of the formulation in aqueous media. When tested for the dissolution behavior, the dosage forms consisting of this formulation neither dissolved nor formed an emulsion in water within the first 30 minutes. Potentially, this formulation could be used for a sustained release formulation. For such applications, chloroform and methylene chloride could be used to clean the system under a fume hood.
- c. **Third formulation** consists of 90% gelucire 44/14 and 10% celecoxib. After unsuccessful formulations of SEDDS, lipids were eliminated from the formulation

and replaced with a solid surfactant. Since gelucire has a melting temperature of 44 °C, the DAMPP process can be run at lower temperatures than the maximum allowable temperatures. The temperatures of the reservoir, tubing and pump temperature controllers were set at 70 °C, 90 °C and 140 °F, respectively. This formulation is used to produce dosage forms, which contain amorphous form of celecoxib and yield self-emulsification. The detailed analysis of dosage forms is presented in the following section.

8.3 Materials and Methods

8.3.1 Materials and Formulation

In this study, celecoxib (CEL) is chosen as the model API to form melt formulations with the surfactant, gelucire 44/14 (Lauroyl macrogol-32 glycerides EP). Celecoxib is purchased from ChemShuttle (Union City, California). Gelucire 44/14 is provided by Gattefosse (Paramus, New Jersey). Celecoxib and gelucire 44/14 are mixed in (10:90) weight ratio. The mixture is comelted at 70 °C until completely melted. The melt formulation is printed both on inert tablets and on polymeric films prepared with hydroxypropyl methylcellulose (HPMC) (E50). Inert tablets are provided by GlaxoSmithKline (Collegeville, Pennsylvania). HPMC (E50) is purchased from Sigma Aldrich Corporation (St. Louis, Missouri).

8.3.1.1 Film Preparation

In order to make a 5% (w/v) polymer solution, 1 gr HPMC powder (E50) are dissolved in 20 ml water at 90 °C. The 5% (w/v) HPMC solution is stirred at room temperature overnight to ensure that the polymeric chains were homogeneously dispersed in the solution and cast onto a Petri glass. After drying is completed, the film is peeled off.

8.3.2 Methodology

After deposition of the drops onto the film, the resulting dosage forms were analyzed for solid-state characteristics, self-emulsifying behavior of the formulation and dissolution behavior of the API. The dosage forms were created and analyzed at the same time and thus varying ambient conditions, such as relative humidity, were not impactful on the results.

8.3.2.1 Reproducibility of Dosage Amounts

In this study, dosage forms are produced with target dosage of 1.5 mg of API. A single dose corresponds to one drop containing dosage form. The drop size can be altered by changing the pump and printing operating parameters such as nozzle diameter, displacement, volume strokes and rate. In addition, by changing the number of drops in a single dose, one can increase the dosage amount. The reproducibility is analyzed both gravimetrically and through image analysis. To analyze reproducibility gravimetrically, substrates are weighed on an Omega AL-201s balance. Next, a specific number of drops (in this study one drop) are deposited on the substrate to reach the target dosage amount.

The dosage forms are then subjected to room temperature until the deposits solidify. After solidification of the drops, the substrates are weighed again to determine the total mass of the deposits on the film. The amount of drug is determined by multiplying this mass of solids by the composition of drug in the solution (10 %). These results are then used to analyze how consistently and accurately the dosage forms are created.

8.3.2.2 Raman Microscopy

A Thermo Scientific DRX Raman Microscope equipped with a 532 nm laser is used to analyze the crystal morphology of the melt formulations. First, the spectra of pure crystalline celecoxib and gelucire 44/14 solid dispersion are obtained. Pure celecoxib and pure gelucire 44/14 are analyzed to obtain the spectra of pure compounds. The spectra of the melt formulation consisting of 10% celecoxib and 90% gelucire 44/14 are obtained by analyzing the drops of the melt formulation deposited using the dropwise additive manufacturing process.

8.3.2.3 X-ray Diffraction

X-ray analysis was performed to ascertain the form of the drug in the formulation. The samples were analyzed using a Rigaku Smartlab diffractometer (The Woodlands, Texas) with CuK_α radiation source and a D/tex ultra-detector. The voltage and current were 40kV and 44mA respectively and the range of data collection was from 5 to 40° 2 θ at scan speed of 10°/min and a step size of 0.04°.

8.3.2.4 Nanoparticle Tracking Analysis

NTA was utilized to characterize the solution formed after dissolving the SEDDS formulation containing 1mg of celecoxib in 160 mL of distilled water. The emulsion that was formed after dissolution of the dosage form was analyzed using the Nanosight LM10 (Malvern instruments, Massachusetts) instrument. The light source of the instrument was a green laser of 532 nm wavelength. The light scattered through the particles was visualized using a 20X magnification objective which was attached to a CMOS camera. Particle size distribution analysis was performed by acquiring a 30 sec video and processing it using the Nanosight NTA 3.0 software.

8.3.2.5 Dissolution Testing and High Performance Liquid Chromatography Analysis

Dissolution testing of crystalline CEL and the SEDDS formulation was performed in 900 mL of pH 6.8 10mM phosphate buffer in USP-I paddle dissolution apparatus. Experiments were performed at 100 rpm at 37°C. Aliquots were taken from the dissolution vessels and filtered through 1 μ glass filter. The volume of the sampled aliquots was replenished using fresh dissolution medium. The filtered samples were then analyzed using Agilent 1100 series HPLC (Santa Clara, California) fitted with a UV detector. Samples were run through a Kinetex 2.6 μ C₁₈ column (150 x 3.0 mm) at a flow rate of 0.5 mL and column temperature of 50°C. The mobile phase consisted of 30% pH 3.5 water adjusted using phosphoric acid and 70% methanol. The injection volume was 20 μ L and the absorbance was monitored at the wavelength of 250 nm. Each experiment was performed in three replicates.

8.4 Results and Discussion

The production of SEDDS is demonstrated with the DAMPP system. The melt-based SEDDS formulation consists of 10% celecoxib and 90% gelucire 44/14 by weight. Celecoxib is a lipophilic and poorly water soluble drug. Gelucire 44/14 is a non-ionic surfactant with a relatively high hydrophilic–lipophilic balance (HLB) of 14. The formulation is comelted at 70 °C and the temperature of the process is controlled at 70 °C during printing. The residence time is less than 5 min.

8.4.1 Reproducibility of Dosage Forms

Using the DAMPP system, dosage forms are produced using the nozzle with internal diameter of 17 AWG, pump displacement of 2.5, pump volume stroke of 1 and pump rate of 500. The reproducibility of the dosage forms produced is shown in Table 8.2. The relative standard deviation (RSD) is less than 2%. These RSD values are well within the 5% RSD limit required by the FDA. The images of the dosages used in the dissolution testing is shown in Figure 8.2. The images are recorded via the online imaging system, after the drops are ejected through the nozzle.

Table 8.2 Reproducibility of SEDDS

Formulation	Number of drops printed	Average dosage amount (mg)	RSD (%)
10% celecoxib 90% gelucire 44/14	1	1.571	1.572 %

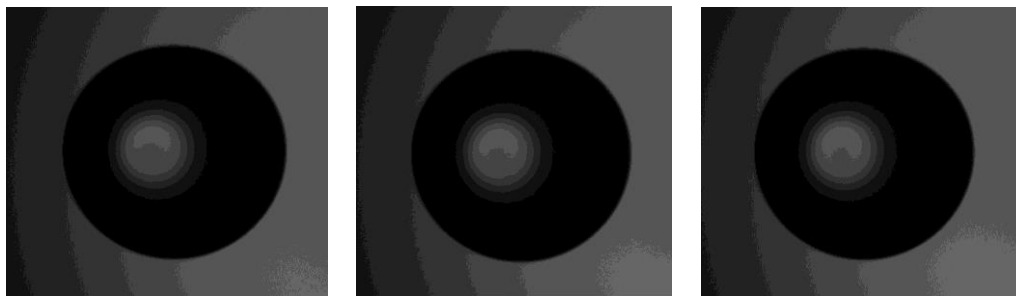


Figure 8.2 Online drop images

8.4.2 Solid-State Analysis

The crystal morphology of the dosage forms are analyzed with a Raman microscopy. Raman spectra of melt-based drug deposits of 90% gelucire and 10% celecoxib, pure gelucire and pure crystalline celecoxib are presented in Figure 8.3. The grey bands are used to clearly show the differences in the peaks of crystalline drug and drug peaks found in the dosage forms. These differences in the peak position, intensity and width are compared with reference spectra of amorphous and crystalline celecoxib from the literature and it is concluded that the celecoxib found in the dosage forms is in amorphous form [91], [92]. The crystalline and amorphous spectra of celecoxib are presented in Figure 8.4, which is modified from Andrews, et al. (2010) [91].

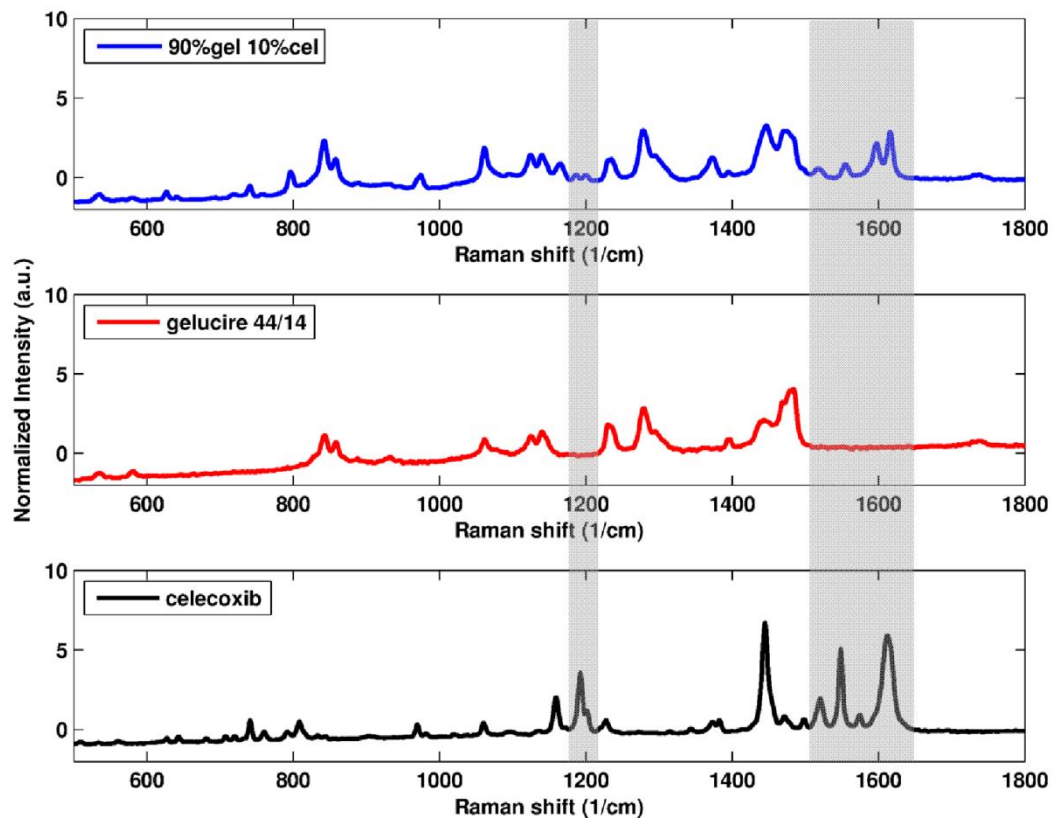


Figure 8.3 Raman spectras of SEDDS formulation, pure gelucire 44/14 and pure crystalline celecoxib

In Figure 8.3., the crystalline spectrum has a double peak at 1614 cm^{-1} with a slight shoulder at 1599 cm^{-1} , whereas the spectrum of the dosage form has a double peak with distinct maximum points at 1616 cm^{-1} and 1597 cm^{-1} . Likewise, the spectrum of the dosage form contains a double peak with distinct maximum points at 1185 and 1200 cm^{-1} whereas the spectrum of crystalline celecoxib contains a double peak with a maximum point at 1192 cm^{-1} and a shoulder at 1201 cm^{-1} .

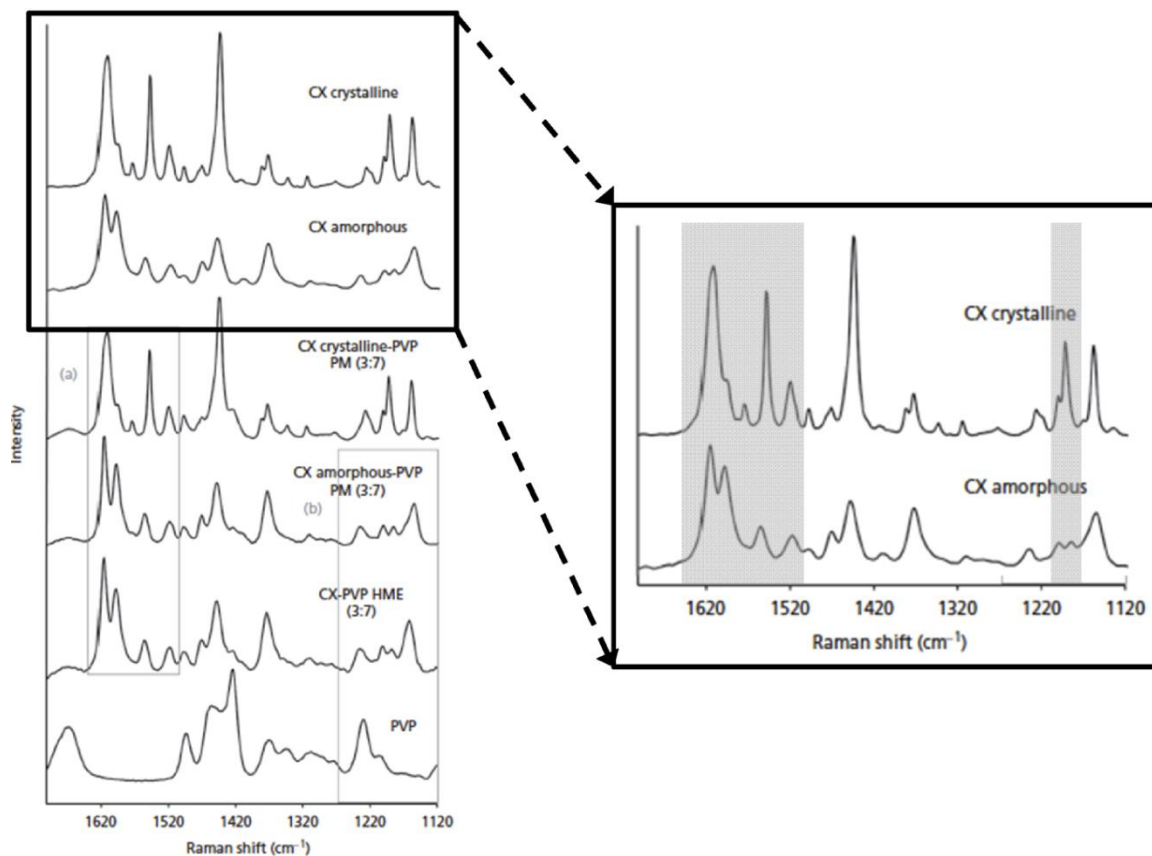


Figure 8.4 Raman spectras of amorphous and crystalline celecoxib. Modified from Andrews, et al. (2010) [91].

The crystallinity of the dosage forms are further analyzed with X-ray diffraction. The XRD spectra of melt-based drug deposits of SEDDS formulation with 90% gelucire and 10% celecoxib, pure gelucire and pure crystalline celecoxib are presented in Figure 8.5. Crystalline peaks of celecoxib were not observed in the dosage forms produced with the SEDDS formulation. Along with the Raman analysis, the presence of amorphous celecoxib in the dosage forms is proven.

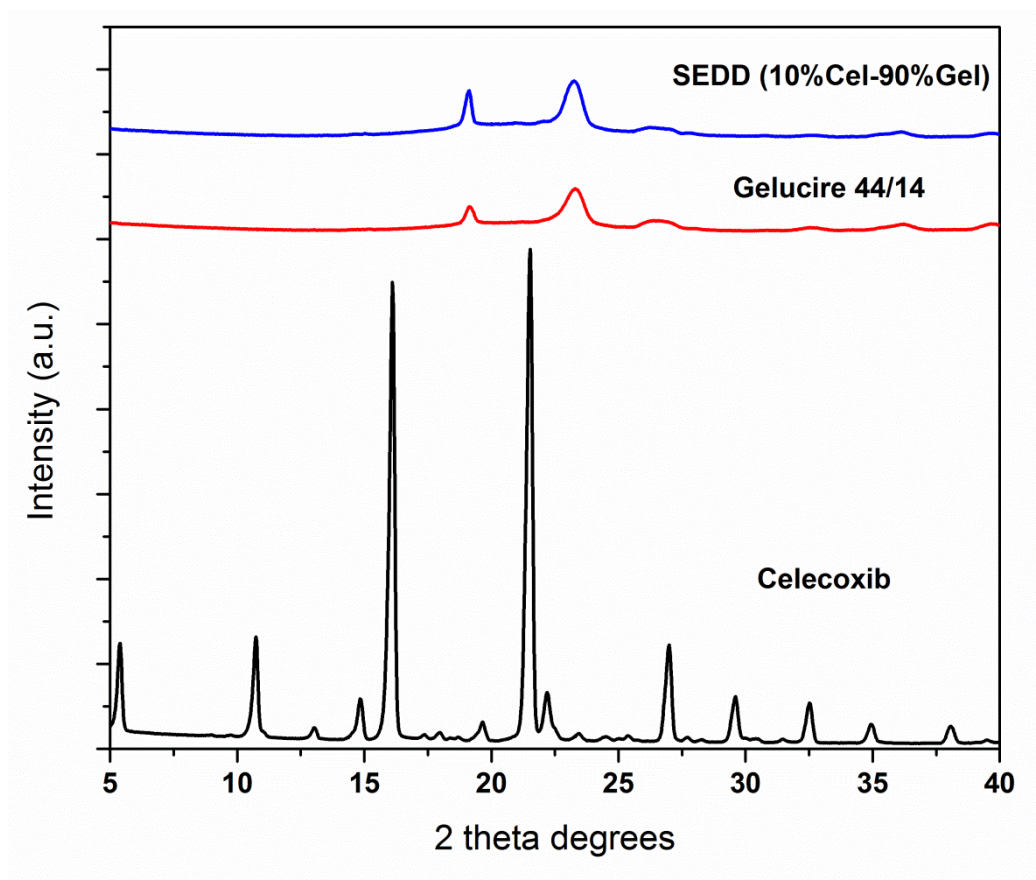


Figure 8.5 XRD spectra of crystalline celecoxib, pure gelucire 44/14 and SEDDS Formulation with 10% celecoxib and 90% gelucire 44/14

8.4.3 Analysis of the Self-Emulsifying Drug Delivery System

The formulation displays spontaneous self-emulsifying characteristics upon dilution in aqueous media. In order to further analyze the resulting emulsion, a technique called nanoparticle tracking analysis (NTA) is used. NTA utilizes the properties of both light scattering and Brownian motion in order to obtain the particle size distribution of nanoparticles in solution [93]. The size distribution profile of emulsion droplets obtained from the SEDDS containing of 10% celecoxib and 90% gelucire is presented in Figure 8.6. NTA also enables visualization and recording of particles. Figure 8.6 also displays a

particle image that is obtained during NTA analysis. White dots correspond to the particles observed in contrast to the black background. Using the software, the mean particle size is found as 160.76 nm. Thus, the celecoxib-gelucire (10:90) formulation results in a submicron spontaneous emulsion.

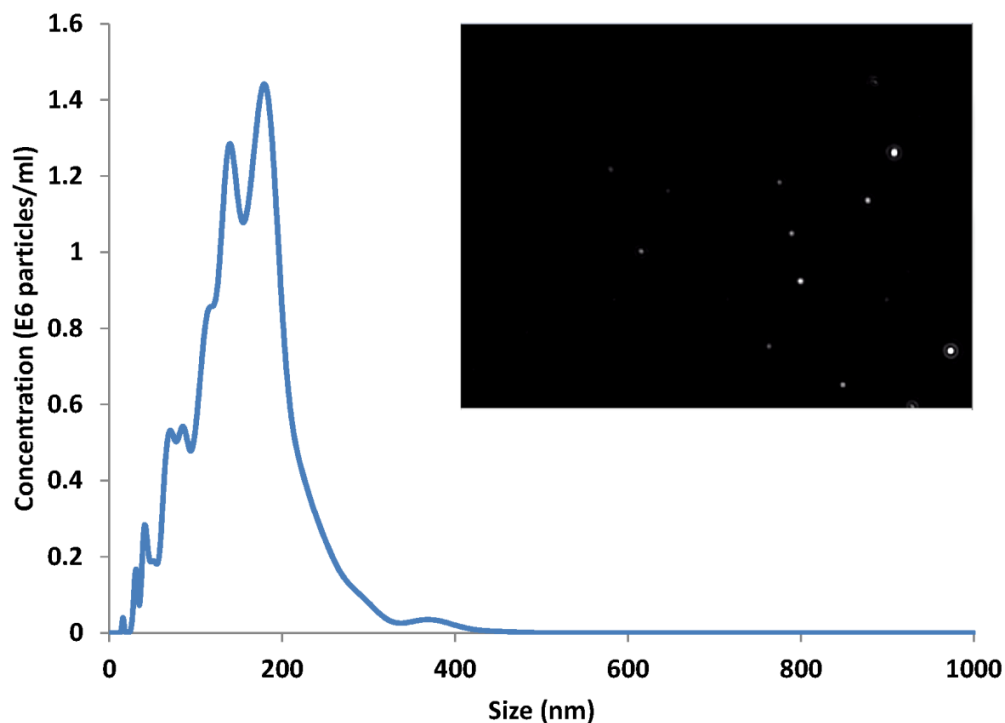


Figure 8.6 Size distribution profiles and particle images for SEDDSs.

8.4.4 Dissolution Testing

Dissolution testing was performed on the dosage forms manufactured of the self-emulsifying formulation. In Figure 8.7, the dissolution profiles of the dosage forms are compared with the crystalline celecoxib. The crystalline solubility limit of celecoxib has been reported in a range of 1.1 to 1.5 $\mu\text{g/ml}$ [94], [95]. The solubility limits are shown as

the dotted black lines, which correspond to a release of 63-85% of the SEDDS dosage forms. The solubility between two limits are shown with the grey band in the figure. For the SEDDS, the dissolution of 70% is reached in 10mins. The dissolution reaches a plateau at around 75% dissolution which indicates that the crystalline solubility limit is reached and increasing the testing time does not affect the release profile. On the other hand, the crystalline celecoxib reaches only 22% in 2 hours under the same conditions. Thus, the SEDDS formulation promotes rapid dissolution and enhances the solubility of celecoxib.

Although celecoxib in the SEDDS is in amorphous form; during dissolution testing it does not exceed crystalline solubility and present amorphous solubility. This can be due to rapid crystallization of celecoxib when dissolved in the buffer solution. Celecoxib is a rapid crystallizer and its crystallization is shown to be inhibited in the presence of polymers [33], [92]. However, the effect of gelucire 44/14 on the crystallization of celecoxib in solution is not known.

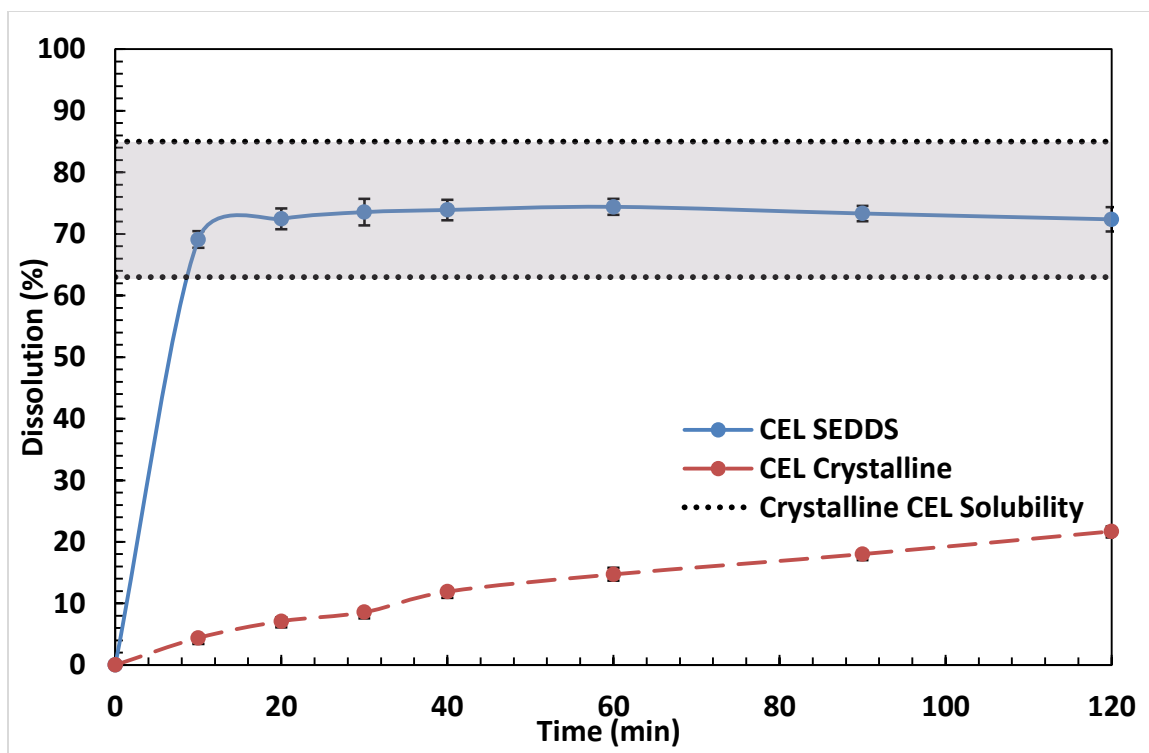


Figure 8.7 Dissolution of celecoxib found in SEEDS formulation and crystalline celecoxib

8.5 Conclusions

The dropwise additive manufacturing process is suitable for the production of various melt-based dosage forms. This temperature controlled process enables the production of lipid-based dosage forms, reproducibly and consistently. In this chapter, the use of DAMPP process for the production of alternative drug formulations such as self-emulsifying drug delivery systems and amorphous dosage forms is investigated. For this purpose, various lipid based excipients are investigated for the use in the DAMPP process. A melt-based formulation consisting of celecoxib and gelucire (10:90) is developed which forms a submicron spontaneous emulsion system upon contact with water. Another

advantage of this formulation is that the celecoxib is present in its amorphous form. This formulation appears to lead to enhancement of the solubility of celecoxib.

The DAMPP process is a viable method for on-demand production of amorphous and self-emulsifying dosage forms. The on-demand production of amorphous dosage form not only solves the solubility issues of the active ingredient but it also reduces concerns with the shelf-life duration in which the active should remain in stable in the amorphous form.

CHAPTER 9. FUTURE DIRECTIONS

The flexibility in adjusting dosage amount makes DAMPP attractive as a mini-manufacturing platform for producing dosages for early clinical trials. As a tool for clinics, hospitals or compounding pharmacies, DAMPP could produce individualized doses of drugs with high inter-patient therapeutic variability. This chapter presents studies that could be used to further advance dropwise additive manufacturing of pharmaceutical products and lead to commercialization of this technology.

Current proto-type DAMPP process is a viable system that can successfully process various solvent- or melt-based formulations. Automation, monitoring and control systems enable control of important process parameters and assure critical quality attributes. Future directions include advancing the manufacturing process, increasing process monitoring and thus process control capabilities and also investigating new product forms.

9.1 Process

The future user of the system is envisioned to be a health professional, who is not required to have a technical background. Therefore, a new version of the proto-type system, DAMPP V2.0, should be developed, which is compact and easy to transport to

medical facilities and easy to operate. As a part of our current commercialization efforts, Dr. Arun Giridhar is working on designing a new version of the DAMPP process.

Here are some recommendations to advance the dropwise additive manufacturing process and simplify process operation, which can immediately be taken into account for DAMPP V2.0:

- All process parameters need to be controlled through the automation program rather than manually. Currently there are some parameters, including pump temperature set point and pump displacement that cannot be changed through the automation program.
- Modification of the process units, such as changing the tubes or the nozzle, needs to be relatively easy. The tubing needs to be changed between different formulations to prevent cross-contamination. The nozzle needs to be changed between manufacturing of different doses. In the current system, either change requires dismantling the whole tubing-nozzle connections and usage of various tools, such as allen keys and flushnut wrench. Eliminating the tubing and connecting the nozzle directly to the pump discharge would significantly simplify process operation, especially for health professionals.
- The current system can be used for melt-based formulations with a melting point up to 70 °C and solidification within the tubing is observed for higher melting temperature formulations. Shortening the processing line would prevent

solidification within the tubing also for formulations with high melting points and expand the operating temperature region.

- The limiting factor for the operating temperature is the maximum operating temperature of the pump. By investing in a pump that has a wider operating range, the product range can be increased.
- The limiting factor for the operating speed of the system is the staging speed. A fast operating staging can be used to further increase the operating rate. Alternatively, the pump can be attached to a moving stage and the substrate can be stationary.
- A compact controller design that will contain all the controllers, i.e. pump, staging and multiple temperature controllers, will significantly reduce the size of the proto-type system and can be an important first step towards a portable design.

9.2 Process Monitoring and Control

Future additions to the DAMPP real time process management system include addition of on-line spectroscopic monitoring of the final dosage form in order to further ensure quality of the final product. Online spectroscopy, preferably Raman, can be used to control the solid state of the products by manipulating the temperature profile in closed-loop. One limitation of a spectroscopy is that the equipment needs to be compact and fit to the mini-manufacturing system. Preliminary studies with a portable Raman spectrometer (Wasatch Photonics, Utah) with size (12.7 x 16.5 x 5.1 cm) showed that the equipment can be attached to the DAMPP process and Raman spectra can be collected using the probe. Thus it can be used to control the crystallinity (or morphology) of the

dosages. For spectroscopic techniques, homogeneity of the deposits is crucial. Previously, NIR spectroscopy could not be used on solvent-based deposits that present coffee ring effect upon evaporation of the solvent. On the other hand, melt-based deposits are shown to be well distributed and are successfully analyzed with a spectroscopic technique.

Currently, IR camera can be used to monitor the spatial distribution of melt deposit temperature. However it is not used as a feedback to the temperature controller. Combined with the online spectroscopy, online IR measurement would allow precisely controlling the drug morphology real time. This would enable achieving a desired morphology regardless of the drop size and also eliminate offline solid-state characterization.

Additional cameras can be added to the system to monitor the drop formation and/or deposition. Currently, camera monitors the primary drop and any satellite drops formed close the primary drop. By placing another camera to monitor drop break up from the nozzle, the satellite drop formation can be monitored more accurately using the arbitrary rotational symmetric shape model. Another camera can be used to monitor the drop deposition on the substrates via stain detection. In the case of drop deposition, a drop would show up as a contrasting material on the substrate by increasing the average pixel value of the image. The stain detection can be implemented in the Labview automation program where the pixel values of an array can be used to detect a presence of abnormality. Stain detection could be useful to detect when a drop does not fall even though it is triggered, or when a drop falls without being triggered, or if satellite drop

generation or splashing would occur. Using the Labview program, the operator can be warned of the possible reasons of the fault.

9.3 Products

DAMPP process is used to demonstrate printing solvent-based and melt-based formulations on a variety of substrates, including polymeric films and placebo tablet. In the future, the product range can be increased by investigating other formulations such as suspensions, which would allow producing both low and high-drug loading dosage forms. Printability of new formulations should be investigated to use them in DAMPP. As shown in previous chapters, DAMPP has its limitations on the selection of formulations. Material rheological properties, e.g., surface tension, viscosity, operating temperature and solubility of the formulations can represent challenges while printing and also while cleaning the system after printing.

Also use of other substrates, such as capsules or tablets with multiple wells, should be investigated. Printing into capsules would eliminate potential peeling of deposits off the substrate. Since increasing number of treatments involve a cocktail of different drugs, combination products is a promising application. Printing on tablets with multiple wells would allow manufacturing of combination products, where multiple formulations do not contact each other thus preventing drug interactions. Another way to manufacture combination products is creating multiple layer dosage forms, where the drug interactions can be prevented through applying an inert coating layer in between. Applying a coating layer could also be used for taste-masking purposes or for sustained release formulations.

In addition to small molecule drug products, DAMPP could also be used to produce sterile drug products for large molecule drugs in large scale. Since sterility is an important concern, small scale manufacturing of the sterile products might not be feasible. However the disposable nature of the tubing used as processing line would simplify sterilization of the system.

REFERENCES

REFERENCES

- [1] L. Mancinelli, M. Cronin, and W. Sadee, "Pharmacogenomics: The Promise of Personalized Medicine," *AAPS PharmSci*, vol. 2, no. 1, pp. 1–13, 2000.
- [2] W. Sadée, "Genomics and Drugs: Finding the Optimal Drug for the Right Patient," *Pharm. Res.*, vol. 15, no. 7, pp. 959–963, 1998.
- [3] W. K. Redekop and D. Mladi, "The Faces of Personalized Medicine: A Framework for Understanding Its Meaning and Scope," *Value Heal.*, vol. 16, no. 6, pp. S4–S9, Sep. 2013.
- [4] F. Collins and H. Varmus, "A new initiative on precision medicine," *N. Engl. J. Med.*, vol. 372, no. 9, pp. 793–795, 2015.
- [5] Food and Drug Administration, "Paving the Way for Personalized Medicine," Silver Spring, Maryland, 2013.
- [6] J. Rantanen and J. Khinast, "The Future of Pharmaceutical Manufacturing Sciences.," *J. Pharm. Sci.*, vol. 104, pp. 3612–3638, Aug. 2015.
- [7] Food and Drug Administration CDER, "Guidance for Industry PAT - A Framework for Innovative Pharmaceutical," Silver Spring, Maryland, 2004.
- [8] A. E. Cervera-Padrell, T. Skovby, S. Kiil, R. Gani, and K. V Gernaey, "Active pharmaceutical ingredient (API) production involving continuous processes--a process system engineering (PSE)-assisted design framework.," *Eur. J. Pharm. Biopharm.*, vol. 82, no. 2, pp. 437–56, Oct. 2012.
- [9] A. Gupta, A. Giridhar, V. Venkatasubramanian, and G. V Reklaitis, "Intelligent Alarm Management Applied to Continuous Pharmaceutical Tablet Manufacturing: An Integrated Approach," *Ind. Eng. Chem. Res.*, vol. 52, no. 35, pp. 12357–12368, 2013.

- [10] B.-J. de Gans, P. C. Duineveld, and U. S. Schubert, "Inkjet Printing of Polymers: State of the Art and Future Developments," *Adv. Mater.*, vol. 16, no. 3, pp. 203–213, Feb. 2004.
- [11] "Engineering Research Center for Structured Organic Particulate Systems." [Online]. Available: www.ercforsops.org.
- [12] J. M. Laínez, E. Schaefer, and G. V. Reklaitis, "Challenges and opportunities in enterprise-wide optimization in the pharmaceutical industry," *Comput. Chem. Eng.*, vol. 47, no. FOCAPO 2012, pp. 19–28, Dec. 2012.
- [13] K. V. Gernaey, A. E. Cervera-Padrell, and J. M. Woodley, "A perspective on PSE in pharmaceutical process development and innovation," *Comput. Chem. Eng.*, vol. 42, pp. 15–29, Jul. 2012.
- [14] L. X. Yu, G. Amidon, M. A. Khan, S. W. Hoag, J. Polli, G. K. Raju, and J. Woodcock, "Understanding pharmaceutical quality by design.," *AAPS J.*, vol. 16, no. 4, pp. 771–83, Jul. 2014.
- [15] L. L. Simon, H. Pataki, G. Marosi, F. Meemken, K. Hungerbu, A. Baiker, S. Tummala, B. Glennon, M. Kuentz, G. Steele, H. J. M. Kramer, J. W. Rydzak, Z. Chen, J. Morris, F. Kjell, R. Singh, K. V Gernaey, M. Louhi-kultanen, J. O. Reilly, N. Sandler, O. Antikainen, J. Yliruusi, P. Frohberg, J. Ulrich, R. D. Braatz, T. Leyssens, M. Von Stosch, R. Oliveira, R. B. H. Tan, H. Wu, M. Khan, D. O. Grady, A. Pandey, R. Westra, E. Delle-case, and D. Pape, "Assessment of Recent Process Analytical Technology (PAT) Trends: A Multiauthor Review," *Org. Process Res. Dev.*, vol. 19, no. 1, pp. 3–62, 2015.
- [16] G. Stephanopoulos and G. V. Reklaitis, "Process systems engineering: From Solvay to modern bio- and nanotechnology.," *Chem. Eng. Sci.*, vol. 66, no. 19, pp. 4272–4306, Jun. 2011.
- [17] G. M. Troup and C. Georgakis, "Process systems engineering tools in the pharmaceutical industry," *Comput. Chem. Eng.*, vol. 51, pp. 157–171, Apr. 2013.
- [18] L. Hirshfield, A. Giridhar, L. S. Taylor, M. T. Harris, and G. V Reklaitis, "Dropwise additive manufacturing of pharmaceutical products for solvent-based dosage forms.," *J. Pharm. Sci.*, vol. 103, no. 2, pp. 496–506, Feb. 2014.

- [19] E. İçten, A. Giridhar, L. S. Taylor, Z. K. Nagy, and G. V Reklaitis, "Dropwise Additive Manufacturing of Pharmaceutical Products for Melt-Based Dosage Forms.," *J. Pharm. Sci.*, vol. 104, no. 5, pp. 1641–1649, Jan. 2015.
- [20] J. M. Laínez, S. Orcun, J. F. Pekny, G. V Reklaitis, A. Suvannasankha, C. Fausel, E. J. Anaissie, and G. E. Blau, "Comparison of an assumption-free Bayesian approach with Optimal Sampling Schedule to a maximum a posteriori Approach for Personalizing Cyclophosphamide Dosing.," *Pharmacotherapy*, vol. 34, no. 4, pp. 330–5, Apr. 2014.
- [21] J. M. Laínez, G. Blau, L. Mockus, S. Orcun, and G. V Reklaitis, "Pharmacokinetic Based Design of Individualized Dosage Regimens Using a Bayesian Approach," *Ind. Eng. Chem. Res.*, vol. 50, pp. 5114–5130, 2011.
- [22] G. E. Blau, S. Orcun, J. M. Laínez, G. V Reklaitis, A. Suvannasankha, C. Fausel, and E. J. Anaissie, "Validation of a novel approach for dose individualization in pharmacotherapy using gabapentin in a proof of principles study.," *Pharmacotherapy*, vol. 33, no. 7, pp. 727–35, Jul. 2013.
- [23] A. J. Clarke, D. G. Doughty, F. H. Fiesser, and D. S. Wagner, "Apparatus for Producing a Pharmaceutical Product," US 8,252,234, 2012.
- [24] B. Derby, "Inkjet Printing of Functional and Structural Materials: Fluid Property Requirements, Feature Stability, and Resolution," *Annu. Rev. Mater. Res.*, vol. 40, no. 1, pp. 395–414, Jun. 2010.
- [25] M. Alomari, F. H. Mohamed, A. W. Basit, and S. Gaisford, "Personalised dosing: Printing a dose of one's own medicine," *Int. J. Pharm.*, vol. 494, no. 2, pp. 568–577, Oct. 2015.
- [26] R. Kolakovic, T. Viitala, P. Ihalainen, N. Genina, J. Peltonen, and N. Sandler, "Printing technologies in fabrication of drug delivery systems.," *Expert Opin. Drug Deliv.*, vol. 10, no. 12, pp. 1711–23, Dec. 2013.
- [27] Z. K. Nagy and R. D. Braatz, "Advances and new directions in crystallization control," *Annu. Rev. Chem. Biomol. Eng.*, vol. 3, pp. 55–75, Jan. 2012.

- [28] E. İcten, Z. K. Nagy, and G. V. Reklaitis, "Supervisory Control of a Drop on Demand Mini-manufacturing System for Pharmaceuticals," *Proc. 24th Eur. Symp. Comput. Aided Process Eng.*, vol. 33, pp. 535–540, 2014.
- [29] E. İçten, A. Giridhar, Z. K. Nagy, and G. V Reklaitis, "Drop-on-Demand System for Manufacturing of Melt-based Solid Oral Dosage: Effect of Critical Process Parameters on Product Quality," *AAPS PharmSciTech*, doi: 10.1208/s12249-015-0348-3, Jun. 2015.
- [30] L. Hirshfield, E. İçten, A. Giridhar, Z. K. Nagy, and G. V. Reklaitis, "Real-Time Process Management Strategy for Dropwise Additive Manufacturing of Pharmaceutical Products," *J. Pharm. Innov.*, vol. 10, no. 2, pp. 140–155, Jun. 2015.
- [31] J. A. Baird, B. Van Eerdenbrugh, and L. S. Taylor, "A Classification System to Assess the Crystallization Tendency of Organic Molecules from Undercooled Melts," *J. Pharm. Sci.*, vol. 99, no. 9, pp. 3787–3806, 2010.
- [32] N. S. Trasi and L. S. Taylor, "Effect of polymers on nucleation and crystal growth of amorphous acetaminophen," *CrystEngComm*, vol. 14, no. 16, p. 5188, 2012.
- [33] L. I. Mosquera-Giraldo, N. S. Trasi, and L. S. Taylor, "Impact of surfactants on the crystal growth of amorphous celecoxib," *Int. J. Pharm.*, vol. 461, no. 1–2, pp. 251–7, Jan. 2014.
- [34] C. Leuner, "Improving drug solubility for oral delivery using solid dispersions," *Eur. J. Pharm. Biopharm.*, vol. 50, no. 1, pp. 47–60, Jul. 2000.
- [35] M. Yang, P. Wang, C.-Y. Huang, M. S. Ku, H. Liu, and C. Gogos, "Solid dispersion of acetaminophen and poly(ethylene oxide) prepared by hot-melt mixing," *Int. J. Pharm.*, vol. 395, no. 1–2, pp. 53–61, Aug. 2010.
- [36] S. Shah, S. Maddineni, J. Lu, and M. A. Repka, "Melt extrusion with poorly soluble drugs," *Int. J. Pharm.*, vol. 453, no. 1, pp. 233–52, Aug. 2013.
- [37] International Conference on Harmonization of Technical Requirements for Registration of Pharmaceuticals for Human Use, "Q1A (R2) - Stability Testing of New Drug Substances and Products," 2003.

- [38] B.-J. de Gans, P. C. Duineveld, and U. S. Schubert, "Inkjet printing of polymers: state of the art and future development," *Adv. Mater.*, vol. 16, no. 3, pp. 203–213, Feb. 2004.
- [39] H. M. Dong, W. W. Carr, and J. F. Morris, "An experimental study of drop-on-demand drop formation," *Phys. Fluids*, vol. 18, no. 7, p. 16, 2006.
- [40] J. Fromm, "Numerical calculation of the fluid dynamics of drop-on-demand jets," *IBM J. Res. Dev.*, vol. 28, pp. 322–333, 1984.
- [41] N. Reis and B. Derby, "Ink Jet Deposition of Ceramic Suspensions : Modeling and Experiments of Droplet Formation," *MRS Proc.*, vol. 624, pp. 65–70, 2000.
- [42] B. Derby, N Reis, "Inkjet printing of highly loaded particulate suspensions.," *MRS Bull*, vol. 28, pp. 815–818, 2003.
- [43] H. Hugli and J. Gonzalez, "Drop volume measurements by vision," *Imaging 2000, SPIE Electron. Imaging Conf. San Diego*, vol. 3966, no. 11, pp. 60–66, 2000.
- [44] A. L. Yarin, "Drop Impact Dynamics: Splashing, Spreading, Receding, Bouncing....," *Annu. Rev. Fluid Mech.*, vol. 38, no. 1, pp. 159–192, Jan. 2006.
- [45] H. Hsu, S. J. Toth, G. J. Simpson, L. S. Taylor, and M. T. Harris, "Effect of Substrates on Naproxen-Polyvinylpyrrolidone Solid Dispersions Formed via the Drop Printing Technique," *J. Pharm. Sci.*, vol. 102, no. 2, pp. 638–648, 2013.
- [46] H. Hsu, O. O. Adigun, L. S. Taylor, S. Murad, and M. T. Harris, "Crystallization of acetaminophen on chitosan films blended with different acids," *Chem. Eng. Sci.*, vol. 126, pp. 1–9, Apr. 2015.
- [47] N. Sandler, A. Määttänen, P. Ihalainen, L. Kronberg, A. Meierjohann, T. Viitala, and J. Peltonen, "Inkjet printing of drug substances and use of porous substrates towards individualized dosing," *J. Pharm. Sci.*, vol. 100, no. 8, pp. 3386–3395, Aug. 2011.
- [48] M. Fujiwara, Z. K. Nagy, J. W. Chew, and R. D. Braatz, "First-principles and direct design approaches for the control of pharmaceutical crystallization," *J. Process Control*, vol. 15, no. 5, pp. 493–504, Aug. 2005.

- [49] T. De Beer, a Burggraeve, M. Fonteyne, L. Saerens, J. P. Remon, and C. Vervaet, "Near infrared and Raman spectroscopy for the in-process monitoring of pharmaceutical production processes.," *Int. J. Pharm.*, vol. 417, no. 1–2, pp. 32–47, Sep. 2011.
- [50] L. X. Yu, R. a Lionberger, A. S. Raw, R. D'Costa, H. Wu, and A. S. Hussain, "Applications of process analytical technology to crystallization processes.," *Adv. Drug Deliv. Rev.*, vol. 56, no. 3, pp. 349–69, Feb. 2004.
- [51] Q. Zhu, S. J. Toth, G. J. Simpson, H.-Y. Hsu, L. S. Taylor, and M. T. Harris, "Crystallization and dissolution behavior of naproxen/polyethylene glycol solid dispersions.," *J. Phys. Chem. B*, vol. 117, no. 5, pp. 1494–500, Feb. 2013.
- [52] A. V Kabanov, E. V Batrakova, and V. Y. Alakhov, "Pluronic® block copolymers as novel polymer therapeutics for drug and gene delivery.," *J. Control. Release*, vol. 82, no. 2–3, pp. 189–212, Aug. 2002.
- [53] K. Patel, P. Bahadur, C. Guo, J. H. Ma, H. Z. Liu, Y. Yamashita, A. Khanal, and K. Nakashima, "Salt induced micellization of very hydrophilic PEO–PPO–PEO block copolymers in aqueous solutions.," *Eur. Polym. J.*, vol. 43, no. 5, pp. 1699–1708, May 2007.
- [54] S. H. Kwon, S. Y. Kim, K. W. Ha, M. J. Kang, J. S. Huh, T. J. Im, Y. M. Kim, Y. M. Park, K. H. Kang, S. Lee, J. Y. Chang, J. Lee, and Y. W. Choi, "Pharmaceutical evaluation of genistein-loaded pluronic micelles for oral delivery.," *Arch. Pharm. Res.*, vol. 30, no. 9, pp. 1138–43, Sep. 2007.
- [55] E. V. Batrakova, H. Y. Han, D. W. Miller, and A. V. Kabanov, "Effects of pluronic P85 unimers and micelles on drug permeability in polarized BBMEC and Caco-2 cells," *Pharm. Res.*, vol. 15, no. 10, pp. 1525–1532, 1998.
- [56] E. V Batrakova and A. V Kabanov, "Pluronic block copolymers: evolution of drug delivery concept from inert nanocarriers to biological response modifiers.," *J. Control. Release*, vol. 130, no. 2, pp. 98–106, Sep. 2008.
- [57] J. Perelaer, P. Krober, J. T. Delaney, and U. S. Schubert, "Fabrication of Two and Three-Dimensional Structures by Using Inkjet Printing," *NIP25 Digit. Fabr.*, pp. 791–794, 2009.

- [58] A. A. Khalate, X. Bombois, and R. Babu, "Performance improvement of a drop-on-demand inkjet printhead using an optimization-based feedforward control method," *Control Eng. Pract.*, vol. 9, no. 19, pp. 771–781, 2011.
- [59] P. Calvert, "Inkjet Printing for Materials and Devices," *Chem. Mater.*, vol. 13, no. 10, pp. 3299–3305, 2001.
- [60] A. Pierik, F. Dijkstra, A. Raaijmakers, T. Wismans, and H. Stapert, "Quality control of inkjet technology for DNA microarray fabrication," *Biotechnol. J.*, vol. 3, no. 12, pp. 1581–1590, 2008.
- [61] Food and Drug Administration CDER, "Q8 (R1) Pharmaceutical Development Revision 1," Silver Spring, Maryland, 2008.
- [62] L. Hirshfield, "Development of Dropwise Additive Manufacturing of Pharmaceutical Products," Purdue University, Doctoral Dissertation, 2013.
- [63] G. S. Joglekar, A. Giridhar, and G. Reklaitis, "A workflow modeling system for capturing data provenance," *Comput. Chem. Eng.*, vol. 67, pp. 148–158, Aug. 2014.
- [64] M. McLennan and R. Kennell, "HUBzero: A Platform for Dissemination and Collaboration in Computational Science and Engineering," *Comput. Sci. Eng.*, vol. 12, no. 2, pp. 48–53, Mar. 2010.
- [65] D. Acevedo and Z. K. Nagy, "Systematic classification of unseeded batch crystallization systems for achievable shape and size analysis," *J. Cryst. Growth*, vol. 394, pp. 97–105, May 2014.
- [66] M. R. A. Bakar, Z. K. Nagy, and C. D. Rielly, "Seeded batch cooling crystallization with temperature cycling for the control of size uniformity and polymorphic purity of sulfathiazole crystals," *Org. Process Res. Dev.*, vol. 13, no. 6, pp. 1343–1356, 2009.
- [67] M. R. Abu Bakar, Z. K. Nagy, and C. D. Rielly, "Investigation of the Effect of Temperature Cycling on Surface Features of Sulfathiazole Crystals during Seeded Batch Cooling Crystallization," *Cryst. Growth Des.*, vol. 10, no. 9, pp. 3892–3900, Sep. 2010.

- [68] E. İçten, Z. K. Nagy, and G. V. Reklaitis, "Process control of a dropwise additive manufacturing system for pharmaceuticals using polynomial chaos expansion based surrogate model," *Comput. Chem. Eng.*, vol. 83, pp. 221–231, Dec. 2015.
- [69] S. L. Lee, T. F. O'Connor, X. Yang, C. N. Cruz, S. Chatterjee, R. D. Madurawe, C. M. V. Moore, L. X. Yu, and J. Woodcock, "Modernizing Pharmaceutical Manufacturing: from Batch to Continuous Production," *J. Pharm. Innov.*, vol. 10, no. 3, pp. 191–199, Mar. 2015.
- [70] J. A. Caballero and I. E. Grossmann, "An algorithm for the use of surrogate models in modular flowsheet optimization," *AIChE J.*, vol. 54, no. 10, pp. 2633–2650, Oct. 2008.
- [71] J. Eason and S. Cremaschi, "Adaptive sequential sampling for surrogate model generation with artificial neural networks," *Comput. Chem. Eng.*, vol. 68, pp. 220–232, Sep. 2014.
- [72] L. T. Biegler, Y. Lang, and W. Lin, "Multi-scale optimization for process systems engineering," *Comput. Chem. Eng.*, vol. 60, pp. 17–30, Jan. 2014.
- [73] V. Dua, "An Artificial Neural Network approximation based decomposition approach for parameter estimation of system of ordinary differential equations," *Comput. Chem. Eng.*, vol. 35, no. 3, pp. 545–553, Mar. 2011.
- [74] K. Kim, D. E. Shen, Z. K. Nagy, and R. D. Braatz, "Wiener's Polynomial Chaos for the Analysis and Control of Nonlinear Dynamical Systems with Probabilistic Uncertainties," *IEEE Control Systems Magazine*, no. October, pp. 58–67, 2013.
- [75] N. Wiener, "The Homogeneous Chaos," *Am. J. Math.*, vol. 60, no. 4, pp. 897–936, 1938.
- [76] R. G. Gahem, P. D. Spanos, R. G. Ghanem, and P. D. Spanos, *Stochastic Finite Elements: A Spectral Approach*. New York: Springer-Verlag, 2003.
- [77] Z. K. Nagy and R. D. Braatz, "Distributional uncertainty analysis using polynomial chaos expansions," in *2010 IEEE International Symposium on Computer-Aided Control System Design*, 2010, pp. 1103–1108.

- [78] D. Zhang and Z. Lu, "An efficient, high-order perturbation approach for flow in random porous media via Karhunen–Loève and polynomial expansions," *J. Comput. Phys.*, vol. 194, no. 2, pp. 773–794, Mar. 2004.
- [79] T. Ghisu, G. T. Parks, J. P. Jarrett, and P. J. Clarkson, "Robust Design Optimization of Gas Turbine Compression Systems," *J. Propuls. Power*, vol. 27, no. 2, pp. 282–295, Mar. 2011.
- [80] Z. K. Nagy and R. D. Braatz, "Distributional uncertainty analysis using power series and polynomial chaos expansions," *J. Process Control*, vol. 17, no. 3, pp. 229–240, Mar. 2007.
- [81] Y. Tsong, M. Shen, and V. Shah, "Three-stage sequential statistical dissolution testing rules," *J. Biopharm. Stat.*, vol. 14, no. 3, pp. 757–779, 2004.
- [82] E. İçten, Z. K. Nagy, and G. V. Reklaitis, "Modelling of Crystallization of Solid Oral Drug Forms in a Dropwise Additive Manufacturing System," *12th Int. Symp. Process Syst. Eng. 25th Eur. Symp. Comput. Aided Process Eng.*, vol. 37, pp. 2195–2200, 2015.
- [83] M. Avrami, "Kinetics of Phase Change. I General Theory," *J. Chem. Phys.*, vol. 7, no. 12, p. 1103, 1939.
- [84] T. Ozawa, "Kinetics of non-isothermal crystallization," *Polymer (Guildf.)*, vol. 12, no. 3, pp. 150–158, Mar. 1971.
- [85] M. Morgen, C. Bloom, R. Beyerinck, A. Bello, W. Song, K. Wilkinson, R. Steenwyk, and S. Shamblin, "Polymeric nanoparticles for increased oral bioavailability and rapid absorption using celecoxib as a model of a low-solubility, high-permeability drug," *Pharm. Res.*, vol. 29, no. 2, pp. 427–40, Feb. 2012.
- [86] D. J. Hauss, "Oral lipid-based formulations," *Adv. Drug Deliv. Rev.*, vol. 59, no. 7, pp. 667–76, Jul. 2007.
- [87] R. Neslihan Gursoy and S. Benita, "Self-emulsifying drug delivery systems (SEDDS) for improved oral delivery of lipophilic drugs," *Biomed. Pharmacother.*, vol. 58, no. 3, pp. 173–182, Apr. 2004.

- [88] M. Soliman and M. A. Khan, "Preparation and in vitro characterization of a semi-solid dispersion of flurbiprofen with Gelucire 44 / 14 and Labrasol," *Die Pharm. - An Int. J. Pharm. Sci.*, vol. 60, no. 4, pp. 288–293, 2005.
- [89] "Hydrophilic lipophilic balance," 2016. [Online]. Available: https://en.wikipedia.org/wiki/Hydrophilic-lipophilic_balance.
- [90] B. Burnside, C. McGuinness, E. Rudnic, R. Couch, X. Guo, and A. Tustian, "Solid Solution Beadlet," US 6,692,767, 2004.
- [91] G. P. Andrews, O. Abu-Diak, F. Kusmanto, P. Hornsby, Z. Hui, and D. S. Jones, "Physicochemical characterization and drug-release properties of celecoxib hot-melt extruded glass solutions," *J. Pharm. Pharmacol.*, vol. 62, no. 11, pp. 1580–1590, Nov. 2010.
- [92] T. Xie and L. S. Taylor, "Dissolution Performance of High Drug Loading Celecoxib Amorphous Solid Dispersions Formulated with Polymer Combinations," *Pharm. Res.*, Nov. 2015.
- [93] V. Filipe, A. Hawe, and W. Jiskoot, "Critical evaluation of Nanoparticle Tracking Analysis (NTA) by NanoSight for the measurement of nanoparticles and protein aggregates," *Pharm. Res.*, vol. 27, no. 5, pp. 796–810, May 2010.
- [94] T. Xie and L. S. Taylor, "Improved Release of Celecoxib from High Drug Loading Amorphous Solid Dispersions Formulated with Polyacrylic Acid and Cellulose Derivatives," *Mol. Pharm.*, doi: 10.1021/acs.molpharmaceut.5b00798, Feb. 2016.
- [95] J. Chen, J. D. Ormes, J. D. Higgins, and L. S. Taylor, "Impact of Surfactants on the Crystallization of Aqueous Suspensions of Celecoxib Amorphous Solid Dispersion Spray Dried Particles," *Mol. Pharm.*, vol. 12, no. 2, pp. 533–541, Feb. 2015.

APPENDICES

Appendix A LabVIEW Flowsheets

The automation program described in Chapter 3 is developed in NI LabVIEW environment. The LabVIEW flowsheets are presented in Appendix A.

First, all of the input parameters are read from the Intermediate Input File generated via the Knowledge Provenance Management System, as shown in Figure A.1.

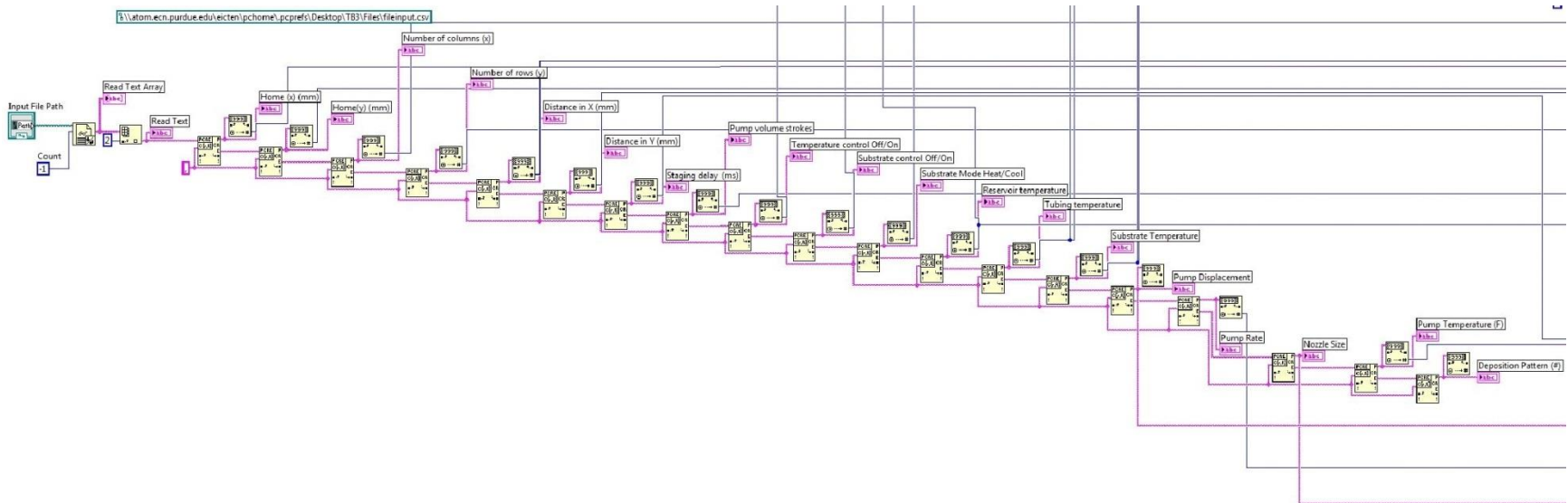


Figure A.1 Reading the input information from the Intermediate file generated by KProMS

For processing melt-based formulations, the temperature control is used. Next, the code connects to all the temperature controllers first through visa ports, as shown in Figure A.2.

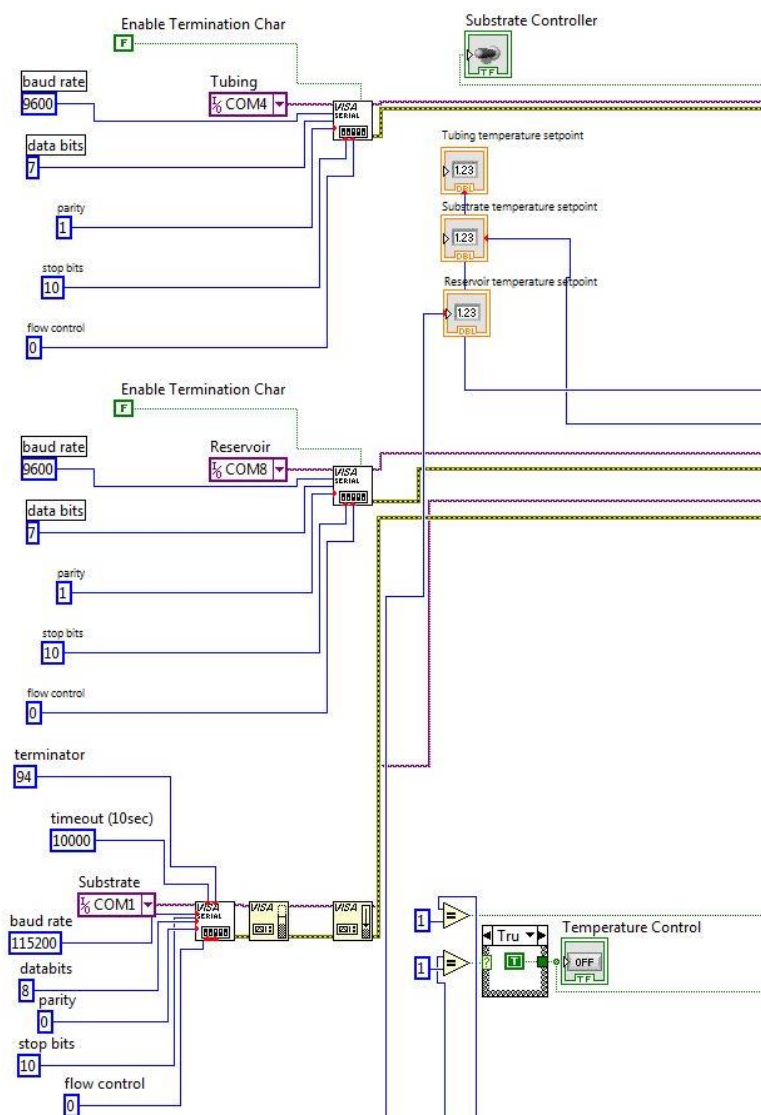


Figure A.2 Connecting to temperature controller visa ports

The substrate temperature controller is set as shown in Figures A.3 through A.10.

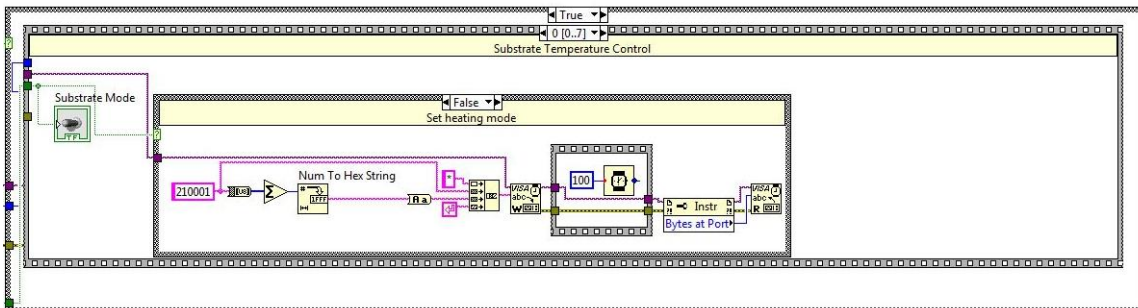


Figure A.3 Setting the substrate temperature controller to heating mode

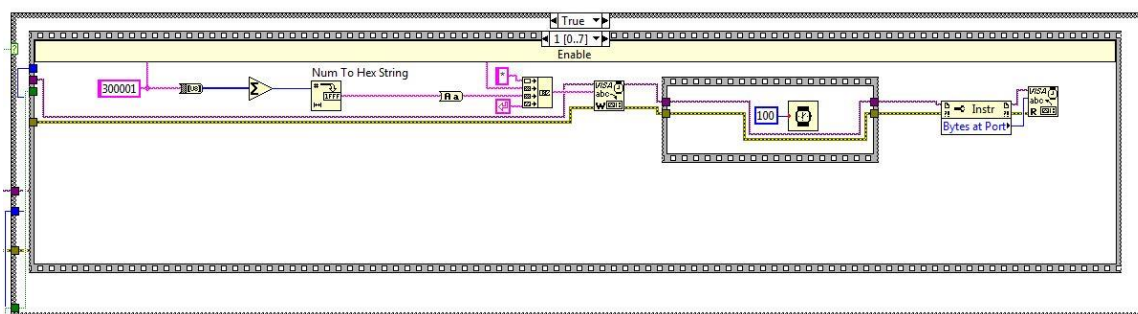


Figure A.4 Turning the substrate temperature controller on

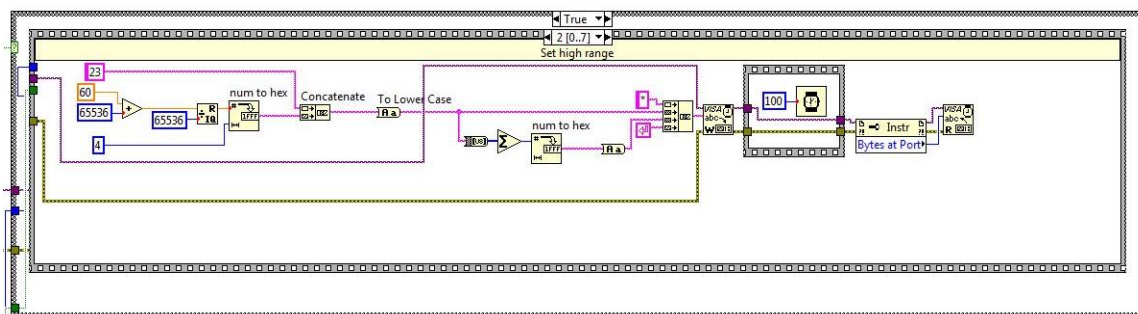


Figure A.5 Setting the substrate temperature controller high operating temperature to 60 °C

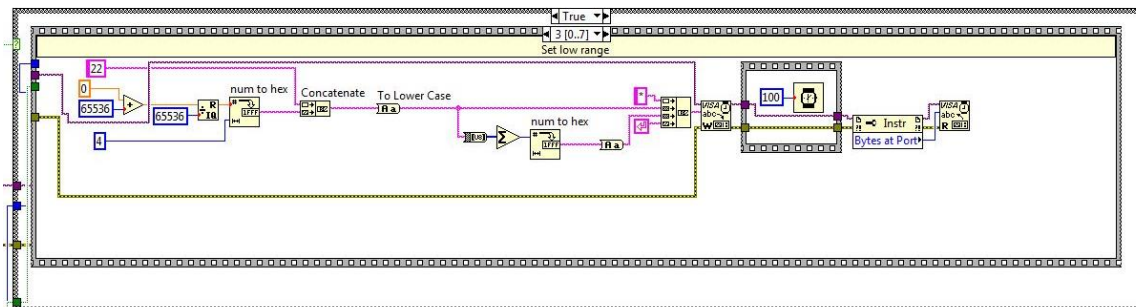


Figure A.6 Setting the substrate temperature controller low operating temperature to 0°C

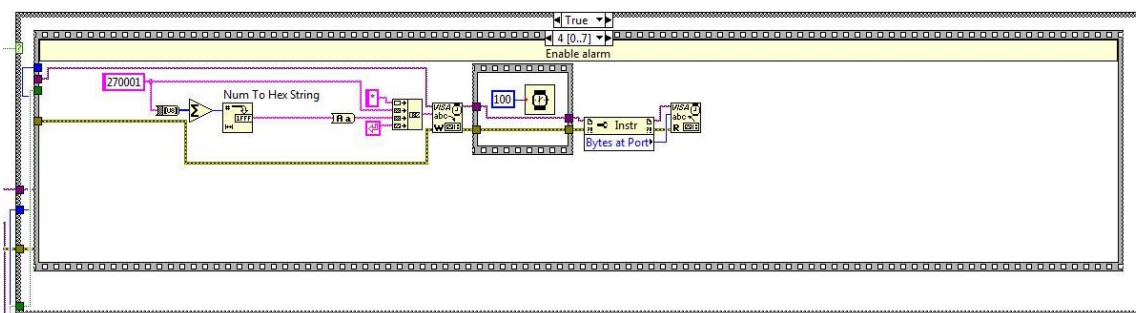


Figure A.7 Turning the substrate temperature controller alarm on

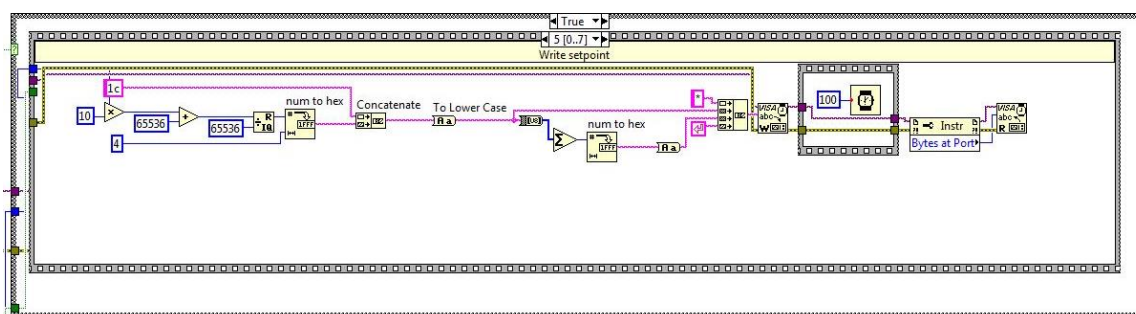


Figure A.8 Setting the setpoint temperature for substrate temperature controller

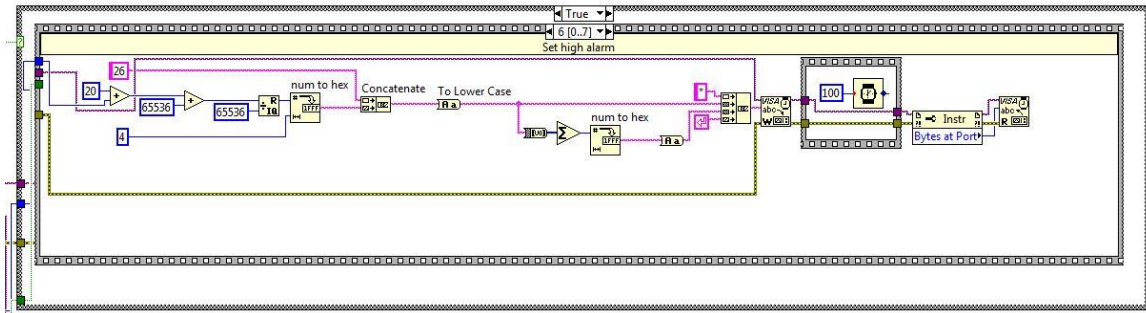


Figure A.9 Setting the substrate temperature controller high alarm 20 °C above the setpoint temperature

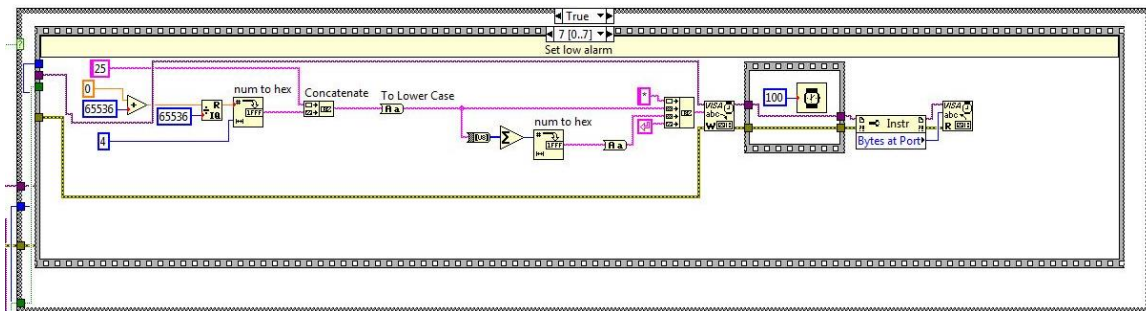


Figure A.10 Setting the substrate temperature controller low alarm at 0 °C

The reservoir temperature controller is set as shown in Figures A.11 through A.14.

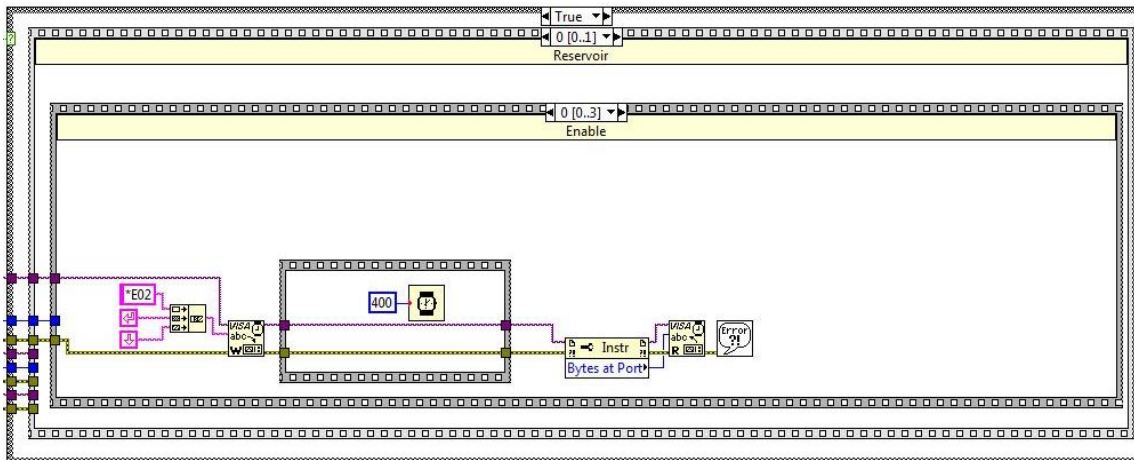


Figure A.11 Turning the reservoir temperature controller on

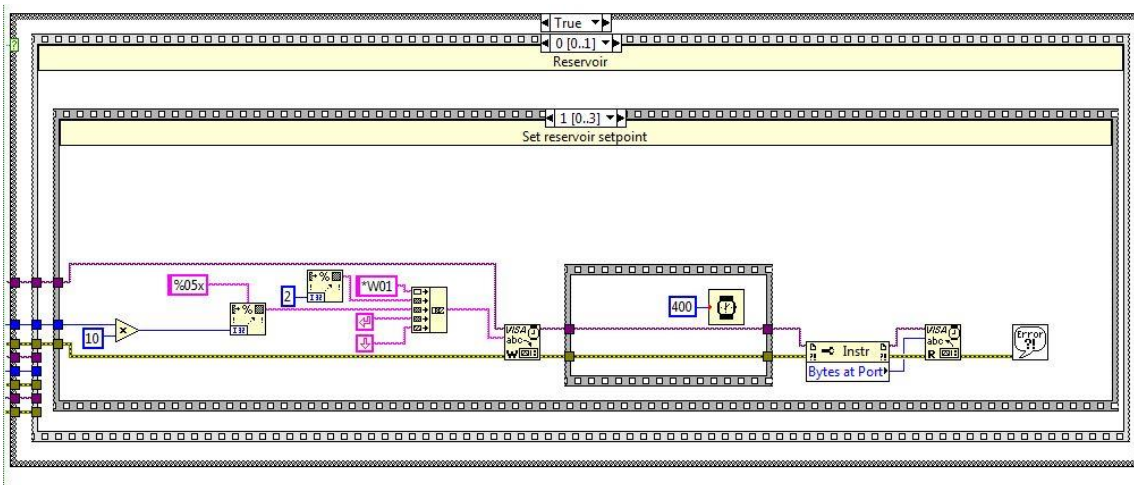


Figure A.12 Setting the reservoir temperature controller setpoint temperature

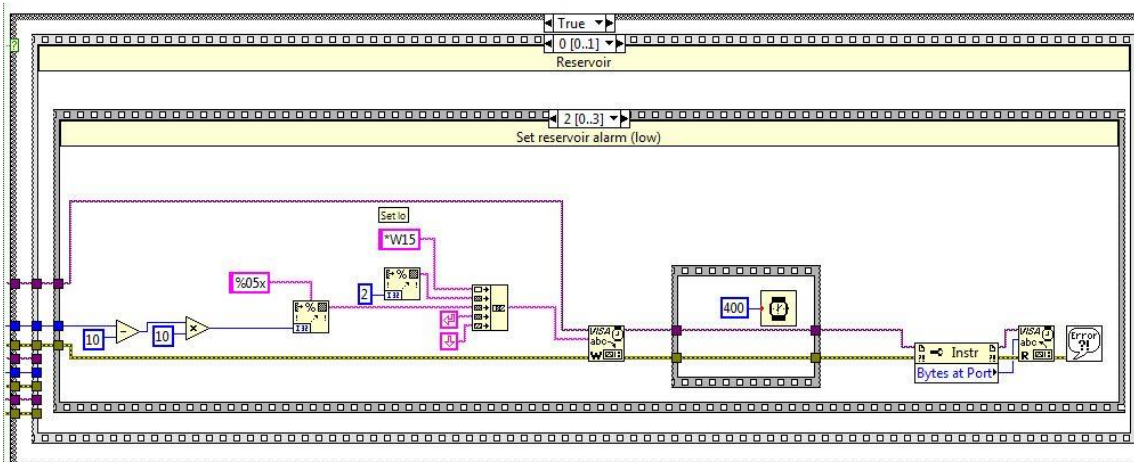


Figure A.13 Setting the reservoir temperature controller alarm low to 10°C lower than setpoint

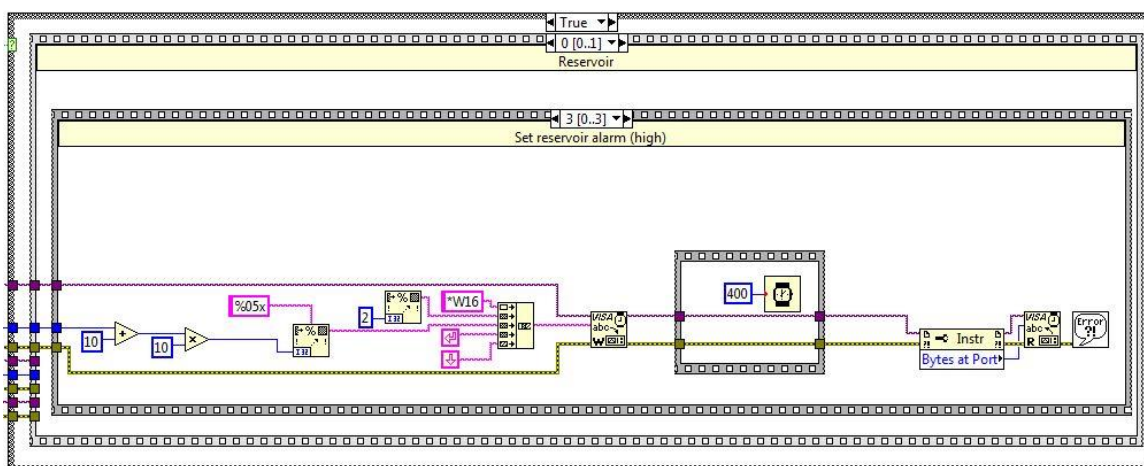


Figure A.14 Setting the reservoir temperature controller alarm high to 10°C higher than setpoint

The tubing temperature controller is set as shown in Figures A.15 through A.18.

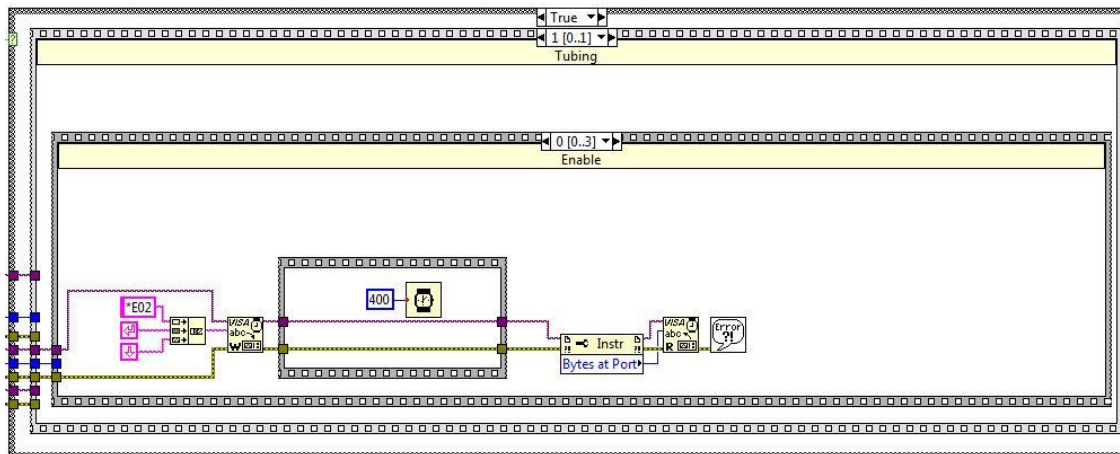


Figure A.15 Turning the tubing temperature controller on

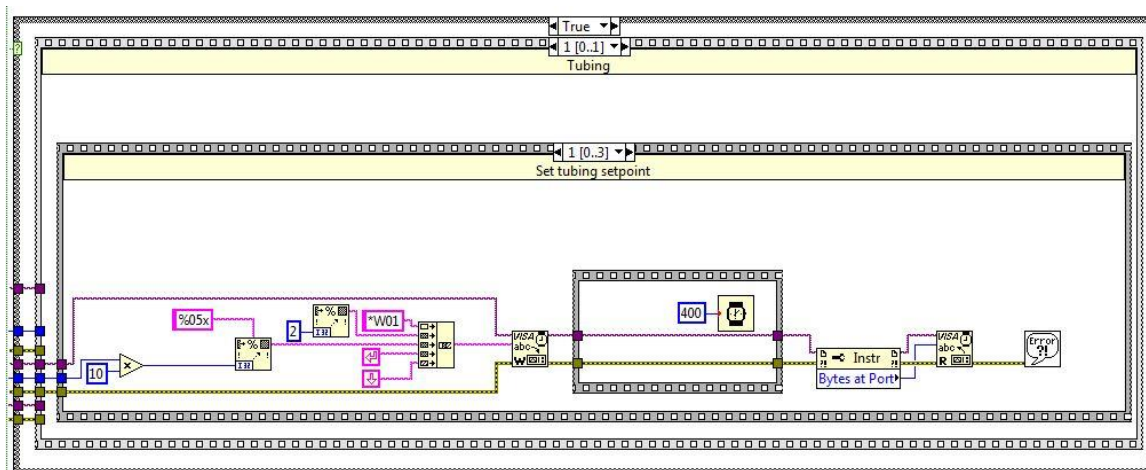


Figure A.16 Setting the tubing temperature controller setpoint temperature

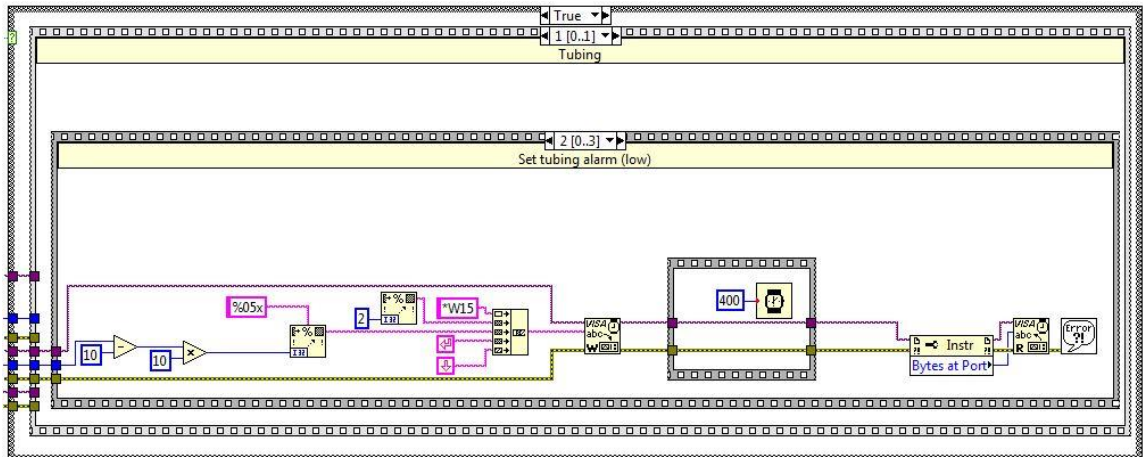


Figure A.17 Setting the tubing temperature controller alarm low to 10°C lower than setpoint

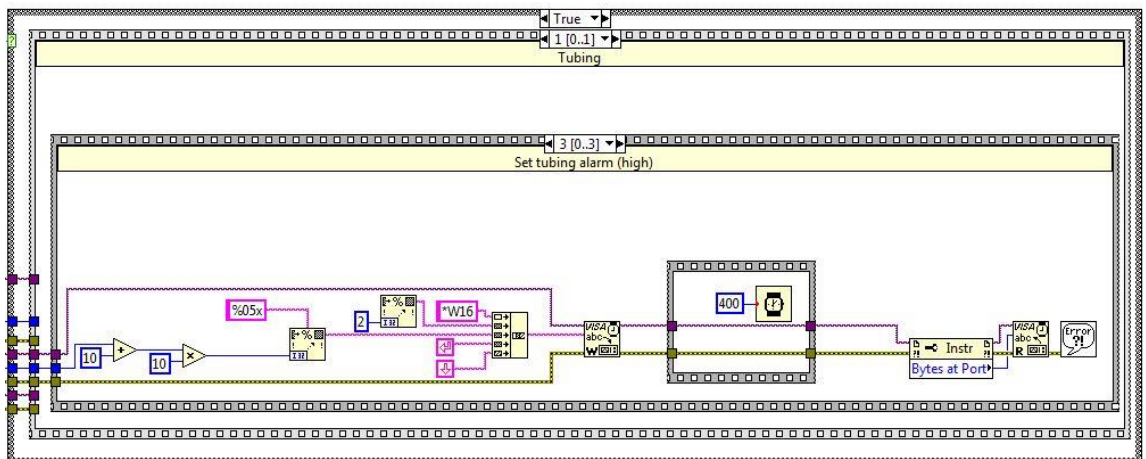


Figure A.18 Setting the tubing temperature controller alarm high to 10°C higher than setpoint

Next, the temperature range is checked before drop deposition starts. If the temperature is not within +/- 3°C within the temperature controller setpoints, drop deposition will not start. The logic is shown in Figures A.19 to A.20.

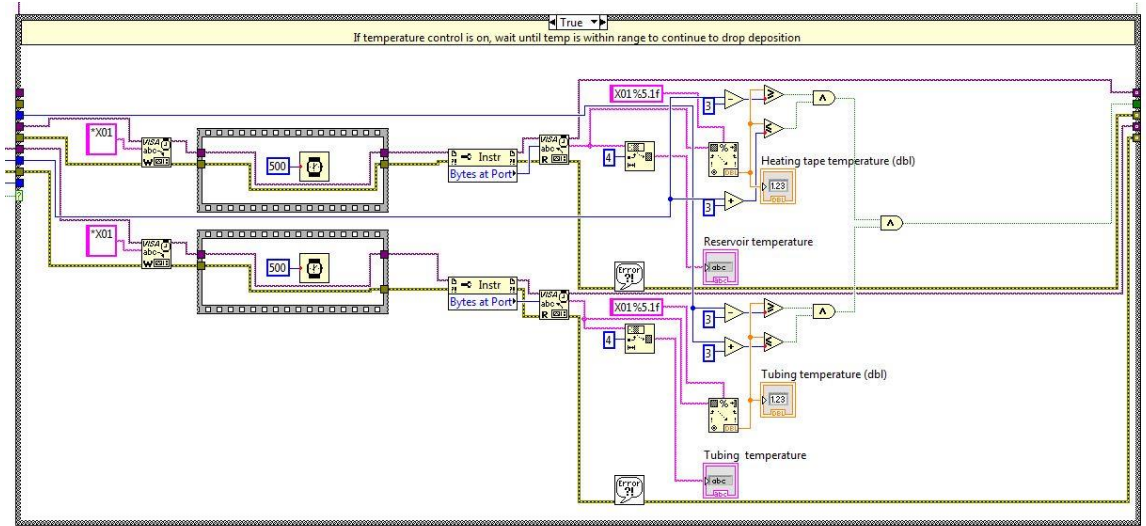


Figure A.19 Checking temperature range for reservoir and tubing controllers

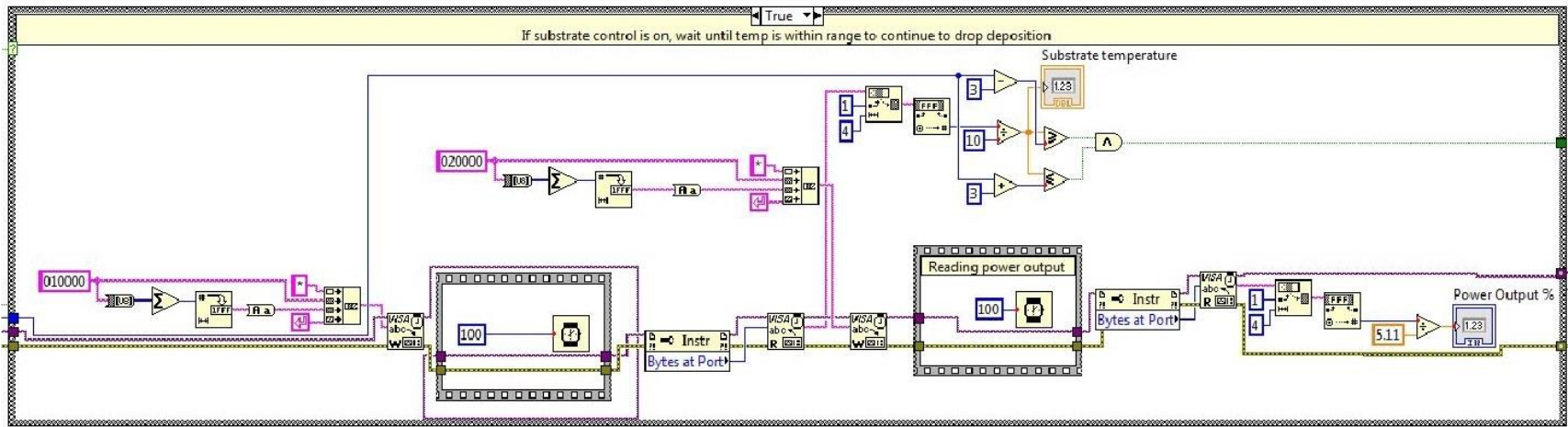


Figure A.20 Checking temperature range for substrate temperature controllers

The next step is initiating the drop deposition process, as shown in Figure A.21. Here, the printing settings are pulled up from the input file; the output file is generated; and it is connected to the pump and staging controllers. If the process is used without temperature control, then the code by passes the previous steps and directly starts with the drop deposition.

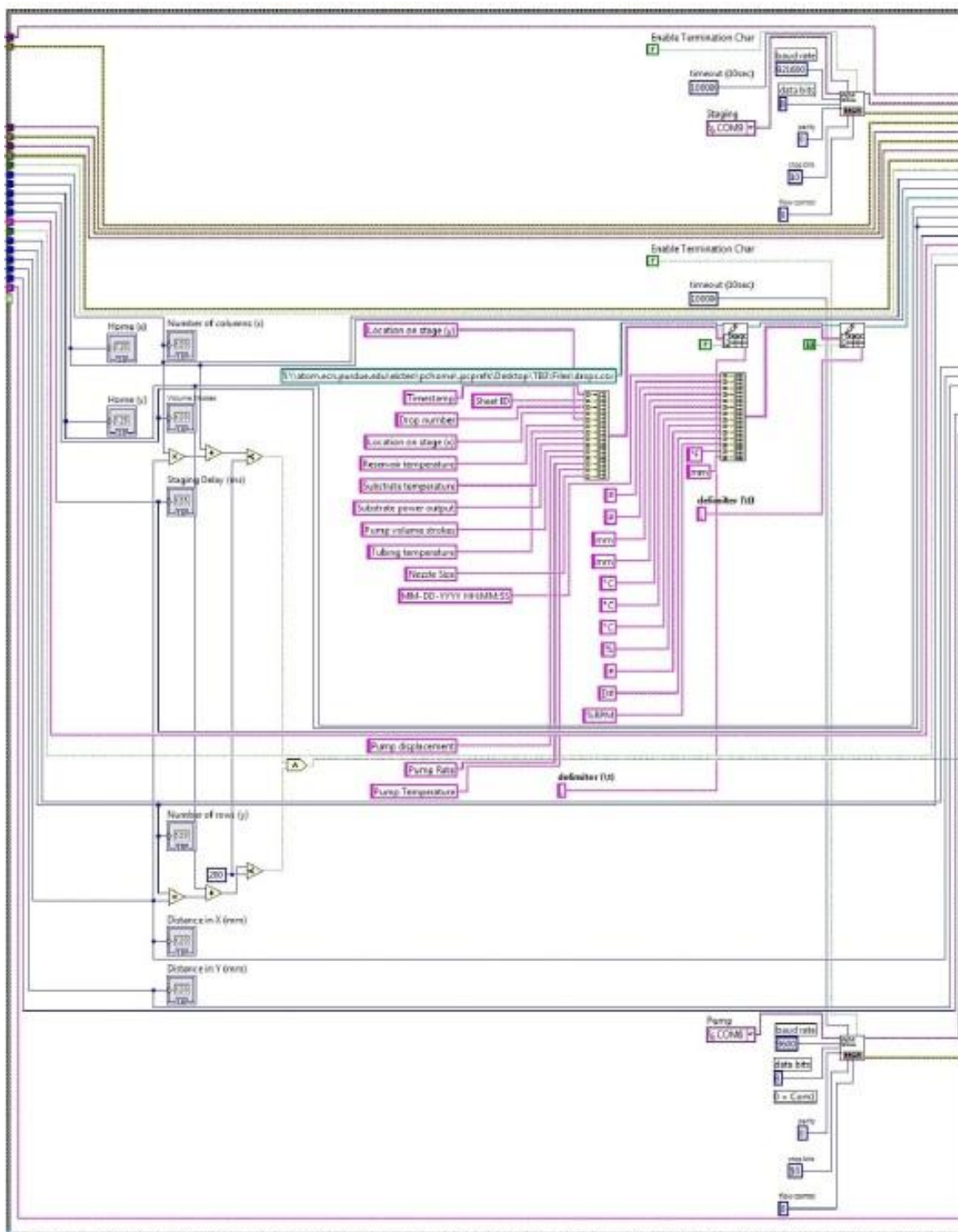


Figure A.21 Generating the output file, pulling up printing settings and connecting to pump and staging controllers

The staging motors are turned on and pump is set to run forward, as shown in Figures A.22 to A.24.

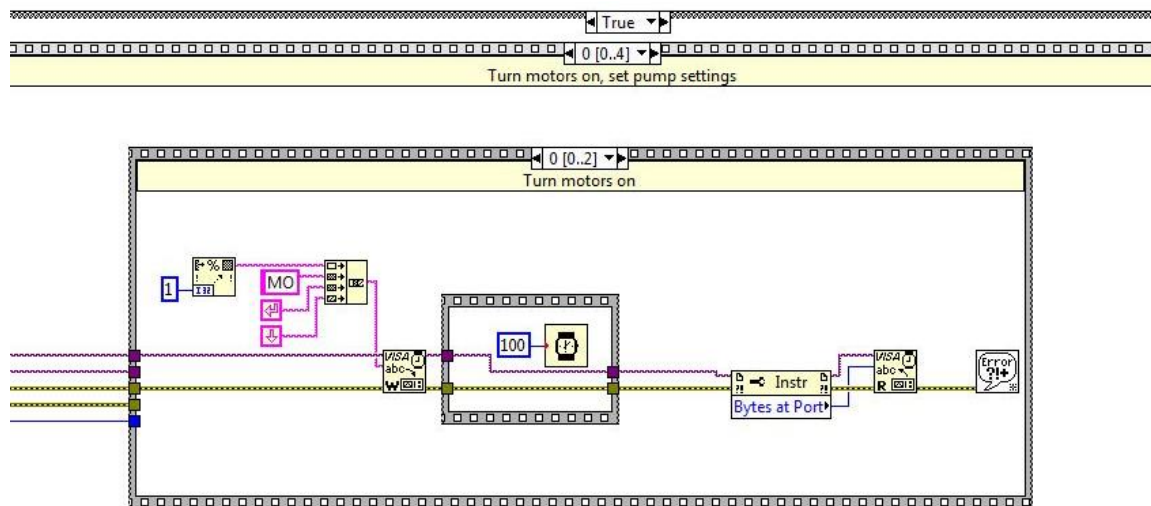


Figure A.22 Turn staging motor for x-direction on

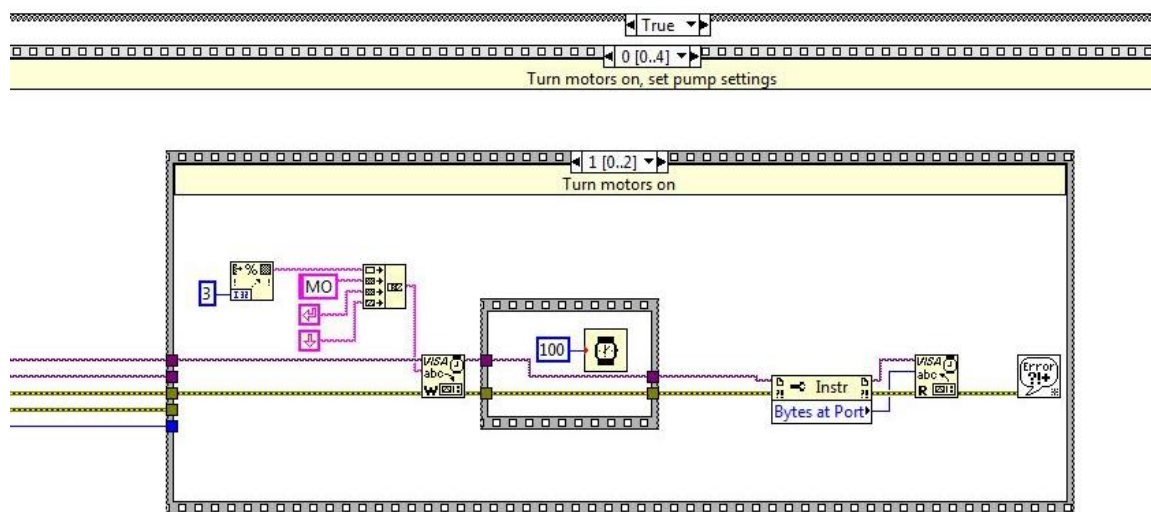


Figure A.23 Turn staging motor for y-direction on

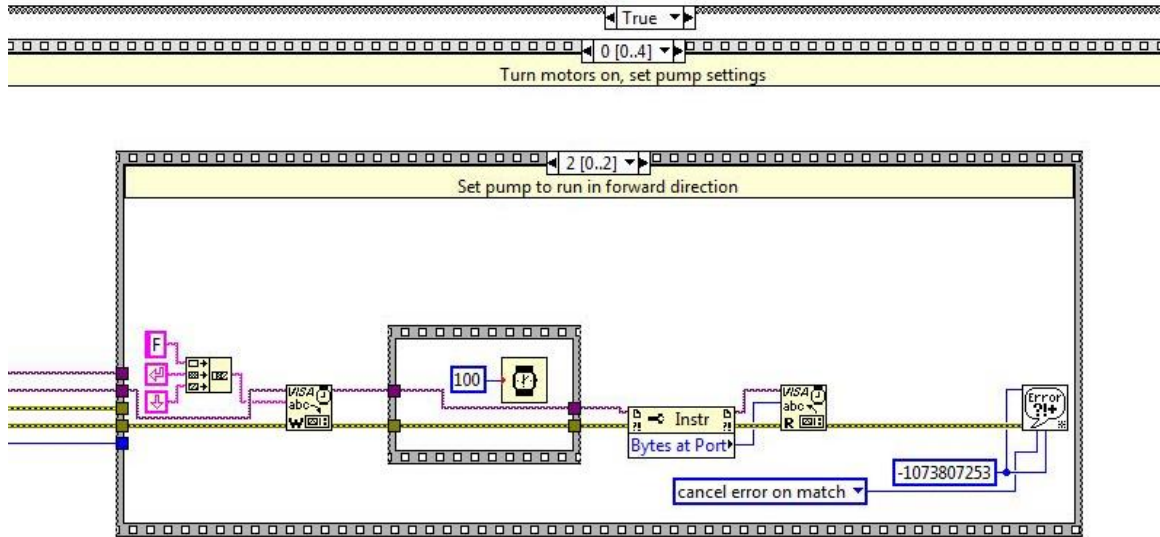


Figure A.24 Setting pump to move in forward direction

The staging is moved to home position in x and y directions, as shown in Figures A.25 to A.26.

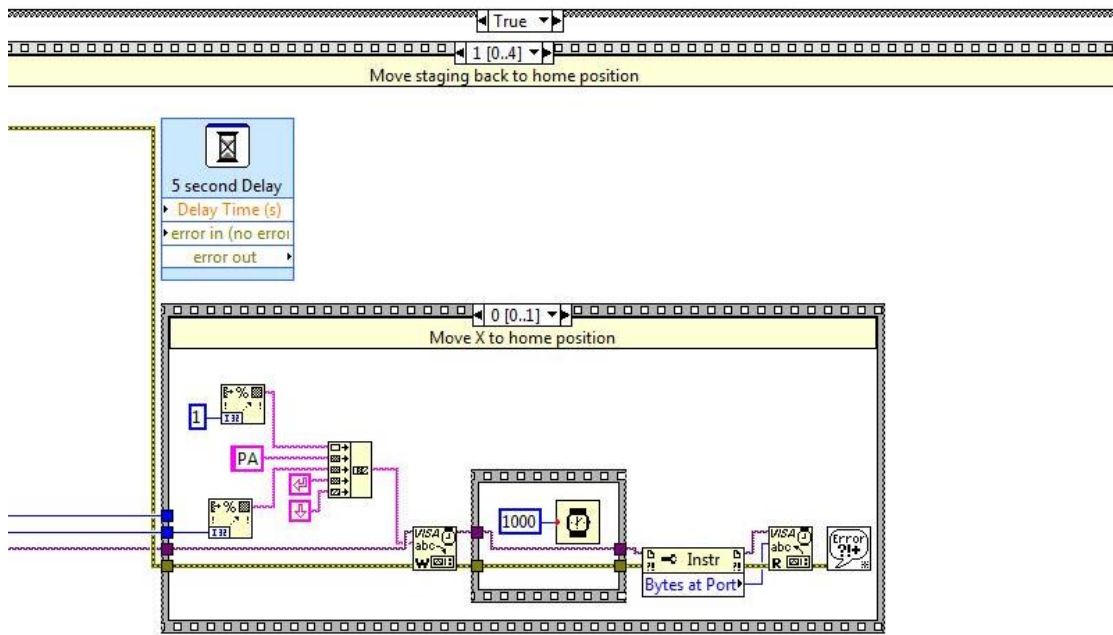


Figure A.25 Moving staging to home position in x-direction

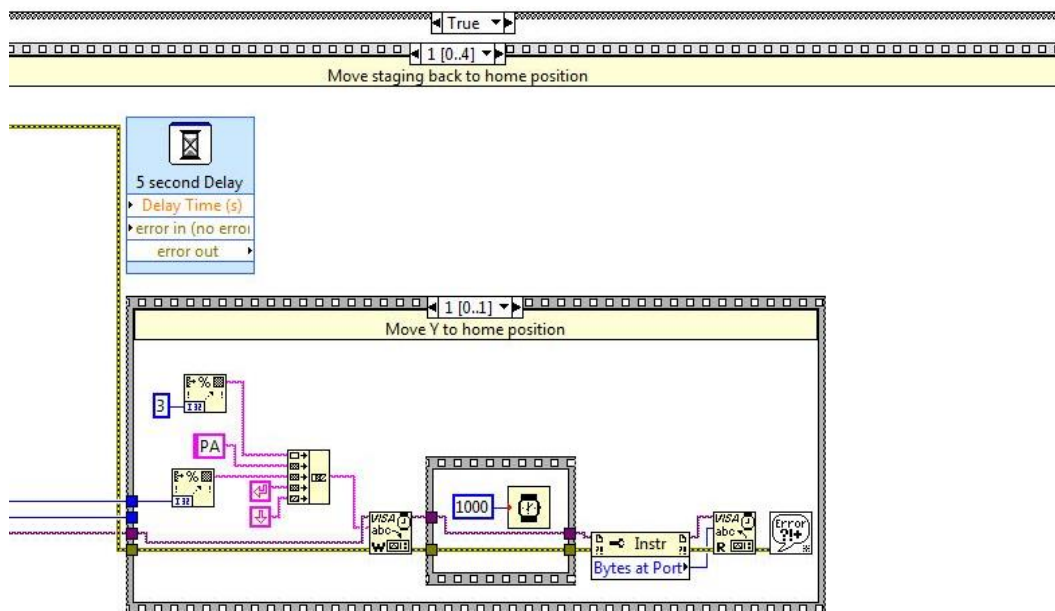


Figure A.26 Moving staging to home position in y-direction

Next, the logic loops allow for the boustrophedon movement to be executed, as shown in Figure A.27. The staging moves in +x direction for even rows and moves in -x direction for odd rows.

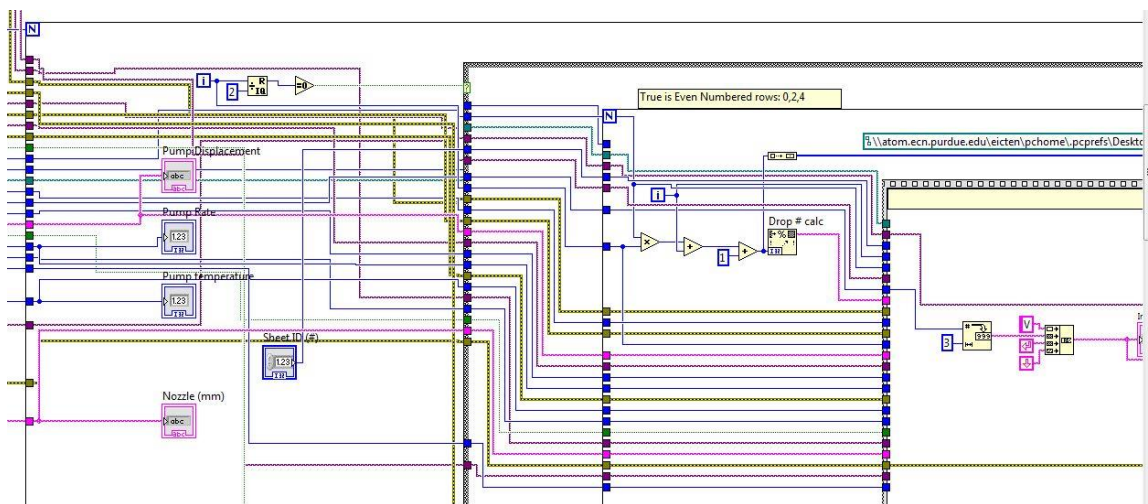


Figure A.27 Logic loops for boustrophedon stage movement

Drop deposition is shown in Figure A.28. After each deposition, the x and y location of the drop are saved as shown in Figures A.29 and A.30.

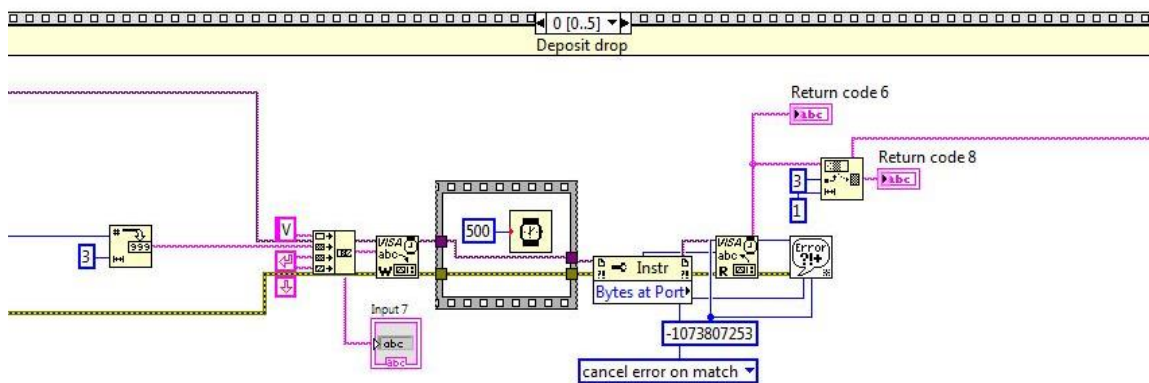


Figure A.28 Depositing drop

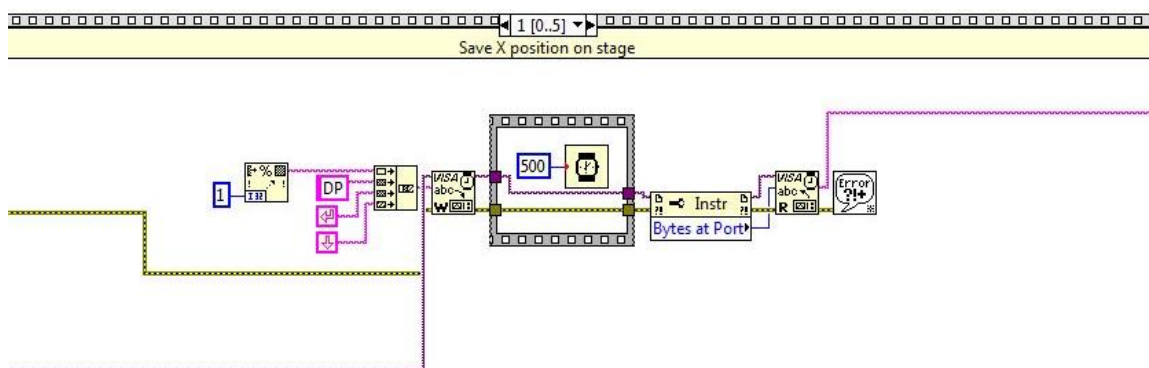


Figure A.29 Saving x-position on stage

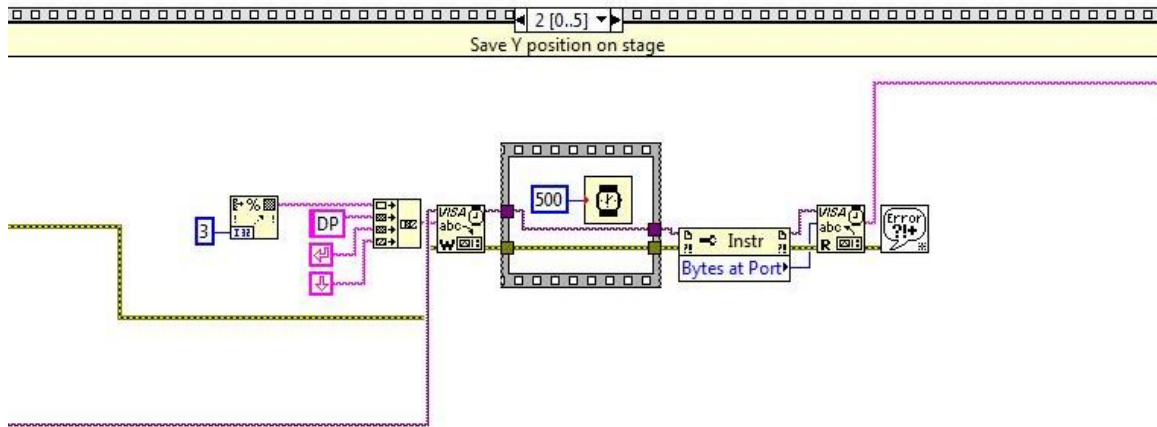


Figure A.30 Saving y-position on stage

The case structure allows continuing printing in the same row and moving to the next row, as shown in Figures A.31 and A.32.

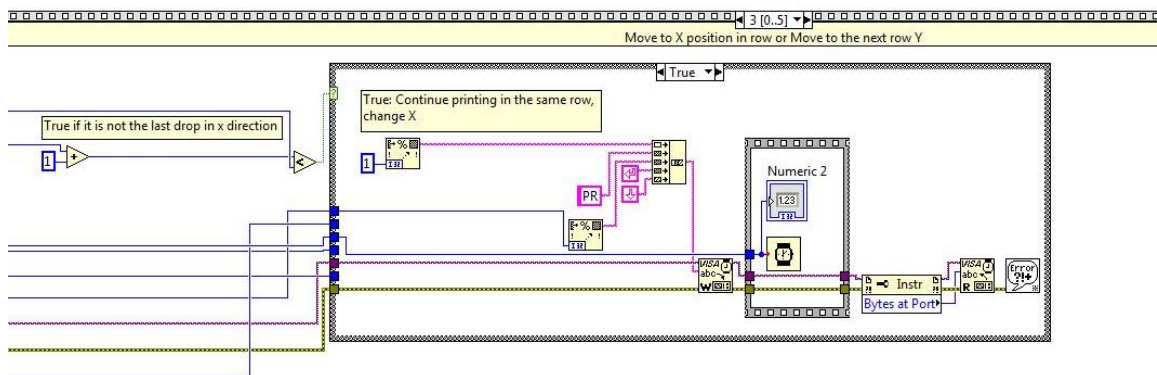


Figure A.31 True: Continue printing in the same row

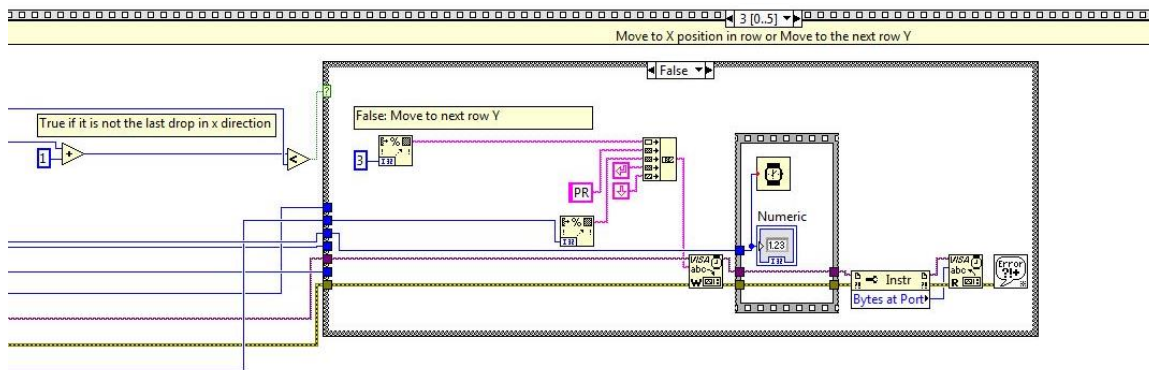


Figure A.32 False: Move to next row y

If temperature controllers are on, record the temperature values as shown in Figure A.33. If temperature control is not used, record default values indicating no temperature control is used, as shown in Figure A.34.

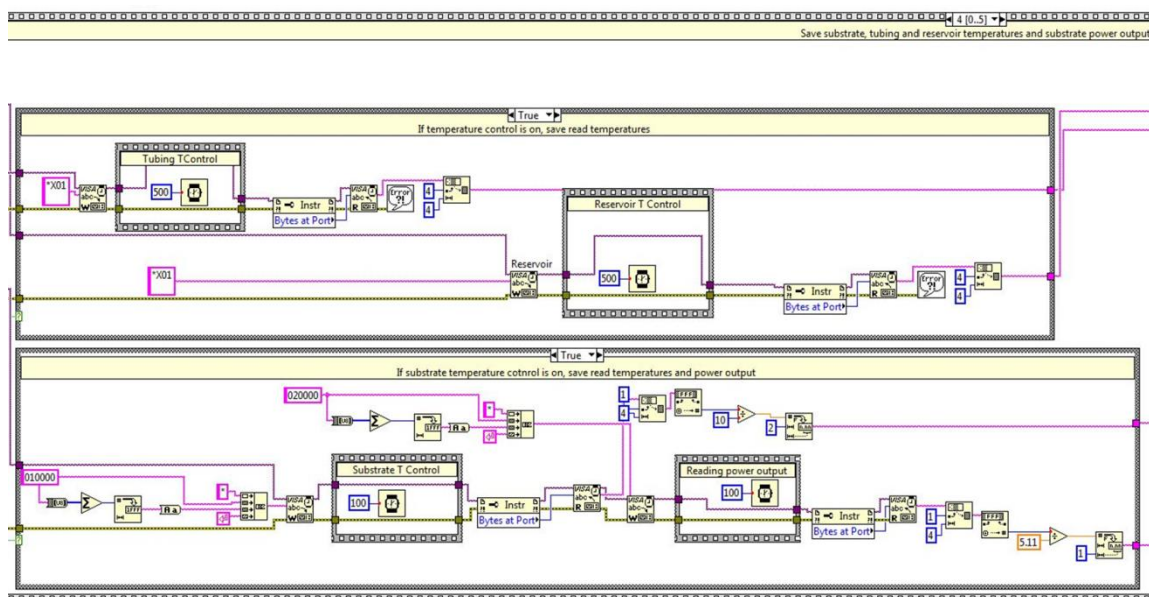


Figure A.33 Read and record temperatures of tubing, reservoir and substrate and substrate power output

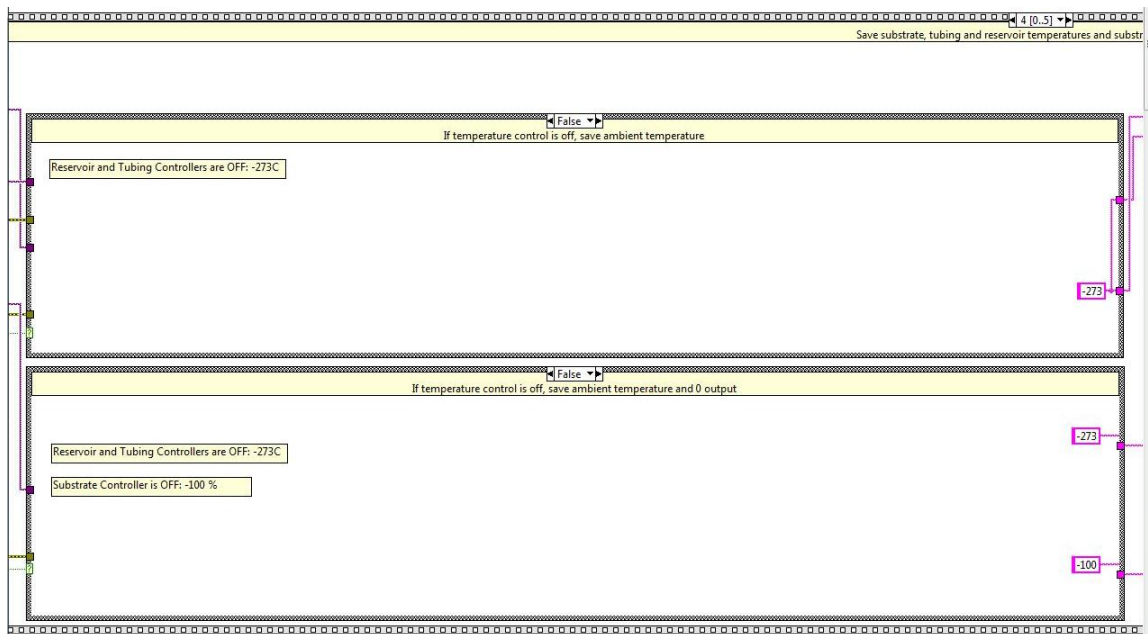


Figure A.34 Record output values for no temperature control

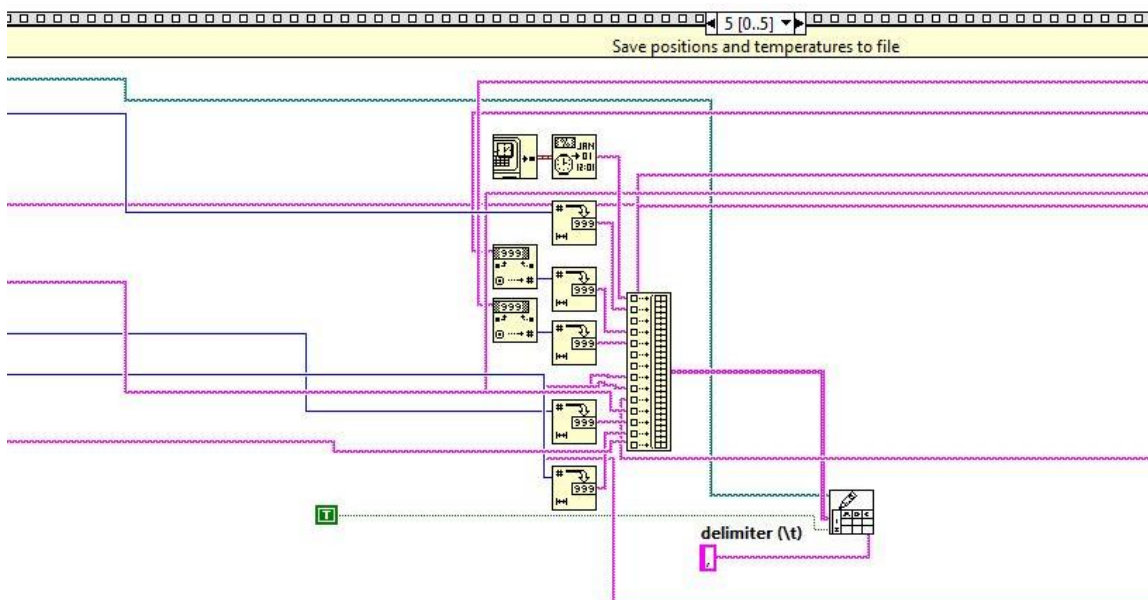


Figure A.35 Saving positions and temperatures to file

In parallel to drop deposition, the camera is operating. The connection to the camera is established as shown in Figure A.36. A camera.csv file is generated to save drop image related calculations.

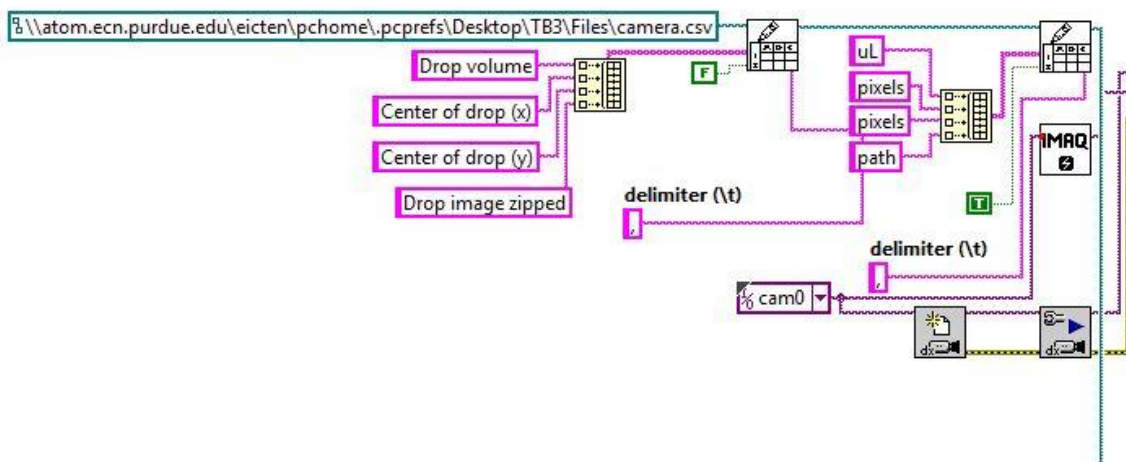


Figure A.36 Connect to camera

The camera code and the image processing is shown in Figure A.37.

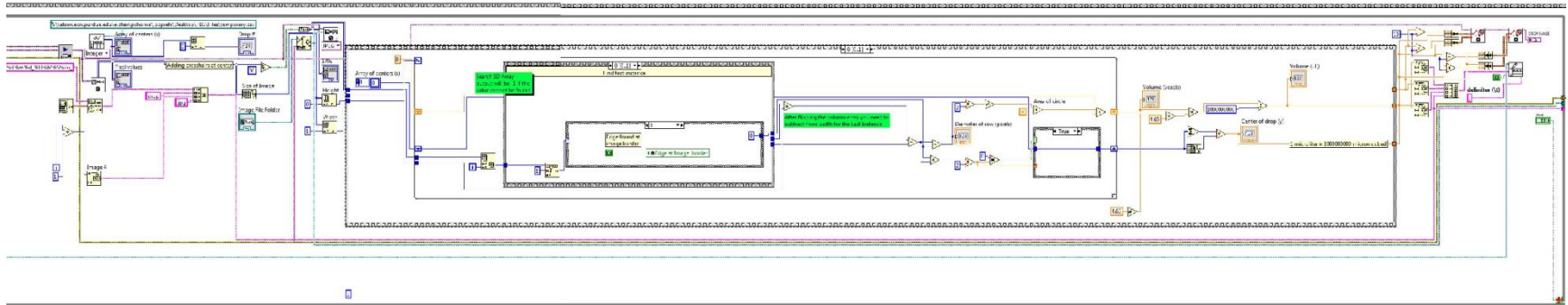


Figure A.37 Image processing code

The csv files containing the drop deposition and camera calculations are merged and saved to the defined output file path, as shown in Figure A.38.

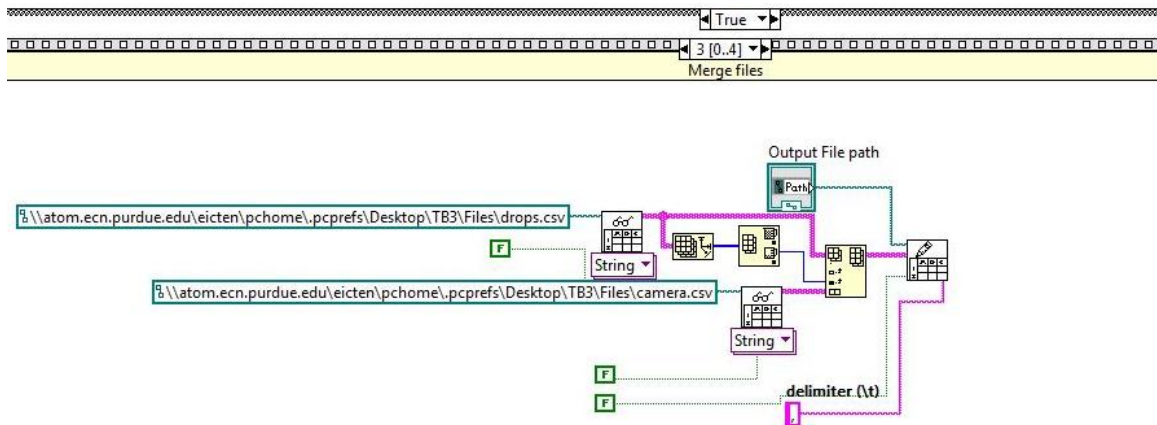


Figure A.38 Merge drop deposition and camera files to the output file

The program stops after drop cycle is executed, as shown in Figure A.39.

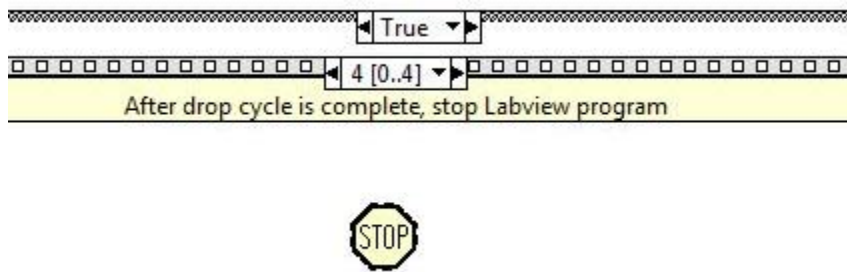


Figure A.39 Stop program after drop cycle is finished

After the drop cycle is executed, the user can design a cooling profile using the substrate cooling temperature as described in Chapters 5 and 6. For that purpose, another LabVIEW program is developed. The user interface of the program is shown in Figures 3.8 and 3.9. The program first connects to the substrate temperature controller via Visa connection, as shown in Figure A.40. The visa connection to substrate temperature controller is shown in Figure A.2 as well. However, at this step, also a spreadsheet is generated to save the data in a user defined location. Real time, setpoint temperature, read temperature and power output are recorded.

Setting the parameters to the substrate controller are shown in Figures A.3 to A.10. These steps are also followed in the substrate temperature control program to setup the controller. Next, the designed temperature profiles are implemented in the substrate temperature controller, as shown in Figure A.41.

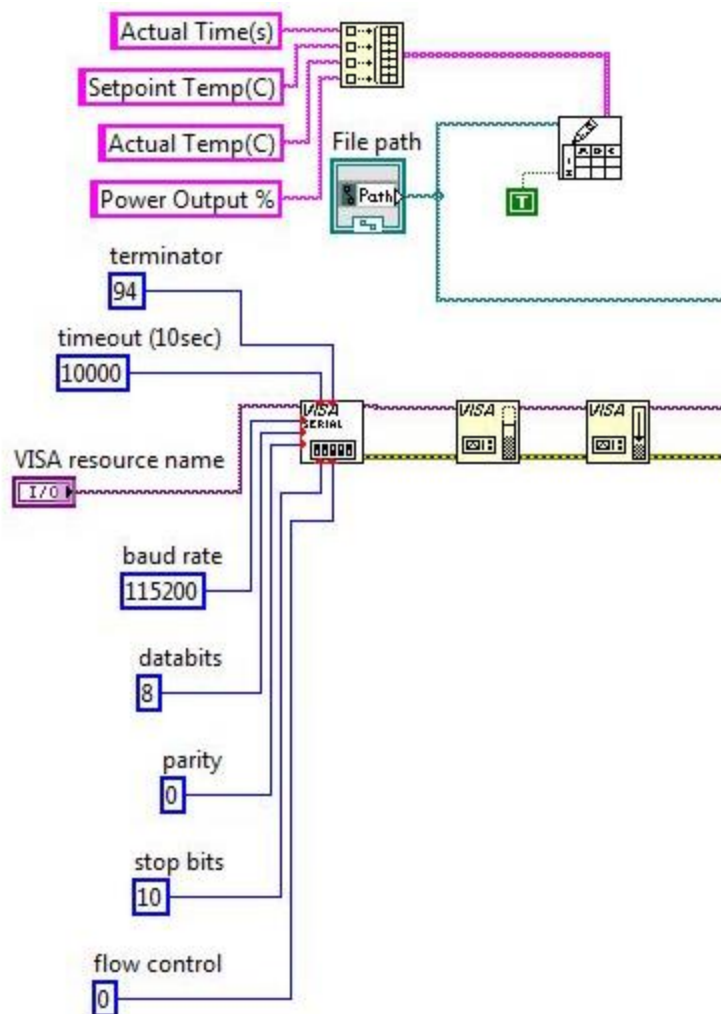


Figure A.40 Connecting to the substrate temperature controller and generating output file

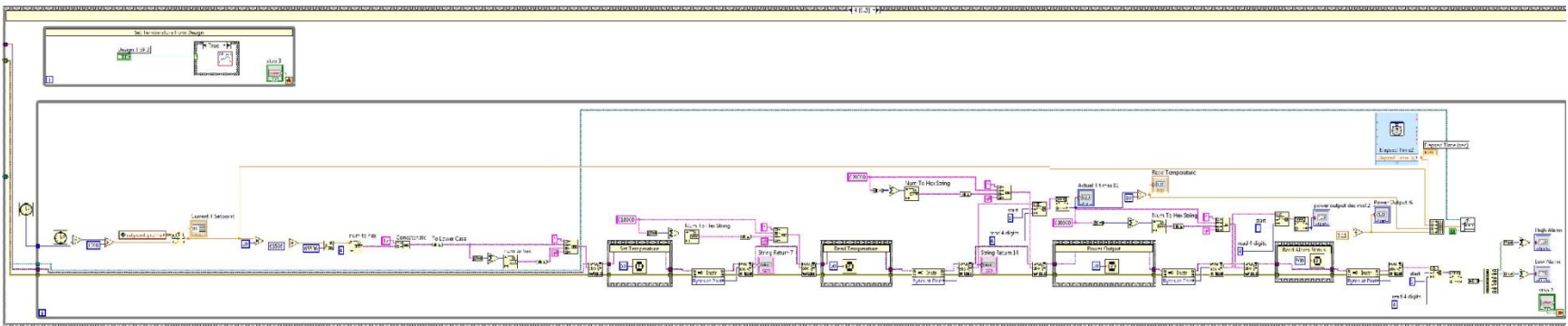


Figure A.41 Executing designed temperature profiles via substrate temperature control program and saving the time series data

Appendix B MATLAB Codes

In this section, the MATLAB codes are presented, which are used for PCE surrogate modelling in Chapter 6. The model for single input single output case is shown below as a representative case.

```

clear all
close all
clc

% Y1 to Y2 dissolution profile time const (min)
% U1 to U2 cooling temperature profile (^oC) or (^oC/min)

% %60% dissoln time
%
% 5 Input 1 Output
% U1= [60 30 30 30 30];
% Y1=[8];
% U2=[60 40 30 30 30];
% Y2=[8.8];
% U3=[60 54 30 30 30];
% Y3=[9.6];
% U4=[60 57 45 30 30];
% Y4=[10.2];
% U5=[60 58 50 30 30];
% Y5=[10.7];
% U6=[60 58.5 52.5 37.5 30];
% Y6=[11.5];
% U7=[60 59 55 45 30];
% Y7=[18.4];

% 1 Input 1 Output
% U1= [15];
% Y1=[8];
U2=[10];
Y2=[8.8];
U3=[3];
Y3=[9.6];
U4=[1.5];
Y4=[10.2];
U5=[1];
Y5=[10.7];
U6=[0.75];
Y6=[11.5];
U7=[0.5];
Y7=[18.4];

```

```

YMat=[Y2',Y3',Y4',Y5',Y6',Y7']';
Temp_Profile=[U2',U3',U4',U5',U6',U7']'
ERR=[];
Yend_alltheta = YMat

% initial condition for 1 temp value and 1st order
X0 = zeros(2,1);
% X0=[100;100];
PCECOEFS = [ones(2,1) X0];
i=0;

while abs(minus(PCECOEFS(:,1),PCECOEFS(:,2)))> 1e-25*(ones(2,1))
    PCECOEFS(:,1)=PCECOEFS(:,2);
    OPTIONS=optimset('TolCon',1e-10,'TolFun',1e-10,'TolX',1e-
    10,'display','iter','Maxiter',1000*1000,'MaxFunEvals',10000000);
    [PCEcoefs1, Fval] =
    fminsearch(@e_f_objPCE_firstorder_1temp_1st,PCECOEFS(:,2),OPTIONS,
    Temp_Profile, Yend_alltheta, 0)
    PCECOEFS(:,2)=PCEcoefs1;
    e_f_objPCE_firstorder_1temp_1st(PCEcoefs1, Temp_Profile, Yend_alltheta,
    1);
    i=i+1
end

function Error = e_f_objPCE_firstorder_1temp_1st(PCEcoef, Temp_Prof,
Yend_alltheta, plotres);
    [m,n] = size(Temp_Prof);

    PCE = zeros(m,1);

    for i = 1:m;
        theta = Temp_Prof(i,:);
        PCE(i) = e_f_PCE_firstorder_1temp_1st(theta, PCEcoef)
    end

    Error = sum((Yend_alltheta(:) - PCE(:)).^2)

    if plotres
        theta_val=[15];
        Y_val_1=[8];
        v_end=size(theta_val)
        for v=1:v_end(:,1)
            Val_PCE_1(v)=e_f_PCE_secondorder_1temp_1st(theta_val(v,:), PCEcoef)
        end

        set(gcf, 'PaperPositionMode', 'manual');
        set(gcf, 'PaperUnits', 'inches');
        set(gcf, 'PaperPosition', [0.25 2.5 5.6 6.0]);

        subplot(5,1,1:2)
        axis([1,6,5,20])
        plot(Yend_alltheta,'ko','MarkerFaceColor','k')

```

```

hold on
plot(PCE,'rd','MarkerFaceColor','r')
hold on

ylabel({'Dissolution Time'; 'Constant \tau
(min)'}, 'fontsize',10,'fontweight','b')
leg=legend('Exp. data','PCE model','Location','Northwest')
legend boxoff
h=gca
h.XTick = [1,2,3,4,5,6];
h.XTickLabel = {'1','2','3','4','5','6'};

subplot(5,1,3)
axis([1,6,-30,30])
h=stem((Yend_alltheta-PCE)./Yend_alltheta*100,'bx' )
RES=(Yend_alltheta-PCE)./Yend_alltheta*100
ylabel('Residual %','fontsize',10,'fontweight','b')
xlabel('Data Points','fontsize',10,'fontweight','b')
leg2=legend('Training Points','Location','Northeast');
hold on
legend boxoff

subplot(5,1,4:5)
axis([7,19,5,20])
plot(Yend_alltheta,Yend_alltheta,'k--')
hold on
plot(Yend_alltheta,PCE,'rd','MarkerFaceColor','r')
hold on
plot(Y_val_1,Val_PCE_1,'gs','MarkerFaceColor','g')
hold on
plot(Y_val_1,Y_val_1,'bp','MarkerFaceColor','b')

xlabel('\tau from Experimental Data
(min)', 'fontsize',10,'fontweight','b')
ylabel({'\tau from (5-1) PCE'; 'Model
(min)'}, 'fontsize',10,'fontweight','b')
leg=legend({'Exp.
data','PCE','Simulated','Actual'}, 'Position',[0.55 0.15 0.25 0.1])
legend boxoff

end

disp(Yend_alltheta-PCE);
disp((Yend_alltheta-PCE).^2);

function [PCE, PCE_terms] = e_f_PCE_firstorder_ltemp_1st(theta, c);
PCE_order = 1;
c = c(:)'; %PCEcoefs
n = length(theta);
nc = length(c);
Npce = 1;

```

```

for i = 1:PCE_order
    Npce = Npce + factorial(n+i-1)/factorial(n-1)/factorial(i);
end

if nc ~=Npce
    error('Wrong number of coefficients!')
end
PCE_terms(1) = 1;

for i=1:n
    PCE_terms(1+i) = theta(i);
end

PCE = sum(c.*PCE_terms);

```

The optimization problem formulated to predict temperature profile is below.

```

clc
clear all
close all
% PCE using U1, U2, U3, U5, U6, U7
% PCE_coeff=[-0.622753317044821;-
0.0149194088038712;0.0660550452915736;-
0.0108792025816413;0.512556063230387;-0.248755439386867;];
% Diss=[13.2];
x0=[1 60 52.5 45 37.5 30]';
Aeq=[1 0 0 0 0 0;0 1 0 0 0 0;0 0 0 0 0 1];
beq=[1;60;30];
A=[0 -1 1 0 0 0;0 0 -1 1 0 0;0 0 0 -1 1 0;0 0 0 0 -1 1];
b=[0;0;0;0];
ub=60;
lb=1;
x = fmincon(@hop,x0,A,b,Aeq,beq,lb,ub)

function res = hop(x)
%U7 is out
PCE_coeff=[0.299121488098244;0.260627000123544;0.0644781150732125;0.036
4433813818839;0.104694900354823;-0.468268250553230;];
Diss=[18.4];
%U6 is out
%PCE_coeff=[6.00308232535602;2.31027050440459;0.0644781144399137;0.0364
433832864824;0.504124282196730;-5.15711667024243;];
% Diss=[11.5];
%U5 is out
% PCE_coeff=[-0.821840939171808;0.0443110978548544;0.0782818185241383;-
0.0694818767352390;0.601255156863062;-0.404404925722324;];
% Diss=[10.7];
%U4 is out
% PCE_coeff=[-0.622753317044821;-
0.0149194088038712;0.0660550452915736;-
0.0108792025816413;0.512556063230387;-0.248755439386867;];

```

```
% Diss=[10.2];
%U3 is out
% PCE_coeff=[-1.43865838038008;0.147055654280234;0.102274182202390;-
0.0475870158806807;0.510654140628079;-0.547566095848332;];
% Diss=[9.6];
%U2 is out
% PCE_coeff=[-0.466895454096701;-0.453160243278553;0.0703231297771442;-
0.00331632471156312;0.492199546171891;0.629343982713687;];
% Diss=[8.8];
%U1 is out
% PCE_coeff=[-0.610241385049950;0.178718323684061;0.0634110776219363;-
0.00193391682608671;0.492199547265658;-0.618575668044410;];
% Diss=[8];
res=((PCE_coeff'*x-Diss)/Diss)*100)^2
end
```


VITA

VITA

Elçin İçten was born and raised in İstanbul, Turkey. After graduating from İstanbul Lisesi (İstanbul High School) in 2005, she attended Boğaziçi University for her bachelor's degree in Chemical Engineering. During the senior year, she participated in a study abroad program and studied at Purdue University in the fall of 2009. After graduating from Boğaziçi University with honors in 2011, she decided to pursue her doctoral degree in Chemical Engineering at Purdue University. Elçin chose to focus her research on process systems engineering applied to pharmaceutical systems and worked on developing a dropwise additive manufacturing system for pharmaceutical drug products. She was supervised by Prof. Zoltan K. Nagy and Prof. Gintaras V. Reklaitis and was part of the Engineering Research Center for Structured Organic Particulate Systems (ERC-SOPS). During her Ph.D., she was awarded with multiple competitive fellowships and awards including AIChE Process Development Division Student Paper Award, Indiana's Next Generation Manufacturing Competitiveness Center (IN-MaC) Fellowship, Women & High-Tech Scholarship, and multiple travel grants including AIChE CAST Division, Purdue College of Engineering, School of Chemical Engineering Eastman and Purdue PGSG travel grants to support her travels for presenting at international conferences. In addition to her research, Elçin also worked on developing her leadership

skills. She served as the vice president of the Student Leadership Committee of ERC-SOPS. She was a graduate woman ambassador of School of Chemical Engineering and in the organization committee of the 2015 Women in Chemical Engineering Seminar. She volunteered in Purdue WIEP program to mentor young students and she also supervised undergraduate researchers in chemical engineering. Elçin is a CMAS 3* diver and enjoys travelling and Scuba-diving around the world. Elçin will graduate with her Ph.D. in March 2016 and will join Amgen in Cambridge, Massachusetts.

PUBLICATIONS

PUBLICATIONS

1. E. Içten, Z. K. Nagy, and G. V. Reklaitis, “Supervisory Control of a Drop on Demand Mini-manufacturing System for Pharmaceuticals,” Proceedings of 24th European Symposium on Computer Aided Process Engineering, vol. 33, pp. 535–540, 2014.
2. E. Içten, A. Giridhar, L. S. Taylor, Z. K. Nagy, and G. V. Reklaitis, “Dropwise Additive Manufacturing of Pharmaceutical Products for Melt-Based Dosage Forms.,” Journal of Pharmaceutical Sciences, vol. 104, no. 5, pp. 1641–1649, 2015.
3. L. Hirshfield, E. Içten, A. Giridhar, Z. K. Nagy, and G. V. Reklaitis, “Real-Time Process Management Strategy for Dropwise Additive Manufacturing of Pharmaceutical Products,” Journal of Pharmaceutical Innovation, vol. 10, no. 2, pp. 140–155, 2015.
4. E. Içten, A. Giridhar, Z. K. Nagy, and G. V. Reklaitis, “Drop-on-Demand System for Manufacturing of Melt-based Solid Oral Dosage: Effect of Critical Process Parameters on Product Quality,” AAPS PharmSciTech, doi: 10.1208/s12249-015-0348-3, 2015.

5. E. İçten, Z. K. Nagy, and G. V. Reklaitis, "Process control of a dropwise additive manufacturing system for pharmaceuticals using polynomial chaos expansion based surrogate model," *Computers & Chemical Engineering*, vol. 83, pp. 221–231, 2015.
6. E. İçten, Z. K. Nagy, and G. V. Reklaitis, "Modelling of Crystallization of Solid Oral Drug Forms in a Dropwise Additive Manufacturing System," in *12th International Symposium on Process Systems Engineering and 25th European Symposium on Computer Aided Process Engineering*, vol. 37, pp. 2195–2200, 2015.